

A Widely Applicable Dual-Catalytic System for Cross-Electrophile Coupling

David Charboneau, Emily L. Barth, Nilay Hazari, Mycah R. Uehling, Susan L. Zultanski

Submitted date: 26/06/2020 • Posted date: 29/06/2020

Licence: CC BY 4.0

Citation information: Charboneau, David; Barth, Emily L.; Hazari, Nilay; Uehling, Mycah R.; Zultanski, Susan L. (2020): A Widely Applicable Dual-Catalytic System for Cross-Electrophile Coupling. ChemRxiv. Preprint. <https://doi.org/10.26434/chemrxiv.12574664.v1>

A new dual catalytic system for cross-electrophile coupling reactions between aryl and alkyl halides that features a Ni catalyst, a Co co-catalyst, and a mild homogeneous reductant, is described. This is a unique combination of reagents for cross-electrophile coupling reactions, which results in one of the most versatile systems reported to date. For example, the coupling of aryl bromides and aryl iodides with alkyl bromides, alkyl iodides, alkyl mesylates, and benzyl chlorides is demonstrated under similar reaction conditions. The system is tolerant of numerous functional groups and is capable of coupling heteroaryl halides, di-ortho-substituted aryl halides, pharmaceutically relevant drug-like aryl halides, and a diverse range of alkyl halides. Additionally, the dual catalytic platform facilitates a series of novel one-pot three-component cross-electrophile coupling reactions of bromo(iodo)arenes with two distinct alkyl halides. Mechanistic studies indicate that the Ni catalyst activates the aryl halide electrophile, while the Co catalyst activates the alkyl electrophile.

File list (2)

Manuscript (1).pdf (1.11 MiB)

[view on ChemRxiv](#) • [download file](#)

Supporting_Information.pdf (7.19 MiB)

[view on ChemRxiv](#) • [download file](#)

A Widely Applicable Dual-Catalytic System for Cross-Electrophile Coupling

David J. Charboneau,^a Emily L. Barth,^a Nilay Hazari,^{a,*} Mycah R. Uehling^b & Susan L. Zultanski^{c,*}

^aDepartment of Chemistry, Yale University, P. O. Box 208107, New Haven, Connecticut, 06520, USA. E-mail: nilay.hazari@yale.edu.

^bMerck & Co., Inc., Discovery Chemistry, HTE and Lead Discovery Capabilities, Kenilworth, New Jersey, 07033, USA.

^cMerck & Co., Inc., Department of Process Research and Development, Rahway, New Jersey, 07065, USA. E-mail: susan_zultanski@merck.com.

Abstract

A new dual catalytic system for cross-electrophile coupling reactions between aryl and alkyl halides that features a Ni catalyst, a Co co-catalyst, and a mild homogeneous reductant, is described. This is a unique combination of reagents for cross-electrophile coupling reactions, which results in one of the most versatile systems reported to date. For example, the coupling of aryl bromides and aryl iodides with alkyl bromides, alkyl iodides, alkyl mesylates, and benzyl chlorides is demonstrated under similar reaction conditions. The system is tolerant of numerous functional groups and is capable of coupling heteroaryl halides, di-*ortho*-substituted aryl halides, pharmaceutically relevant drug-like aryl halides, and a diverse range of alkyl halides. Additionally, the dual catalytic platform facilitates a series of novel one-pot three-component cross-electrophile coupling reactions of bromo(iodo)arenes with two distinct alkyl halides. Mechanistic studies indicate that the Ni catalyst activates the aryl halide electrophile, while the Co catalyst activates the alkyl electrophile.

Introduction

Ni-catalyzed cross-electrophile coupling (CEC) reactions to generate new C(sp²)–C(sp³) bonds have received significant attention over the last decade due to the prevalence of these linkages in natural products and pharmaceuticals, and the limitations of current synthetic methods to form these bonds (Figure 1a).^[1] Despite the widespread interest, reaction development has relied heavily on the empirical screening of reaction parameters, such as the identity of the ancillary ligand and presence of pyridine and alkali halide additives.^[2] Consequently, reaction conditions developed using this strategy are often specific to a limited range of substrates.^[3] For example, typical reaction conditions for the coupling of aryl halides with primary alkyl bromides, primary alkyl iodides, or primary benzyl chlorides utilize different ligand sets, additives, solvents, and reductants.^[1a,1b,2,4] Further, even within a particular substrate class, for instance nitrogen-containing heteroaryl halides, significant changes are often required depending on the exact identity of the substrates.^[5] Unfortunately, it is often unclear why a given alteration of reaction conditions or the presence of an additive results in the desired reactivity, which complicates the translation of the method to other substrates. These challenges have limited the application of CEC in synthetic chemistry, especially for the functionalization of complex pharmaceutically relevant substrates.^[6]

A potential reason for the lack of generalizable conditions for CEC is related to the proposed mechanism,^[7] in which it is difficult to independently control key on- and off-cycle reactions (Figure 1b). Specifically, in CEC reactions between aryl and alkyl halides, complexes of the type LNi^{II}(Ar)X (X = Cl, Br, or I) are proposed to be crucial intermediates, as they are both the catalyst resting state and responsible for capturing free alkyl radicals (Figure 1b).^[7a] *In an ideal CEC reaction, the LNi^{II}(Ar)X intermediate would be stable and the rate at which radicals are generated would be controlled relative to the concentration of LNi^{II}(Ar)X to facilitate effective radical capture* (Figure 2). However, the rate of alkyl radical generation by a Ni^I halide intermediate cannot be tuned separately from the concentration of LNi^{II}(Ar)X because both complexes are intermediates on the same catalytic cycle. Additionally, under the reaction conditions typically utilized, LNi^{II}(Ar)X complexes are unstable and can undergo two deleterious side reactions: (i) bimolecular decomposition to produce biaryl,^[7d,8] which is especially problematic when high catalyst loadings are employed, or (ii) direct reduction to produce

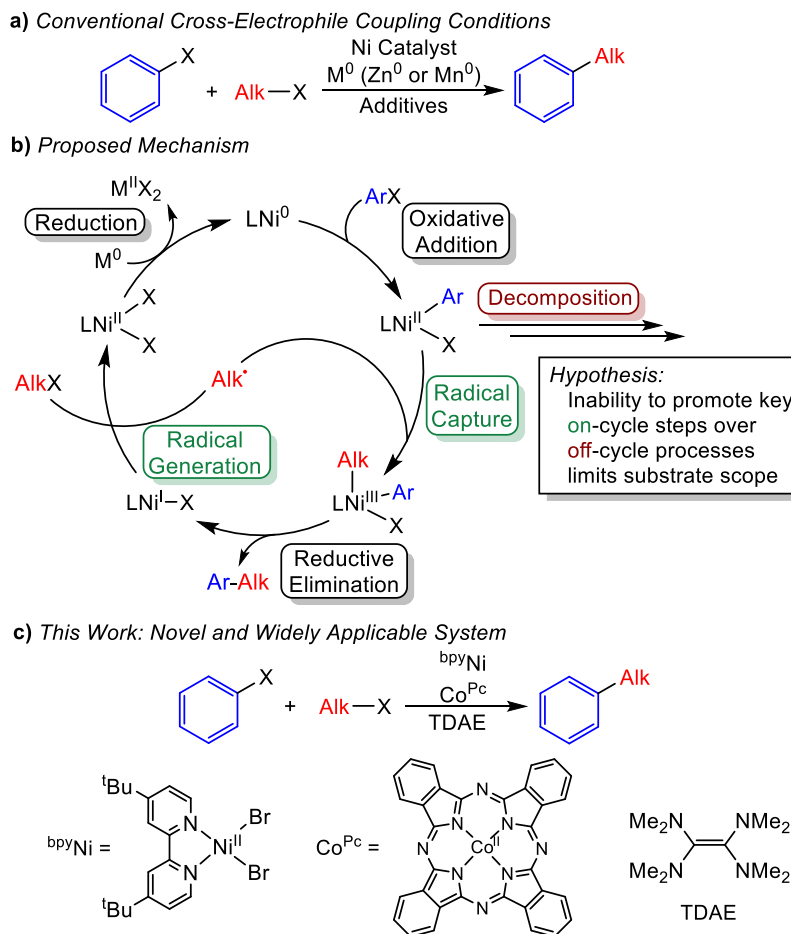


Figure 1. a) General depiction and **b)** mechanism of conventional Ni-catalyzed CEC reactions.^[7] **c)** CEC reaction described in this work.

protodehalogenated and biaryl products, which can readily occur when using strong heterogeneous Zn^0 or Mn^0 reductants.^[7c,7d,9] Further, heterogeneous reductants present practical limitations, including challenges with process scale reactions, flow chemistry, and automated chemical synthesis,^[10] and typically require the use of toxic amide-based solvents and additives^[4c,9b,11] for efficient electron transfer to solution state catalysts.^[10d,12] We hypothesized that by addressing the challenges related to the stability of the $\text{LNi}^{\text{II}}(\text{Ar})\text{X}$ intermediate and the inability to discretely control radical generation we could develop a general and practical system for $\text{C}(\text{sp}^2)\text{-C}(\text{sp}^3)$ CEC (Figure 2).

Here, we report an operationally simple protocol for CEC reactions between aryl and alkyl halides by using a Ni catalyst, a radical generating Co co-catalyst and a weak homogeneous reductant (Figure 1c). The Co co-catalyst activates the alkyl halide, which allows for control of

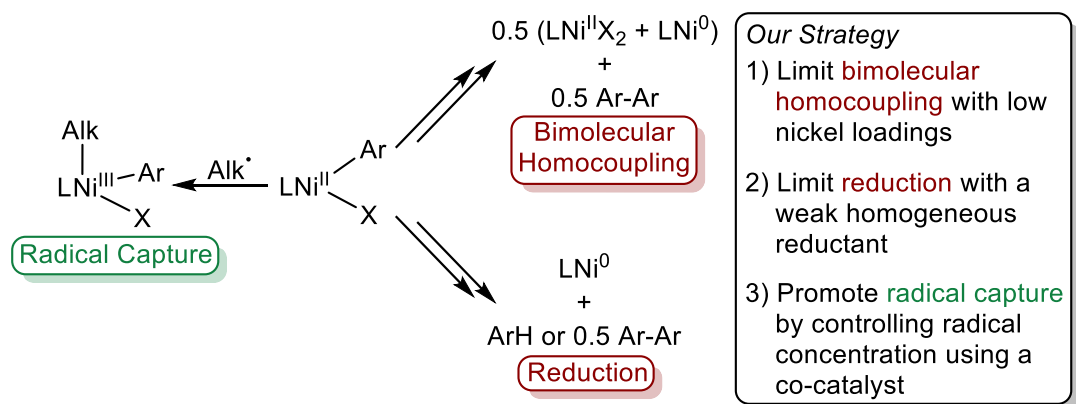


Figure 2. Potential reactions of $\text{LNi}^{\text{II}}(\text{Ar})\text{X}$ in catalysis and our strategy for system development.

the concentration of the alkyl radical relative to the concentration of the $\text{LNi}^{\text{II}}(\text{Ar})\text{X}$ intermediate (*vide infra*). The weak homogeneous reductant and generally low Ni loadings limit decomposition of $\text{LNi}^{\text{II}}(\text{Ar})\text{X}$. The reactions do not require additives and are easy to optimize because the product profile contains information about how to vary the ratio of the catalysts to promote radical capture at $\text{LNi}^{\text{II}}(\text{Ar})\text{X}$ before its decomposition in catalysis. As a result, a wide range of aryl and alkyl halides can be coupled in high yield, including substrates that are rarely utilized in CEC, such as di-*ortho*-substituted arenes and a diverse array of medically relevant substrates. Further, we show that our general strategy can facilitate the discovery of novel reactions by performing a series of one-pot three-component dialkylations of bromo(iodo)arenes with two distinct alkyl electrophiles. Finally, owing to the wide range of transformations that propose radical capture at intermediates of the type $\text{LNi}^{\text{II}}(\text{Ar})\text{X}$,^[13] our general strategy of controlling key processes associated with this complex may be relevant to both improving a range of current reactions and developing new methods.

Results and Discussion

Method for Reaction Optimization

We sought to identify appropriate reagents to explore our strategy of inhibiting off-cycle reactivity at $\text{LNi}^{\text{II}}(\text{Ar})\text{X}$ intermediates by using a weak homogeneous reductant and promoting productive radical capture through the use of a co-catalyst capable of generating a radical from an alkyl halide. An established method for activating an alkyl electrophile to generate an alkyl radical under reductive conditions is to use a Co catalyst.^[14] Based on its previous compatibility in CEC with heterogeneous Zn^0 or Mn^0 reductants, we selected $\text{Co}^{\text{II}}(\text{Pc})$ (Co^{Pc} ; Pc = phthalocyanine).^[15] Next, we selected the weak homogeneous reductant tetrakis(dimethylamino)ethylene (TDAE),

which is known to be compatible with Ni-catalyzed reductive coupling reactions.^[4c,16] Importantly, TDAE ($E^\circ = -0.57$ V vs NHE) is a weaker reductant than Mn^0 ($E^\circ = -1.19$ V vs NHE) or Zn^0 ($E^\circ = -0.76$ V vs NHE),^[9b] which should limit deleterious reduction of $LNi^{II}(Ar)X$ species (Figure 2a), but it is still capable of reducing Co^{Pc} (*vide infra*) and the commonly utilized Ni catalyst $(dtbbpy)Ni^{II}Br_2$ (^{bpy}Ni ; $dtbbpy = 4,4'$ -di-*tert*-butyl-2,2'-bipyridine).^[7d]

To test our strategy, we performed CEC reactions between 4-*tert*-butylbromobenzene and 1-bromo-3-phenylpropane using 2.5 mol% Co^{Pc} , 120 mol% TDAE, and variable loadings of ^{bpy}Ni (Table 1). We selected 1,4-dioxane as the solvent due its ability to stabilize intermediates of the type $LNi^{II}(Ar)X$ (see SI), which is crucial for efficient radical capture in our envisioned pathway. Gratifyingly, we observed yields ranging from 53-84% depending on the loading of ^{bpy}Ni , with the highest yield obtained at 1 mol% loading (Entry 3). Our data also highlight how the reaction can be simply optimized by varying the relative loadings of ^{bpy}Ni and Co^{Pc} . When a ^{bpy}Ni loading below 1 mol% is utilized, reduced yields are obtained presumably because the rate of alkyl halide consumption is faster than the rate of aryl halide consumption as evidenced by the presence of unreacted aryl bromide when all of the alkyl bromide has been consumed (Entries 1 & 2). In contrast, when a ^{bpy}Ni loading above 1 mol% is utilized, lower yields are obtained because the rate of aryl halide consumption is faster than the rate of alkyl halide consumption as evidenced by the presence of unreacted alkyl bromide when all of the aryl bromide has been consumed (Entries 4 & 5). We suggest that these trends occur because *the aryl electrophile is primarily activated by*

Table 1. CEC of 4-*tert*-butyl-bromobenzene with 1-bromo-3-phenylpropane with varying amounts of ^{bpy}Ni .^{a,b}

Entry	^{bpy}Ni (X mol%)	Product (%)	Unreacted ArBr (%)	Unreacted AlkBr (%) ^c
1 ^d	0.1	55	29	3
2 ^d	0.5	68	22	6
3	1	84	6	<1
4 ^e	2.5	66	4	10
5 ^f	5	53	<1	30

^aReaction conditions: 1-bromo-4-*tert*-butylbenzene (0.0625 mmol), 1-bromo-3-phenylpropane (0.075 mmol), Co^{Pc} (0.0016 mmol), and TDAE (0.075 mmol) in 1,4-dioxane (0.5 mL) at 80 °C for 24 hours. ^bYields are reported as the average of two trials and were determined by integration of 1H NMR spectra against a standard (hexamethyl benzene). ^cYield of recovered 1-bromo-3-phenylpropane reported relative to 4-*tert*-butyl-bromobenzene. ^d48 h. ^e12 h. ^f4 h.

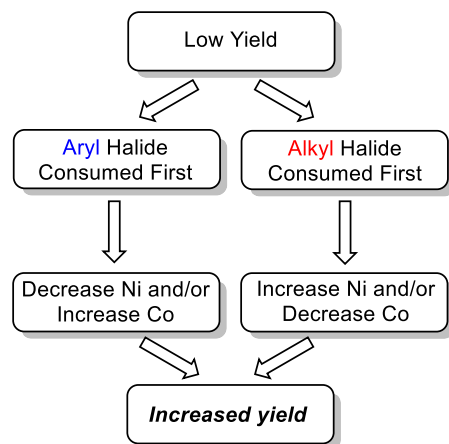
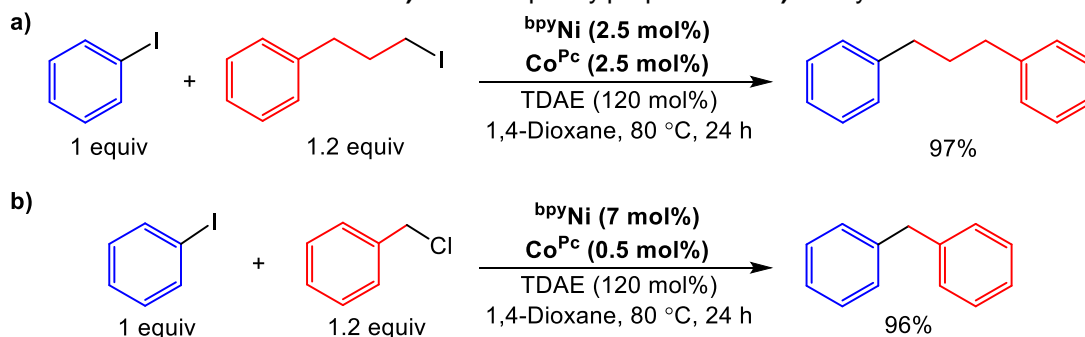


Figure 3. Optimization strategy for CEC reactions used in this work.

the Ni catalyst and the alkyl electrophile is primarily activated by the Co catalyst (*vide infra*). To obtain high yields, the rate of consumption of the aryl electrophile needs to be the same as the rate of consumption of the alkyl electrophile, which is accomplished by efficient alkyl radical capture at the $\text{LNi}^{\text{II}}(\text{Ar})\text{X}$ intermediate and can be easily controlled by the loadings of $^{\text{bpy}}\text{Ni}$ and Co^{Pc} (Figure 3). Further, this approach to optimization has not previously been utilized in reductive coupling reactions and provides potential advantages over methods where optimization is performed by empirical ligand and additive screening.

Using our method, we hypothesized that it would be possible to perform a diverse range of CEC reactions under the same conditions by modifying the loadings of $^{\text{bpy}}\text{Ni}$ and Co^{Pc} to match the reactivity of the aryl and alkyl halides, respectively. Specifically, we proposed that an aryl halide, such as iodobenzene, could be coupled with alkyl electrophiles of varying reactivities, such as unactivated alkyl iodides and highly activated benzyl chlorides, by optimizing the loadings of $^{\text{bpy}}\text{Ni}$ and Co^{Pc} under the same general conditions we employed to couple aryl bromides with alkyl bromides (Scheme 1). In agreement with this model, we were able to couple iodobenzene with 1-iodo-3-phenylpropane using 2.5 mol% $^{\text{bpy}}\text{Ni}$ and 2.5 mol% Co^{Pc} in 97% yield under the same reaction conditions utilized in Table 1 (Scheme 1a and see SI for optimization). Further, we can also couple iodobenzene with benzyl chloride using 7 mol% $^{\text{bpy}}\text{Ni}$ and 0.5 mol% Co^{Pc} in 96% yield (Scheme 1b and *vide infra* for optimization). We propose that the reason a much higher loading of $^{\text{bpy}}\text{Ni}$ to Co^{Pc} is required in the coupling of benzyl chlorides is because they are more easily activated than alkyl iodides by Co^{Pc} in catalysis. To our knowledge the ability to couple substrates with such diverse reactivity under the same general reaction conditions with high efficiency is unprecedented in $\text{C}(\text{sp}^2)\text{-C}(\text{sp}^3)$ CEC (*vide supra*).

Scheme 1. CEC of iodobenzene with **a)** 1-iodo-3-phenylpropane and **b)** benzyl chloride.



Substrate Scope for Aryl and Alkyl Bromide Coupling

Starting from the optimized conditions established for the coupling of 4-*tert*-butylbromobenzene and 1-bromo-3-phenylpropane we evaluated the substrate scope of the dual catalyzed method (Figure 4). Initially, we explored the coupling of a range of aryl bromides, as these are more synthetically valuable than aryl iodides, with 1-bromo-3-phenylpropane (or *N*-(3-bromopropyl)phthalimide^[17]). Our system exhibits a wide functional group tolerance, as demonstrated by the coupling of electronically diverse substrates (**4a-4c**) and substrates with reducible functional groups, such as nitriles (**4d**), sulfones (**4e**), aldehydes (**4f**), ketones (**4g**), esters (**4h**), and amides (**4i**). When 1-bromo-4-chlorobenzene (**4j**) is used as a substrate, our system is selective for coupling the aryl bromide, which offers opportunities for orthogonal reactivity with traditional cross-coupling reactions. Substrates with protic functionality, such as 4-bromophenethyl alcohol (**4k**) and 5-bromoindole (**4l**) could also be coupled in high yield, although 4-bromoaniline gives a reduced yield (see SI) and the more activated 4-iodoaniline (**4m**) is required to give a high yield. Mono-*ortho*-substituted substrates with moderate steric bulk (**4n** & **4o**) are also effectively coupled.

To show the generality and simplicity of our optimization protocol, we optimized each substrate to a yield greater than 75% by ¹H NMR spectroscopy using the procedure outlined in Figure 3 (see SI).^[18] Notably, the optimized conditions for each substrate deviate only slightly from our standard reaction conditions, indicating the ease by which high yields can be obtained. Further, good yields can be attained over more than an order of magnitude in ^{bpy}Ni or Co^{Pc} loadings (Tables 1 & 3). This suggests that a wide range of substrates may be successfully coupled under a standard set of conditions even without performing the simple catalyst loading optimization. Although many of substrates **4a-4o** have been coupled previously in the literature using heterogeneous Mn⁰ or Zn⁰ reductants, our system is the first to utilize a homogeneous reductant

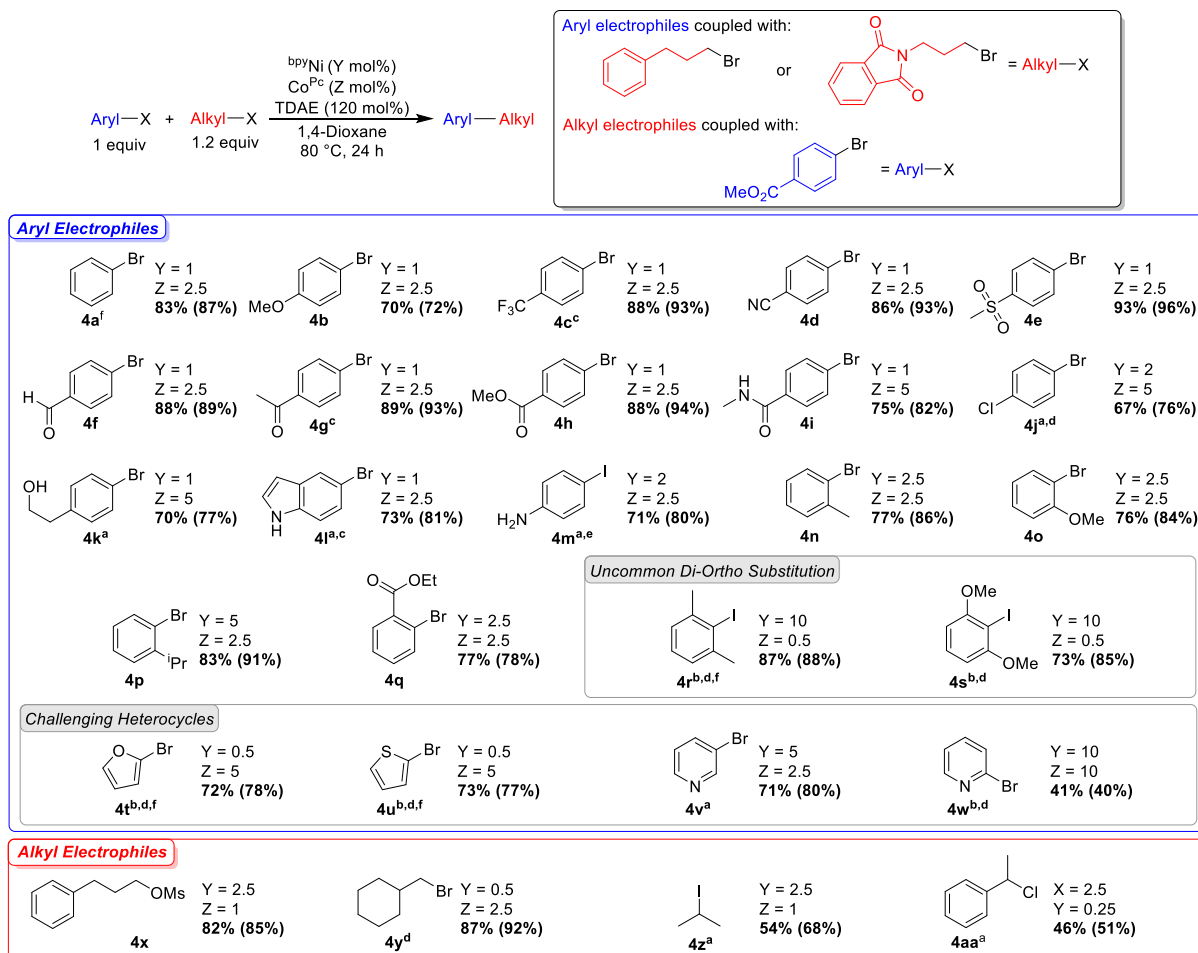


Figure 4. Substrate scope for CEC of aryl halides with alkyl halides or pseudohalides. Values outside of parentheses are isolated yields and values inside of parentheses are NMR yields, which were determined by integration of ^1H NMR spectra against a standard (hexamethylbenzene). ^a1.6 equiv. of alkyl substrate, 140 mol% TDAE. ^b2.0 equiv. of alkyl substrate, 160 mol% TDAE. ^c36 h. ^d48 h. ^e1-iodo-3-phenylpropane used as alkyl substrate. ^fN-(3-bromopropyl)phthalimide used as alkyl substrate.

with such a broad substrate scope, which provides significant practical advantages (*vide supra*). Further, our system achieves high yields using lower than typical catalyst loadings, only uses commercially available reaction components, and does not require inscrutable additives for any of the substrates. All of these factors are advantageous for translating our results to different substrate classes.

Another significant advantage of our system is that it is compatible with some substrates that have not been traditionally used in CEC. For example, aryl halides with sterically demanding substituents in the *ortho*-position are a challenging class of substrates in conventional CEC. This is likely because oxidative addition of the sterically hindered aryl electrophile is difficult relative to the activation of the alkyl halide coupling partner, which results in incompatible rates of

substrate activation in catalysis. We hypothesized that our system could overcome this challenge through modulation of catalyst loadings (*vide supra*). Consistent with this proposal, mono-*ortho*-substituted aryl bromides with significant steric bulk (**4p** & **4q**) could be coupled in high yield using increased loadings of ^{bpy}Ni compared to reactions between bromobenzene (**4a**) and 1-bromo-3-phenylpropane. In particular, the coupling of **4q** is significant, as Weix *et al.* previously reported that it was difficult to couple aryl halides with bulky *ortho*-directing groups.^[2] By further increasing the loading of ^{bpy}Ni and decreasing the loading of Co^{Pc}, this strategy could be extended to di-*ortho*-substituted aryl iodides (**4r** & **4s**), for which there is virtually no precedent in the CEC literature.^[2,19]

Heteroaryl halides are important substrates because heteroaromatic groups are common structures in medicinal chemistry,^[20] but are traditionally difficult substrates in CEC. In particular, it has proven challenging to use 2-halofurans and 2-halothiophenes as substrates in CEC, especially when there is no substitution in the 5-position.^[1j,12f] Our system can couple several heteroaryl substrates in high yield, including 2-bromofuran (**4t**), 2-bromothiophene (**4u**), and 3-bromopyridine (**4v**). Importantly, the same optimization strategy that was utilized for simple arenes can be applied to heteroaryl substrates to overcome potential challenges associated with substrates binding to catalysts (see SI). We note, however, that we can only couple 2-bromopyridine (**4w**) in 41% yield using 10 mol% ^{bpy}Ni and 10 mol% of Co^{Pc}.

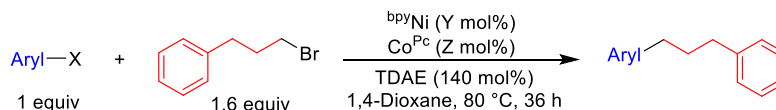
The alkyl electrophile scope was examined using the same optimization strategy that was utilized for exploring the scope of the aryl electrophile. Primary benzyl chlorides (*vide supra*) as well as unactivated primary alkyl iodides (*vide supra*) and bromides (**4a-4w**) can be readily coupled under our reaction conditions. However, Co^{Pc} activates alkyl substrates via an S_N2 mechanism,^[21] which differentiates it from conventional CEC systems that activate alkyl substrates through a radical pathway.^[7a] One advantage of this difference is that our system can couple primary alkyl mesylates, such as 3-phenylpropyl methanesulfonate (**4x**), with methyl 4-bromobenzoate in high yield. This result is notable because alkyl mesylates can be readily generated *in situ* from the corresponding alcohols,^[15b,22] which are abundant and diverse building blocks that are commonly used in pharmaceutical research.^[14a] In contrast, while substrates with some steric bulk at the α -carbon of alkyl bromides, such as (bromomethyl)cyclohexane (**4y**), can be coupled with methyl 4-bromobenzoate, no product is generated when either neopentyl bromide or iodide are used as substrates (see SI). Similarly, branched secondary alkyl halides such as

iodides (**4z**) and benzyl chlorides (**4aa**) can be coupled in moderate yields, but branched secondary alkyl bromides and iodocyclohexane are unreactive (see SI). In a subsequent section we explore the types of functionalized alkyl bromides and iodides and benzyl chlorides that are compatible with our system.

Applications to Medicinal Chemistry

Despite the significant attention that C(sp²)–C(sp³) cross-electrophile reactions have received over the past decade, it remains difficult to translate this methodology to complex, medicinally relevant substrates.^[6,23] Given the high value of compounds containing alkylated arene groups in the development and study of pharmaceuticals, a robust and generalizable method to form C(sp²)–C(sp³) linkages with medicinally relevant substrates would be valuable for drug discovery.^[24] To this end, we tested the compatibility of our reaction conditions with aryl halides from the MSD Aryl Halide Informer Library, as these compounds were at one time intermediates in drug discovery programs.^[25] Using standard high-throughput experimentation (HTE) techniques, we were able to rapidly optimize the reactions by varying the catalyst loadings for eight substrates in a single experiment using a standard 96 well reaction plate (see SI).^[26] Aryl halides **5a–5h** were successfully coupled in moderate to high yields (42–91% yield by ¹H NMR spectroscopy) with 1-bromo-3-phenylpropane using catalyst loadings between 0.5 and 5 mol% of both ^{bpy}Ni and Co^{Pc} without altering any other reaction parameters (Figure 5). The range of functional groups present in these aryl halides highlights the power of our method. For example, successful reactions were observed in the presence of esters, amides, sulfones, alcohols, triazoles, thiophenes, pyridines, and both free and protected amines among many other functional groups. Notably, the challenging di-*ortho* substituted aryl halide containing a pendant primary amine, **5i**, was coupled in lower, but still medicinally useful, yield (22% by ¹H NMR spectroscopy) with 1-iodo-3-phenylpropane. Additionally, we isolated the product from the reaction of **5a** with 1-bromo-3-phenylpropane in good yield (72%) and demonstrated that the reaction is scalable through a coupling using 3 mmol of **5f** (see SI) as proof-of-principle that our method will enable the generation of compounds for drug discovery.

To further investigate the potential applicability of our reaction conditions to C(sp²)–C(sp³) bond formation in molecules relevant to drug discovery, we performed a parallel library synthesis via late-stage diversification of aryl halide **5f**, a precursor to oxazolidinone antibacterials, with



Medically Relevant Aryl Electrophiles

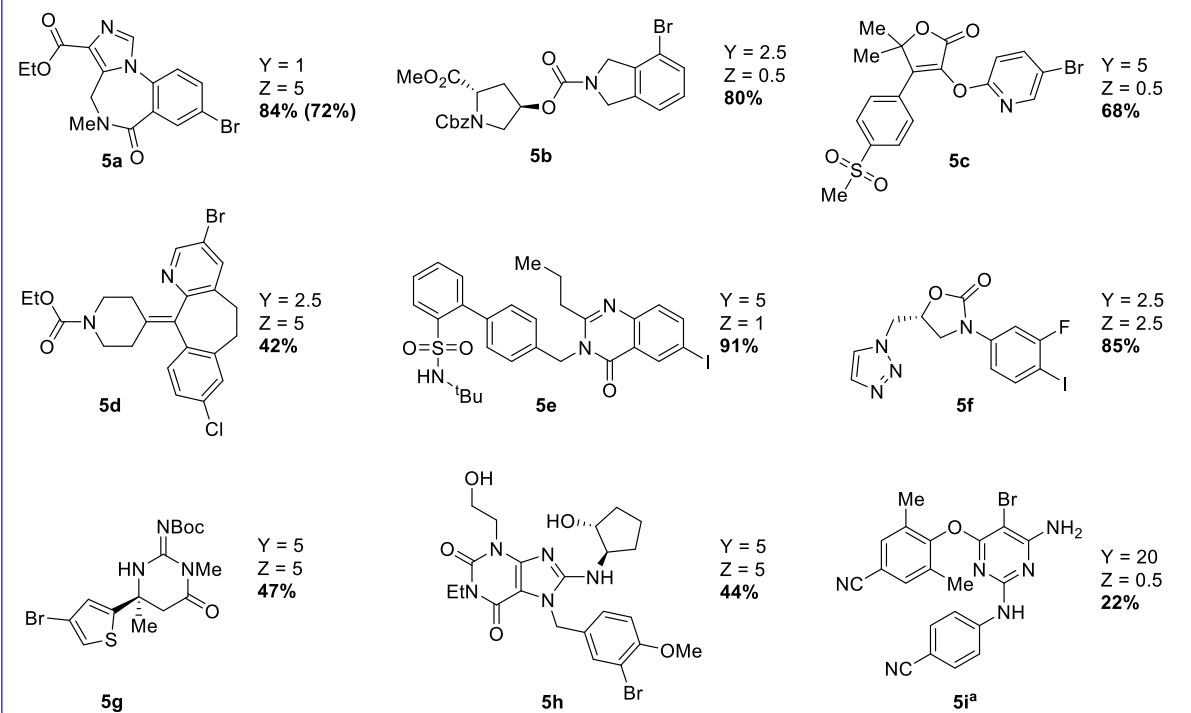


Figure 5. Substrate scope for CEC between examples from the MSD Aryl Halide Informer Library and 1-bromo-3-phenylpropane. Values outside of parentheses are NMR yields, which were determined by integration of ^1H NMR spectra against a standard (hexamethylbenzene), and values inside of parentheses are isolated yields. ^a2 equivalents of 1-iodo-3-phenylpropane alkyl substrate, 160 mol% TDAE, 48 h.

different alkyl halides (Figure 6).^[27] First, we optimized the loadings of bpyNi and Co^{Pc} for the reactions of **5f** with a benzylic chloride, an alkyl iodide, and an alkyl bromide (see SI). We then used the optimized conditions for each class of alkyl halide to evaluate the coupling of a series of functionalized derivatives with **5f** using HTE techniques (see SI). For example, all primary alkyl bromides used in the experiment were coupled under the optimal conditions determined for the coupling of **5f** with 1-bromo-3-phenylpropane (**6r**). Using our strategy, we observed that 25 out of 32 products were formed in greater than 10% conversion, an overall 78% success rate. A range of functionalized primary benzyl chloride electrophiles could be coupled, including substrates containing a tetrazole (**6b**) or thiophene (**6d**) ring, or a protic amide substituent (**6f**). Further, various primary alkyl iodide and bromide electrophiles could be coupled, such as substrates containing an unprotected indole (**6o**) and terminal alkenes (**6x**), which are susceptible to Giese-

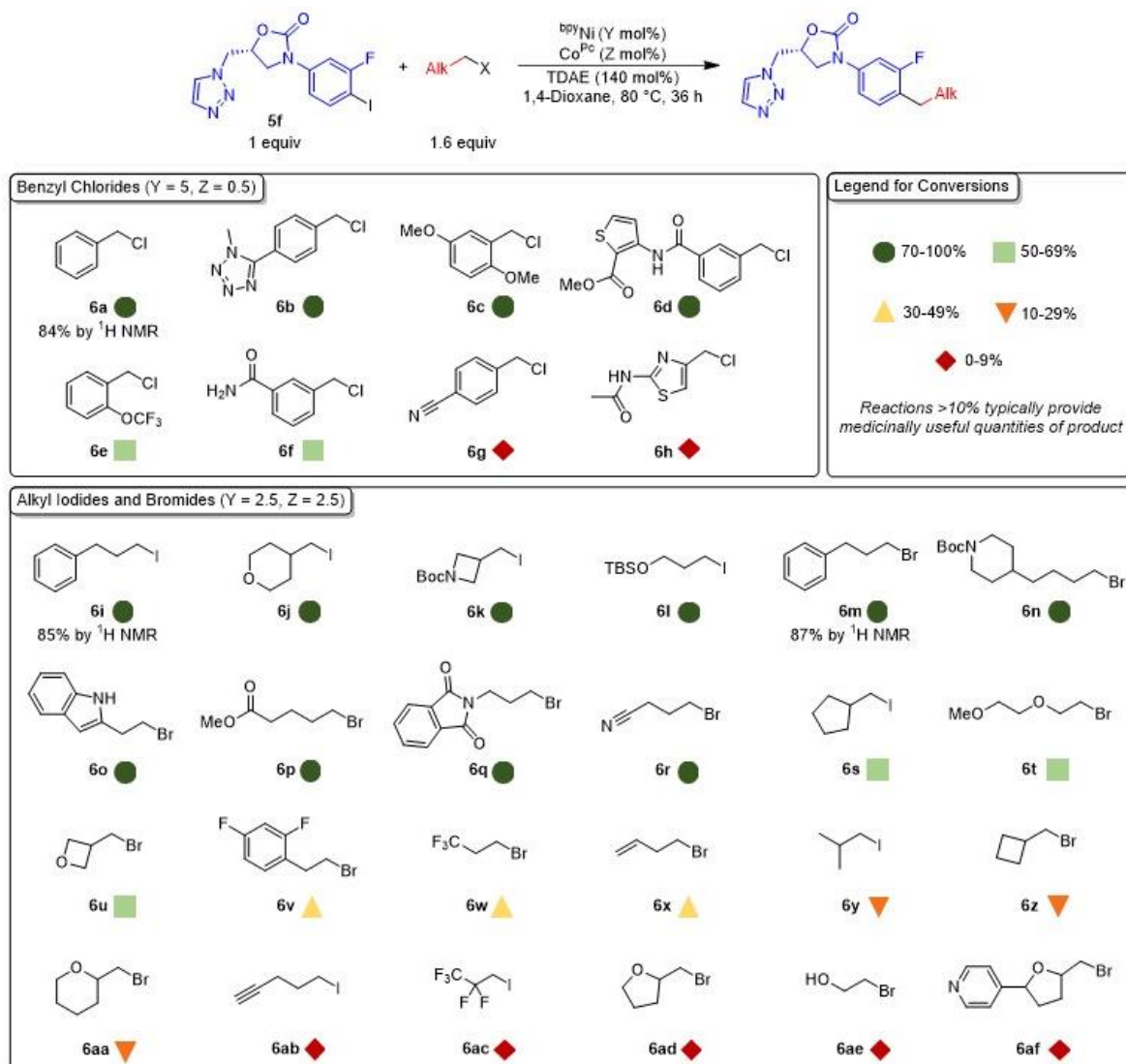


Figure 6. CEC between **5f** and a series of benzylic chlorides, alkyl iodides, and alkyl bromides. Values are reported as the conversion to product relative to all known species derived from **5f** determined by UV-Visible spectroscopy (see SI for details). NMR yields were determined by integration of ^1H NMR spectra against a standard (hexamethylbenzene).

type additions in related reactions.^[16b,16c] Additionally, heterocyclic rings, which are prevalent in medicinal chemistry, such as azetidine (**6k**), piperidine (**6n**), and cyclic ethers (**6j**, **6u**, **6aa**) are compatible with our method.^[28] Overall, this experiment shows that our methodology can tolerate a large number of functional groups on the alkyl halide substrate. *It also shows that the optimized reactions conditions obtained for an individual aryl halide substrate can be readily translated to a broad range of alkyl halides without reoptimization, which enables efficient parallel library synthesis and should be valuable in medicinal chemistry.*

Apart from the improved substrate scope, our system offers practical advantages for

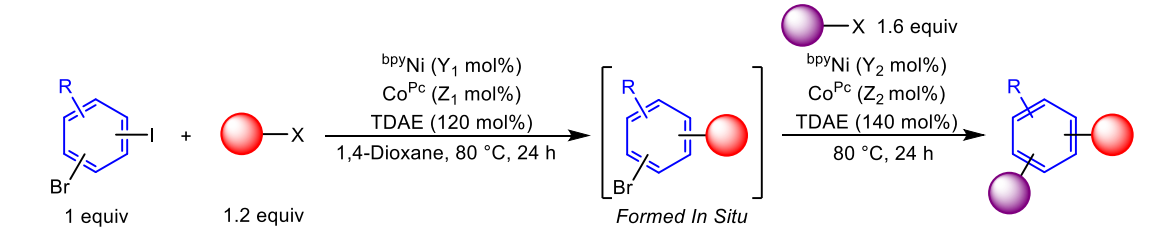
performing CEC reactions in a medicinal chemistry setting compared to existing methodology. (i) Experimental setup is straightforward because all reactions utilize the same reaction components under the same reaction conditions. In contrast, conventional CEC protocols operate within an almost indeterminate optimization space as various reaction parameters, such as ancillary ligand, solvent, and inscrutable additives, are all typically individually optimized for each substrate. (ii) It is compatible with a wide range of solvents, including green solvents (see SI), which assists in finding conditions where substrates are fully soluble and reduces environmental impact.^[29] (iii) It utilizes a homogeneous reductant as opposed to a heterogeneous reductant, which is important for scale-up.

Three-Component Coupling Reactions

Reactions that enable the modification of simple aryl rings in a modular fashion are valuable for the creation of diverse libraries of compounds, which often facilitate the discovery of lead structures in medicinal chemistry.^[30] To this end, readily accessible dihaloarenes represent promising starting materials from which to directly and efficiently construct a wide range of structures.^[31] Although there are currently numerous methods for the sequential introduction of aryl groups into dihaloarenes via standard $C(sp^2)-C(sp^2)$ cross-coupling reactions,^[30-32] there is only a single report that demonstrates the sequential introduction of alkyl groups,^[33] and no reports that utilize CEC. Using our method, we performed one-pot three-component CEC reactions involving the sequential addition of two alkyl halides to an iodo(bromo)arene (Table 2). These reactions take advantage of the increased reactivity of iodoarenes over bromoarenes. Initially, upon completion of a reaction between 1-bromo-4-iodo-2-methoxybenzene and benzyl chloride to selectively form the monoalkylated bromoarene product, we added ethyl 4-bromobutyrate and TDAE and continued the reaction. The *in situ* generated bromoarene product underwent a second CEC with the alkyl bromide, without the need to add additional amounts of either catalyst, suggesting that there is no catalyst death either during or upon completion of the initial alkylation (Entry 1, see SI for optimization). Across the two steps, the isolated yield for the bis-alkylated product was 82%. Under the same reaction conditions, 1-bromo-2-iodo-4-methylbenzene can also be coupled with benzyl chloride and ethyl 4-bromobenzoate in 91% yield (Entry 2).

Using the sequential addition strategy, reactions that require different catalyst loadings for the first and second coupling can be performed by introducing additional equivalents of either catalyst after the completion of the initial coupling. Through this method, 1-iodo-3-phenylpropane

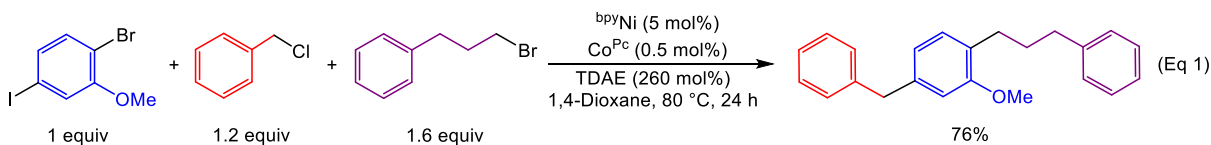
Table 2. One-pot three-component CEC of bromo(iodo)arenes with alkyl halides.^a

						
Entry				Y ₁ , Z ₁ (mol%)	Y ₂ , Z ₂ (mol%)	Yield (%)
1				5, 0.5	0, 0	82 (88)
2				5, 0.5	0, 0	91 (95)
3 ^b				1, 2.5	4, 0	84 (91)
4				2.5, 0.1	0, 5	70 (76)

^aYields outside of parentheses are isolated yields and yields inside of parentheses are NMR yields, which were determined by integration of ¹H NMR spectra against a standard (hexamethylbenzene). ^b1.1 equivalents of 1-iodo-3-phenylpropane and 110 mol% TDAE used in initial coupling.

and ethyl 4-bromobutyrate could be sequentially coupled with 1-bromo-4-iodo-2-methoxybenzene in 84% yield through the addition of 4 mol% ^{bpy}Ni after the initial coupling (Entry 3). Additionally, an unsubstituted bromo(iodo)arene, 1-bromo-4-iodobenzene, was coupled with benzyl chloride and ethyl 4-bromobutyrate in 70% yield through the addition of 5 mol% Co^{Pc} after the initial coupling (Entry 4). Further, in some cases, it is possible to perform these transformations in a single-step, as demonstrated by the coupling of 1-bromo-4-iodo-2-methoxybenzene with benzyl chloride and 1-bromo-3-phenylpropane with high regioselectivity to generate the desired product in 76% yield (see Eq 1 and SI for further details), which extends the practicality of the method. The examples presented here serve as proof-of-principle that our dual catalytic platform can be used for the one-pot construction of multiple C(sp²)–C(sp³) bonds using readily available bromo(iodo)arene and alkyl halide starting materials and highlight the potential utility of our CEC strategy towards the discovery of novel reactions. *Our method is a significant advancement over*

existing methodology for dialkylolation of bromo(iodo)arenes, which cannot be performed in one-pot and require the use of preformed organometallic nucleophiles, such as alkylbis(catecholato)silicates, that are not commercially available and generally require multi-step syntheses.^[33]



Preliminary Mechanistic Investigation

To gain further insight into the reaction mechanism, we explored a CEC reaction between the activated substrates phenyl iodide and benzyl chloride (Table 3). In the absence of Co^{Pc} , the reaction proceeded in 40% yield (Entry 1). Significant quantities of benzyl chloride were still present at the end of the reaction, showing that alkyl halide consumption is slow relative to aryl halide consumption. Notably, Ni is able to engage the alkyl electrophile to promote catalysis in the absence of Co^{Pc} with the highly activated benzyl chloride substrate. In contrast, when reactions are performed with weakly activated alkyl halides, such as primary alkyl bromides, no product formation is observed in the absence of Co^{Pc} (see SI). These observations align with our hypothesis and suggest that $^{\text{bpy}}\text{Ni}$ primarily activates the aryl electrophile, while Co^{Pc} primarily activates the alkyl electrophile.

The addition of varying amounts of Co^{Pc} into the reaction results in clear trends, which mirror those observed in Table 1. We propose that the reaction can be broken down into three distinct regimes which are related to the relative loadings of $^{\text{bpy}}\text{Ni}$ and Co^{Pc} . Regime 1 occurs when the rate of radical formation and capture at $(\text{dtbbpy})\text{Ni}^{\text{II}}(\text{Ar})\text{X}$ is slow relative to the rate of decomposition of $(\text{dtbbpy})\text{Ni}^{\text{II}}(\text{Ar})\text{X}$, which deleteriously consumes the aryl halide to produce biaryl and protodehalogenated products (Figure 2).^[12c] Further, unreacted alkyl halide remains after all of the aryl electrophile has been consumed (Entry 2). Regime 2 occurs when the rate of alkyl radical formation and capture at $(\text{dtbbpy})\text{Ni}^{\text{II}}(\text{Ar})\text{X}$ is optimal relative to the formation and decomposition of $(\text{dtbbpy})\text{Ni}^{\text{II}}(\text{Ar})\text{X}$. In this regime, high product yields are observed and no unreacted starting material remains at the end of the reaction (Entries 3-6). Regime 3 occurs when alkyl radical formation is faster than the generation of $(\text{dtbbpy})\text{Ni}^{\text{II}}(\text{Ar})\text{X}$, and, as a result, the alkyl radical decomposes before it can be trapped by Ni and unreacted aryl halide remains after the alkyl halide has been consumed (Entries 7 & 8). The same trends are also obtained when the loading of

^{bpy}Ni is varied at a fixed loading of Co^{Pc} in the coupling of iodobenzene with benzyl chloride (see SI).

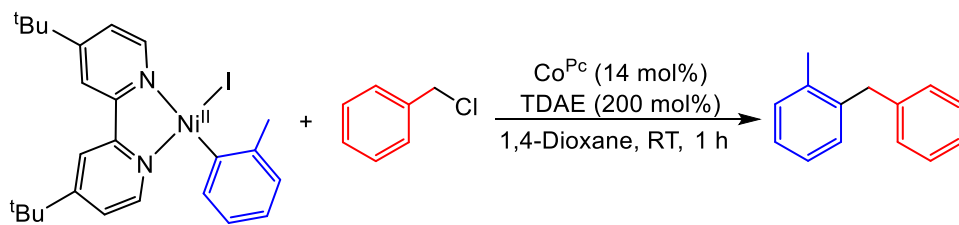
Table 3. CEC of iodobenzene and benzyl chloride with varying amounts of Co^{Pc}.^{a,b}

Entry	Co ^{Pc} (X mol%)	Product (%)	Unreacted Arl (%)	Biphenyl (%)	Unreacted BnCl (%) ^c	Catalytic Regime
1	0	40	3	21	28	1
2	0.01	77	<1	6	16	
3	0.1	90	5	2	4	2
4	0.25	87	4	2	<1	
5	0.5	96	3	1	<1	
6	1	90	4	2	<1	
7	2.5	75	14	1	<1	3
8	5	62	21	1	<1	

^aReaction conditions: iodobenzene (0.0625 mmol), benzyl chloride (0.075 mmol), ^{bpy}Ni (0.0044 mmol), and TDAE (0.075 mmol) in 1,4-dioxane (0.5 mL) at 80 °C for 24 h. ^bYields are reported as the average of two trials and were determined by integration of ¹H NMR spectra against a standard (hexamethylbenzene). Yield of recovered benzyl chloride reported relative to iodobenzene loading.

To further explore the proposed interplay between Ni and Co in catalysis, we performed a stoichiometric reaction between (dtbbpy)Ni^{II}(*o*-tol)I and benzyl chloride in the presence of excess TDAE and catalytic amounts of Co^{Pc} (Table 4). This resulted in the generation of the diarylmethane cross-product, (*o*-tolyl)(phenyl)methane, in 76% yield (Entry 1). No product formation, however, was observed without Co^{Pc} in either the presence or absence of TDAE (Entries 2 & 3), consistent with our hypothesis that Co primarily activates the alkyl electrophile in catalysis. Furthermore, the use of stoichiometric Co^{Pc} without TDAE also yielded no cross-product (Entry 4), suggesting that the activation of alkyl electrophiles occurs at a reduced Co center. In agreement with this proposal, the reduction potential of TDAE^{2+/0} is more negative than that of the Co^{II/I} couple of Co^{Pc}.^[34] Low-valent Co complexes similar to [Co^I(Pc)]⁻ are known to undergo oxidative addition with alkyl halides through an S_N2 mechanism to form Co^{III}(Pc)(Alk) species.^[21] In turn, these high valent Co^{III} complexes can undergo homolysis of the Co^{III}–Alk bond, which produces an alkyl radical and regenerates Co^{Pc}.^[35] Further support for the proposal that Co^{Pc} is capable of generating alkyl radicals in the presence of TDAE was obtained by performing an analogous radical trapping experiment using 2,2,6,6-tetramethyl-1-piperidinyloxy (TEMPO) as the radical acceptor instead of (dtbbpy)Ni^{II}(*o*-tol)I.^[36] In a similar fashion to our experiment with (dtbbpy)Ni^{II}(*o*-tol)I, trapping

Table 4. Reaction of (dtbbpy)Ni^{II}(*o*-tol)I with benzyl chloride under various conditions.^{a,b}



Entry	Deviation From Conditions	Yield (%)
1	None	76
2	No Co(Pc)	<1
3	No Co(Pc) & no TDAE	<1
4	100 mol% Co(Pc) & no TDAE	<1

^aReaction Conditions: (dtbbpy)Ni^{II}(*o*-tol)I (0.0132 mmol), benzyl chloride (0.0264 mmol), Co^{Pc} (0.00185 mmol), TDAE (0.0264 mmol), in 1,4-dioxane (1.5 mL) at RT for 1 h. ^bYields are reported as the average of two trials and were determined by integration of ¹H NMR spectra against a standard (hexamethylbenzene).

of the benzyl radical by TEMPO is only observed in the presence of excess TDAE and catalytic amounts of Co^{Pc} (see SI). Altogether, these experiments provide evidence for the Co-mediated generation of free radicals from an alkyl electrophile and subsequent radical capture by (dtbbpy)Ni^{II}(Ar)X species in catalysis.

On the basis of our experimental results, we propose a mechanism containing two cycles for the coupling of phenyl iodide and benzyl chloride catalyzed by ^{bpv}Ni and Co^{Pc} (Figure 7). Initially, the ^{bpv}Ni precatalyst is reduced by TDAE to generate a catalytically active Ni⁰ species. The Ni⁰ species undergoes oxidative addition with an aryl halide to form a (dtbbpy)Ni^{II}(Ar)X intermediate, which is likely the resting state of the Ni catalyst. Subsequently, the (dtbbpy)Ni^{II}(Ar)X intermediate captures an alkyl radical, which is liberated upon the homolysis of

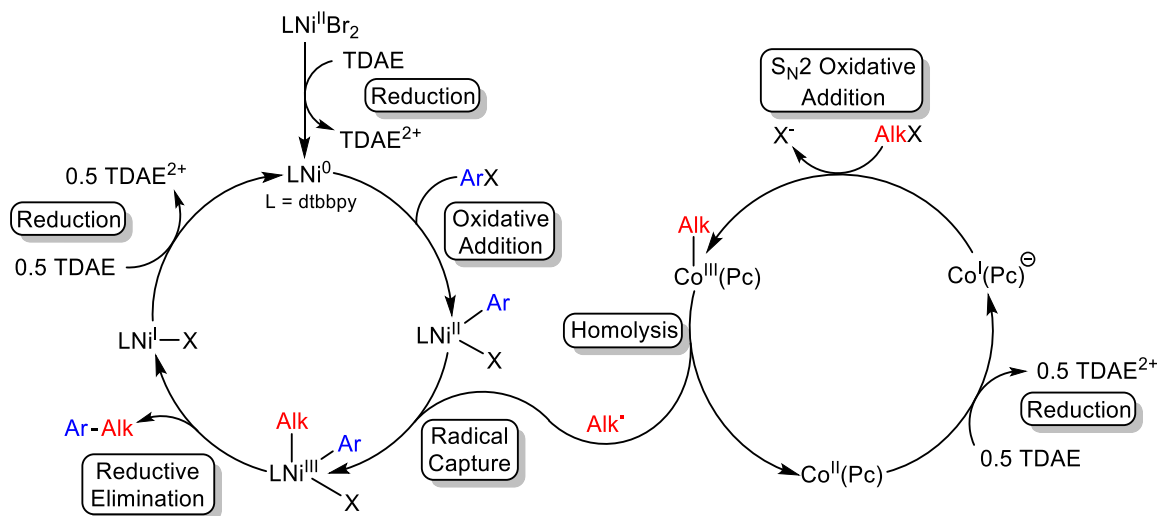


Figure 7. Proposed mechanism for the CEC of aryl and alkyl halides in the presence of Co^{Pc} and TDAE.

a $\text{Co}^{\text{III}}(\text{Pc})(\text{Alk})$ species. The $\text{Co}^{\text{III}}(\text{Pc})(\text{Alk})$ species is generated in an independent catalytic cycle through initial reduction of Co^{Pc} to form an anionic $[\text{Co}^{\text{I}}(\text{Pc})]^-$ complex, which can react with an alkyl halide via an $\text{S}_{\text{N}}2$ mechanism. Following radical capture at $(\text{dtbbpy})\text{Ni}^{\text{II}}(\text{Ar})\text{X}$, a putative $(\text{dtbbpy})\text{Ni}^{\text{III}}(\text{Ar})(\text{Alk})\text{X}$ species is produced, which rapidly reductively eliminates at the Ni^{III} center to liberate the product and form a $(\text{dtbbpy})\text{Ni}^{\text{I}}\text{X}$ species. Finally, we propose that the $(\text{dtbbpy})\text{Ni}^{\text{I}}\text{X}$ species is reduced by TDAE to regenerate Ni^0 , closing the catalytic cycle. Further mechanistic work to explore all of the potential roles of Ni^{I} species is ongoing.

Conclusions

We have developed a novel system for $\text{C}(\text{sp}^2)\text{-C}(\text{sp}^3)$ CEC reactions of aryl and alkyl halides. Our system uses a Ni and Co dual catalytic platform in tandem with a relatively weak homogenous reductant to ensure that the key $\text{LNi}^{\text{II}}(\text{Ar})\text{X}$ intermediate undergoes on-cycle reactions. Our system is able to efficiently couple a wide a range of substrates including heteroaryl halides, di-*ortho*-substituted aryl iodides, drug-like aryl halides and functionally diverse alkyl halides, all of which are rarely compatible with traditional methods for $\text{C}(\text{sp}^2)\text{-C}(\text{sp}^3)$ CEC. Additionally, we are able to perform a series of novel one-pot, three-component dialkylations of bromo(iodo)arenes. Given the importance of $\text{LNi}^{\text{II}}(\text{Ar})\text{X}$ intermediates in Ni-catalyzed radical coupling reactions, we suggest that our strategy of selecting reaction conditions that stabilize this complex and allow for controlled generation of alkyl radicals are relevant to a large number of other reactions.

Acknowledgements

NH acknowledges support from the NIHGMs under Award Number R01GM120162. We thank Professor Jon Ellman and Dr. Louis-Charles Campeau for valuable discussions. We also thank Sr. Scientist Scott Borges, May Ann Desaca, and Sr. Scientist Tao Meng for purification support, Assoc. Scientist Ming Wang for assistance with high-throughput analytical sample processing, and Dr. Fabian Menges for help with mass spectrometry.

Supporting information

Additional information about selected experiments, NMR spectra, and other details are available via the Internet.

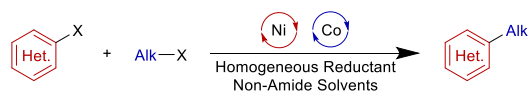
References

- [1] For leading references, see: (a) D. A. Everson, R. Shrestha, D. J. Weix, *J. Am. Chem. Soc.* **2010**, *132*, 920; (b) D. A. Everson, B. A. Jones, D. J. Weix, *J. Am. Chem. Soc.* **2012**, *134*, 6146; (c) A. C. Wotal, D. J. Weix, *Org. Lett.* **2012**, *14*, 1476; (d) D. A. Everson, D. J. Weix, *J. Org. Chem.* **2014**, *79*, 4793; (e) C. Zhao, X. Jia, X. Wang, H. Gong, *J. Am. Chem. Soc.* **2014**, *136*, 17645; (f) J. Gu, X. Wang, W. Xue, H. Gong, *Org. Chem. Front.* **2015**, *2*, 1411; (g) D. J. Weix, *Acc. Chem. Res.* **2015**, *48*, 1767; (h) Y. Zhao, D. J. Weix, *J. Am. Chem. Soc.* **2015**, *137*, 3237; (i) K. M. Arendt, A. G. Doyle, *Angew. Chem. Int. Ed.* **2015**, *54*, 9876; (j) N. T. Kadunce, S. E. Reisman, *J. Am. Chem. Soc.* **2015**, *137*, 10480; (k) G. A. Molander, K. M. Traister, B. T. O'Neill, *J. Org. Chem.* **2015**, *80*, 2907; (l) X. Wang, S. Wang, W. Xue, H. Gong, *J. Am. Chem. Soc.* **2015**, *137*, 11562; (m) L. Hu, X. Liu, X. Liao, *Angew. Chem. Int. Ed.* **2016**, *55*, 9743; (n) K. A. Johnson, S. Biswas, D. J. Weix, *Chem. Eur. J.* **2016**, *22*, 7399; (o) M. O. Konev, L. E. Hanna, E. R. Jarvo, *Angew. Chem. Int. Ed.* **2016**, *55*, 6730; (p) F. Chen, K. Chen, Y. Zhang, Y. He, Y.-M. Wang, S. Zhu, *J. Am. Chem. Soc.* **2017**, *139*, 13929; (q) K. E. Poremba, N. T. Kadunce, N. Suzuki, A. H. Cherney, S. E. Reisman, *J. Am. Chem. Soc.* **2017**, *139*, 5684; (r) B. P. Woods, M. Orlandi, C.-Y. Huang, M. S. Sigman, A. G. Doyle, *J. Am. Chem. Soc.* **2017**, *139*, 5688; (s) P. Schneider, G. Schneider, *Angew. Chem. Int. Ed.* **2017**, *56*, 7971; (t) L. Peng, Y. Li, Y. Li, W. Wang, H. Pang, G. Yin, *ACS Catal.* **2018**, *8*, 310; (u) X. Wang, G. Ma, Y. Peng, C. E. Pitsch, B. J. Moll, T. D. Ly, X. Wang, H. Gong, *J. Am. Chem. Soc.* **2018**, *140*, 14490; (v) S. Ni, C.-X. Li, Y. Mao, J. Han, Y. Wang, H. Yan, Y. Pan, *Sci. Adv.* **2019**, *5*, 9516; (w) Y. Ye, H. Chen, J. L. Sessler, H. Gong, *J. Am. Chem. Soc.* **2019**, *141*, 820; (x) H. Yue, C. Zhu, L. Shen, Q. Geng, K. J. Hock, T. Yuan, L. Cavallo, M. Rueping, *Chem. Sci.* **2019**, *10*, 4430.
- [2] E. C. Hansen, D. J. Pedro, A. C. Wotal, N. J. Gower, J. D. Nelson, S. Caron, D. J. Weix, *Nature Chem.* **2016**, *8*, 1126.
- [3] E. S. Isbrandt, R. J. Sullivan, S. G. Newman, *Angew. Chem. Int. Ed.* **2019**, *58*, 7180.
- [4] (a) C.-S. Yan, Y. Peng, X.-B. Xu, Y.-W. Wang, *Chem. Eur. J.* **2012**, *18*, 6039; (b) G. A. Molander, K. M. Traister, B. T. O'Neill, *J. Org. Chem.* **2014**, *79*, 5771; (c) L. L. Anka-Lufford, K. M. M. Huihui, N. J. Gower, L. K. G. Ackerman, D. J. Weix, *Chem. Eur. J.* **2016**, *22*, 11564; (d) J. Zhang, G. Lu, J. Xu, H. Sun, Q. Shen, *Org. Lett.* **2016**, *18*, 2860.
- [5] E. C. Hansen, C. Li, S. Yang, D. Pedro, D. J. Weix, *J. Org. Chem.* **2017**, *82*, 7085.
- [6] (a) J. M. E. Hughes, P. S. Fier, *Org. Lett.* **2019**, *21*, 5650; (b) K. M. Mennie, B. A. Vara, S. M. Levi, *Org. Lett.* **2020**, *22*, 556.
- [7] (a) S. Biswas, D. J. Weix, *J. Am. Chem. Soc.* **2013**, *135*, 16192; (b) J. B. Diccianni, J. Katigbak, C. Hu, T. Diao, *J. Am. Chem. Soc.* **2019**, *141*, 1788; (c) Q. Lin, T. Diao, *J. Am. Chem. Soc.* **2019**, *141*, 17937; (d) M. Mohadjer Beromi, G. W. Brudvig, N. Hazari, H. M. C. Lant, B. Q. Mercado, *Angew. Chem. Int. Ed.* **2019**, *58*, 6094.
- [8] K. Osakada, T. Yamamoto, *Coord. Chem. Rev.* **2000**, *198*, 379.
- [9] (a) M. Mohadjer Beromi, G. Banerjee, G. W. Brudvig, N. Hazari, B. Q. Mercado, *ACS Catal.* **2018**, *8*, 2526; (b) D. J. Charboneau, G. W. Brudvig, N. Hazari, H. M. C. Lant, A. K. Saydjari, *ACS Catal.* **2019**, *9*, 3228.
- [10] For representative examples, see: (a) R. L. Hartman, *Org. Proc. Res. Devel.* **2012**, *16*, 870; (b) K. F. Jensen, *AIChE J.* **2017**, *63*, 858; (c) D. Perera, J. W. Tucker, S. Brahmabhatt, C. J. Helal, A. Chong, W. Farrell, P. Richardson, N. W. Sach, *Science* **2018**, *359*, 429; (d) R. J. Perkins, A. J. Hughes, D. J. Weix, E. C. Hansen, *Org. Proc. Res. Devel.* **2019**, *23*, 1746.
- [11] L. Huang, L. K. G. Ackerman, K. Kang, A. M. Parsons, D. J. Weix, *J. Am. Chem. Soc.* **2019**, *141*, 10978.
- [12] Systems that utilize light, via a photocatalyst, or electricity have been reported. While these methods address some limitations associated with heterogeneous reductants, they have other practical challenges. For selected systems, see: (a) P. Zhang, C. C. Le, D. W. C. MacMillan, *J. Am. Chem. Soc.* **2016**, *138*, 8084; (b) R. J. Perkins, D. J. Pedro, E. C. Hansen, *Org. Lett.* **2017**, *19*, 3755; (c) H. Li, C. P. Breen, H. Seo, T. F. Jamison, Y.-Q. Fang, M. M. Bio, *Org. Lett.* **2018**, *20*, 1338; (d) T. J. DeLano, S. E. Reisman, *ACS Catal.* **2019**, *9*, 6751; (e) R. Martin-Montero, V. R. Yatham, H. Yin, J. Davies, R. Martin, *Org. Lett.* **2019**, *21*, 2947; (f) J. Yi, S. O. Badir, L. M. Kammer, M. Ribagorda, G. A. Molander, *Org. Lett.* **2019**, *21*, 3346; (g) Z. G. Brill, C. B. Ritts, U. F. Mansoor, N. Sciammetta, *Org. Lett.* **2020**, *22*, 410; (h) B. L. Truesdell, T. B. Hamby, C. S. Sevov, *J. Am. Chem. Soc.* **2020**, *142*, 5884.
- [13] For select examples, see: (a) J. C. Tellis, D. N. Primer, G. A. Molander, *Science* **2014**, *345*, 433; (b) Z. Zuo, D. T. Ahneman, L. Chu, J. A. Terrett, A. G. Doyle, D. W. C. MacMillan, *Science* **2014**, *345*, 437; (c) S. A. Green, T. R. Huffman, R. O. McCourt, V. van der Puy, R. A. Shenvi, *J. Am. Chem. Soc.* **2019**, *141*, 7709; (d) H. Yin, G. C. Fu, *J. Am. Chem. Soc.* **2019**, *141*, 15433.
- [14] (a) K. Komeyama, R. Ohata, S. Kiguchi, I. Osaka, *Chem. Commun.* **2017**, *53*, 6401; (b) K. Komeyama, Y. Yamahata, I. Osaka, *Org. Lett.* **2018**, *20*, 4375; (c) K. Komeyama, T. Michiyuki, I. Osaka, *ACS Catal.* **2019**, *9*, 9285; (d) M. Ociepa, A. J. Wierzb, J. Turkowska, D. Gryko, *J. Am. Chem. Soc.* **2020**, *142*, 5355.
- [15] (a) K. Takai, K. Nitta, O. Fujimura, K. Utimoto, *J. Org. Chem.* **1989**, *54*, 4732; (b) L. K. G. Ackerman, L. L. Anka-Lufford, M. Naodovic, D. J. Weix, *Chem. Sci.* **2015**, *6*, 1115; (c) J. L. Hofstra, A. H. Cherney, C. M. Ordner, S. E. Reisman, *J. Am. Chem. Soc.* **2018**, *140*, 139.

- [16] (a) M. Kuroboshi, M. Tanaka, S. Kishimoto, K. Goto, M. Mochizuki, H. Tanaka, *Tetrahedron Lett.* **2000**, *41*, 81; (b) A. García-Domínguez, Z. Li, C. Nevado, *J. Am. Chem. Soc.* **2017**, *139*, 6835; (c) W. Shu, A. García-Domínguez, M. T. Quirós, R. Mondal, D. J. Cárdenas, C. Nevado, *J. Am. Chem. Soc.* **2019**, *141*, 13812.
- [17] In some cases, *N*-(3-bromopropyl)phthalimide was used as the alkyl electrophile because the polar functional group assists with isolation.
- [18] An alternative method for optimizing reactions involves utilizing additional equivalents of the alkyl electrophile. See the SI for further details.
- [19] H. Yin, J. Sheng, K.-F. Zhang, Z.-Q. Zhang, K.-J. Bian, X.-S. Wang, *Chem. Commun.* **2019**, *55*, 7635.
- [20] S. D. Roughley, A. M. Jordan, *J. Med. Chem.* **2011**, *54*, 3451.
- [21] F. Alonso, I. P. Beletskaya, M. Yus, *Chem. Rev.* **2002**, *102*, 4009.
- [22] H.-Q. Do, E. R. R. Chandrashekar, G. C. Fu, *J. Am. Chem. Soc.* **2013**, *135*, 16288.
- [23] (a) V. Bacauanu, S. Cardinal, M. Yamauchi, M. Kondo, D. F. Fernández, R. Remy, D. W. C. MacMillan, *Angew. Chem. Int. Ed.* **2018**, *57*, 12543; (b) C. Xu, W.-H. Guo, X. He, Y.-L. Guo, X.-Y. Zhang, X. Zhang, *Nature Commun.* **2018**, *9*, 1170.
- [24] (a) F. Lovering, J. Bikker, C. Humblet, *J. Med. Chem.* **2009**, *52*, 6752; (b) F. Lovering, *Med. Chem. Comm.* **2013**, *4*, 515.
- [25] P. S. Kutchukian, J. F. Dropinski, K. D. Dykstra, B. Li, D. A. DiRocco, E. C. Streckfuss, L.-C. Campeau, T. Cernak, P. Vachal, I. W. Davies, S. W. Krska, S. D. Dreher, *Chem. Sci.* **2016**, *7*, 2604.
- [26] S. W. Krska, D. A. DiRocco, S. D. Dreher, M. Shevlin, *Acc. Chem. Res.* **2017**, *50*, 2976.
- [27] (a) F. Reck, F. Zhou, C. J. Eyermann, G. Kern, D. Carcanague, G. Ioannidis, R. Illingworth, G. Poon, M. B. Gravestock, *J. Med. Chem.* **2007**, *50*, 4868; (b) T. Komine, A. Kojima, Y. Asahina, T. Saito, H. Takano, T. Shibue, Y. Fukuda, *J. Med. Chem.* **2008**, *51*, 6558.
- [28] R. D. Taylor, M. MacCoss, A. D. G. Lawson, *J. Med. Chem.* **2014**, *57*, 5845.
- [29] P. G. Jessop, *Green Chem.* **2011**, *13*, 1391.
- [30] M. Mendel, I. Kalvet, D. Hupperich, G. Magnin, F. Schoenebeck, *Angew. Chem. Int. Ed.* **2020**, *59*, 2115.
- [31] I. Kalvet, G. Magnin, F. Schoenebeck, *Angew. Chem. Int. Ed.* **2017**, *56*, 1581.
- [32] (a) L.-Y. He, M. Schulz-Senft, B. Thiedemann, J. Linshoeft, P. J. Gates, A. Staubitz, *Eur. J. Org. Chem.* **2015**, *2015*, 2498; (b) J. W. B. Fyfe, N. J. Fazakerley, A. J. B. Watson, *Angew. Chem. Int. Ed.* **2017**, *56*, 1249.
- [33] K. Lin, R. J. Wiles, C. B. Kelly, G. H. M. Davies, G. A. Molander, *ACS Catal.* **2017**, *7*, 5129.
- [34] (a) S.-i. Mho, B. Ortiz, N. Doddapaneni, S. M. Park, *J. Electrochem. Soc.* **1995**, *142*, 1047; (b) B. Eberle, O. Hübner, A. Ziesak, E. Kaifer, H.-J. Himmel, *Chem. Eur. J.* **2015**, *21*, 8578.
- [35] J. Demarteau, A. Debuigne, C. Detrembleur, *Chem. Rev.* **2019**, *119*, 6906.
- [36] F. T. T. Ng, G. L. Rempel, C. Mancuso, J. Halpern, *Organometallics* **1990**, *9*, 2762.

TOC Graphic

Rationally Designed C(sp²)-C(sp³) Cross-Electrophile Coupling...



... Enables

Broad and expanded substrate scope	One-pot dialkylation of bromo(iodo)arenes	Compatibility with medically relevant aryl halides
<p>27 examples (76% avg yield)</p>	<p>4 examples (82% avg yield)</p>	<p>9 examples (63% avg yield)</p>

Manuscript (1).pdf (1.11 MiB)

[view on ChemRxiv](#) • [download file](#)

Supporting Information: A Widely Applicable Dual-Catalytic System for Cross-Electrophile Coupling

David J. Charboneau,^a Emily L. Barth,^a Nilay Hazari,^{a,*} Mycah R. Uehling^b & Susan L. Zultanski^{c,*}

^aDepartment of Chemistry, Yale University, P. O. Box 208107, New Haven, Connecticut, 06520, USA. E-mail: nilay.hazari@yale.edu.

^bMerck & Co., Inc., Discovery Chemistry, HTE and Lead Discovery Capabilities, Kenilworth, New Jersey, 07033, USA.

^cMerck & Co., Inc., Department of Process Research and Development, Rahway, New Jersey, 07065, USA. E-mail: susan_zultanski@merck.com.

Table of Contents

<i>SI</i>	<i>S4</i>	<i>General Methods (Not Including High Throughput Experimentation)</i>
<i>SII</i>	<i>S5</i>	<i>Instrumentation Methods (Not Including High Throughput Experimentation)</i>
<i>SIII</i>	<i>S6</i>	<i>General Methods Used in High Throughput Experimentation</i>
<i>SIV</i>	<i>S7</i>	<i>Hardware and Instrumentation Methods for High Throughput Experimentation</i>
<i>SV</i>	<i>S9</i>	<i>General Procedure for Cross-Electrophile Coupling of Aryl and Alkyl Halides</i>
<i>SVI</i>	<i>S11</i>	<i>Optimization of Concentration</i>
<i>SVII</i>	<i>S12</i>	<i>Solvent Screen</i>
<i>SVIII</i>	<i>S13</i>	<i>Stability of (dtbbpy)Ni^{II}(<i>o</i>-tol)I in the Presence and Absence of TDAE in Varying Solvents</i>
<i>SIX</i>	<i>S16</i>	<i>Varying (dtbbpy)Ni^{II}Br₂ Loading in Dual-Catalyzed Cross-Electrophile Coupling of Iodobenzene with Benzyl Chloride</i>
<i>SX</i>	<i>S17</i>	<i>Representative Optimizations of Substrates in Figure 4</i>
<i>SXI</i>	<i>S21</i>	<i>Additional Reactions for Two-Component Cross-Electrophile Coupling</i>
<i>SXII</i>	<i>S23</i>	<i>High Throughput Experimentation for Optimization of Drug-Like Aryl Halides</i>
<i>SXIII</i>	<i>S26</i>	<i>Additional Reactions for Drug-Like Aryl Halide Cross-Electrophile Coupling</i>
<i>SXIV</i>	<i>S27</i>	<i>Parallel Library Synthesis Using Substrate 5f</i>
<i>SXV</i>	<i>S29</i>	<i>Procedure and General Information for 3 mmol Scale Reaction of 5f with 1-Iodo-3-Phenylpropane</i>
<i>SXVI</i>	<i>S32</i>	<i>Optimization of Single-Step One-Pot Three-Component Coupling</i>
<i>SXVII</i>	<i>S33</i>	<i>Procedure for and Optimization of Two-step One-Pot Three-Component Component Coupling for ¹H NMR Yields</i>
<i>SXVIII</i>	<i>S35</i>	<i>Additional Reactions for Three-Component Cross-Electrophile Coupling</i>
<i>SXIX</i>	<i>S36</i>	<i>Stoichiometric C(sp²)-C(sp³) Bond Formation with (dtbbpy)Ni^{II}(<i>o</i>-tol)I</i>
<i>SXX</i>	<i>S37</i>	<i>Radical Trapping Experiments with TEMPO</i>
<i>SXXI</i>	<i>S38</i>	<i>Isolation Procedures and Characterization for Products of Two-Component Cross-Electrophile Coupling</i>

<i>SXXII</i>	<i>S44</i>	<i>Isolation Procedures and Characterization for Products of Two-Component Cross-Electrophile Coupling with Drug-Like Aryl Halides</i>
<i>SXXIII</i>	<i>S49</i>	<i>Procedure for ¹H NMR Yields of Products from Two-Component Cross-Electrophile Coupling with Drug-Like Aryl Halides</i>
<i>SXXIV</i>	<i>S50</i>	<i>Isolation Procedures and Characterization for Products of Two-Step One-Pot Three-Component Component Coupling</i>
<i>SXXV</i>	<i>S52</i>	<i>NMR Spectra of Isolated Products</i>
<i>SXXVI</i>	<i>S84</i>	<i>UPLC Traces from HTE Experiments for Optimization of Drug-Like Aryl Halides with 1-Bromo-3-Phenylpropane</i>
<i>SXXVII</i>	<i>S89</i>	<i>UPLC Traces from HTE Experiments for Parallel Library Synthesis Using Substrate 5f</i>
<i>SXXVIII</i>	<i>S106</i>	<i>References</i>

SI. General Methods (Not Including High Throughput Experimentation)

Experiments were performed under an atmosphere of dinitrogen in an MBRAUN glovebox or using standard Schlenk techniques, unless specified otherwise. Purging of the glovebox atmosphere was not performed between uses of pentane, benzene, toluene, diethyl ether, 1,4-dioxane and tetrahydrofuran (THF); as such, trace amounts of the solvents may have been present in the box atmosphere and intermixed in the solvent bottles. 1,4-Dioxane, *N,N*-dimethylformamide (DMF), pentane, tetrahydrofuran (THF), benzene, and toluene were dried via passage through a column of activated alumina on an Inert Technologies PureSolv MD7 solvent purification system and subsequently stored under dinitrogen unless otherwise noted. Acetonitrile (CH_3CN) was purchased from Honeywell (Cat. No. CS017-56) and used without further purification. Methyl ethyl ketone (MEK) was purchased as <0.005% H_2O from EMD Chemicals then degassed and used without further purification. Other solvents used for catalysis, such as isopropyl acetate (IPAc, Sigma Aldrich), 2-methyltetrahydrofuran (2-MeTHF, Acros), and 1,2-dimethoxyethane (DME, Acros) were degassed then dried via passage through a small pipette of neutral activated alumina in a glovebox under an N_2 atmosphere until they reached <50 ppm H_2O content by KF titration. Neutral alumina was activated by heating at 250 °C under vacuum overnight. Deuterated solvents were obtained from Cambridge Isotope Laboratories and were dried by passage through a short column of neutral activated alumina. Chemicals were used as received unless otherwise stated. 4,4'-di-*tert*-butyl-2,2'-bipyridine (dtbbpy) was purchased from Sigma Aldrich or Santa Cruz at >97% purity. Substrates were purchased at $\geq 97\%$ purity. All liquid substrates were degassed by sparging with dinitrogen or by three consecutive freeze-pump-thaw cycles, then handled inside of a nitrogen filled glovebox. Liquid substrates that had a yellow color instead of being colorless were purified by passage through a short column of neutral activated alumina prior to use. Tetrakis(dimethylamino)ethylene (TDAE) was purchased from Sigma-Aldrich, TCI, AstaTech, or Santa Cruz and was used without further purification. $\text{Co}^{\text{II}}(\text{Pc})$ was purchased from Sigma-Aldrich and used without further purification. The following compounds were synthesized according to literature procedures: $(\text{dtbbpy})\text{Ni}^{\text{II}}(o\text{-tol})\text{I}$,^[1] $(\text{dtbbpy})\text{Ni}^{\text{II}}\text{Br}_2$.^[2]

SII. Instrumentation Methods (Not Including High Throughput Experimentation)

NMR spectra were recorded on Agilent-400, -500, or -600 MHz spectrometers at ambient probe temperatures unless otherwise stated. Chemical shifts for ^1H NMR spectra are reported with respect to residual protio solvent in ppm. Chemical shifts for other nuclei are referenced through the gyromagnetic ratio method described by Harris *et al.*^[3] High resolution mass spectra were acquired with a Waters Xevo QToF Mass Spectrometer (spray needle held at 3kV, source temperature set to 125 °C, N₂ cone gas flow rate 24 L/h, N₂ desolvation gas flow rate 720 L/h). Liquid chromatography was used for sample separation with a gradient from 95% H₂O (0.1% formic acid) and 5% acetonitrile to 5% H₂O and 95% acetonitrile at a flow rate of 0.6 L/min over 3 minutes using an Acquity UPLC BEH C18 column (1.7 μm , 2.1 mm x 50 mm). In some instances, poor ionization of compounds precluded high resolution data collection, so low resolution gas chromatography/mass spectrometry or liquid chromatography/mass spectrometry was utilized. Low resolution gas chromatography/mass spectrometry was performed on an Agilent 6890N Network GC and an Agilent 5973 Mass Selective Detector system using the following parameters: flow rate 1.0 mL/min, column temperature 50 °C (held for 3 min), 20 °C/min increase to 300 °C (held for 2 min), total time 17.5 min. For information on liquid chromatography/mass spectroscopy see section SIV.

SIII. General Methods Used in High Throughput Experimentation

All coupling partners, catalysts, and reductants were dosed as mixtures in 1,4-dioxane inside a nitrogen filled glovebox. If the mixture in 1,4-dioxane was not soluble (slurry), the mixture was dosed while it was stirred. The 1,4-dioxane that was used was purchased from Millipore Sigma in an air-free, Sure/SealTM bottle, and used as is, after opening inside a nitrogen-filled glove box. Solutions of aryl and alkyl halide dissolved in 1,4-dioxane were prepared by independently weighing the aryl and alkyl halides into different dram vials under air (each with a stir bar), then bringing the vials inside a nitrogen filled glove box and adding 1,4-dioxane. The mixtures of Co^{II}(Pc) and TDAE were prepared by weighing Co^{II}(Pc) and TDAE into different dram vials (each with a stir bar) inside a nitrogen filled glovebox, then adding 1,4-dioxane. The mixture of (dtbbpy)Ni^{II}Br₂ was prepared by weighing Ni^{II}Br₂ (1 equiv) and dtbbpy (1 equiv) in a dram vial (with a stir bar) inside a nitrogen filled glove box, and adding 1,4-dioxane. The mixture was allowed to stir for 20 min at 25 °C before use. The concentration of the mixtures of each reaction component in 1,4-dioxane is outlined in section SXII.

SIV. Hardware and Instrumentation Methods for High Throughput Experimentation

Reactions were performed in a 96 well reaction block (Analytical Sales & Services, Inc. catalog # 96960) using 1 mL reaction vials (Analytical Sales & Services, Inc. catalog # 884001), a PFA sheet (Analytical Sales & Services, Inc. catalog #: 96967) and rubber mat (Analytical Sales & Services, Inc. catalog #: 96965) for sealing the block, and 96 parylene coated stir dowels (1.98mm diameter, 4.80 mm length, V&P Scientific, Inc. product # VP 711D-1) for stirring. The reaction block was stirred using a tumble stirrer (tumble stirrer: V&P Scientific, Inc. Model # VP710 S) and heating was applied using a heating jacket (V&P Scientific, Inc. Model VP 741ABZ-R-MB).



Figure S1. Representative image of a reaction block, reaction vessels, stir bar, PFA sheet, and rubber mat used in high throughput experimentation.

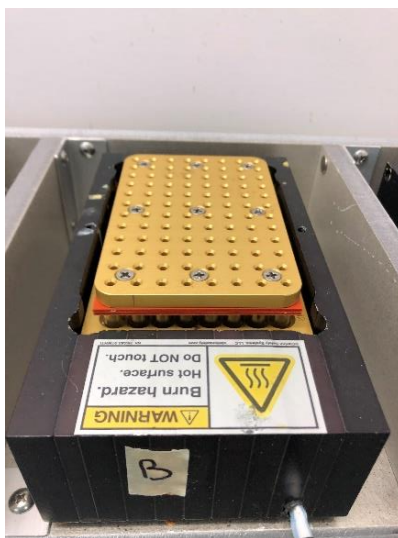


Figure S2. Representative image of a reaction block inside a heating jacket on a tumble stirrer used in high throughput experimentation.

UPLC/MS (ESI) was performed using a Waters Acquity UPLC I-Class system equipped with a binary pump, sample manager, column manager, sample organizer, a photodiode array detector, Single Quad Detector 2 with ESI source and MassLynx® software.

Analytical separations were performed using one of two methods (see below):

Method 1:

Inject volume: 1 μ L

Column Temperature: 45 °C

UV scan: 210 – 400 nM

CORTECS UPLC C18 1.6 μ M, 2.1 mm x 50 mm

Mobile Phase A: 0.1 % TFA in Water

Mobile Phase B: 0.1 % TFA in Acetonitrile

Details of Elution

Time (min)	Flow (mL/min)	% A	% B
0.00	0.700	95	5
1.70	0.700	0	100
1.95	0.700	0	100
1.96	0.700	95	100
2.00	0.700	95	5

Method 2:

Inject volume: 1 μ L

Column temperature: 55 °C

UV scan: 210 – 500 nM

ACQUITY UPLC C18 BEH 1.7 μ M, 1 mm x 50 mm

Mobile Phase A: 0.1 % TFA in Water

Mobile Phase B: 0.1 % TFA in Acetonitrile

Details of Elution

Time (min)	Flow (mL/min)	% A	% B
0.00	0.350	95	5
1.40	0.350	0	100
1.80	0.350	0	100
1.82	0.350	95	100
2.00	0.350	95	5

SV. General Procedure for Cross-Electrophile Coupling of Aryl and Alkyl Halides

General Information:

In general, aryl halides and alkyl halides were found to be unreactive with (dtbbpy)Ni^{II}Br₂ and Co^{II}(Pc) over hours at room temperature in the absence of TDAE. Therefore, reactions were typically set up by first generating a fresh stock solution of substrate with catalysts under an N₂ solution. However, if the substrates were a solid at room temperature, the solid was added directly to the reaction flask. In many solvents, the catalysts are not fully soluble, so the mixtures were sonicated into a fine suspension, which was then added as a slurry to a reaction vial equipped with a magnetic stir bar. TDAE was then added to initiate the reaction.

The quantity of TDAE utilized in a given reaction was determined by:

$$(\text{mmol aryl halide} + \text{mmol alkyl halide})/2 + (0.1 \times \text{mmol aryl halide}) = \text{mmol TDAE}$$

In the above equation, the left term describes the amount of TDAE required to stoichiometrically reduce aryl and alkyl electrophiles. The right term shows that 10% excess of TDAE was employed relative to the aryl electrophile, which was employed to reduce Ni^{II} and Co^{II} catalysts to low-valent oxidation states (Ni⁰ and Co^I).

In general, (dtbbpy)Ni^{II}Br₂ was employed as a well-defined precatalyst. However, comparable activity was observed when a slurry of premixed Ni^{II}Br₂ (anhydrous) and free dtbbpy in dioxane was utilized (See SXII).

Unless otherwise stated, all reported yields were performed in duplicate and quantified by ¹H NMR (*vide infra*) with the exception of isolated yields, which were quantified once by ¹H NMR and once by product isolation. In general, product yields for duplicate reactions agreed within 10% of one another regardless of quantification method.

Representative Procedure:

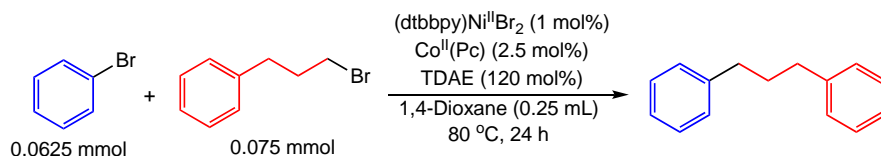


Figure S3. Cross-electrophile coupling of bromobenzene with 1-bromo-3-phenylpropane.

Outside of a glovebox to a 1 dram vial was added 1.2 mg (0.0025 mmol) (dtbbpy)Ni^{II}Br₂ and 3.6 mg (0.00625 mmol) Co^{II}(Pc). The vial was pumped into a glovebox containing an N₂ atmosphere, where 1 mL 1,4-dioxane was added via syringe transfer using a 1 mL disposable

syringe. To the same vial, 26.3 μL (0.25 mmol) bromobenzene and 45.6 μL (0.30 mmol) 1-bromo-3-phenylpropane were added via a 100 μL gas-tight Hamilton syringe. The vial was capped tightly with a PTFE seal cap and removed from the glovebox, sonicated until the mixture was a uniform suspension, then brought back into the glovebox. To a separate 1 dram vial equipped with a magnetic stir bar, 270 μL of the prepared suspension was added as a slurry via syringe transfer with a disposable 1 mL syringe, followed by 17.5 μL (0.075 mmol) TDAE via 50 μL gas-tight Hamilton syringe, which initiates the reaction. The reaction vial was capped tightly with a PTFE seal cap and stirred at 80 $^{\circ}\text{C}$ for 24 hours.

General Workup for ^1H NMR Yields:

The reaction vial was removed from heat, allowed to cool to room temperature, and diluted with 0.5 mL of ethyl acetate (EtOAc). The mixture was passed through a short silica plug (~1.5 inches) in a glass pipette, which was rinsed with 5 mL EtOAc. The filtrate was concentrated to dryness and the crude residue was taken up in CDCl_3 with added hexamethylbenzene as an internal standard. The reaction yields were determined using ^1H NMR spectroscopy.

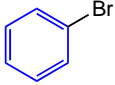
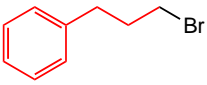
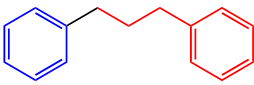
SVI. Optimization of Concentration

Procedure:

See section SV for representative experimental setup and workup. For individual reaction conditions, see Table S1 below. Higher concentrations were not utilized because, at these concentrations, as TDAE oxidized and precipitated out of solution, insufficient stirring of the thick mixture was observed.

Data:

Table S1. Optimization of dual catalyzed cross-electrophile coupling of bromobenzene with 1-bromo-3-phenylpropane.

	+		$\xrightarrow[\text{80 } ^\circ\text{C, 24 h}]{\begin{array}{l} \text{(dtbbpy)Ni}^{\text{II}}\text{Br}_2 \text{ (1 mol\%)} \\ \text{Co}^{\text{II}}(\text{Pc}) \text{ (2.5 mol\%)} \\ \text{TDAE (120 mol\%)} \\ \text{1,4-Dioxane (X mL)} \end{array}}$	
0.0625 mmol		0.075 mmol		
1,4-Dioxane (X mL)			Product Yield (%)	
0.5			84	
0.25			87	

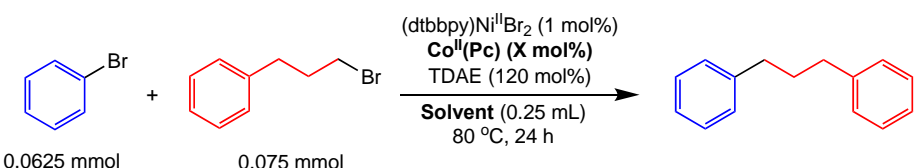
SVII. Solvent Screen

Procedure:

See section SV for representative experimental setup and workup. For individual reaction conditions, see Table S2 below.

Data:

Table S2. Solvent screen for dual-catalyzed cross-electrophile coupling of bromobenzene with 1-bromo-3-phenylpropane.

		
Solvent	Yield (%) X = 2.5%	Yield (%) X = 0%
1,4-Dioxane	87	<1
Isopropylacetate	72	<1
2-MeTHF	83	<1
Dimethoxyethane	56 (79) ^a	<1
Methyl ethyl ketone	13 (66) ^b	<1

^aReaction performed with 1 mol% Co^{II}(Pc). ^bReaction performed with 0.25 mol% Co^{II}(Pc).

SVIII. Stability of (dtbbpy)Ni^{II}(*o*-tol)I in the Presence and Absence of TDAE in Varying Solvents

General Information:

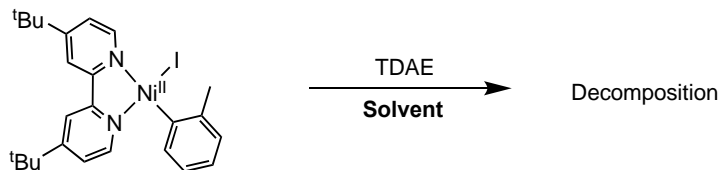
(dtbbpy)Ni^{II}(*o*-tol)I showed no decomposition in the absence of TDAE in the solvents in Table S3 over the measured course of the reaction with TDAE (<10 minutes for acetonitrile). Decomposition was measured as conversion to free ligand, which was the most significant decomposition product observed by ¹H NMR spectroscopy. Paramagnetic species were not observed during these reactions. The color of (dtbbpy)Ni^{II}(*o*-tol)I was deep red in nonpolar solvents, such as toluene and dioxane, but bright orange to pale red in more polar solvents, such as acetone, acetonitrile, and dimethylsulfoxide (DMSO). We hypothesize that the color difference arises from the iodide ligand being inner sphere in nonpolar solvents and outersphere in polar solvents so that complexes of the type [(dtbbpy)Ni^{II}(*o*-tol)(solv)]⁺I⁻ are formed. In acetonitrile, ¹H NMR spectroscopy indicates that the dtbbpy ligand may also be displaced by acetonitrile.

Representative Procedure:

In a nitrogen-filled glovebox, to a 1 dram vial was added 0.0040 g (0.0073 mmol) (dtbbpy)Ni^{II}(*o*-tol)I, 600 μ L of 1,4-dioxane, and 2.9 mg (0.014 mmol) TDAE. The solution was transferred to a J-young NMR tube and the reaction was monitored by ¹H NMR spectroscopy. For individual reaction conditions, see Table S3 below.

Reactivity Data:

Table S3. Reactivity of (dtbbpy)Ni^{II}(*o*-tol)I with TDAE in various solvents over time.



Solvent	Dielectric Constant (ε)	Solution Color Before TDAE Addition	¹ H NMR After 12 Hours at Room Temperature with TDAE
Toluene	2.38	Dark Red	No Reaction
1,4-Dioxane	2.25	Dark Red	No Reaction
Acetone	20.7	Bright Orange	20% Conversion to New Signal
Acetonitrile	37.5	Bright Orange	Complete Conversion (in <10 min)
DMSO	46.7	Bright Orange	10% Conversion to New Signal

Representative ^1H NMR data in d_6 -acetone:

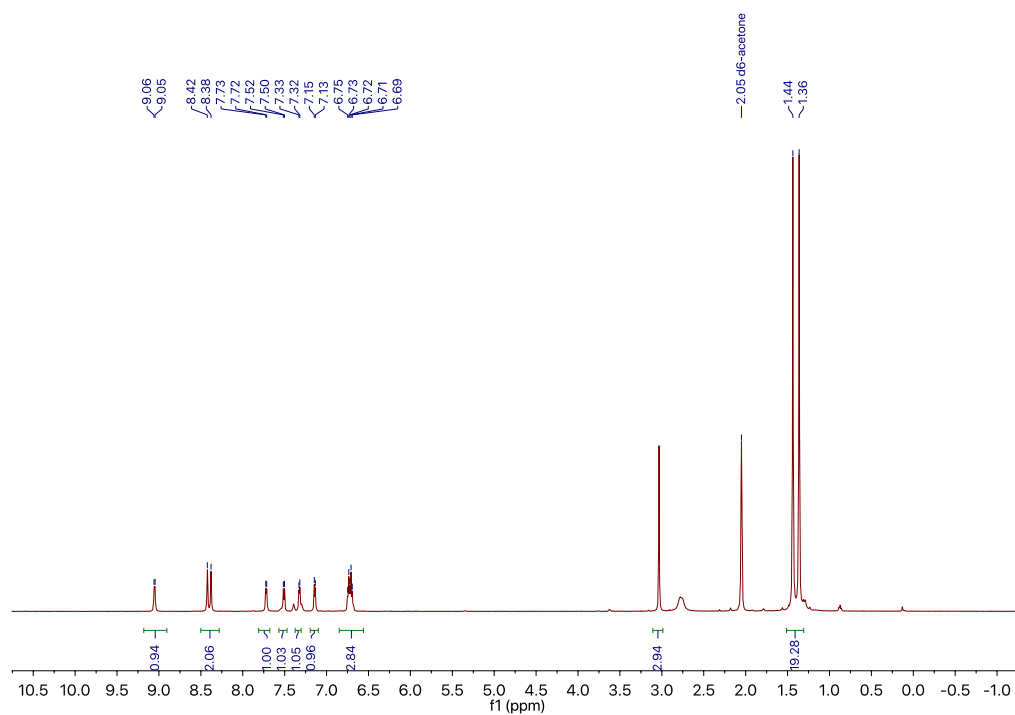


Figure S4. $(\text{dtbbpy})\text{Ni}^{\text{II}}(\text{o-tol})\text{I}$ in d_6 -acetone.

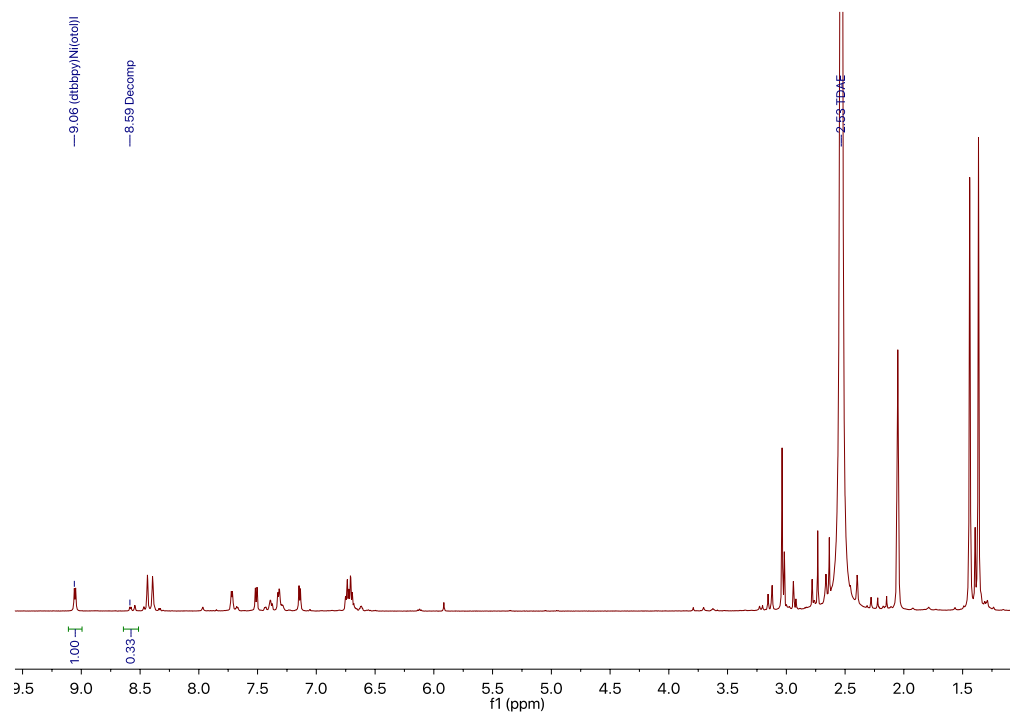


Figure S5. Reaction of $(\text{dtbbpy})\text{Ni}^{\text{II}}(\text{o-tol})\text{I}$ with TDAE in d_6 -acetone after 12 hours.

SIX. Varying (dtbbpy)Ni^{II}Br₂ Loading in Dual-Catalyzed Cross-Electrophile Coupling of Iodobenzene with Benzyl Chloride

General Information:

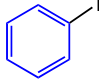
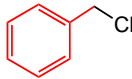
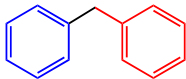
When varying the loading of (dtbbpy)Ni^{II}Br₂ while maintaining constant loading of Co^{II}(Pc), biphenyl is observed at high loading and iodobenzene is observed at low catalyst loadings, consistent with our hypotheses (Table S4).

Procedure:

See section SV for representative experimental setup and workup. For individual reaction conditions, see Table S4, below.

Data:

Table S4. Dual catalyzed cross-electrophile coupling of iodobenzene with benzyl chloride using varying amounts of (dtbbpy)Ni^{II}Br₂.

<div style="display: flex; align-items: center; justify-content: center;"> <div style="text-align: center; margin-right: 10px;">  0.0625 mmol </div> <div style="margin-right: 10px;">+</div> <div style="text-align: center; margin-right: 10px;">  0.075 mmol </div> <div style="text-align: center; margin-right: 10px;"> $\xrightarrow[\text{80 } ^\circ\text{C, 24 h}]{\begin{array}{l} \text{(dtbbpy)Ni}^{\text{II}}\text{Br}_2 \text{ (X mol\%)} \\ \text{Co}^{\text{II}}(\text{Pc}) \text{ (2.5 mol\%)} \\ \text{TDAE (120 mol\%)} \\ \text{1,4-Dioxane (0.5 mL)} \end{array}}$ </div> <div style="text-align: center;">  </div> </div>						
(dtbbpy)Ni ^{II} Br ₂ (X mol%)	Product Yield (%)	Phenyl iodide (%)	Biphenyl (%)	PhI Mass Balance (%)	Benzyl Chloride (%)	
1.75	52	38	<1	90	<1	
3.5	61	27	<1	88	<1	
7	75	14	1	91	<1	
14	85	2	8	103	<1	

SX. Representative Optimizations of Substrates in Figure 4

Procedure:

See section SV for representative experimental setup and workup. For individual reaction conditions, see Tables S5-S9 below.

General Information:

These data are to demonstrate the methods by which substrates in Figure 4 of the manuscript were optimized and to show that the general strategy depicted in Figure 3 for substrate optimization can be applied to a wide range of substrates. Representative optimization sequences are provided and, in some instances, superfluous data points are omitted.

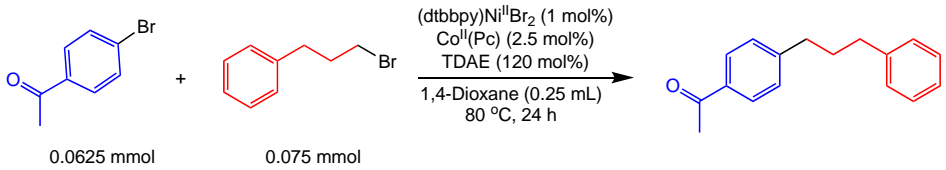
Data and Analysis:

Table S5. Optimization of dual catalyzed cross-electrophile coupling of 4-bromo-*N*-methylbenzamide (**4i**) with 1-bromo-3-phenylpropane.

<div><div><div>0.0625 mmol 0.075 mmol</div></div></div>					
Deviation From Conditions	Product Yield (%)	ArBr (%)	ArH (%)	Biaryl (%)	AlkBr (%)
None	62	<1	<1	12	18
5 mol% Co	82	<1	<1	7	8

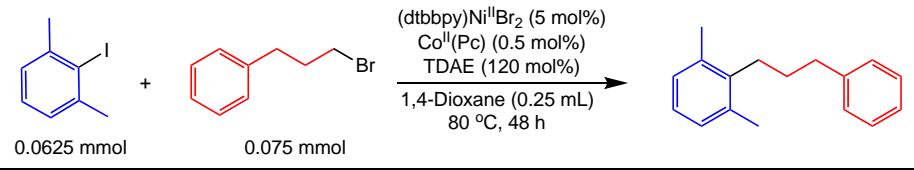
Using our standard catalyst loadings for bromobenzene (**4a**), 1 mol% (dtbbpy)Ni^{II}Br₂ and 2.5 mol% Co^{II}(Pc), 4-bromo-*N*-methylbenzamide (**4i**) was coupled with 1-bromo-3-phenylpropane in 62% yield. Under these conditions, alkyl bromide was left unreacted upon complete consumption of the aryl electrophile. Therefore, in accord with the strategy outlined in Figure 3, the loading of Co^{II}(Pc) was increased to 5 mol%, resulting in an 82% yield. Further optimization was not attempted, however, using 5 mol% Co^{II}(Pc), alkyl bromide still remained after consumption of the aryl bromide, indicating that higher yields could be obtained by either increasing Co^{II}(Pc) loading or decreasing (dtbbpy)Ni^{II}Br₂ loadings.

Table S6. Optimization of dual catalyzed cross-electrophile coupling of 4-bromoacetophenone (**4g**) with 1-bromo-3-phenylpropane.

					
Deviation From Conditions	Product Yield (%)	ArBr (%)	ArH (%)	Biaryl (%)	AlkBr (%)
None	80	17	<1	<1	20
36 h	93	6	<1	1	2

Using our standard catalyst loadings for bromobenzene (**4a**), 1 mol% (dtbbpy)Ni^{II}Br₂ and 2.5 mol% Co^{II}(Pc), 4-bromoacetophenone (**4g**) was coupled with 1-bromo-3-phenylpropane in 80% yield. Under these conditions, alkyl bromide and aryl bromide remained unreacted, indicating that the reaction had not reached completion. Therefore, the reaction was allowed to run for 36 hours, resulting in a 93% yield.

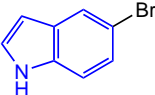
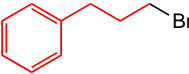
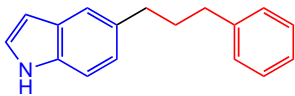
Table S7. Optimization of dual catalyzed cross-electrophile coupling of 2-iodo-1,3-dimethylbenzene (**4r**) with 1-bromo-3-phenylpropane.

					
Deviation From Conditions	Product Yield (%)	ArBr (%)	ArH (%)	Biaryl (%)	AlkBr (%)
None	37	54	<1	<1	20
10 mol% Ni, 0.125 mmol AlkBr, 160 mol% TDAE	88	<1	<1	<1	<1

Based on reactivity observed with mono-*ortho*-substituted aryl halide substrates, which required a higher ratio of (dtbbpy)Ni^{II}Br₂ to Co^{II}(Pc), we started reaction optimization for the coupling of 2-iodo-1,3-dimethylbenzene (**4r**) with 1-bromo-3-phenylpropane at 5 mol% (dtbbpy)Ni^{II}Br₂ and 0.5 mol% Co^{II}(Pc). Additionally, the reaction was performed for 48 hours

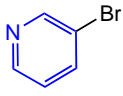
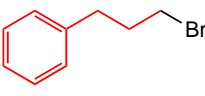
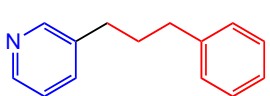
owing to the expected sluggish oxidative addition of **4r**. Under these conditions, a 37% yield was observed. While both alkyl bromide and aryl bromide were present at the end of the reaction, the rate of alkyl bromide consumption outpaced the rate of aryl bromide consumption. Therefore, the loading of (dtbbpy)Ni^{II}Br₂ was increased and the loadings of alkyl bromide and TDAE were increased. It is probable that high yields could also be obtained in this reaction without increasing the equivalents of alkyl bromide, however, these reactions were not attempted.

Table S8. Optimization of dual catalyzed cross-electrophile coupling of 5-bromoindole (**4j**) with 1-bromo-3-phenylpropane.

<div style="display: flex; align-items: center; justify-content: center;"> <div style="text-align: center;">  <p>0.0625 mmol</p> </div> <div style="margin: 0 10px;">+</div> <div style="text-align: center;">  <p>0.075 mmol</p> </div> <div style="margin-left: 20px;"> <p>(dtbbpy)Ni^{II}Br₂ (1 mol%) Co^{II}(Pc) (2.5 mol%) TDAE (120 mol%) 1,4-Dioxane (0.25 mL) 80 °C, 24 h</p> </div> <div style="text-align: center;">  </div> </div>					
Deviation From Conditions	Product Yield (%)	ArBr (%)	ArH (%)	Biaryl (%)	AlkBr (%)
None	64	20	6	<1	15
36 hours	68	24	6	<1	2
0.1 mmol AlkBr, 140 mol% TDAE, 36h	81	<1	12	1	<1

Using our standard catalyst loadings for bromobenzene (**4a**), 1 mol% (dtbbpy)Ni^{II}Br₂ and 2.5 mol% Co^{II}(Pc), 5-bromoindole (**4j**) was coupled with 1-bromo-3-phenylpropane in 64% yield. Under these conditions, alkyl bromide and aryl bromide remained unreacted, indicating that the reaction had not reached completion. Therefore, the reaction was allowed to run for 36 hours, resulting in a modest increase in yield to 68%. After 36 hours, alkyl bromide was fully consumed but aryl bromide remained unreacted. According to our general strategy, the nickel loading should be increased or the cobalt loading should be decreased. However, another alternative solution for reaction optimization when alkyl bromide is consumed more quickly than aryl bromide is to increase the loadings of alkyl bromide and TDAE. In this case, when the loadings of alkyl bromide and TDAE are increased, the yield was improved to 81%.

Table S9. Optimization of dual catalyzed cross-electrophile coupling of 3-bromopyridine (**4v**) with 1-bromo-3-phenylpropane.

<div style="display: flex; align-items: center; justify-content: center;"> <div style="text-align: center;">  0.0625 mmol </div> <div style="margin: 0 10px;">+</div> <div style="text-align: center;">  0.075 mmol </div> <div style="margin-left: 20px;"> $\xrightarrow[\text{80 } ^\circ\text{C, 24 h}]{\begin{array}{l} \text{(dtbbpy)Ni}^{\text{II}}\text{Br}_2 \text{ (1 mol\%)} \\ \text{Co}^{\text{II}}(\text{Pc}) \text{ (2.5 mol\%)} \\ \text{TDAE (120 mol\%)} \\ \text{1,4-Dioxane (0.25 mL)} \end{array}}$ </div> <div style="text-align: center;">  </div> </div>					
Deviation From Conditions	Product Yield (%)	ArBr (%) ^a	ArH (%)	Biaryl (%)	AlkBr (%)
None	52	16	<1	<1	3
0.1 mmol AlkBr, 140% TDAE	65	12	<1	<1	7
5 mol% Ni, 0.1 mmol AlkBr, 140% TDAE	80	<1	<1	1	<1

^a3-bromopyridine is volatile enough to be partially removed through evaporation during workup. Therefore, values reported represent the lower limit of unreacted aryl bromide in catalysis.

Using our standard catalyst loadings for bromobenzene (**4a**), 1 mol% (dtbbpy)Ni^{II}Br₂ and 2.5 mol% Co^{II}(Pc), 3-bromopyridine (**4v**) was coupled with 1-bromo-3-phenylpropane in 52% yield. Under these conditions, aryl bromide was left unreacted upon complete consumption of the alkyl electrophile. According to our optimization guidelines, the options for improving the reaction yield are to: (1) increase the loading of (dtbbpy)Ni^{II}Br₂, (2) decrease the loading of Co^{II}(Pc), or (3) increase the loadings of alkyl bromide and TDAE. Through option (3), increasing the loadings of alkyl bromide and TDAE, the yield was improved to 65%. However, aryl bromide still remained after near consumption of alkyl bromide. In addition to option (3), using option (1), increasing the loading of (dtbbpy)Ni^{II}Br₂, an 80% yield was obtained.

SXI. Additional Reactions for Two-Component Cross-Electrophile Coupling

Procedure:

See section SV for representative experimental setup and workup. For individual reaction conditions, see Figures S6 and S7 below.

Aryl Halide Substrates:

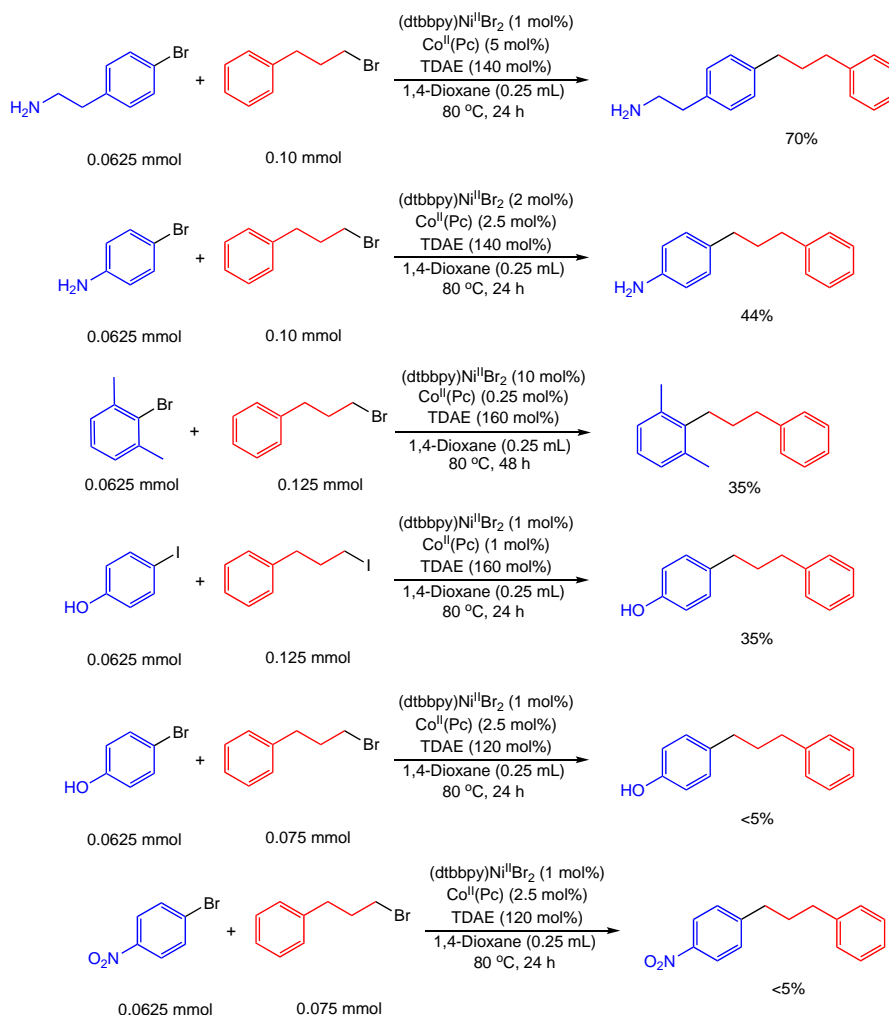


Figure S6. Additional reactions for two-component cross-electrophile coupling aryl halide substrate scope.

Alkyl Halide Substrates:

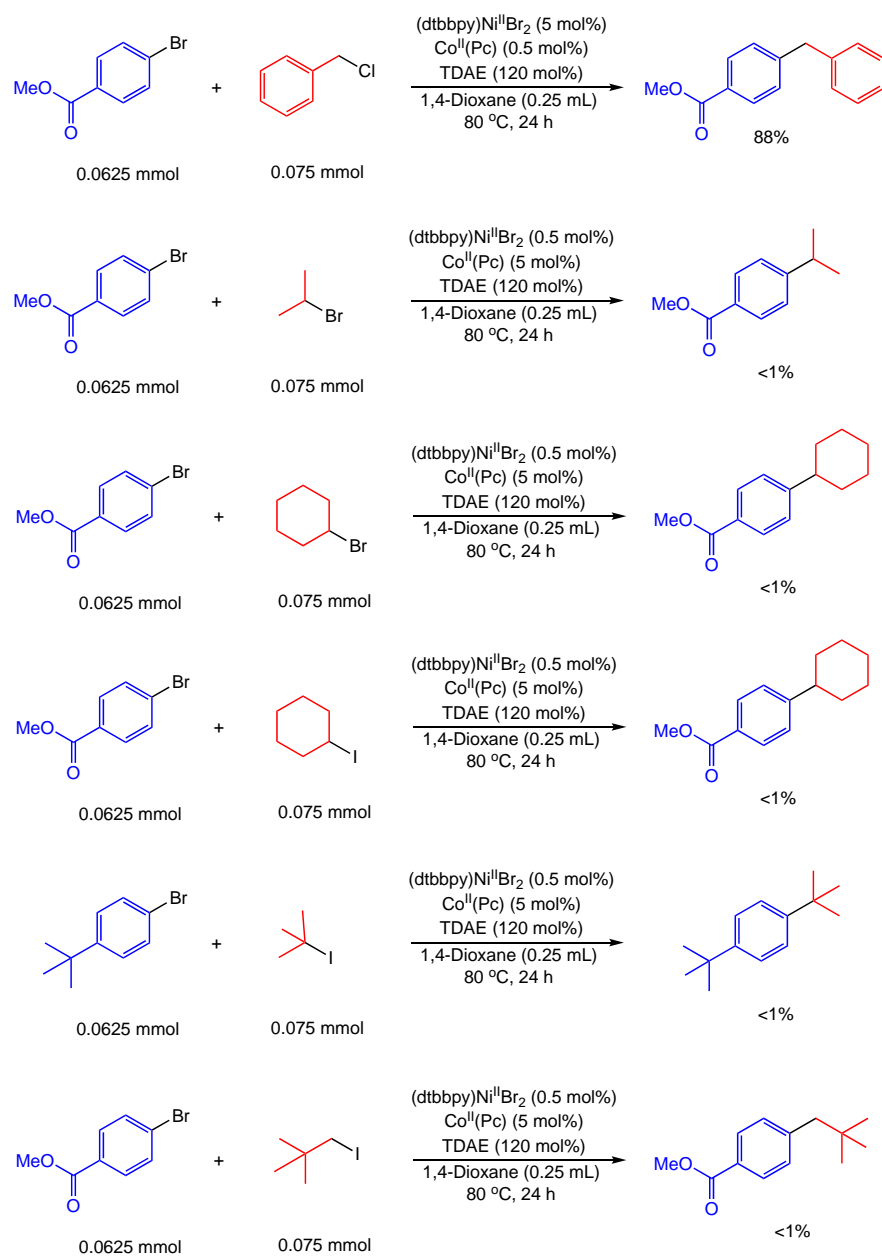


Figure S7. Additional reactions for two-component cross-electrophile coupling alkyl halide substrate scope.

SXII. High Throughput Experimentation for Optimization of Drug-Like Aryl Halides

Representative Procedure:

Using Eppendorf pipettes in a nitrogen filled glove box, each 1 mL reaction vial (containing a parylene coated stir dowel) was charged with a 1,4-dioxane mixture of aryl halide (50 μ L, 10 μ mol, 1 equiv, 0.2 M), (dtbbpy)Ni^{II}Br₂ (12.5 μ L, 0.5 μ mol, 0.05 equiv, 0.04 M, *for 5 mol% loading, volumes scaled appropriately for other loadings*), Co^{II}(Pc) (12.5 μ L, 0.5 μ mol, 0.05 equiv, 0.04 M, *for 5 mol% loading, volumes scaled appropriately for other loadings*), alkyl halide (16 μ L, 16 μ mol, 1.6 equiv, 1 M), and TDAE (14 μ L, 14 μ mol, 1.4 equiv, 1 M). The final concentration of all reactions was 0.1 M. If multiple catalyst loadings were used on the same reaction block (different volumes of catalyst added to different vials), after the dosing of TDAE, 1,4-dioxane was added to vials, where required, to reach a final concentration of 0.1 M. The reaction plate was then sealed and placed in a preheated (80 °C) tumble stirrer. The reaction block was stirred at 80 °C for 36 hours. At this time, the reaction block was allowed to cool to 25 °C and removed from the tumble stirrer and glove box. The plate was centrifuged, opened to air, and diluted with 100 μ L DMSO. The plate was then sealed, and the mixtures were stirred for 5 minutes on a tumble stirrer. The plate was opened, and 4 μ L of the crude material was diluted in 200 μ L DMSO. These solutions were used for analytical analysis. The reaction mixtures were analyzed by comparing the UV210 peak area for the product, aryl halide, protodehalogenation product, and aryl homocoupling product. Reactions that had the most product relative to aryl halide starting material and associated byproducts were repeated and the yield measured using ¹H NMR calibrated with hexamethylbenzene external standard. See section SXXIII for NMR yields.

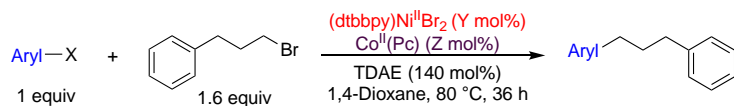
Representative Schematics of HTE Plate Design for Reaction Optimization:

Ni (mol%)		1				2.5				5				ArX
Co (mol%)		0.5	1	2.5	5	0.5	1	2.5	5	0.5	1	2.5	5	
Column		1	2	3	4	5	6	7	8	9	10	11	12	
Row	A	●	●	●	●	●	●	●	●	●	●	●	●	ArX ¹
	B	●	●	●	●	●	●	●	●	●	●	●	●	ArX ²
	C	●	●	●	●	●	●	●	●	●	●	●	●	ArX ³
	D	●	●	●	●	●	●	●	●	●	●	●	●	ArX ⁴
	E	●	●	●	●	●	●	●	●	●	●	●	●	ArX ⁵
	F	●	●	●	●	●	●	●	●	●	●	●	●	ArX ⁶
	G	●	●	●	●	●	●	●	●	●	●	●	●	ArX ⁷
	H	●	●	●	●	●	●	●	●	●	●	●	●	ArX ⁸



Conditions for well H2: ArX⁸, 1 mol% Ni, 1 mol% Co.

Figure S8. Generic scheme for reaction optimization of drug-like aryl halides using HTE. Table represents a 12x8 well plate (see Figure S1).



Y = 1 mol% Z = 0.5 mol% Aryl = 1	Y = 1 mol% Z = 1 mol% Aryl = 1	Y = 1 mol% Z = 2.5 mol% Aryl = 1	Y = 1 mol% Z = 5 mol% Aryl = 1	Y = 2.5 mol% Z = 0.5 mol% Aryl = 1	Y = 2.5 mol% Z = 1 mol% Aryl = 1	Y = 2.5 mol% Z = 2.5 mol% Aryl = 1	Y = 2.5 mol% Z = 5 mol% Aryl = 1	Y = 5 mol% Z = 0.5 mol% Aryl = 1	Y = 5 mol% Z = 1 mol% Aryl = 1	Y = 5 mol% Z = 2.5 mol% Aryl = 1	Y = 5 mol% Z = 5 mol% Aryl = 1
Y = 1 mol% Z = 0.5 mol% Aryl = 2	Y = 1 mol% Z = 1 mol% Aryl = 2	Y = 1 mol% Z = 2.5 mol% Aryl = 2	Y = 1 mol% Z = 5 mol% Aryl = 2	Y = 2.5 mol% Z = 0.5 mol% Aryl = 2	Y = 2.5 mol% Z = 1 mol% Aryl = 2	Y = 2.5 mol% Z = 2.5 mol% Aryl = 2	Y = 2.5 mol% Z = 5 mol% Aryl = 2	Y = 5 mol% Z = 0.5 mol% Aryl = 2	Y = 5 mol% Z = 1 mol% Aryl = 2	Y = 5 mol% Z = 2.5 mol% Aryl = 2	Y = 5 mol% Z = 5 mol% Aryl = 2
Y = 1 mol% Z = 0.5 mol% Aryl = 3	Y = 1 mol% Z = 1 mol% Aryl = 3	Y = 1 mol% Z = 2.5 mol% Aryl = 3	Y = 1 mol% Z = 5 mol% Aryl = 3	Y = 2.5 mol% Z = 0.5 mol% Aryl = 3	Y = 2.5 mol% Z = 1 mol% Aryl = 3	Y = 2.5 mol% Z = 2.5 mol% Aryl = 3	Y = 2.5 mol% Z = 5 mol% Aryl = 3	Y = 5 mol% Z = 0.5 mol% Aryl = 3	Y = 5 mol% Z = 1 mol% Aryl = 3	Y = 5 mol% Z = 2.5 mol% Aryl = 3	Y = 5 mol% Z = 5 mol% Aryl = 3
Y = 1 mol% Z = 0.5 mol% Aryl = 4	Y = 1 mol% Z = 1 mol% Aryl = 4	Y = 1 mol% Z = 2.5 mol% Aryl = 4	Y = 1 mol% Z = 5 mol% Aryl = 4	Y = 2.5 mol% Z = 0.5 mol% Aryl = 4	Y = 2.5 mol% Z = 1 mol% Aryl = 4	Y = 2.5 mol% Z = 2.5 mol% Aryl = 4	Y = 2.5 mol% Z = 5 mol% Aryl = 4	Y = 5 mol% Z = 0.5 mol% Aryl = 4	Y = 5 mol% Z = 1 mol% Aryl = 4	Y = 5 mol% Z = 2.5 mol% Aryl = 4	Y = 5 mol% Z = 5 mol% Aryl = 4
Y = 1 mol% Z = 0.5 mol% Aryl = 5	Y = 1 mol% Z = 1 mol% Aryl = 5	Y = 1 mol% Z = 2.5 mol% Aryl = 5	Y = 1 mol% Z = 5 mol% Aryl = 5	Y = 2.5 mol% Z = 0.5 mol% Aryl = 5	Y = 2.5 mol% Z = 1 mol% Aryl = 5	Y = 2.5 mol% Z = 2.5 mol% Aryl = 5	Y = 2.5 mol% Z = 5 mol% Aryl = 5	Y = 5 mol% Z = 0.5 mol% Aryl = 5	Y = 5 mol% Z = 1 mol% Aryl = 5	Y = 5 mol% Z = 2.5 mol% Aryl = 5	Y = 5 mol% Z = 5 mol% Aryl = 5
Y = 1 mol% Z = 0.5 mol% Aryl = 6	Y = 1 mol% Z = 1 mol% Aryl = 6	Y = 1 mol% Z = 2.5 mol% Aryl = 6	Y = 1 mol% Z = 5 mol% Aryl = 6	Y = 2.5 mol% Z = 0.5 mol% Aryl = 6	Y = 2.5 mol% Z = 1 mol% Aryl = 6	Y = 2.5 mol% Z = 2.5 mol% Aryl = 6	Y = 2.5 mol% Z = 5 mol% Aryl = 6	Y = 5 mol% Z = 0.5 mol% Aryl = 6	Y = 5 mol% Z = 1 mol% Aryl = 6	Y = 5 mol% Z = 2.5 mol% Aryl = 6	Y = 5 mol% Z = 5 mol% Aryl = 6
Y = 1 mol% Z = 0.5 mol% Aryl = 7	Y = 1 mol% Z = 1 mol% Aryl = 7	Y = 1 mol% Z = 2.5 mol% Aryl = 7	Y = 1 mol% Z = 5 mol% Aryl = 7	Y = 2.5 mol% Z = 0.5 mol% Aryl = 7	Y = 2.5 mol% Z = 1 mol% Aryl = 7	Y = 2.5 mol% Z = 2.5 mol% Aryl = 7	Y = 2.5 mol% Z = 5 mol% Aryl = 7	Y = 5 mol% Z = 0.5 mol% Aryl = 7	Y = 5 mol% Z = 1 mol% Aryl = 7	Y = 5 mol% Z = 2.5 mol% Aryl = 7	Y = 5 mol% Z = 5 mol% Aryl = 7
Y = 1 mol% Z = 0.5 mol% Aryl = 8	Y = 1 mol% Z = 1 mol% Aryl = 8	Y = 1 mol% Z = 2.5 mol% Aryl = 8	Y = 1 mol% Z = 5 mol% Aryl = 8	Y = 2.5 mol% Z = 0.5 mol% Aryl = 8	Y = 2.5 mol% Z = 1 mol% Aryl = 8	Y = 2.5 mol% Z = 2.5 mol% Aryl = 8	Y = 2.5 mol% Z = 5 mol% Aryl = 8	Y = 5 mol% Z = 0.5 mol% Aryl = 8	Y = 5 mol% Z = 1 mol% Aryl = 8	Y = 5 mol% Z = 2.5 mol% Aryl = 8	Y = 5 mol% Z = 5 mol% Aryl = 8

Medicinally Relevant Aryl Electrophiles

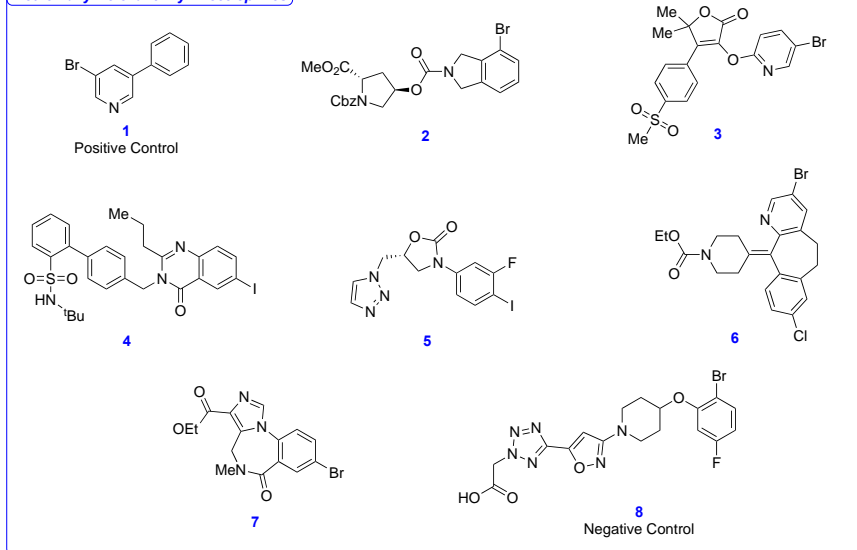


Figure S9. Example experimental design for HTE optimization of drug-like aryl halides. Table represents a 12x8 well plate (See Figure S1).

SXIII. Additional Reactions for Drug-Like Aryl Halides Cross-Electrophile Coupling

Procedure:

See section SXII for representative experimental setup, permutations of attempted reaction optimization conditions, and data analysis.

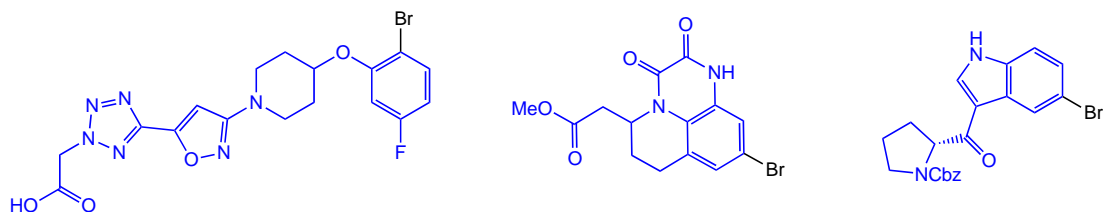


Figure S10. Drug-like aryl halides that did not show conversion to product when reacted with 1-bromo-3-phenylpropane.

SXIV. Parallel Library Synthesis Using Substrate **5f**

Procedure for ^1H NMR Yields:

Reactions to obtain ^1H NMR yields were performed on 0.03 mmol scale. See SV for representative experimental setup and workup.

Procedure for High Throughput Experimentation:

See SXII for representative experimental setup. Values are reported as area percent of product relative to all known species derived from **5f** as determined by UV-Visible spectroscopy (see section SXII for details). The species observed include **5f**, the cross-electrophile coupling product of **5f**, the homocoupled product of **5f** (Aryl-Aryl), and the protodehalogenated product of **5f** (Aryl-H).

Data:

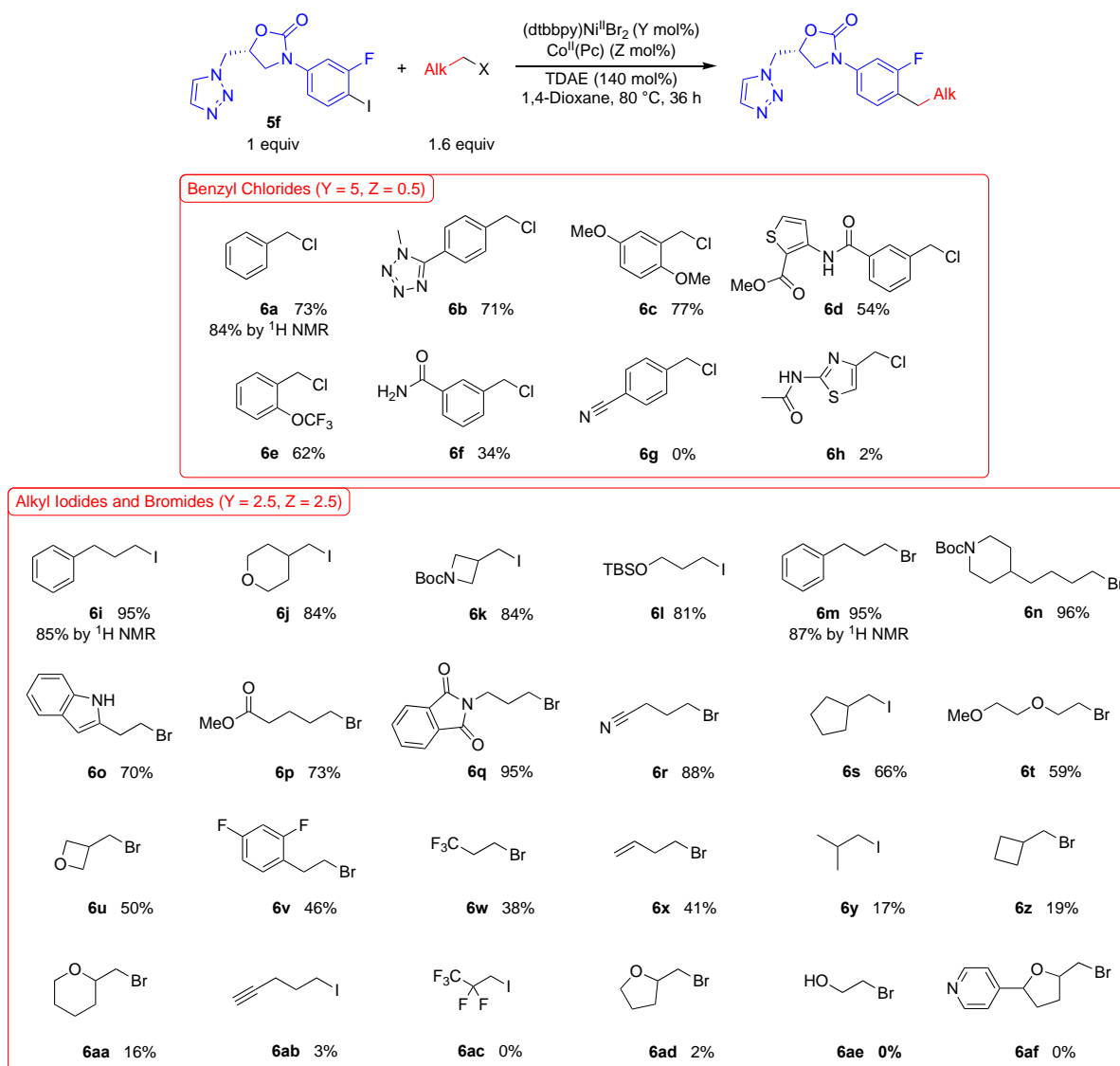


Figure S11. Dual catalyzed cross-electrophile coupling reactions between **5f** and a series of benzyl chlorides, alkyl iodides, and alkyl bromides. Values are reported as the conversion to product relative to all known species derived from **5f** determined by UV-Visible spectroscopy. NMR yields were determined by integration of ¹H NMR spectra against a hexamethylbenzene external standard.

SXV. Procedure and General Information for 3 mmol Scale Reaction of **5f** with 1-Iodo-3-Phenylpropane

Procedure:

A 100-mL round bottom flask with a Kontes seal was charged with a stir bar, aryl halide **5f** (1.165 g, 3 mmol, 1.0 equiv), (dtbbpy)Ni^{II}Br₂ (36.2 mg, 2.5 mol %), and Co^{II}(Pc) (42.9 mg, 2.5 mol %). The flask was then moved into a nitrogen-filled glovebox. To the flask was then added 30 mL 1,4-dioxane and 1-iodo-3-phenylpropane (0.772 mL, 4.8 mmol, 1.6 equiv). The flask was then sealed and removed from the glovebox and sonicated for approximately 5 minutes or until the mixture was a fine slurry. The flask was then moved back into the glovebox and TDAE (0.977 mL, 4.2 mmol, 1.4 equiv) was added. The flask was quickly removed from the glovebox, and placed into an oil bath with a thermocouple. The reaction was stirred at 80 °C for 36 hours, during which time the color was deep blue and a precipitate formed (Figure S12). After 36 hours, the flask was opened and about 30 mL EtOAc was added. The reaction mixture was filtered through a celite pad, which was rinsed with EtOAc (3 x 30 mL). The filtrate was then concentrated under reduced pressure. The resulting residue was purified by column chromatography on silica gel in 100% EtOAc. The clean fractions were collected and concentrated under reduced pressure until about 10 mL of EtOAc remained. Pentane was then added, which caused the precipitation of an off-white solid. The solid was collected via filtration, washed with pentane, and dried on a high vacuum line. The product was obtained in 64% yield (729 mg) (see general information below for further details, including discussion of isolated yield on large scale relative to ¹H NMR yield on small scale).

¹H NMR (400 MHz, CDCl₃) δ 7.77 (d, *J*=15.2 Hz, 2H), 7.30-7.23 (m, 3H), 7.20-7.11 (m, 4H), 7.01-6.99 (m, 1H), 5.06 (sextet, *J*=4.4 Hz, 1H), 4.79-4.74 (m, 2H), 4.14 (t, *J*=9.1 Hz, 1H), 3.92-3.88 (m, 1H), 2.66-2.62 (m, 4H), 1.91 (quintet, *J*=7.8 Hz, 2H). ¹³C{¹H} NMR (151 MHz, CDCl₃) δ 161.97, 160.34, 153.37, 142.05, 136.7 (d, *J*=10.6 Hz), 134.77 (br s), 130.99 (d, *J*=6.7 Hz), 128.50 (d, *J*=9.4 Hz), 125.95, 125.52 (d, *J*=16.5 Hz), 125.21 (br s), 113.67 (d, *J*=3.3 Hz), 106.5 (d, *J*=28.2 Hz), 70.51, 52.11, 47.38, 35.52, 31.70, 28.29. ¹⁹F{¹H} NMR (470 MHz, CDCl₃) δ -115.75 (quartet, *J*=8.9 Hz). (HRMS) TOF MS ES+ (*m/z*) [M+H]⁺ calculated for [C₂₁H₂₁FN₄O₂+H]⁺ 381.1721; found 381.1727.



Figure S12. Image showing scaled-up reaction after approximately 24 hours (left) and isolated product (right).

General Information:

When the reaction was performed on a 3 mmol scale, ^{19}F NMR analysis of the crude reaction mixture showed 95:5 ratio of product to starting material, with no other species present (Figure S13). This result is consistent with the 96:4 ratio of product to starting material observed by ^{19}F NMR analysis of the crude reaction mixture when the same reaction was performed on 0.03 mmol scale (Figure S14). These data suggest that our reaction conditions can be readily used to scale up synthetic protocols for medicinally relevant substrates. However, there was a discrepancy in product yield between the 85% yield obtained on 0.03 mmol scale, which was determined by ^1H NMR integration of the crude reaction mixture against a hexamethylbenzene external standard, with the 64% yield obtained on 3 mmol scale, which was determined by the mass of the isolated product after purification. We propose that this discrepancy is likely due to the fact that product was lost during purification for the quantification of the 3 mmol scale reaction. One possible explanation is that significant amounts of product remained in solution after filtration and the filtrate was not recovered.

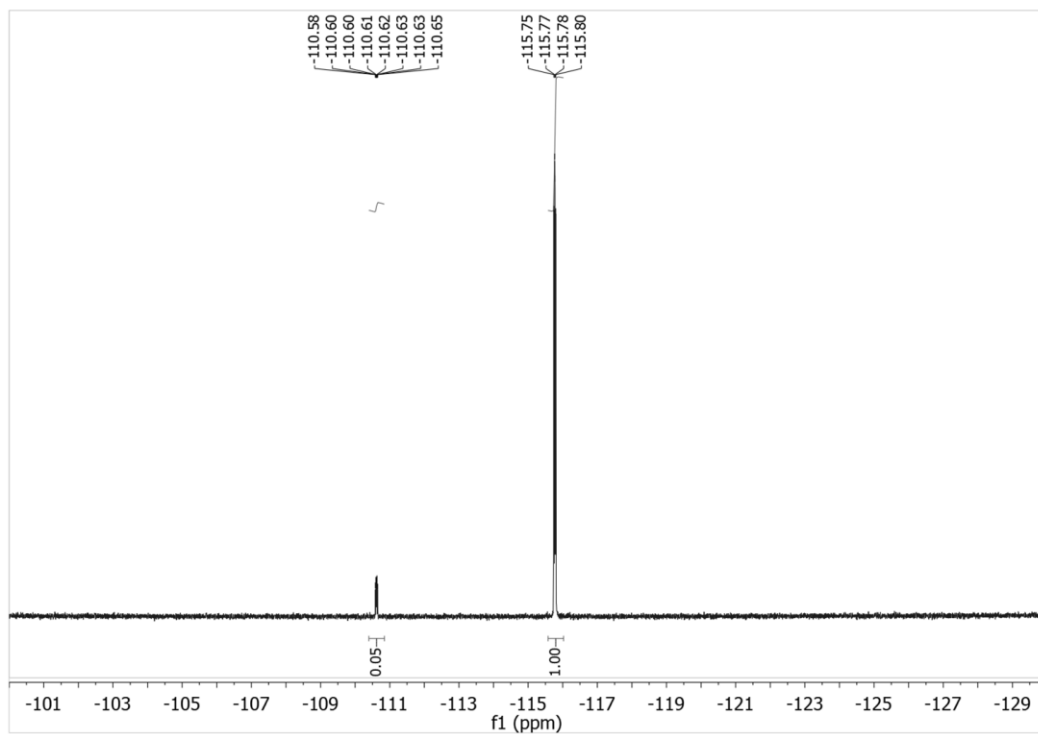


Figure S13. ^{19}F NMR spectrum (CDCl_3) of crude reaction mixture for product derived from the cross-electrophile coupling of **5f** with 1-iodo-3-phenylpropane on a 3 mmol scale.

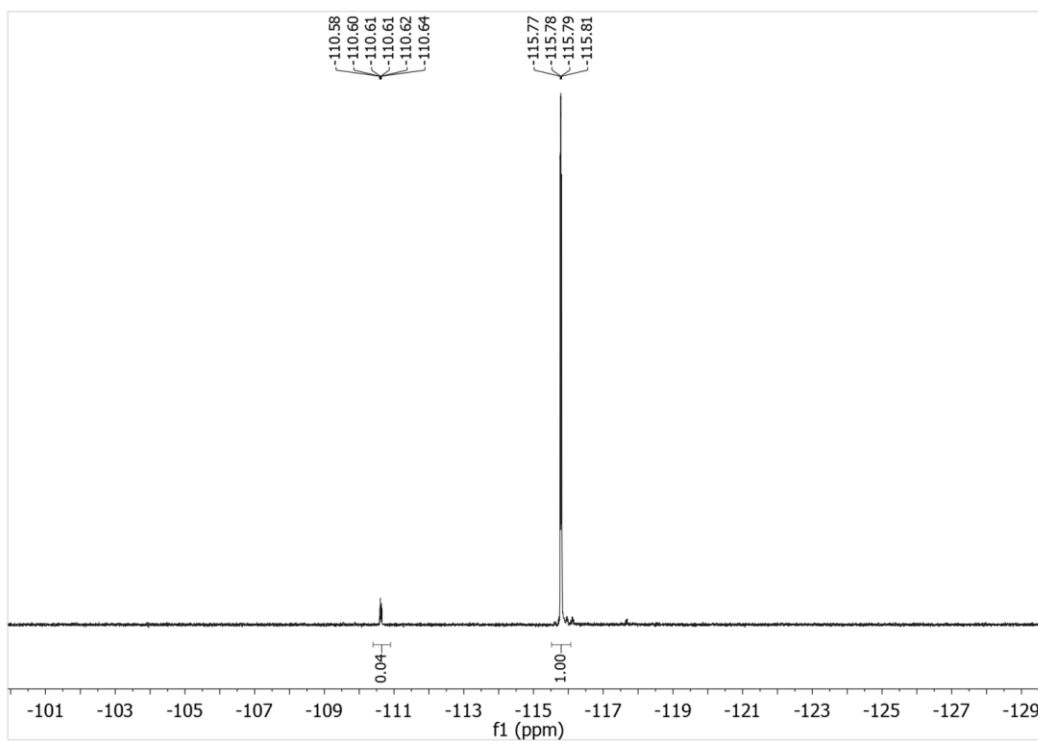


Figure S14. ^{19}F NMR spectrum (CDCl_3) of crude reaction mixture for product derived from the cross-electrophile coupling of **5f** with 1-iodo-3-phenylpropane on a 0.03 mmol scale.

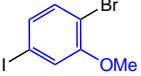
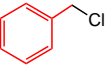
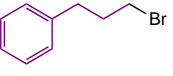
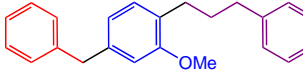
SXVI. Optimization of Single-Step One-Pot Three-Component Coupling

Procedure:

See section SV for representative experimental setup and workup. For individual reaction conditions, see Table S10 below.

Reaction Optimization Data:

Table S10. Reaction optimization of single-step one-pot cross-electrophile coupling of 1-bromo-4-iodo-2-methoxybenzene with 1-bromo-3-phenylpropane and benzyl chloride.

	+		+		$\xrightarrow[\text{Dioxane (Z mL), 80 } ^\circ\text{C, 24 h}]{\begin{array}{l} \text{(dtbbpy)Ni}^{\text{II}}\text{Br}_2 \text{ (5 mol\%)} \\ \text{Co}^{\text{II}}(\text{Pc}) \text{ (0.5 mol\%)} \\ \text{TDAE (Y mol\%)} \end{array}}$	
0.0625 mmol		0.075 mmol		X mmol		
1-bromo-3-phenylpropane (X mmol)		TDAE (X mol%)		1,4-Dioxane (Z mL)		Product Yield (%)
0.75		240		0.5		48
0.75		240		0.25		59
0.1		260		0.25		76
0.125		280		0.25		68

SXVII. Procedure for and Optimization of Two-step One-Pot Three-Component Component Coupling for ^1H NMR Yields

Representative Procedure:

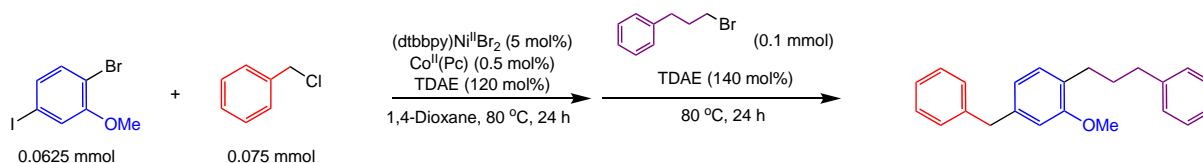


Figure S15. Two-step three-component cross-electrophile coupling of 1-bromo-4-iodo-2-methoxybenzene with 1-bromo-3-phenylpropane and benzyl chloride.

Outside of a glovebox 1.4 mg (0.0025 mmol) Co^{II}(Pc) was added to a 1 dram vial. The vial was pumped into a glovebox containing an N₂ atmosphere, where 2 mL 1,4-dioxane was added via syringe transfer using a 1 mL disposable syringe. To the same vial, 69.0 μL (0.6 mmol) benzyl chloride was added via a 100 μL gas-tight Hamilton syringe. The vial was capped tightly with a PTFE seal cap and removed from the glovebox, sonicated until the mixture was homogeneous, then brought back into the glovebox. Outside of a glovebox, 19.6 mg (0.0625 mmol) 1-bromo-4-iodo-2-methoxybenzene and 1.5 mg (0.00313 mmol) (dtbbpy)Ni^{II}Br₂ were weighed into a separate 1 dram vial equipped with a magnetic stir bar, which was pumped into a glovebox. Next, 260 μL of the prepared Co^{II}(Pc) solution was added via syringe transfer with a disposable 1 mL syringe, followed by 17.5 μL (0.075 mmol) TDAE via 50 μL gas-tight Hamilton syringe. The reaction vial was capped tightly with a PTFE seal cap and stirred at 80 °C for 24 hours. Next, the reaction vial was removed from heat and pumped into a nitrogen filled glovebox, where the cap was removed and 14.3 μL (0.1 mmol) ethyl 4-bromobutyrate was added via 50 μL gas-tight Hamilton syringe transfer followed by addition of 20.2 μL (0.0875 mmol) TDAE. The reaction was then tightly capped and stirred at 80 °C for 24 hours. The reaction vial was removed from heat, allowed to cool to room temperature, and diluted with 0.5 mL of ethyl acetate (EtOAc). The mixture was passed through a short silica plug (~1.5 inches) in a glass pipette, which was rinsed with 5 mL EtOAc. The filtrate was concentrated to dryness and the crude residue was taken up in CDCl₃ with added hexamethylbenzene as an internal standard. The reaction yields were determined by ^1H NMR spectroscopy. For individual reaction conditions, see Table 2 in the manuscript.

General Information:

Two-step three-component reactions were optimized by initially performing the first alkylation at the iodide site of the bromo(iodo)arene to ensure high yields, then performing the combination of the two alkylation reactions. See below for representative example.

Representative Data for Quantifying the First Alkylation Reaction of a Bromo(iodo)arene in a Discrete Step Followed by Two-Step One-Pot Cross-Electrophile Coupling:

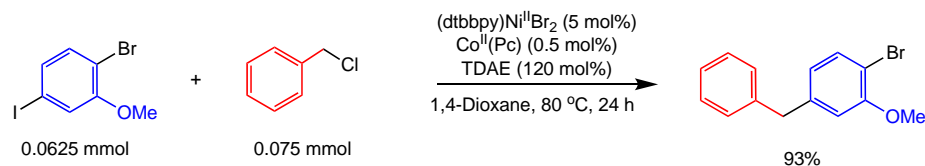


Figure S16. Cross-electrophile coupling of 1-bromo-4-iodo-2-methoxybenzene with benzyl chloride.

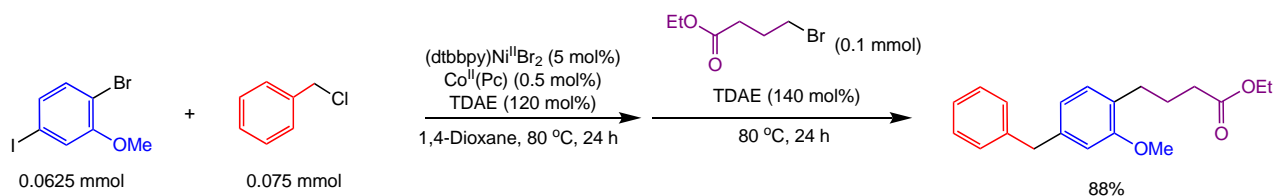


Figure S17. Cross-electrophile coupling of 1-bromo-4-iodo-2-methoxybenzene with benzyl chloride.

SXVIII. Additional Reactions for Three-Component Cross-Electrophile Coupling

Procedure:

See section SXVII for representative experimental setup and workup. For individual reaction conditions, see Figure S18 below.

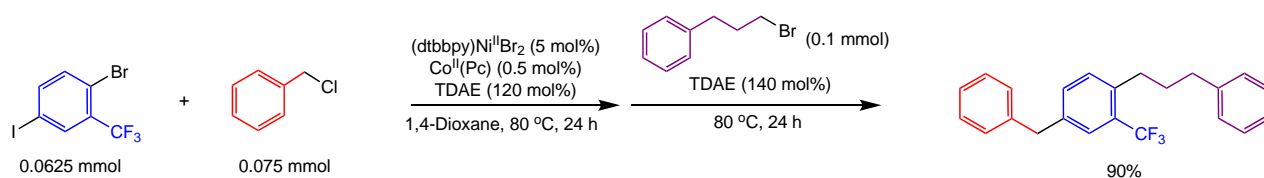


Figure S18. Additional reactions for alkyl halide substrate scope.

SXIX. Stoichiometric C(sp²)-C(sp³) Bond Formation with (dtbbpy)Ni^{II}(*o*-tol)I

Representative Procedure:

In a nitrogen filled glovebox, to a 1 dram vial equipped with a magnetic stir bar was added 6.8 mg (0.013 mmol) (dtbbpy)Ni^{II}(*o*-tol)I, 1.1 mg (0.0019 mmol) Co^{II}(Pc), 1.5 mL 1,4-dioxane, 3.3 mg (0.026 mmol) benzyl chloride, then 5.2 mg (0.026 mmol) TDAE. The vial was fit with a PTFE cap and stirred at room temperature for one hour. The reaction was then diluted with 0.5 mL of ethyl acetate (EtOAc). The mixture was passed through a short silica plug (~1.5 inches) in a glass pipette, which was rinsed with 5 mL EtOAc. The filtrate was concentrated to dryness and the crude residue was taken up in CDCl₃ with added hexamethylbenzene as an internal standard. The reaction yields were determined by ¹H NMR spectroscopy. For individual reaction conditions, see Table 4 in the manuscript.

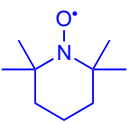
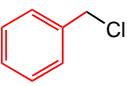
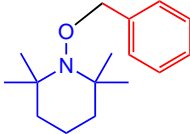
SXX. Radical Trapping Experiments with TEMPO

Representative Procedure:

In a nitrogen filled glovebox, to a 1 dram vial equipped with a magnetic stir bar was added 2.0 mg (0.013 mmol) TEMPO, 1.1 mg (0.0019 mmol) $\text{Co}^{\text{II}}(\text{Pc})$, 1.5 mL 1,4-dioxane, 3.3 mg (0.026 mmol) benzyl chloride, then 5.2 mg (0.026 mmol) TDAE. The vial was fit with a PTFE cap and stirred at room temperature for one hour. The reaction was then diluted with 0.5 mL of ethyl acetate (EtOAc). The mixture was passed through a short silica plug (~1.5 inches) in a glass pipette, which was rinsed with 5 mL EtOAc. The filtrate was concentrated to dryness and the crude residue was taken up in CDCl_3 with added hexamethylbenzene as an internal standard. The reaction yields were determined by ^1H NMR spectroscopy. For individual reaction conditions, see Table S11 below.

Data:

Table S11. Stoichiometric reaction of TEMPO with benzyl chloride under various reaction conditions.

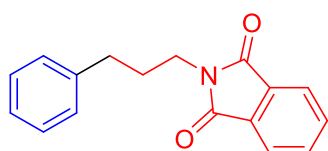
 0.013 mmol	+	 0.026 mmol	$\xrightarrow[\text{RT, 1 h}]{\text{Co}^{\text{II}}(\text{Pc}) (14 \text{ mol}\%) \text{ TDAE } (200 \text{ mol}\%) \text{ 1,4-Dioxane } (1.5 \text{ mL})}$	
Deviation From Conditions		Product Yield (%)		
None		41		
No $\text{Co}^{\text{II}}(\text{Pc})$		<1		
No $\text{Co}^{\text{II}}(\text{Pc})$ and no TDAE		<1		
100 mol% $\text{Co}^{\text{II}}(\text{Pc})$ and no TDAE		<1		

SXXI. Isolation Procedures and Characterization for Products of Two-Component Cross-Electrophile Coupling

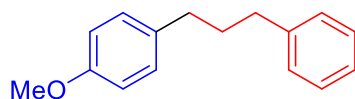
Procedure for Isolation Scale Reactions of Following Substrates:

See section SV for representative experimental setup. Reactions were typically performed on 0.1875 mmol scale of aryl electrophile (other reagents scaled linearly). See Figure 4 in the manuscript for individual reaction conditions. The reaction vial was removed from heat, allowed to cool to room temperature, and diluted with 0.5 mL of ethyl acetate (EtOAc). The mixture was passed through a short celite plug (~1.5 inches) in a glass pipette, which was rinsed with 5 mL EtOAc. The filtrate was concentrated to dryness and the crude residue was purified by silica gel column chromatography.

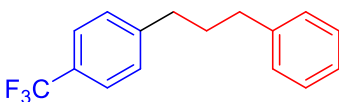
Aryl Electrophiles



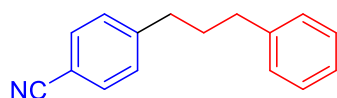
2-(3-phenylpropyl)isoindoline-1,3-dione, derived from **4a**: Eluent: gravity column in 10% EtOAc in petroleum ether. White solid, 83% yield (41.4 mg). ^1H NMR (400 MHz, CDCl_3) δ 7.84-7.82 (m, 2H), 7.71-7.70 (m, 2H), 7.27-7.24 (m, 2H), 7.25 (t, $J=7.4$ Hz, 2H), 7.20 (d, $J=7.1$ Hz, 2H), 7.14 (t, $J=7.2$ Hz, 1H), 3.75 (t, $J=7.2$ Hz, 2H), 2.69 (t, $J=8.0$ Hz, 2H), 2.04 (quintet, $J=8.0$ Hz, 2H). The ^1H NMR data are consistent with a previous literature report.^[4]



1-phenyl-3-(4-methoxyphenyl)propane, derived from **4b**: Eluent: 5% EtOAc in hexanes. Colorless oil, 70% yield (42.4 mg). ^1H NMR (400 MHz, CDCl_3) δ 7.29 (t, 2H), 7.20-7.18 (m, 3H), 7.11 (d, $J=8.5$ Hz, 2H), 6.84 (d, $J=8.5$ Hz, 2H), 3.79 (s, 3H), 2.67-2.59 (m, 4H), 1.94 (quintet, $J=7.8$ Hz, 2H). The ^1H NMR data are consistent with a previous literature report.^[5]

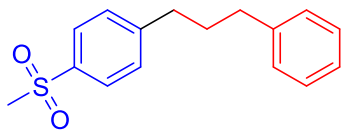


1-phenyl-3-(4-trifluoromethylphenyl)propane, derived from **4c**: Eluent: 100% pentane. Colorless oil, 88% yield (43.6 mg). ^1H NMR (400 MHz, CDCl_3) δ 7.55 (d, $J=8.0$ Hz, 2H), 7.32-7.29 (m, 4H), 7.23-7.19 (m, 3H), 2.74-2.65 (m, 4H), 1.99 (quintet, $J=7.8$ Hz, 2H). $^{19}\text{F}\{^1\text{H}\}$ NMR (470 MHz, CDCl_3) δ -62.29 (s). The ^1H NMR data are consistent with a previous literature report.^[6]

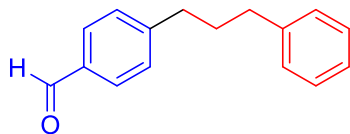


4-(3-phenylpropyl)benzonitrile, derived from **4d**: Eluent: 5% EtOAc in hexanes. Colorless oil, 86% yield (35.7 mg). ^1H NMR (400

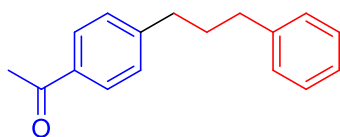
MHz, CDCl₃) δ 7.57 (d, J =8.1 Hz, 2H), 7.32-7.26 (m, 4H), 7.22-7.17 (m, 3H), 2.72-2.64 (m, 4H), 1.97 (quintet, J =7.8 Hz, 2H). The ¹H NMR data are consistent with a previous literature report.^[6]



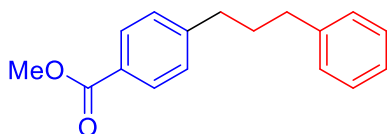
1-(methylsulfonyl)-4-(3-phenylpropyl)benzene, derived from **4e**: Eluent: 30% EtOAc in hexanes. Pale yellow oil, 93% yield (47.7 mg). ¹H NMR (400 MHz, CDCl₃) δ 7.85 (d, J =7.9 Hz, 2H), 7.37 (d, J =8.0 Hz, 2H), 7.31-7.26 (m, 2H), 7.22-7.17 (m, 3H), 3.04 (s, 3H), 2.74 (t, J =7.7 Hz, 2H), 2.66 (t, J =7.7 Hz, 2H), 1.99 (quintet, J =7.9 Hz, 2H). ¹³C{¹H} NMR (151 MHz, CDCl₃) δ 149.09, 141.71, 138.19, 129.51, 128.57, 128.53, 127.62, 126.13, 44.74, 35.45, 35.43, 32.66. (LRMS) GCMS EI (m/z) [M]⁺ calculated for [C₁₆H₁₈O₂S]⁺ 274.1; found 274.1.



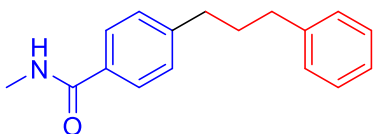
4-(3-phenylpropyl)benzaldehyde, derived from **4f**: Eluent: 5% EtOAc in hexanes. Colorless oil, 88% yield (37.0 mg). ¹H NMR (400 MHz, CDCl₃) δ 9.96 (s, 1H), 7.79 (d, J =8.1 Hz, 2H), 7.32 (d, J =8.0 Hz, 2H), 7.29-7.24 (m, 2H), 7.20-7.15 (m, 3H), 2.71 (t, J =7.7 Hz, 2H), 2.65 (t, J =7.7 Hz, 2H), 1.98 (quintet, J =7.8 Hz, 2H). The ¹H NMR data are consistent with a previous literature report.^[7]



4-(3-phenylpropyl)benzophenone, derived from **4g**: Eluent: 5% EtOAc in hexanes. Colorless oil, 89% yield (39.7 mg). ¹H NMR (400 MHz, CDCl₃) δ 7.89 (d, J =8.1 Hz, 2H), 7.31-7.27 (m, 4H), 7.21-7.17 (m, 3H), 2.73-2.64 (m, 4H), 2.59 (s, 3H), 1.98 (quintet, J =7.9 Hz, 2H). The ¹H NMR data are consistent with a previous literature report.^[8]

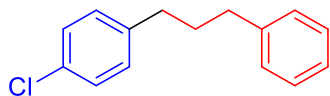


4-(3-phenylpropyl)methyl benzoate, derived from **4h**: Eluent: 5% EtOAc in hexanes. Colorless oil, 88% yield (41.9 mg). ¹H NMR (400 MHz, CDCl₃) δ 7.97 (d, J =8.0 Hz, 2H), 7.30-7.27 (t, J =7.4 Hz, 2H), 7.25 (d, J =8.1 Hz, 2H), 7.21-7.17 (m, 3H), 3.90 (s, 3H), 2.70 (t, J =7.8 Hz, 2H), 2.65 (t, J =7.8 Hz, 2H), 1.98 (quintet, J =7.7 Hz, 2H). The ¹H NMR data are consistent with a previous literature report.^[9]

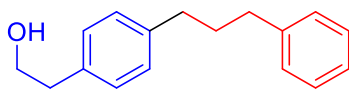


N-methyl-4-(3-phenylpropyl)benzamide, derived from **4i**: Eluent: 70% EtOAc in hexanes. White solid, 75% yield (35.5 mg). ¹H NMR (400 MHz, CDCl₃) δ 7.68 (d, J =8.1 Hz, 2H), 7.30-7.26 (m, 2H), 7.24-7.16 (m, 5H), 6.16 (br s, 1H), 3.00 (d, J =4.9 Hz, 3H), 2.66

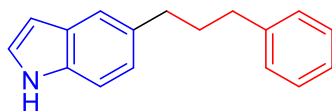
(quintet, $J=8.0$ Hz, 4H), 1.96 (quintet, $J=7.8$ Hz, 2H). $^{13}\text{C}\{^1\text{H}\}$ NMR (151 MHz, CDCl_3) δ 168.31, 146.14, 142.08, 132.31, 128.73, 128.54, 128.48, 127.03, 125.97, 35.46, 35.35, 32.80, 26.93. (LRMS) GCMS EI (m/z) [M] $^+$ calculated for $[\text{C}_{17}\text{H}_{19}\text{NO}]^+$ 253.2; found 253.2.



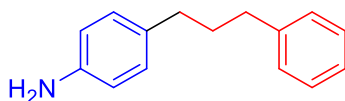
1-chloro-4-(3-phenylpropyl)benzene, derived from **4j**: Eluent: 100% pentane. Colorless oil, 67% yield (43.3 mg). ^1H NMR (400 MHz, CDCl_3) δ 7.36 (m, 2H), 7.31-7.29 (m, 2H), 7.25-7.22 (m, 3H), 7.16 (d, $J=8.3$ Hz, 2H), 2.71-2.66 (m, 4H), 1.99 (quintet, $J=7.8$ Hz, 2H). The ^1H NMR data are consistent with a previous literature report.^[10]



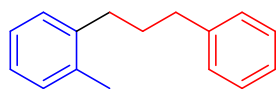
2-(4-(3-phenylpropyl)phenyl)ethanol, derived from **4k**: Eluent: 5% EtOAc in hexanes. Colorless oil, 70% yield (31.5 mg). ^1H NMR (400 MHz, CDCl_3) δ 7.28 (quartet, $J=7.2$ Hz, 2H), 7.21-7.18 (m, 3H), 7.15 (s, 4H), 3.85 (t, $J=6.5$ Hz, 2H), 2.84 (t, $J=6.6$ Hz, 2H), 2.65 (quartet, $J=7.3$ Hz, 4H), 1.96 (quintet, $J=7.8$ Hz, 2H), 1.46 (br s, 1H). $^{13}\text{C}\{^1\text{H}\}$ NMR (151 MHz, CDCl_3) δ 142.39, 140.60, 135.83, 129.10, 128.80, 128.56, 128.43, 125.86, 63.87, 38.92, 35.58, 35.16, 33.08. (LRMS) GCMS EI (m/z) [M] $^+$ calculated for $[\text{C}_{17}\text{H}_{20}\text{O}]^+$ 240.2; found 240.2.



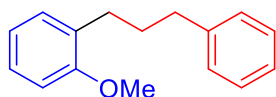
5-(3-phenylpropyl)-1H-indole, derived from **4l**: Eluent: 22% EtOAc in hexanes. Pale yellow oil, 73% yield (32.1 mg). ^1H NMR (400 MHz, CDCl_3) δ 8.01 (br s, 1H), 7.44 (s, 1H), 7.30-7.23 (m, 3H), 7.20-7.15 (m, 4H), 7.03 (d, $J=8.3$ Hz, 1H), 6.48 (br s, 1H), 2.75 (t, $J=7.9$ Hz, 2H), 2.67 (t, $J=7.9$ Hz, 2H), 2.01 (quintet, $J=7.8$ Hz, 2H). $^{13}\text{C}\{^1\text{H}\}$ NMR (151 MHz, CDCl_3) δ 142.77, 134.46, 133.80, 128.61, 128.38, 128.18, 125.75, 124.37, 120.02, 110.87, 102.40, 35.70, 35.63, 33.86. (LRMS) GCMS EI (m/z) [M] $^+$ calculated for $[\text{C}_{17}\text{H}_{17}\text{N}]^+$ 235.1; found 235.2.



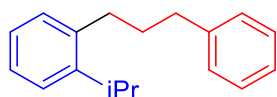
4-(3-phenylpropyl)aniline, derived from **4m**: Eluent: Gradient of 35-40% EtOAc in hexanes. Pale yellow oil, 71% yield (28.1 mg). ^1H NMR (400 MHz, CDCl_3) δ 7.28-7.24 (m, 2H), 7.17 (d, $J=6.8$ Hz, 3H), 6.96 (d, $J=8.1$ Hz, 2H), 6.61 (d, $J=8.1$ Hz, 2H), 3.50 (br s, 2H), 2.62 (t, $J=7.7$ Hz, 2H), 2.54 (t, $J=7.7$ Hz, 2H), 1.89 (quintet, $J=7.8$ Hz, 2H). The ^1H NMR data are consistent with a previous literature report.^[11]



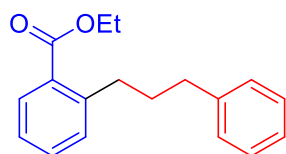
2-(3-phenylpropyl)toluene, derived from **4n**: Eluent: gradient of 0-5% diethyl ether in pentane. Colorless oil, 77% yield (30.4 mg). ^1H NMR (400 MHz, CDCl_3) δ 7.29 (t, $J=7.6$ Hz, 2H), 7.22-7.18 (m, 3H), 7.14-7.10 (m, 4H), 2.71 (t, $J=7.6$ Hz, 2H), 2.65 (t, $J=7.6$ Hz, 2H), 2.28 (s, 3H), 1.93 (quintet, $J=7.9$ Hz, 2H). The ^1H NMR data are consistent with a previous literature report.^[1]



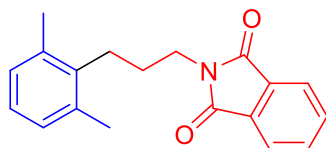
1-phenyl-3-(2-methoxyphenyl)propane, derived from **4o**: Eluent: gradient of 0-5% diethyl ether in pentane. Colorless oil, 76% yield (33.0 mg). ^1H NMR (400 MHz, CDCl_3) δ 7.29-7.25 (m, 2H), 7.21-7.12 (m, 5H), 6.90-6.83 (m, 2H), 3.80 (s, 3H), 2.67 (t, $J=7.7$ Hz, 4H), 1.93 (quintet, $J=7.8$, 2H). The ^1H NMR data are consistent with a previous literature report.^[12]



1-phenyl-3-(2-isopropylphenyl)propane, derived from **4p**: Eluent: Gradient of 0-3% diethyl ether in pentane. Colorless oil, 83% yield (37.1 mg). ^1H NMR (400 MHz, CDCl_3) δ 7.32-7.26 (m, 3H), 7.22-7.18 (m, 4H), 7.14-7.09 (m, 2H), 3.11 (septet, $J=6.9$ Hz, 1H), 2.71 (quartet, $J=7.9$ Hz, 4H), 1.93 (quintet, $J=7.9$ Hz, 2H), 1.22 (d, $J=6.9$ Hz, 6H). $^{13}\text{C}\{^1\text{H}\}$ NMR (151 MHz, CDCl_3) δ 146.69, 142.40, 139.15, 129.46, 128.54, 128.44, 126.40, 125.90, 125.65, 125.39, 36.03, 33.36, 32.57, 28.69, 24.19. (LRMS) GCMS EI (m/z) [M] $^+$ calculated for [$\text{C}_{18}\text{H}_{22}$] $^+$ 238.2; found 238.2.

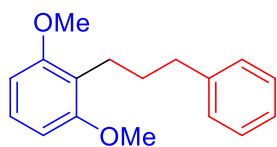


2-(3-phenylpropyl)ethyl benzoate, derived from **4q**: Eluent: 5% EtOAc in hexanes. Colorless oil, 77% yield (38.7 mg). ^1H NMR (400 MHz, CDCl_3) δ 7.86 (d, $J=7.4$ Hz, 1H), 7.40 (t, $J=8.6$ Hz, 1H), 7.30-7.16 (m, 7H), 4.34 (quartet, $J=7.1$ Hz, 2H), 3.01 (t, $J=7.9$ Hz, 2H), 2.70 (t, $J=7.9$ Hz, 2H), 1.95 (quintet, $J=7.9$ Hz, 2H), 1.39 (t, $J=7.1$ Hz, 3H). $^{13}\text{C}\{^1\text{H}\}$ NMR (151 MHz, CDCl_3) δ 167.99, 143.99, 142.47, 131.83, 130.99, 130.70, 130.12, 128.55, 128.39, 125.94, 125.82, 60.92, 36.07, 34.29, 33.53, 14.45. (LRMS) GCMS EI (m/z) [M] $^+$ calculated for [$\text{C}_{18}\text{H}_{20}\text{O}_2$] $^+$ 268.1; found 268.1.

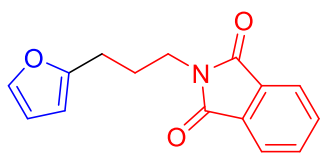


2-(3-(2,6-dimethylphenyl)propyl)isoindoline-1,3-dione, derived from **4r**: Eluent: gravity column in 10% EtOAc in petroleum ether. White solid, 87% yield (47.8 mg). ^1H NMR (400 MHz, CDCl_3) δ 7.87-7.85 (m, 2H), 7.73-7.71 (m, 2H), 6.98 (s, 3H), 3.82 (t, $J=7.3$ Hz, 2H), 2.69-2.66 (m, 2H), 2.29 (s, 6H), 1.89-1.83 (m, 2H). $^{13}\text{C}\{^1\text{H}\}$ NMR (151 MHz, CDCl_3) δ 168.49, 138.08, 136.00, 134.04, 132.18, 128.25, 125.90, 123.33, 38.45, 27.84, 27.14, 19.83. (LRMS)

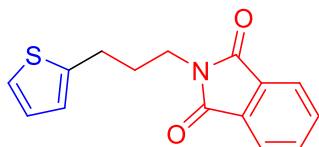
GCMS EI (m/z) [M]⁺ calculated for [$C_{19}H_{19}NO_2$]⁺ 293.1; found 293.1.



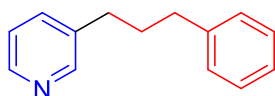
3-(3-phenylpropyl)-2,6-dimethoxybenzene, derived from **4s**: Eluent: 4% EtOAc in hexanes. Colorless oil, 73% yield (48.1 mg). ¹H NMR (400 MHz, CDCl₃) δ 7.25 (t, J =7.3 Hz, 2H), 7.21 (d, J =7.9 Hz, 2H), 7.15 (t, J =7.3 Hz, 1H), 7.11 (t, J =8.3 Hz, 1H), 6.53 (d, J =8.3 Hz, 1H), 3.78 (s, 6H), 2.72 (t, J =7.7 Hz, 2H), 2.66 (t, J =7.7 Hz, 2H), 1.82 (quintet, J =7.9 Hz, 2H). ¹³C{¹H} NMR (151 MHz, CDCl₃) δ 158.45, 143.21, 128.52, 128.21, 126.71, 125.53, 119.16, 103.77, 55.77, 36.11, 30.79, 22.99. (LRMS) GCMS EI (m/z) [M]⁺ calculated for [$C_{17}H_{20}O_2$]⁺ 256.2; found 256.1.



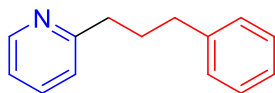
2-(3-(2-furanyl)propyl)isoindoline-1,3-dione, derived from **4t**: Eluent: gravity column in 10% EtOAc in petroleum ether. White solid, 72% yield (34.3 mg). ¹H NMR (400 MHz, CDCl₃) δ 7.85-7.83 (m, 2H), 7.72-7.70 (m, 2H), 7.26 (s, 1H), 6.23 (t, J =1.9 Hz, 1H), 6.04 (d, J =2.8 Hz, 1H), 3.76 (t, J =7.2 Hz, 2H), 2.70 (t, J =7.5 Hz, 2H), 2.05 (quintet, J =7.2 Hz, 2H). ¹³C{¹H} NMR (151 MHz, CDCl₃) δ 168.43, 154.78, 141.11, 133.99, 132.21, 123.27, 110.19, 105.32, 37.59, 26.90, 25.59. (LRMS) GCMS EI (m/z) [M]⁺ calculated for [$C_{15}H_{13}NO_3$]⁺ 255.1; found 255.1.



2-(3-(2-thiophenyl)propyl)isoindoline-1,3-dione, derived from **4u**: Eluent: gravity column in 10% EtOAc in petroleum ether. White solid, 73% yield (37.1 mg). ¹H NMR (400 MHz, CDCl₃) δ 7.84-7.83 (m, 2H), 7.71-7.70 (m, 2H), 7.09 (d, J =5.1 Hz, 1H), 6.88 (t, J =4.9 Hz, 1H), 6.83 (br s, 1H), 3.77 (t, J =7.1 Hz, 2H), 2.90 (t, J =7.7 Hz, 2H), 2.09 (quintet, J =7.4 Hz, 2H). The ¹H NMR data are consistent with a previous literature report.^[13]

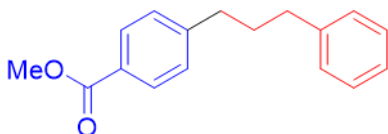


3-(3-phenylpropyl)pyridine, derived from **4v**: Eluent: 50% EtOAc in hexanes. Colorless oil, 71% yield (26.3 mg). ¹H NMR (400 MHz, CDCl₃) δ 8.46 (s, 2H), 7.49 (d, J =7.7 Hz, 1H), 7.29 (quartet, J =7.4 Hz, 2H), 7.22-7.17 (m, 4H), 2.66 (quartet, J =7.7 Hz, 4H), 1.97 (quintet, J =7.8 Hz, 2H). The ¹H NMR data are consistent with a previous literature report.^[14]

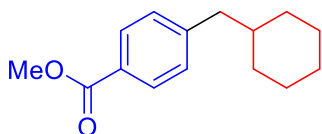


2-(3-phenylpropyl)pyridine, derived from **4w**: Eluent: 20% EtOAc and 1% Et₃N in hexanes. Colorless oil, 41% yield (37.0 mg). Isolated yield accounts for a roughly 1% impurity of 4,4'-diterbutyl-2,2'-bipyridine. ¹H NMR (400 MHz, CDCl₃) δ 8.54 (d, *J*=4.4 Hz, 1H), 7.58 (td, *J*=7.7, 1.7 Hz, 1H), 7.29-7.26 (m, 2H), 7.20-7.16 (m, 3H), 7.13 (d, *J*=7.8, 1H), 7.11-7.08 (m, 1H), 2.83 (t, *J*=7.8 Hz, 2H), 2.69 (t, *J*=7.8 Hz, 2H), 2.08 (quintet, *J*=7.8, 2H). The ¹H NMR data are consistent with a previous literature report.^[15]

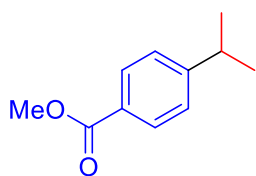
Alkyl Electrophiles



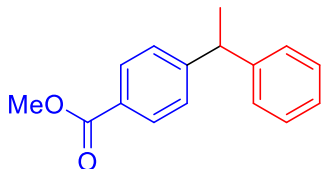
4-(3-phenylpropyl)methyl benzoate, derived from **4x**: Eluent: 10% EtOAc in hexanes. Colorless oil, 82% yield (39.2 mg). ¹H NMR (400 MHz, CDCl₃) δ 7.96 (d, *J*=8.1 Hz, 2H), 7.28 (t, *J*=7.4 Hz, 2H), 7.24 (d, *J*=8.0 Hz, 2H), 7.20-7.17 (m, 3H), 3.90 (s, 3H), 2.70 (t, *J*=7.8 Hz, 2H), 2.65 (t, *J*=7.8 Hz, 2H), 1.97 (quintet, *J*=7.6 Hz, 2H). The ¹H NMR data are consistent with a previous literature report.^[9]



Methyl 4-(cyclohexylmethyl)benzoate, derived from **4y**: Eluent: gravity column in 10% EtOAc in hexanes. Colorless oil, 87% yield (40.4 mg). ¹H NMR (400 MHz, CDCl₃) δ 7.94 (d, *J*= Hz, 2H), 7.20 (d, *J*= Hz, 2H), 3.90 (s, 3H), 2.53 (d, *J*= Hz, 2H), 1.69-1.64 (m, 5H), 1.57-1.51 (m, 1H), 1.22-1.13 (m, 3H), 0.97-0.91 (m, 2H). ¹³C{¹H} NMR (151 MHz, CDCl₃) δ 167.34, 147.13, 129.30, 127.74, 52.07, 44.24, 39.77, 33.23, 26.59, 26.37. (LRMS) GCMS EI (*m/z*) [*M*]⁺ calculated for [C₁₅H₂₀O₂]⁺ 232.2; found 232.2.



Methyl 4-isopropylbenzoate, derived from **4z**: Eluent: 40% EtOAc in hexanes by preparative TLC. Pale yellow oil, 54% yield (18.1 mg). ¹H NMR (400 MHz, CDCl₃) δ 7.96 (d, *J*=8.3 Hz, 2H), 7.29 (d, *J*= 8.2 Hz, 2H), 3.90 (s, 3H), 2.96 (quintet, *J*=6.9 Hz, 1H), 1.27 (d, *J*=6.9 Hz, 6H). The ¹H NMR data are consistent with a previous literature report.^[16]



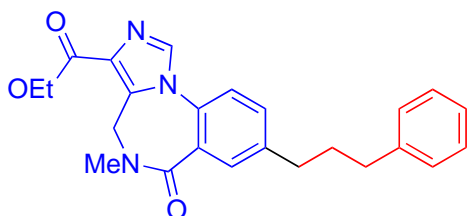
Methyl 4-(1-phenylethyl)benzoate, derived from **4aa**: Eluent: 5% EtOAc in hexanes. Colorless oil, 46% yield (20.4 mg). ¹H NMR (400 MHz, CDCl₃) δ 7.96 (d, *J*=8.3 Hz, 2H), 7.31-7.28 (m, 4H), 7.22-7.19 (m, 3H), 4.21 (quartet, *J*=7.2 Hz, 1H), 3.90 (s, 3H), 1.66 (d, *J*=7.2 Hz, 3H). The ¹H NMR data are consistent with a previous literature report.^[17]

SXXII. Isolation Procedures and Characterization for Products of Two-Component Cross-Electrophile Coupling with Drug-Like Aryl Halides

General Information:

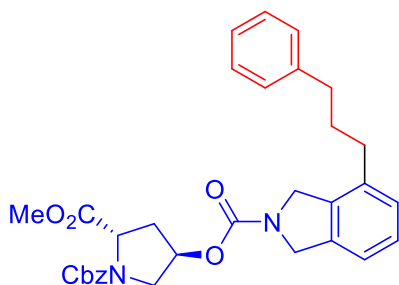
Products derived from the cross-electrophile coupling of 1-bromo-3-phenylpropane with aryl halides **5a** and **5f** were isolated using silica gel chromatography according to the corresponding procedures (see below for product derived from **5a** and see section SXV for product derived from **5f**).

Products derived from the cross-electrophile coupling of 1-bromo-3-phenylpropane with all other drug-like aryl halides were isolated from purification of the combined fractions for a given aryl halide from HTE experiments (see section SXII for representative HTE experimental setup). This mixture was purified by initial filtration using a 0.45 μ M syringe filter and followed by preparatory scale reverse-phase HPLC (aqueous phase: 8% NH_4OH , organic phase: MeCN, column: Waters XBridge Prep C18, 5 μ M, 19x100 mm, unless otherwise specified). The isolated products were used to confirm the ^1H NMR yields reported in Figure 5 (see section SXXIII). The products were purified using mass-directed purification, with priority weighted on purity, not material recovery, so in some cases, only milligram quantities of products were isolated, obscuring the physical appearance of some samples. In these cases, the sample is described as: “oil (residue)”.

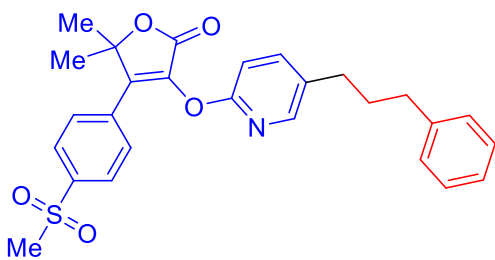


Product derived from 5a, Figure 5: The isolation scale experimental setup follows that which is described in section SV on a 0.100 mmol scale of aryl halide (all other reagents scaled linearly), see Figure 5 exact reaction conditions. The reaction vial was removed from heat, allowed to cool to room temperature, and diluted with 0.5 mL of ethyl acetate (EtOAc). The mixture was passed through a short celite plug (~1.5 inches) in a glass pipette, which was rinsed with 5 mL EtOAc. The filtrate was concentrated to dryness and the crude residue was purified by silica gel column chromatography. Eluent: 100% EtOAc. Off-white powder, 72% yield (29.0 mg). ^1H NMR (400 MHz, CDCl_3) δ 7.87 (d, $J=6.6$ Hz, 2H), 7.42 (d, $J=8.2$ Hz, 1H), 7.33-7.26 (m, 3H), 7.20-7.16 (m, 3H), 5.17 (br s, 1H), 4.42-4.35 (br m, overlapping signals, 3H), 3.23 (s, 3H), 2.74 (t, $J=7.6$ Hz, 2H), 2.68 (t, $J=7.6$ Hz, 2H), 2.01 (quintet,

$J=7.7$ Hz, 2H), 1.44 (t, $J=7.2$ Hz, 3H). $^{13}\text{C}\{^1\text{H}\}$ NMR (151 MHz, CDCl_3) δ 166.77, 163.21, 143.36, 141.72, 135.68, 135.00, 132.83, 132.38, 130.05, 129.01, 128.64, 128.51, 126.06, 121.89, 61.05, 42.51, 35.97, 35.45, 34.84, 32.64, 14.52. (HRMS) TOF MS ES+ (m/z) $[\text{M}+\text{H}]^+$ calculated for $[\text{C}_{24}\text{H}_{25}\text{N}_3\text{O}_2+\text{H}]^+$ 404.1969; found 404.1962.

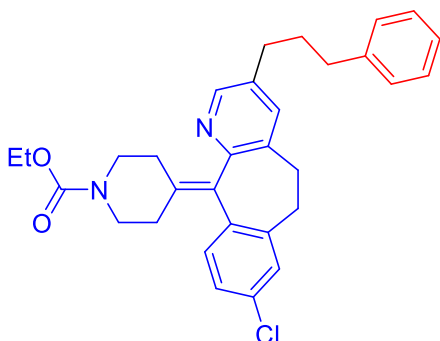


Product derived from 5b, Figure 5: Pale yellow oil. Purification method: 25 mL/min, 12-minute run, ramp from 52% to 82% MeCN. ^1H NMR (400 MHz, DMSO-d_6) δ 7.38-7.25 (m, 7H), 7.24-7.10 (m, 6H), 5.20 (br s, 1H), 5.15-4.98 (m, overlapping signals, 2H), 4.66-4.56 (m, 3H), 4.52-4.41 (m, 2H), 3.77-3.63 (m, overlapping signals, 3H), 3.58 (d, $J=7.1$ Hz, 1H), 2.61 (quartet, $J=7.7$ Hz, 2H), 2.55 (t, $J=7.8$ Hz, 1H), 2.48-2.42 (br m, overlapping with DMSO, 1H), 2.28-2.17 (m, 1H), 1.84 (quintet, $J=7.7$ Hz, 2H). $^{13}\text{C}\{^1\text{H}\}$ NMR (151 MHz, DMSO-d_6) δ 172.45, 172.09, 154.07, 153.48, 153.42, 153.39, 153.37, 141.80, 141.70, 136.73, 136.68, 136.64, 136.48, 136.42, 136.15, 135.26, 134.77, 128.36, 128.33, 128.27, 127.86, 127.84, 127.80, 127.73, 127.37, 126.97, 125.75, 120.26, 120.24, 73.19, 72.49, 66.44, 66.40, 66.27, 57.74, 57.66, 57.30, 57.23, 52.68, 52.42, 52.24, 52.18, 52.11, 52.09, 51.08, 50.41, 36.29, 36.21, 35.26, 35.17, 34.88, 34.68, 31.98, 31.56, 31.17, 30.96. Complexity observed in ^1H NMR and ^{13}C NMR due to presence of rotamers and possibly diastereomers.^[18] (LRMS) LCMS ES+ (m/z) $[\text{M}+\text{H}]^+$ calculated for $[\text{C}_{32}\text{H}_{34}\text{N}_2\text{O}_6+\text{H}]^+$ 543.2; found 543.5.

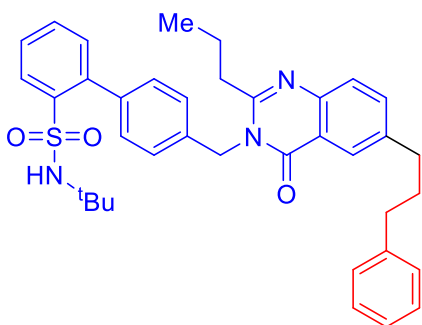


Product derived from 5c, Figure 5: colorless oil (residue). Purification method: 25 mL/min, 8-minute run, ramp from 45% to 80% MeCN. ^1H NMR (400 MHz, CDCl_3) δ 8.00-7.97 (m, 2H), 7.94 (d, $J=2.3$ Hz, 1H), 7.77-7.76 (m, 2H), 7.53 (dd, $J=8.4$, 2.4 Hz, 1H), 7.30-7.27 (m, 2H), 7.21-7.16 (m, 3H), 6.93 (d, $J=8.4$ Hz, 1H), 3.05 (s, 3H), 2.65 (t, $J=7.7$ Hz, 2H), 2.59 (t, $J=7.9$ Hz, 2H), 1.92 (quintet, $J=7.8$ Hz, 2H), 1.76 (s, 6H). $^{13}\text{C}\{^1\text{H}\}$ NMR (151 MHz, CDCl_3) δ 166.06, 159.82, 148.20, 146.93, 141.79, 141.36, 140.08, 138.16, 135.16, 133.66, 129.09, 128.53, 128.52, 128.00, 126.06, 110.76, 84.42, 44.49, 35.36, 32.72, 31.66, 26.55. (LRMS) LCMS ES+ (m/z)

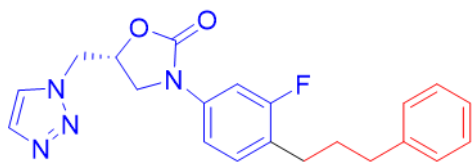
$[M+H]^+$ calculated for $[C_{27}H_{27}NO_5S]^+$ 478.17; found 478.0.



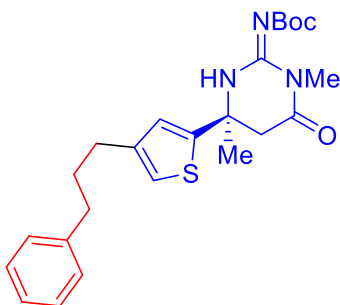
Product derived from 5d, Figure 5: Yellow oil. Purification method: 25 mL/min, 8-minute run, ramp from 65% to 98% MeCN. 1H NMR (400 MHz, $CDCl_3$) δ 8.21 (d, $J=7.1$ Hz, 1H), 7.26-7.21 (m, 3H), 7.17-7.11 (m, 4H), 7.10-7.08 (m, 2H), 4.11 (quartet, $J=7.7$ Hz, 2H), 3.79 (br s, 2H), 3.39-3.33 (m, 1H), 3.31-3.25 (m, 1H), 3.11-3.06 (m, 2H), 2.82-2.72 (m, 2H), 2.63 (t, $J=8.0$ Hz, 2H), 2.56 (t, $J=8.0$ Hz, 2H), 2.49-2.44 (m, 1H), 2.32-2.29 (br m, 3H), 1.91 (quintet, $J=7.7$ Hz, 2H), 1.22 (t, $J=7.1$ Hz, 3H). $^{13}C\{^1H\}$ NMR (151 MHz, $CDCl_3$) δ 155.62, 154.37 (br s), 146.69 (br s), 141.82, 139.78, 138.18, 137.77 (br s), 137.61 (br s), 136.22, 134.06 (br s), 132.95, 130.53, 128.97, 128.51, 128.50, 126.29, 126.03, 61.44, 44.91, 35.48, 32.59, 32.15, 31.75, 31.70, 30.90, 30.66, 14.82. (HRMS) TOF MS ES+ (m/z) $[M+H]^+$ calculated for $[C_{31}H_{33}ClN_2O_2+H]^+$ 501.2303; found 501.2300.



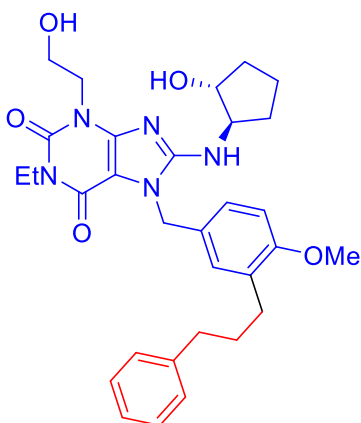
Product derived from 5e, Figure 5: Light brown solid. Purification method: 25 mL/min, 8-minute run, ramp from 65% to 98% MeCN. 1H NMR (400 MHz, $DMSO-d_6$) δ 8.01 (d, $J=7.9$ Hz, 1H), 7.99 (s, 1H), 7.70-7.68 (m, 1H), 7.63-7.58 (m, 2H), 7.57-7.53 (m, 1H), 7.38 (d, $J=8.2$ Hz, 2H), 7.28 (t, $J=7.2$ Hz, 3H), 7.23-7.16 (m, 5H), 6.57 (s, 1H), 5.45 (br s, 2H), 2.79-2.74 (m, 4H), 2.63 (t, $J=7.8$ Hz, 2H), 1.95 (quintet, $J=7.6$ Hz, 2H), 1.75 (sextet, $J=7.4$ Hz, 2H), 0.95-0.92 (m, overlapping signals, 12H). $^{13}C\{^1H\}$ NMR (151 MHz, $DMSO-d_6$) δ 161.65, 156.52, 145.32, 142.06, 141.82, 140.55, 139.59, 138.77, 135.84, 135.17, 132.59, 131.76, 129.64, 128.31, 128.29, 128.05, 127.75, 126.92, 125.76, 125.56, 125.19, 119.63, 53.34, 45.35, 35.73, 34.66, 34.41, 32.62, 29.29, 19.45, 13.57. (HRMS) TOF MS ES+ (m/z) $[M+H]^+$ calculated for $[C_{37}H_{41}N_3O_3S+H]^+$ 608.2941; found 608.2947.



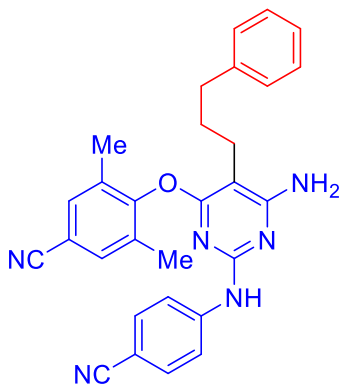
Product derived from 5f, Figure 5: see section SXXI for purification and characterization data.



Product derived from 5g, Figure 5: white solid. Purification method: 25 mL/min, 12-minute run, ramp from 53% to 83% MeCN. ^1H NMR (400 MHz, DMSO- d_6) δ 7.29-7.26 (m, 2H), 7.20-7.16 (m, 3H), 7.08 (s, 1H), 6.93 (s, 1H), 3.33 (s, 1H), 3.19-3.11 (m, 2H), 3.04 (s, 3H), 2.57 (t, $J=7.8$ Hz, 2H), 2.52 (t, overlapping with DMSO, $J=7.7$ Hz, 2H), 1.84 (quintet, $J=7.9$ Hz, 2H), 1.68 (s, 3H), 1.43 (s, 9H). $^{13}\text{C}\{^1\text{H}\}$ NMR (151 MHz, DMSO- d_6) δ 167.66, 163.11, 156.85, 148.17, 142.45, 141.85, 128.31, 128.27, 125.72, 125.23, 119.74, 78.55, 52.90, 44.42, 34.76, 31.48, 29.49, 29.45, 27.91. (HRMS) TOF MS ES+ (m/z) [$\text{M}+\text{H}$] $^+$ calculated for $[\text{C}_{24}\text{H}_{31}\text{N}_3\text{O}_3\text{S}+\text{H}]^+$ 442.2159; found 442.2164.



Product derived from 5h, Figure 5: white solid. Purification method: 25 mL/min, 12-minute run, ramp from 40% to 70% MeCN. ^1H NMR (400 MHz, DMSO- d_6) δ 7.28-7.25 (m, 2H), 7.18-7.16 (m, 4H), 7.12-7.10 (m, 1H), 6.96 (d, $J=$ Hz, 1H), 6.89 (d, $J=$ Hz, 1H), 5.22 (s, 2H), 4.81 (t, $J=$ Hz, 1H), 4.78 (d, $J=$ Hz, 1H), 3.98-3.94 (m, 3H), 3.91-3.82 (m, 3H), 3.72 (s, 3H), 3.60 (quartet, $J=$ Hz, 2H), 2.56 (t, $J=$ Hz, 2H), 2.05-1.98 (m, 1H), 1.85-1.74 (m, 3H), 1.66-1.56 (m, 2H), 1.48-1.42 (m, 2H), 1.05 (t, $J=$ Hz, 3H). $^{13}\text{C}\{^1\text{H}\}$ NMR (151 MHz, DMSO- d_6) δ 156.44, 153.42, 152.54, 150.39, 148.66, 141.95, 129.52, 128.98, 128.84, 128.22, 126.43, 125.66, 110.58, 101.14, 76.12, 61.42, 57.76, 55.32, 44.73, 44.56, 35.11, 34.89, 32.39, 30.82, 29.88, 28.92, 20.55, 13.31. (HRMS) TOF MS ES+ (m/z) [$\text{M}+\text{H}$] $^+$ calculated for $[\text{C}_{31}\text{H}_{39}\text{N}_5\text{O}_5+\text{H}]^+$ 562.3024; found 562.3029.



Product derived from 5i, Figure 5: white solid. First purification: 0.1% TFA aqueous phase, 25 mL/min, 12-minute run, ramp from 45% to 75% MeCN (column: Waters Sunfire Prep C18, 5 μ M, 19x100 mm). Second purification: 0.8% NH₄OH aqueous phase, 25 mL/min, 15 minute run, 48% to 78% MeCN. ¹H NMR (400 MHz, DMSO-d₆) δ 9.33 (s, 1H), 7.71 (s, 2H), 7.50 (d, J =8.6 Hz, 2H), 7.36 (d, J =8.9 Hz, 2H), 7.28-7.25 (t, J =7.3 Hz, 2H), 7.22 (d, J =6.9 Hz, 2H), 7.15 (t, J =7.1 Hz, 1H), 6.67 (s, 2H) 2.73-2.69 (t, J =8.0 Hz, 2H), 2.66-2.63 (t, J =7.6 Hz, 2H), 2.08 (s, 6H), 1.82 (quintet, J =7.2 Hz, 2H). ¹³C{¹H} NMR (151 MHz, DMSO-d₆) δ 165.02, 164.23, 156.11, 154.67, 145.50, 142.37, 132.89, 132.36, 132.28, 128.30, 128.12, 125.65, 119.68, 118.82, 117.56, 107.65, 101.14, 91.39, 35.12, 30.27, 22.26, 15.93. (HRMS) TOF MS ES+ (m/z) [M+H]⁺ calculated for [C₂₉H₂₆N₆O+H]⁺ 475.2241; found 475.2246.

SXXIII. Procedure for ¹H NMR Yields of Products from Two-Component Cross-Electrophile Coupling with Drug-Like Aryl Halides

Procedure:

See section SV for representative experimental setup and workup, but reactions were performed on 0.03 mmol scale of aryl electrophile at 0.1 M in 1,4-dioxane for 36 hours (other reagents scaled linearly). For individual reaction conditions and yields, see Figure 5 in the manuscript.

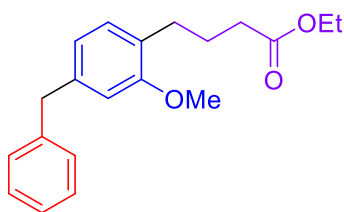
General Comments:

Optimized reaction conditions were determined through HTE (see section SXII), so reactions to determine ¹H NMR yields were not performed in duplicate as long as results agreed well with data obtained from HTE optimization. In the case of aryl halide **5i**, the reaction was optimized using ¹H NMR yields beyond the initial optimization performed using HTE. As a result, this reaction was performed in duplicate to report a yield as the average of two trials.

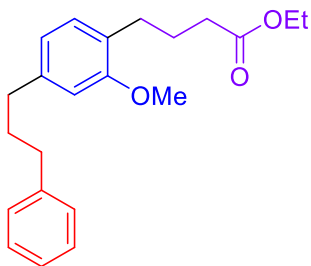
SXXIV. Isolation Procedures and Characterization for Products of Two-step One-Pot Three-Component Component Coupling

Procedure:

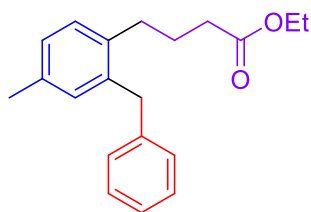
See section SXVII for representative experimental setup, but reactions were performed on 0.125 mmol scale of aryl electrophile (other reagents scaled linearly). See Table 2 in manuscript for individual reaction conditions. The reaction vial was removed from heat, allowed to cool to room temperature, and diluted with 0.5 mL of ethyl acetate (EtOAc). The mixture was passed through a short celite plug (~1.5 inches) in a glass pipette, which was rinsed with 5 mL EtOAc. The filtrate was concentrated to dryness and the crude residue was purified by silica gel column chromatography.



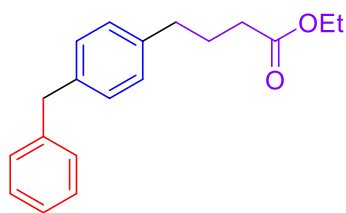
Ethyl 4-(4-benzyl-3-methoxyphenyl)butanoate, Table 2, Entry 1: Eluent: 10% EtOAc in hexanes. Colorless oil, 82% yield (32.0 mg). ^1H NMR (400 MHz, CDCl_3) δ 7.31-7.26 (m, 2H), 7.21-7.19 (m, 3H), 7.03 (d, $J=7.5$ Hz, 1H), 6.71 (d, $J=7.6$ Hz, 1H), 6.66 (s, 1H), 4.11 (quartet, $J=7.1$ Hz, 2H), 3.95 (s, 2H), 3.76 (s, 3H), 2.61 (t, $J=7.6$ Hz, 2H), 2.31 (t, $J=7.7$ Hz, 2H), 1.90 (quintet, $J=7.5$ Hz, 2H), 1.24 (t, $J=7.1$ Hz, 3H). $^{13}\text{C}\{^1\text{H}\}$ NMR (151 MHz, CDCl_3) δ 173.92, 157.64, 141.30, 140.37, 130.06, 128.99, 128.57, 127.67, 126.17, 120.94, 111.12, 60.29, 55.31, 42.07, 34.11, 29.37, 25.23, 14.41. (LRMS) GCMS EI (m/z) [M] $^+$ calculated for $[\text{C}_{20}\text{H}_{24}\text{O}_3]^+$ 312.2; found 312.2.



Ethyl 4-(3-methoxy-4-(3-phenylpropyl)phenyl)butanoate, Table 2, Entry 2: Eluent: 5% EtOAc in hexanes. Colorless oil, 84% yield (35.8 mg). ^1H NMR (400 MHz, CDCl_3) δ 7.26 (quartet, $J=6.8$ Hz, 2H), 7.19-7.15 (m, 3H), 7.00 (d, $J=7.5$ Hz, 1H), 6.69 (d, $J=7.6$ Hz, 1H), 6.64 (s, 1H), 4.10 (quartet, $J=7.1$ Hz, 2H), 3.78 (s, 3H), 2.67-2.58 (m, overlapping signals, 6H), 2.30 (t, $J=7.7$ Hz, 2H), 1.98-1.85 (m, 4H), 1.23 (t, $J=7.1$ Hz, 3H). $^{13}\text{C}\{^1\text{H}\}$ NMR (151 MHz, CDCl_3) δ 173.92, 157.54, 142.44, 141.67, 129.93, 128.58, 128.43, 127.29, 125.86, 120.36, 110.70, 60.27, 55.33, 35.65, 34.13, 33.08, 29.37, 25.29, 14.41. (LRMS) GCMS (m/z) EI [M] $^+$ calculated for $[\text{C}_{22}\text{H}_{28}\text{O}_3]^+$ 340.2; found 340.2.



Ethyl 4-(2-benzyl-4-methylphenyl)butanoate, Table 2, Entry 3: Eluent: 5% EtOAc in hexanes. Colorless oil, 91% yield (26.6 mg). ^1H NMR (400 MHz, CDCl_3) δ 7.28-7.24 (m, 2H), 7.19-7.15 (m, 1H), 7.12-7.06 (m, 3H), 7.00 (d, $J=7.8$ Hz, 1H), 6.93 (s, 1H), 4.10 (quartet, $J=7.1$ Hz, 2H), 3.99 (s, 2H), 2.57 (t, $J=8.1$ Hz, 2H), 2.30-2.26 (m, overlapping signals, 5H), 1.81 (quintet, $J=7.7$ Hz, 2H), 1.23 (t, $J=7.1$ Hz, 3H). $^{13}\text{C}\{^1\text{H}\}$ NMR (151 MHz, CDCl_3) δ 173.59, 141.11, 138.34, 136.94, 135.81, 131.43, 129.52, 128.80, 128.49, 127.42, 126.02, 60.38, 38.85, 34.13, 31.92, 26.19, 21.13, 14.39. (LRMS) GCMS EI (m/z) $[\text{M}]^+$ calculated for $[\text{C}_{20}\text{H}_{24}\text{O}_2]^+$ 296.2; found 296.1.



Ethyl 4-(4-benzylphenyl)butanoate, Table 2, Entry 4: Eluent: 8% EtOAc in hexanes. Colorless oil, 70% yield (24.8 mg). ^1H NMR (400 MHz, CDCl_3) δ 7.30-7.26 (m, 2H), 7.21-7.18 (m, 3H), 7.10 (s, 4H), 4.12 (quartet, $J=7.1$ Hz, 2H), 3.95 (s, 2H), 2.62 (t, $J=7.5$ Hz, 2H), 2.31 (t, $J=7.5$ Hz, 2H), 1.94 (quintet, $J=7.5$ Hz, 2H), 1.25 (t, $J=7.1$ Hz, 3H). $^{13}\text{C}\{^1\text{H}\}$ NMR (151 MHz, CDCl_3) δ 173.64, 141.40, 139.28, 138.87, 129.04, 128.71, 128.57, 126.15, 60.38, 41.69, 34.88, 33.86, 26.71, 14.40. (LRMS) GCMS EI (m/z) $[\text{M}]^+$ calculated for $[\text{C}_{19}\text{H}_{22}\text{O}_2]^+$ 282.2; found 282.1.

SXXV. NMR Spectra of Isolated Products

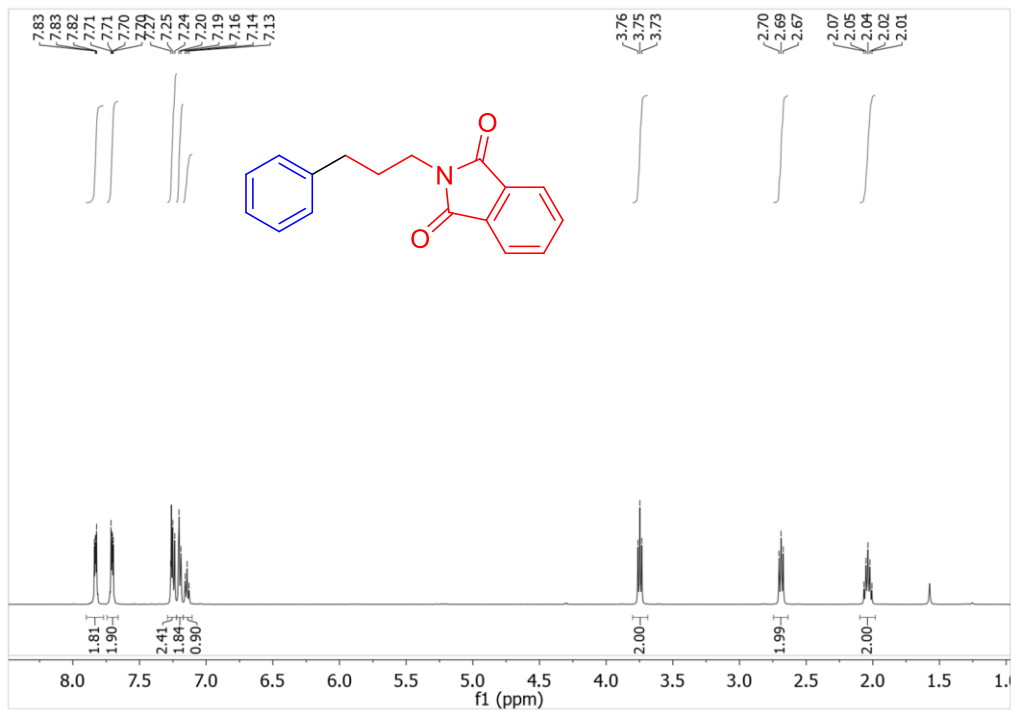


Figure S19. ¹H NMR spectrum (400 MHz, CDCl₃) of 2-(3-phenylpropyl)isoindoline-1,3-dione, derived from substrate **4a**.

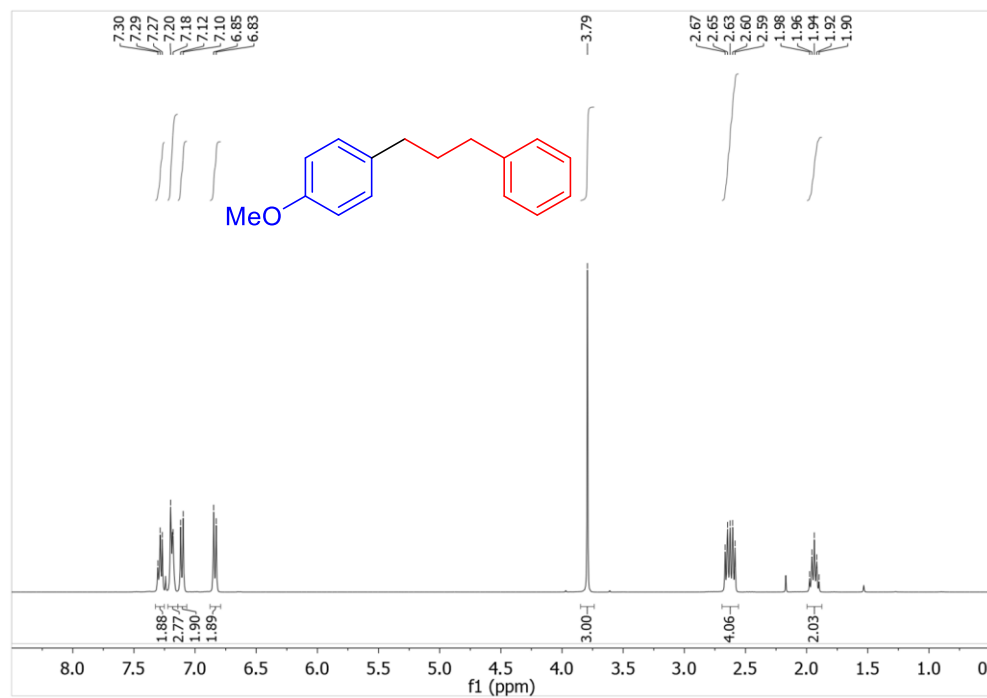


Figure S20. ¹H NMR spectrum (400 MHz, CDCl₃) of 1-phenyl-3-(4-methoxyphenyl)propane, derived from substrate **4b**.

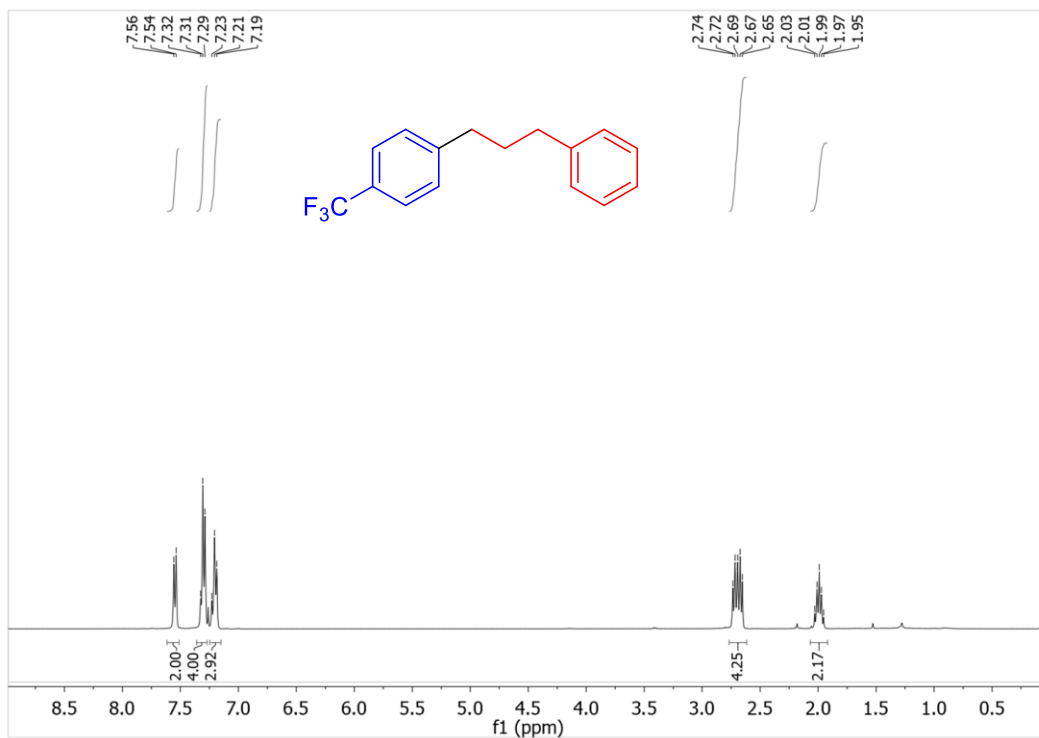


Figure S21. ¹H NMR spectrum (400 MHz, CDCl₃) of 1-phenyl-3-(4-trifluoromethylphenyl)propane, derived from substrate **4c**.

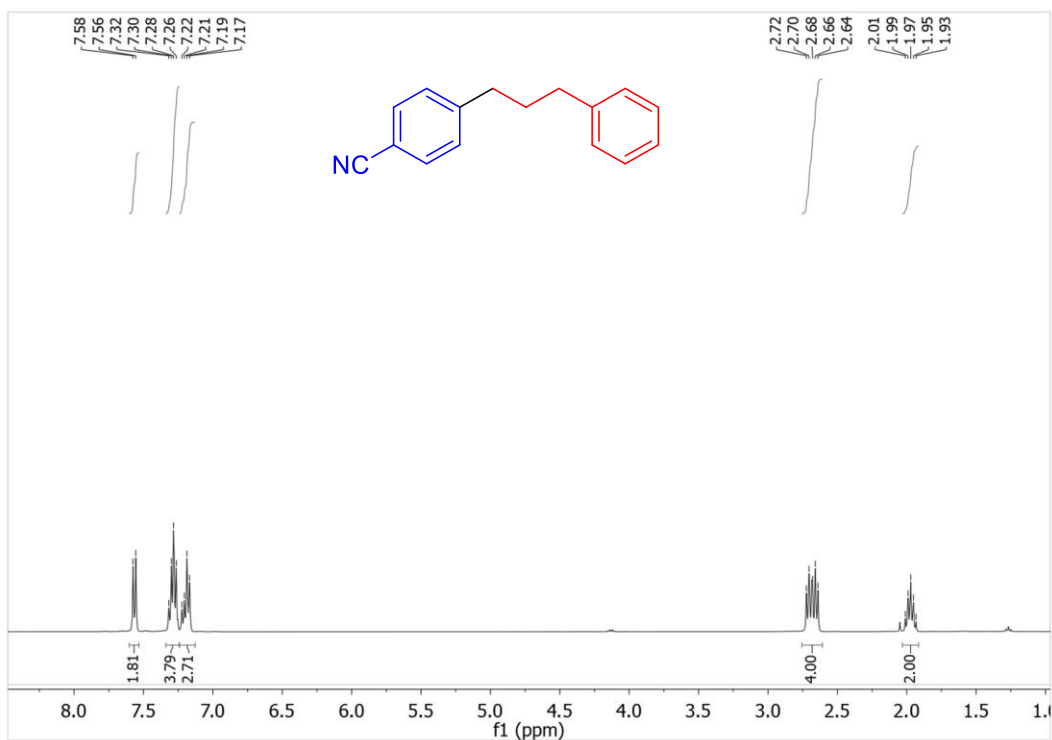


Figure S22. ¹H NMR spectrum (400 MHz, CDCl₃) of 4-(3-phenylpropyl)benzonitrile, derived from substrate **4d**.

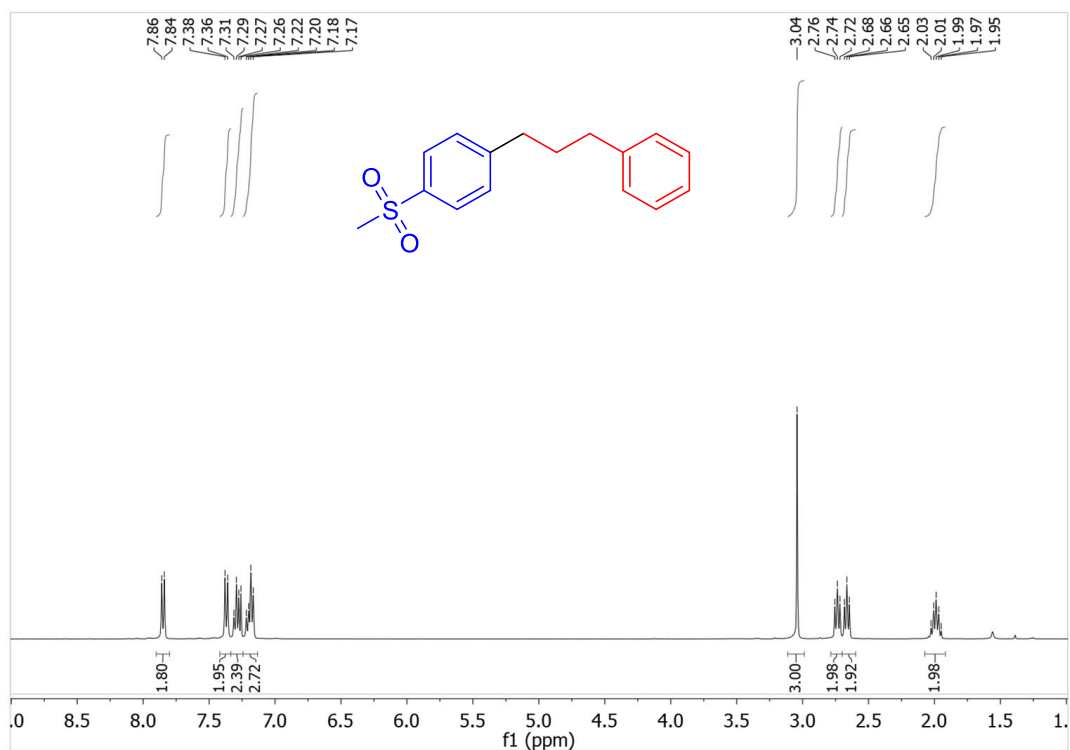


Figure S23. ^1H NMR spectrum (400 MHz, CDCl_3) of 1-(methylsulfonyl)-4-(3-phenylpropyl)benzene, derived from substrate **4e**.

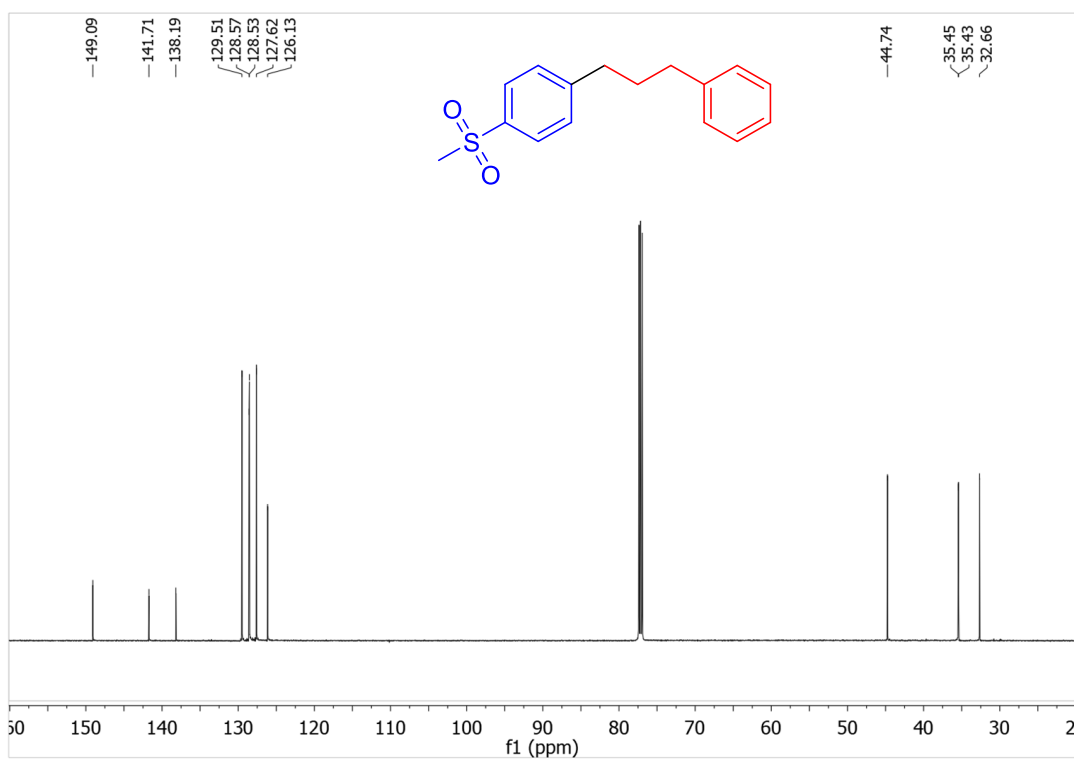


Figure S24. $^{13}\text{C}\{^1\text{H}\}$ NMR spectrum (151 MHz, CDCl_3) of 1-(methylsulfonyl)-4-(3-phenylpropyl)benzene, derived from substrate **4e**.

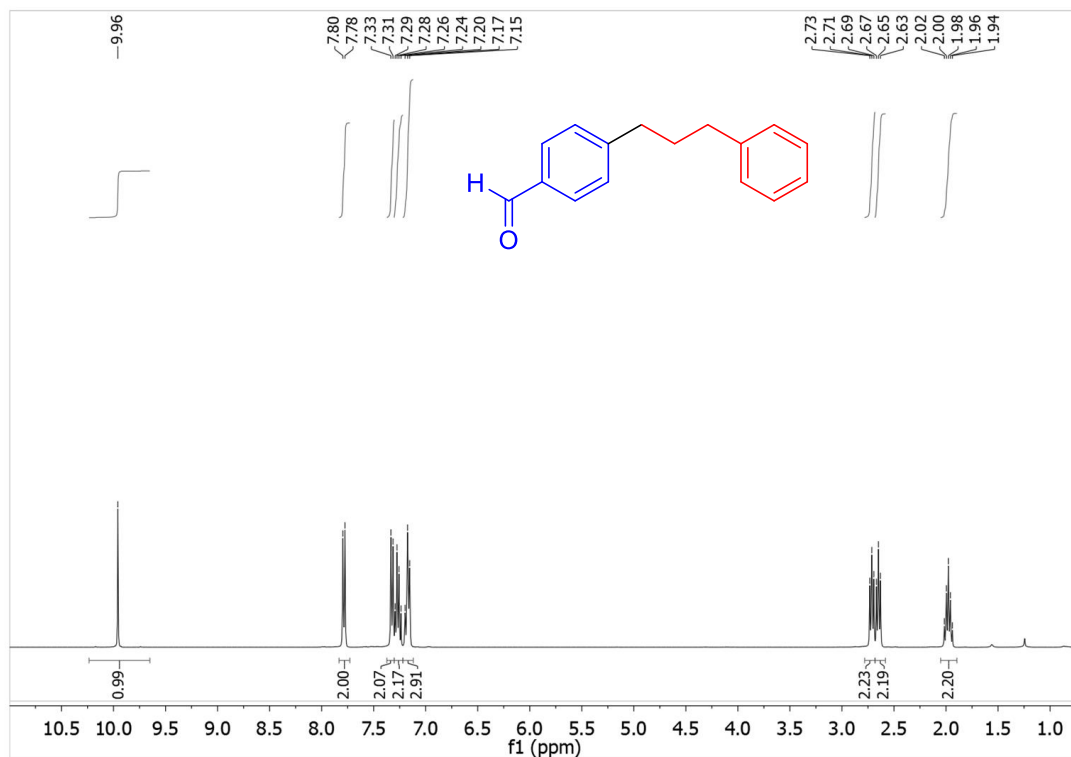


Figure S25. ¹H NMR spectrum (400 MHz, CDCl₃) of 4-(3-phenylpropyl)benzaldehyde, derived from substrate **4f**.

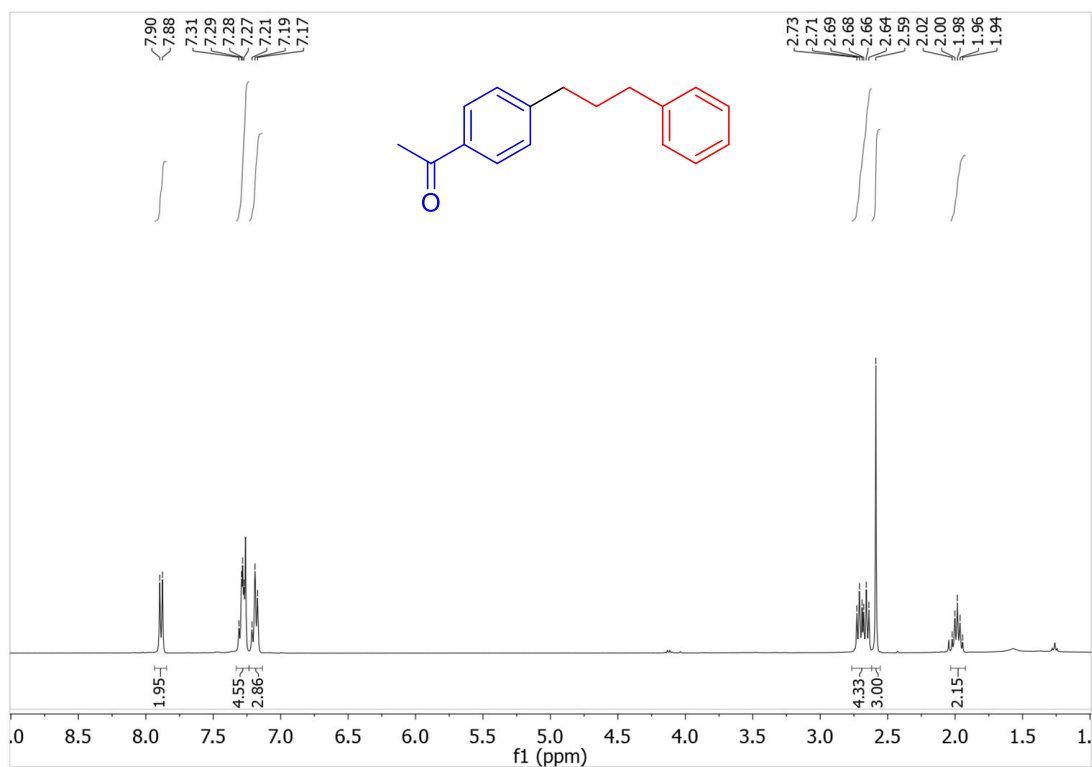


Figure S26. ¹H NMR spectrum (400 MHz, CDCl₃) of 4-(3-phenylpropyl)benzophenone, derived from substrate **4g**.

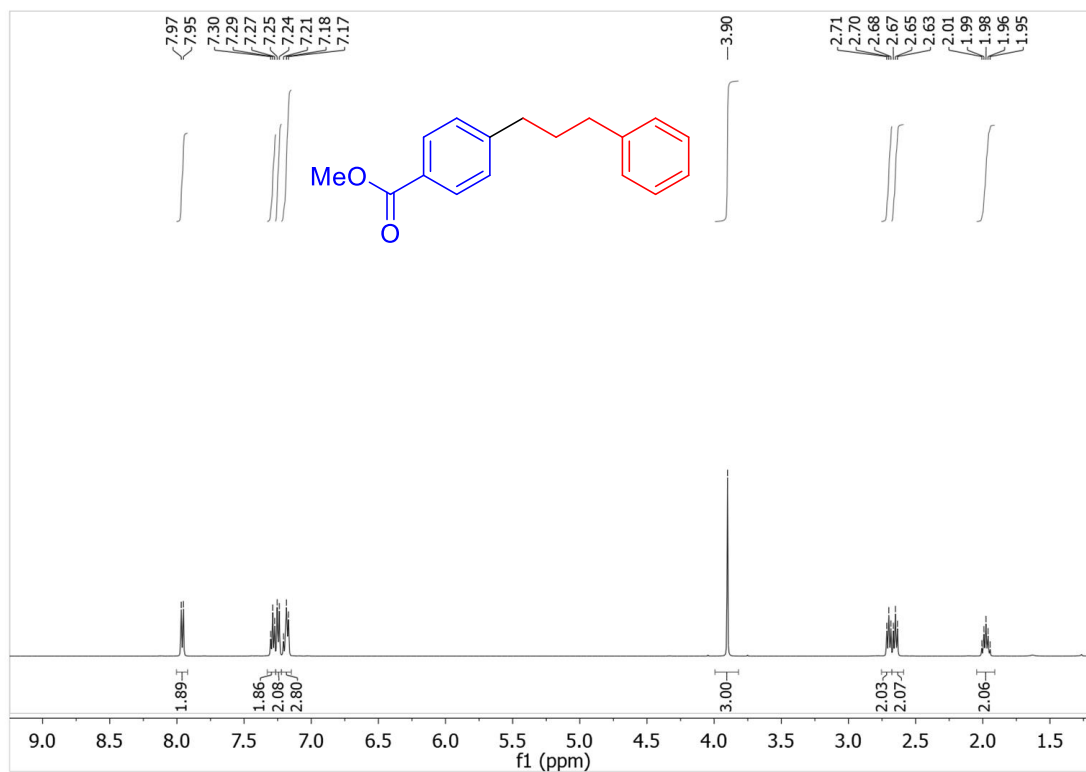


Figure S27. ¹H NMR spectrum (400 MHz, CDCl₃) of 4-(3-phenylpropyl)methyl-benzoate, derived from substrate **4h**.

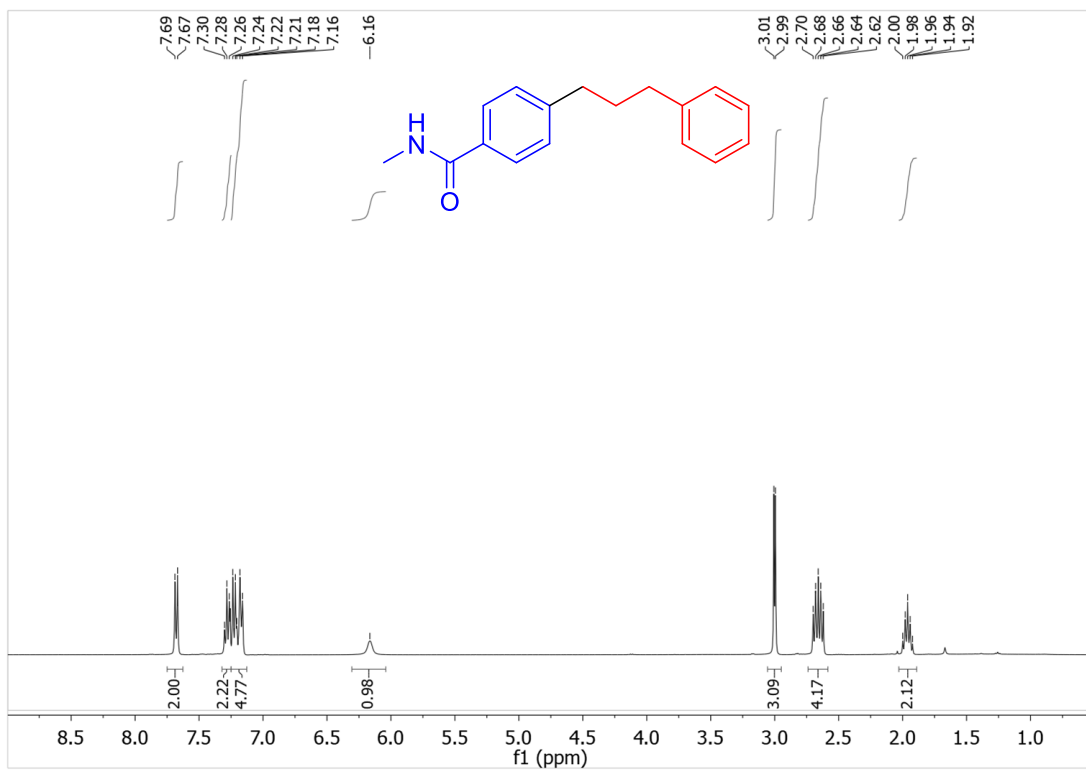
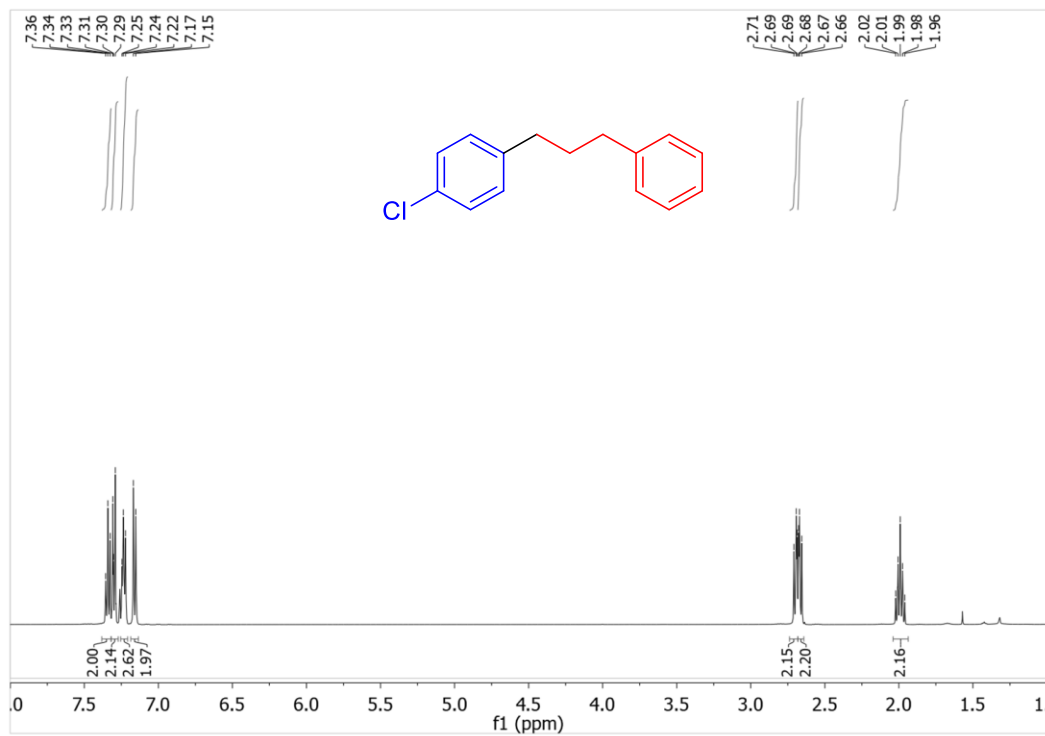
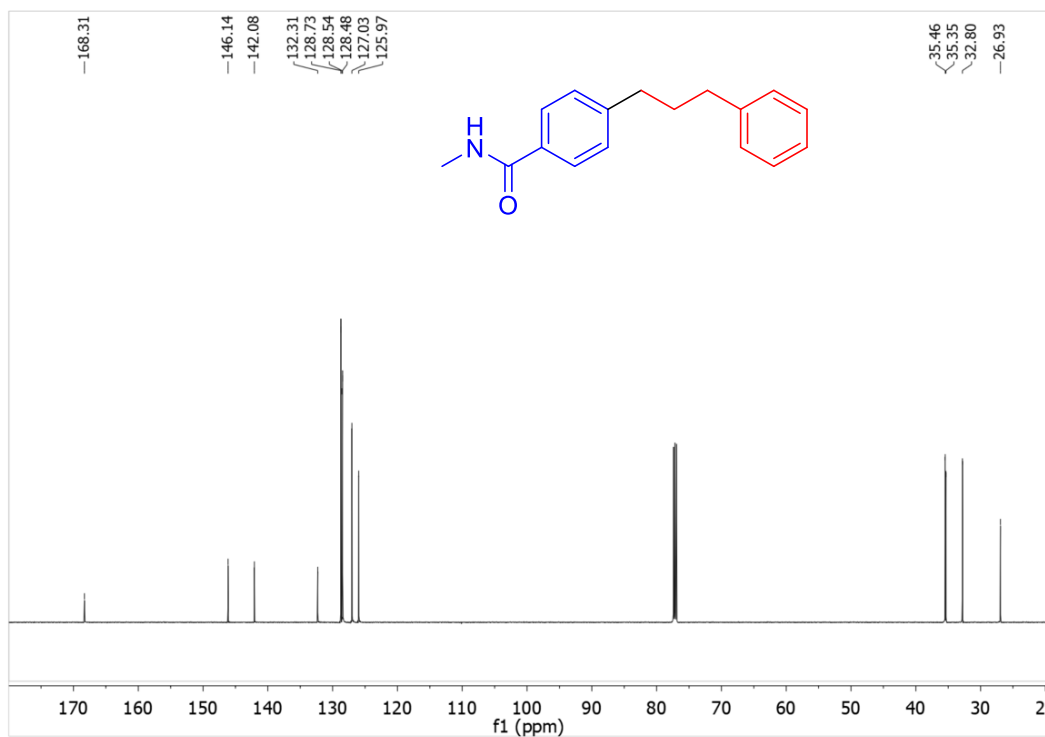


Figure S28. ¹H NMR spectrum (400 MHz, CDCl₃) of *N*-methyl-4-(3-phenylpropyl)benzamide, derived from substrate **4i**.



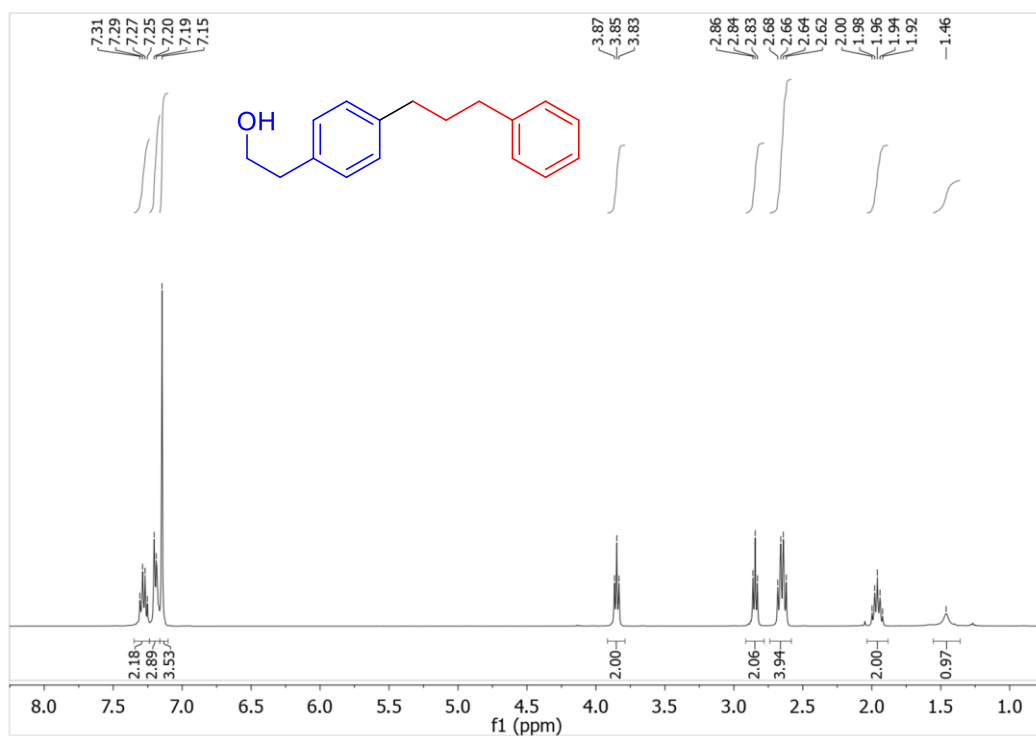


Figure S31. ¹H NMR spectrum (400 MHz, CDCl₃) of 2-(4-(3-phenylpropyl)phenyl)ethanol, derived from substrate **4k**.

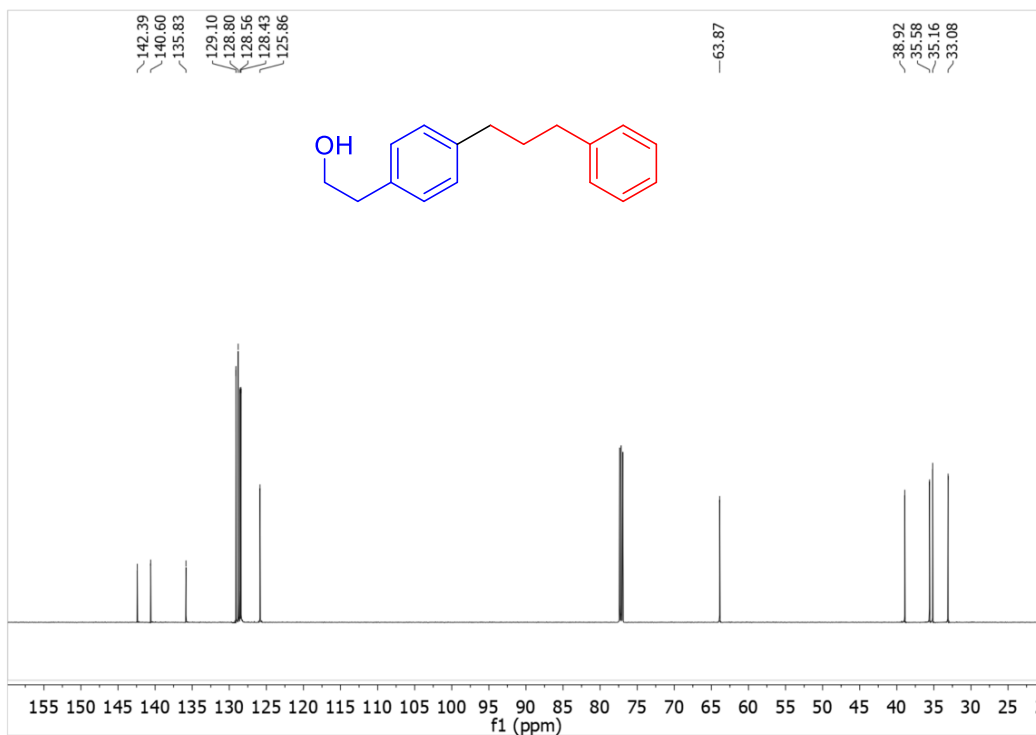


Figure S32. ¹³C{¹H} NMR spectrum (151 MHz, CDCl₃) of 2-(4-(3-phenylpropyl)phenyl)ethanol, derived from substrate **4k**.

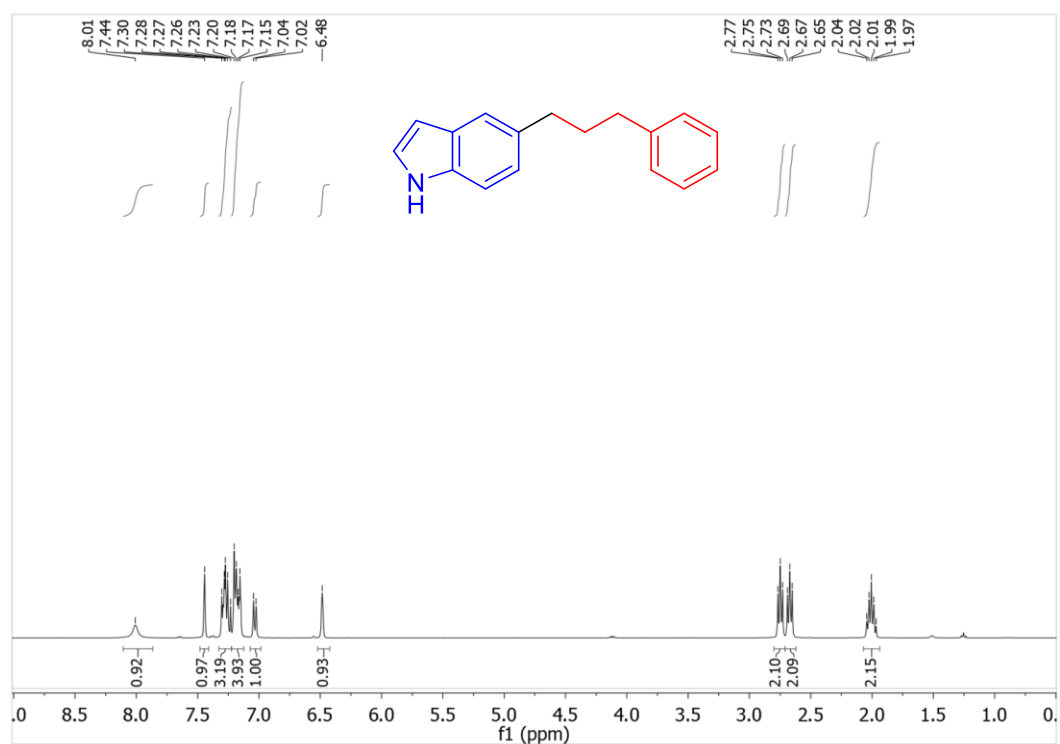


Figure S33. ¹H NMR spectrum (400 MHz, CDCl₃) of 5-(3-phenylpropyl)-1*H*-indole, derived from substrate **4I**.

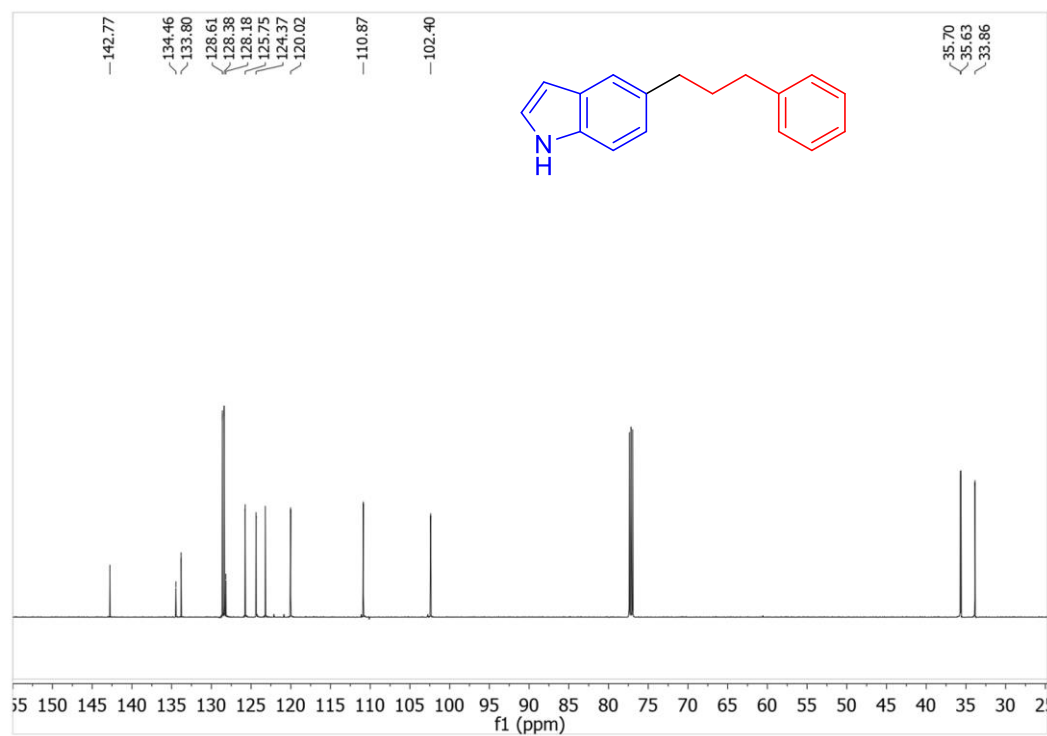


Figure S34. ¹³C{¹H} NMR spectrum (151 MHz, CDCl₃) of 5-(3-phenylpropyl)-1*H*-indole, derived from substrate **4I**.

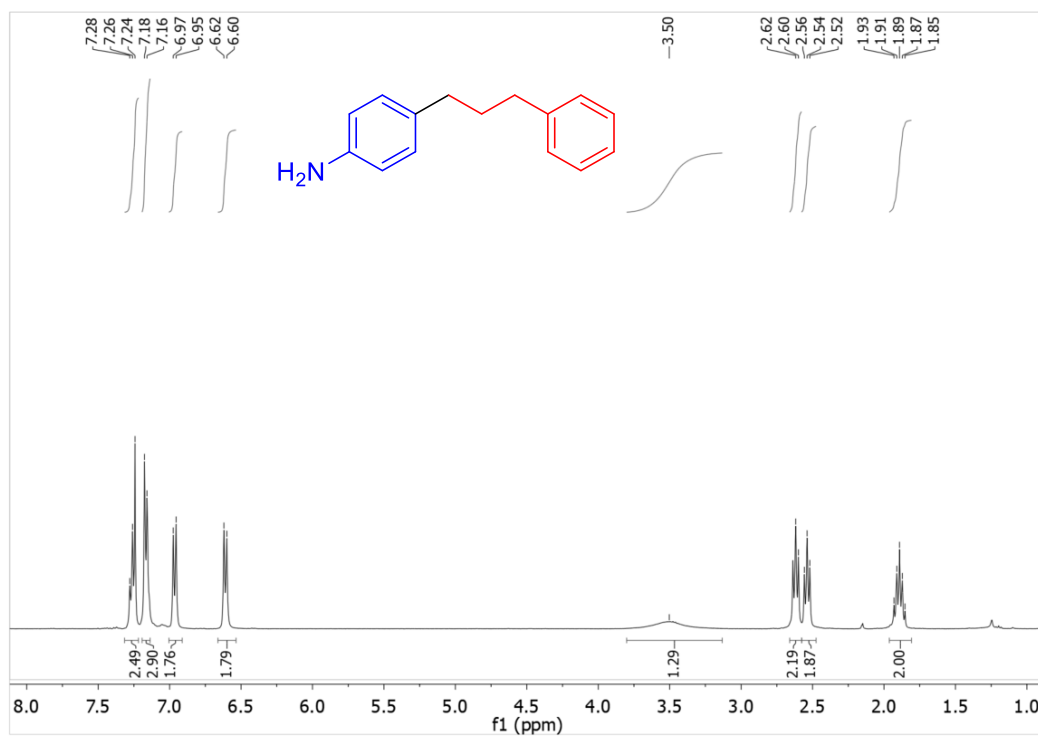


Figure S35. ¹H NMR spectrum (400 MHz, CDCl₃) of 4-(3-phenylpropyl)aniline, derived from substrate **4m**.

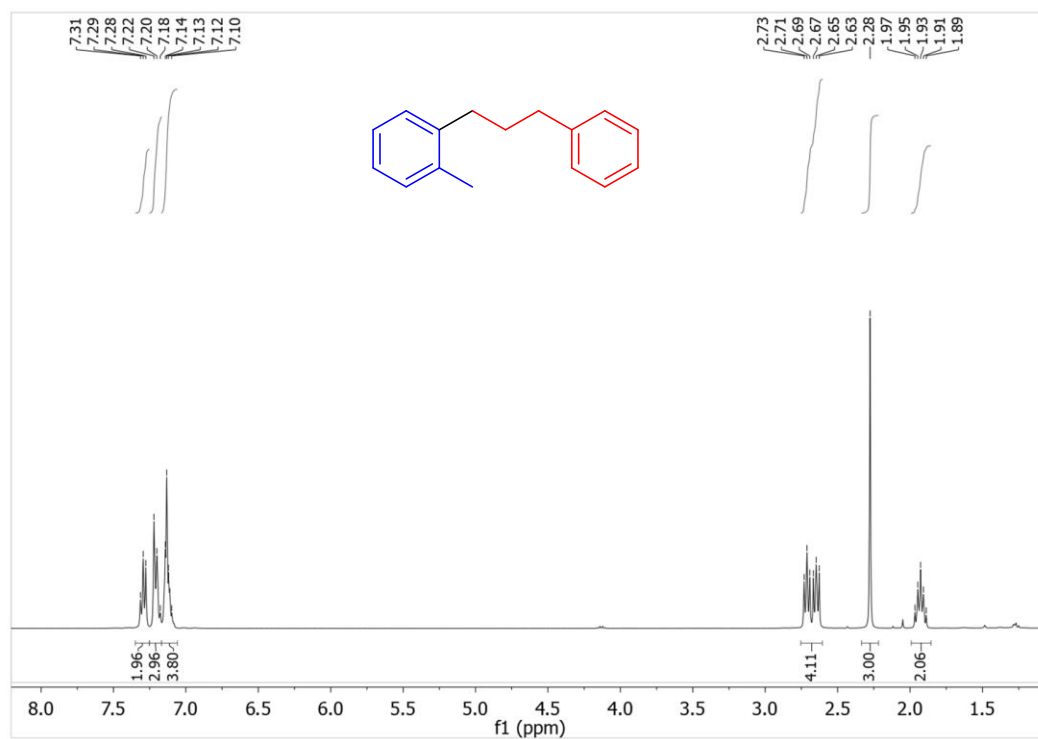


Figure S36. ¹H NMR spectrum (400 MHz, CDCl₃) of 2-(3-phenylpropyl)toluene, derived from substrate **4n**.

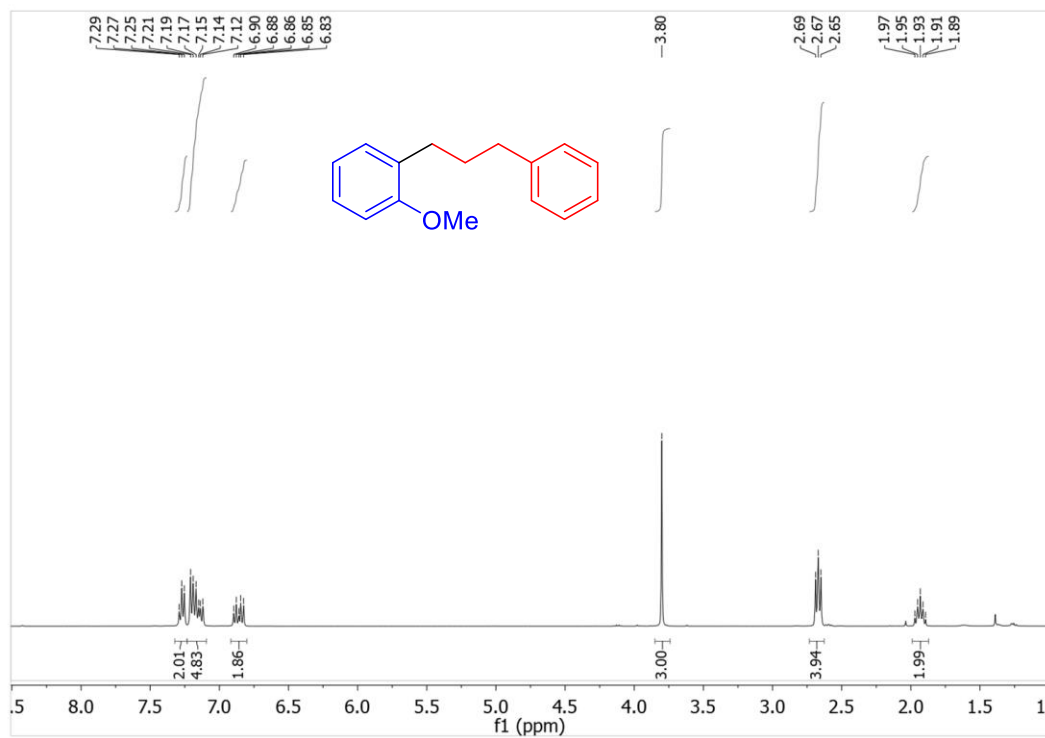


Figure S37. ¹H NMR spectrum (400 MHz, CDCl₃) of 1-phenyl-3-(2-methoxyphenyl)propane, derived from substrate **4o**.

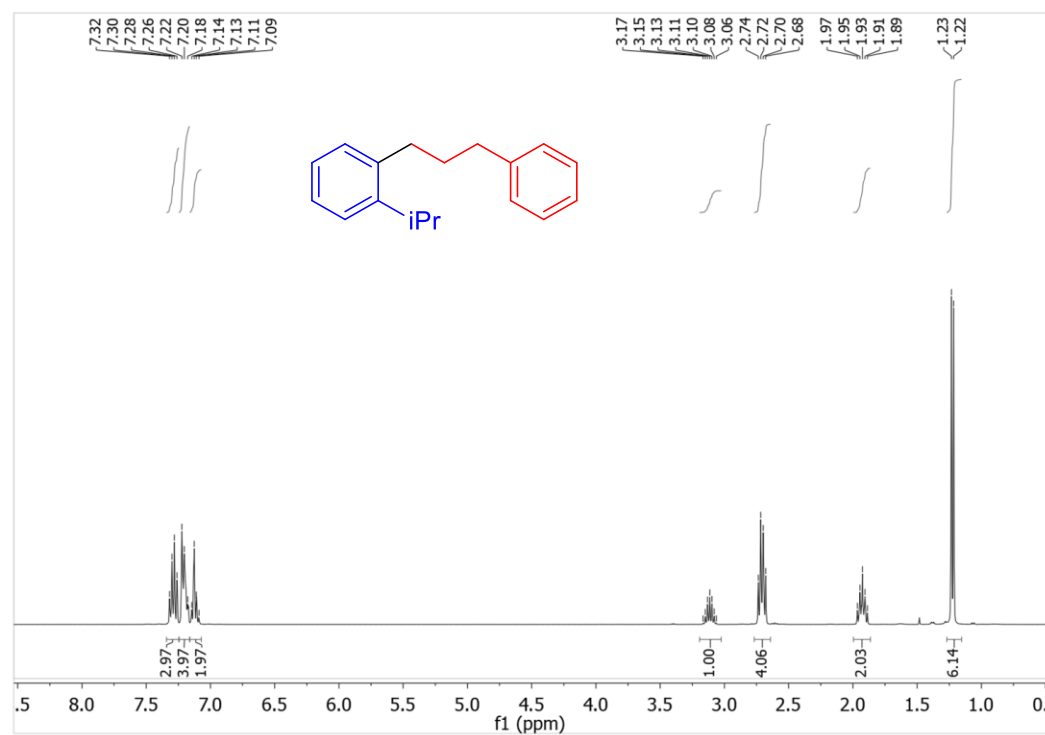


Figure S38. ¹H NMR spectrum (400 MHz, CDCl₃) of 1-phenyl-3-(2-isopropylphenyl)propane, derived from substrate **4p**.

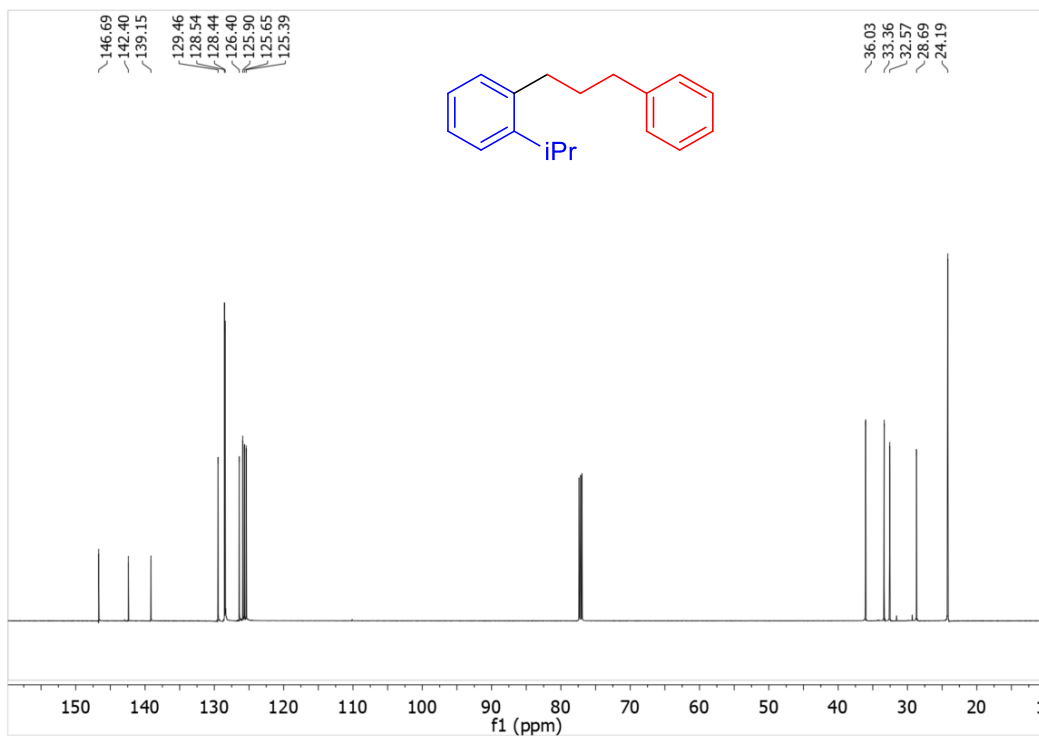


Figure S39. ¹³C{¹H} NMR spectrum (151 MHz, CDCl₃) of 1-phenyl-3-(2-isopropylphenyl)propane, derived from substrate **4p**.

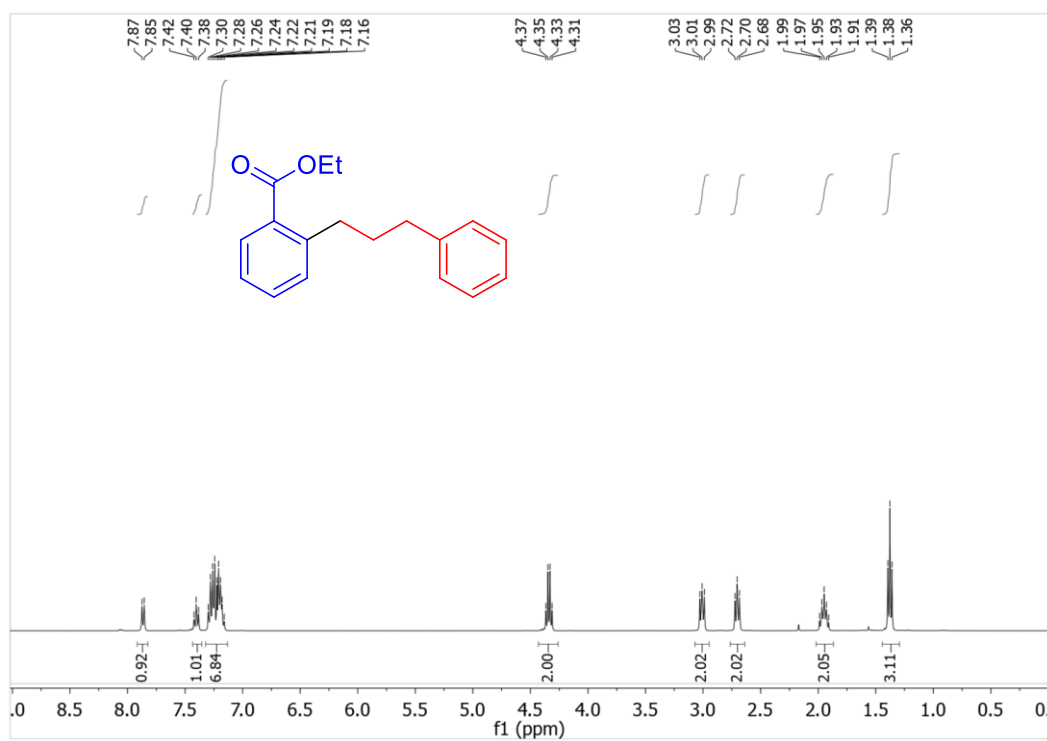


Figure S40. ¹H NMR spectrum (400 MHz, CDCl₃) of 2-(3-phenylpropyl)ethylbenzoate, derived from substrate **4q**.

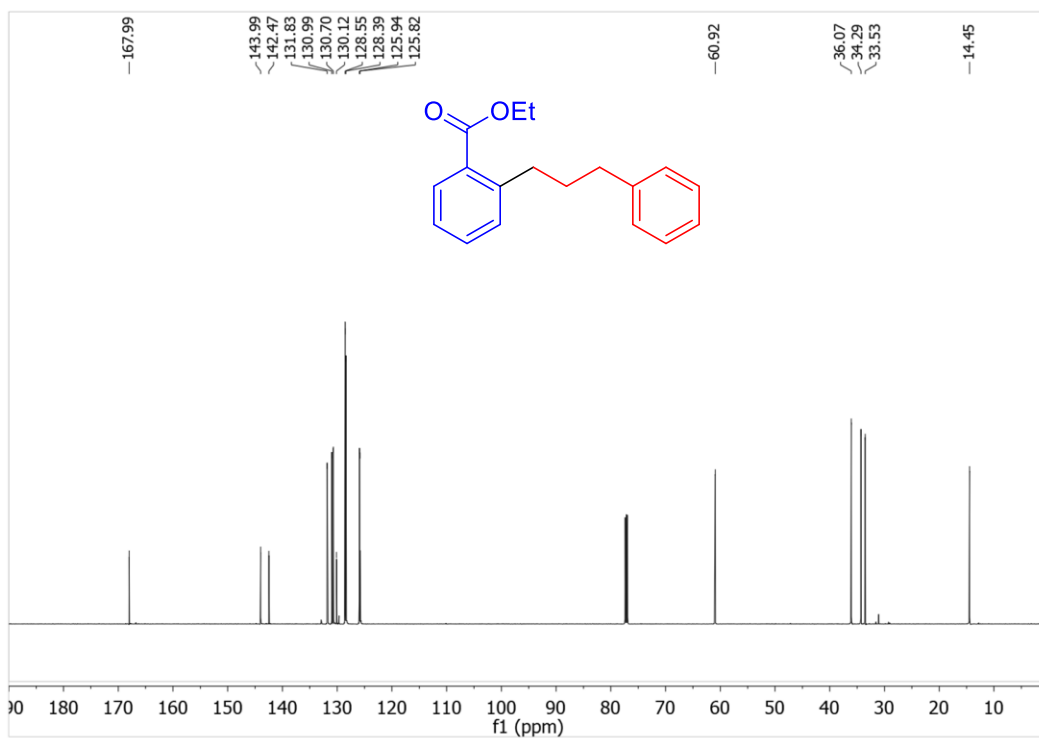


Figure S41. ¹³C{¹H} NMR spectrum (151 MHz, CDCl₃) of 2-(3-phenylpropyl)ethylbenzoate, derived from substrate **4q**.

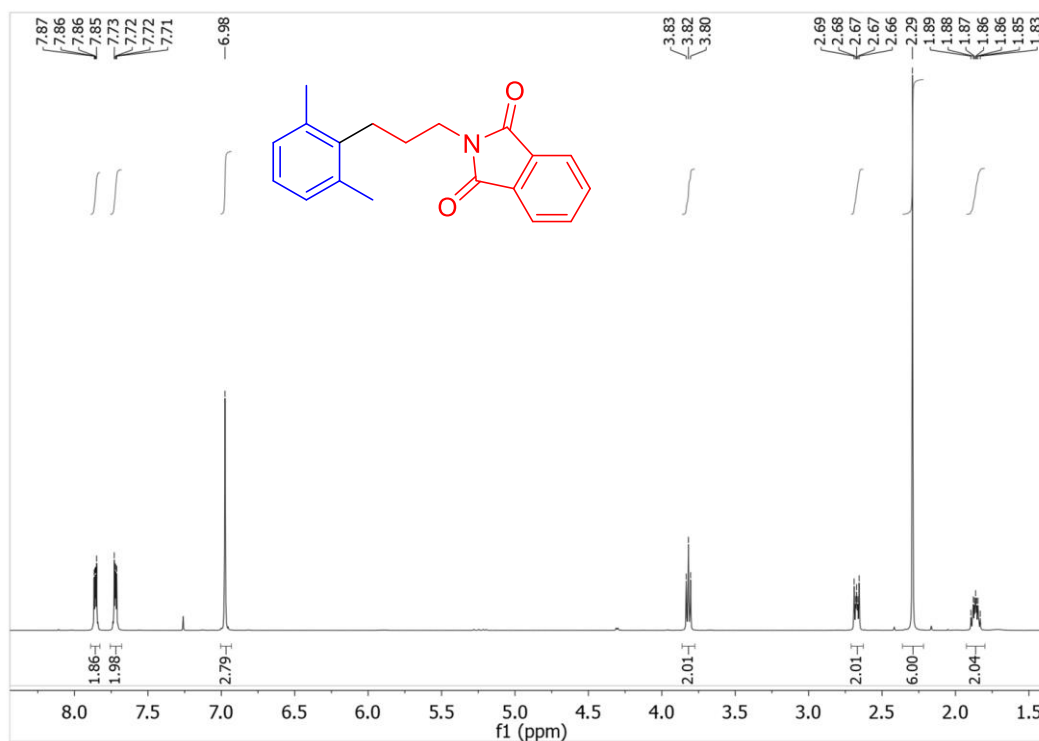


Figure S42. ¹H NMR spectrum (400 MHz, CDCl₃) of 2-(3-(2,6-dimethylphenyl)propyl)isoindoline-1,3-dione, derived from substrate **4r**.

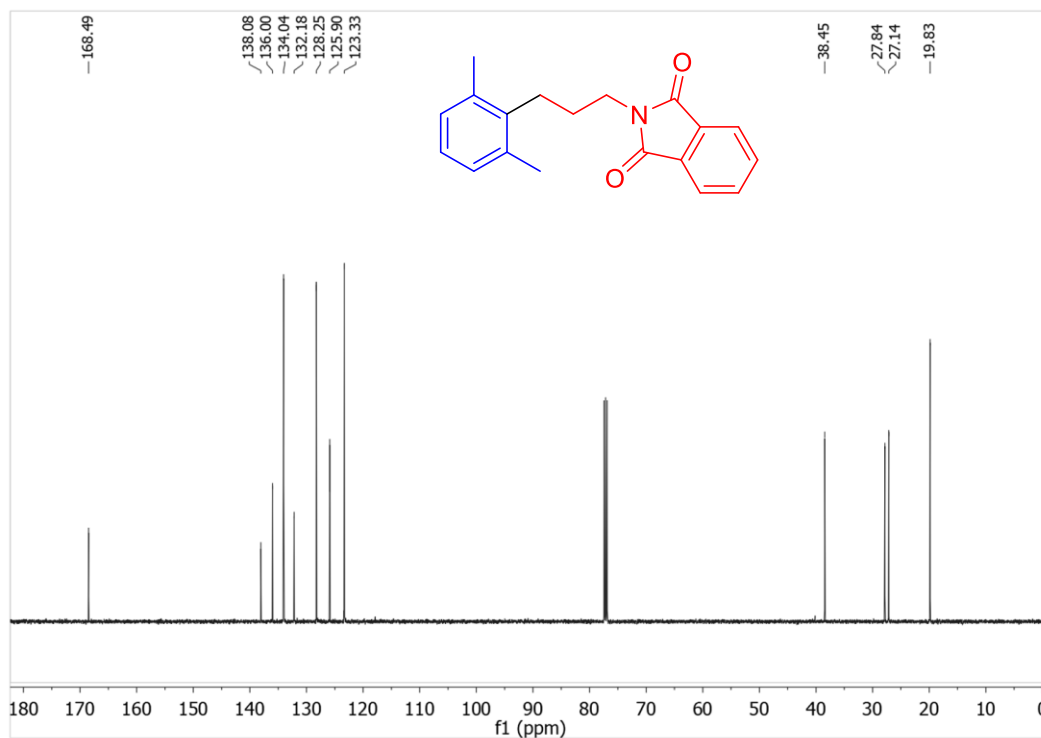


Figure S43. ¹³C{¹H} NMR spectrum (151 MHz, CDCl₃) of 2-(3-(2,6-dimethylphenyl)propyl)isoindoline-1,3-dione, derived from substrate **4r**.

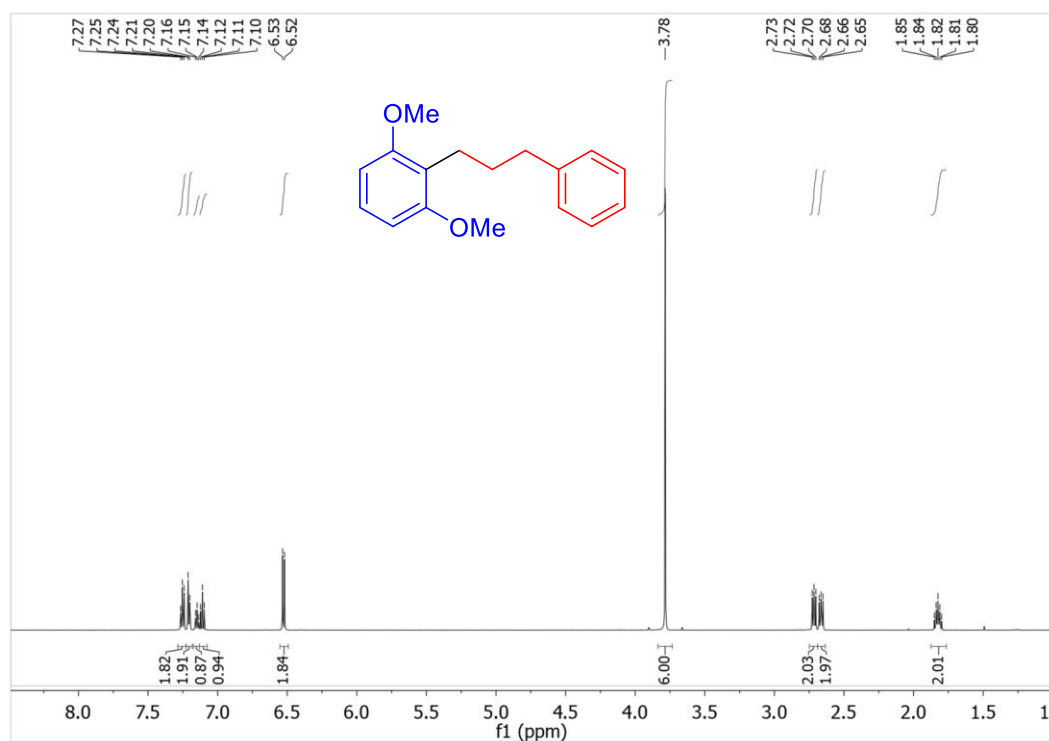


Figure S44. ¹H NMR spectrum (400 MHz, CDCl₃) of 3-(3-(2,6-dimethoxyphenyl)propyl)benzene, derived from substrate **4s**.

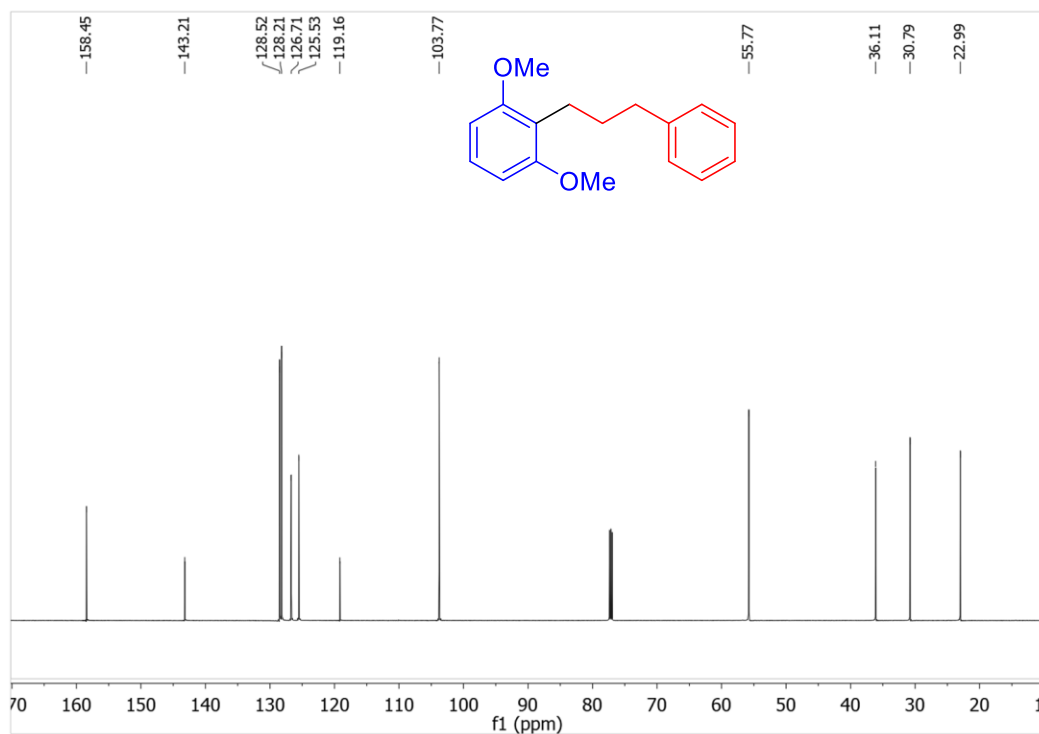


Figure S45. ¹³C{¹H} NMR spectrum (151 MHz, CDCl₃) of 3-(3-phenylpropyl)-2,6-dimethoxybenzene, derived from substrate **4s**.

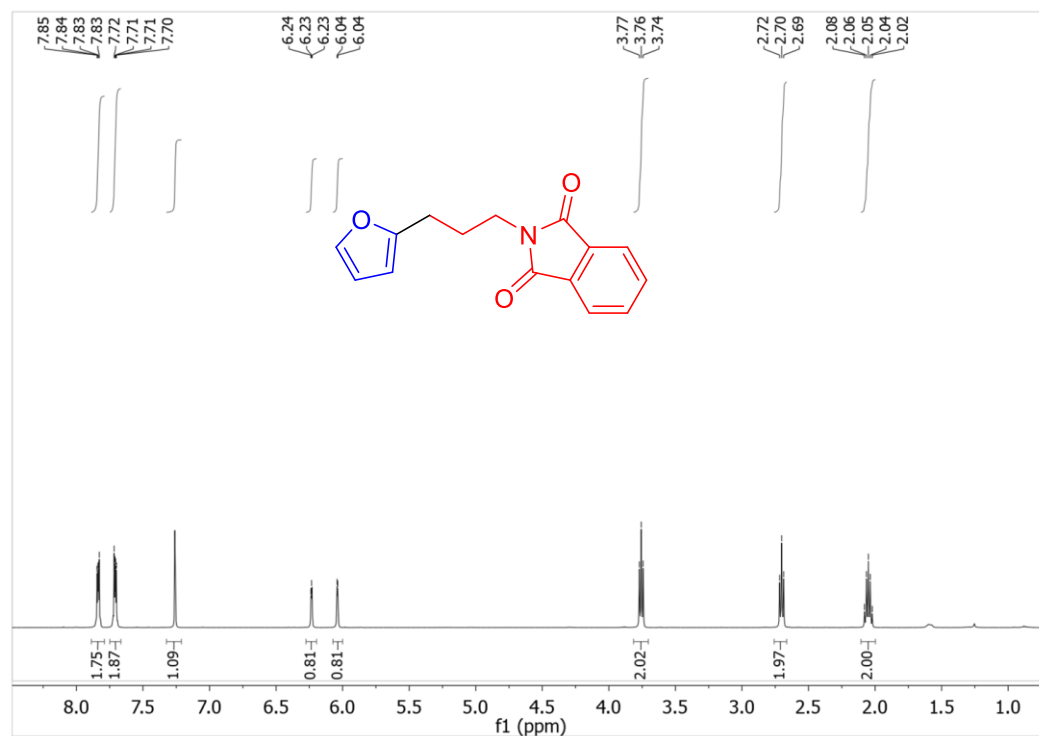


Figure S46. ¹H NMR spectrum (400 MHz, CDCl₃) of 2-(3-(2-furanyl)propyl)isoindoline-1,3-dione, derived from substrate **4t**.

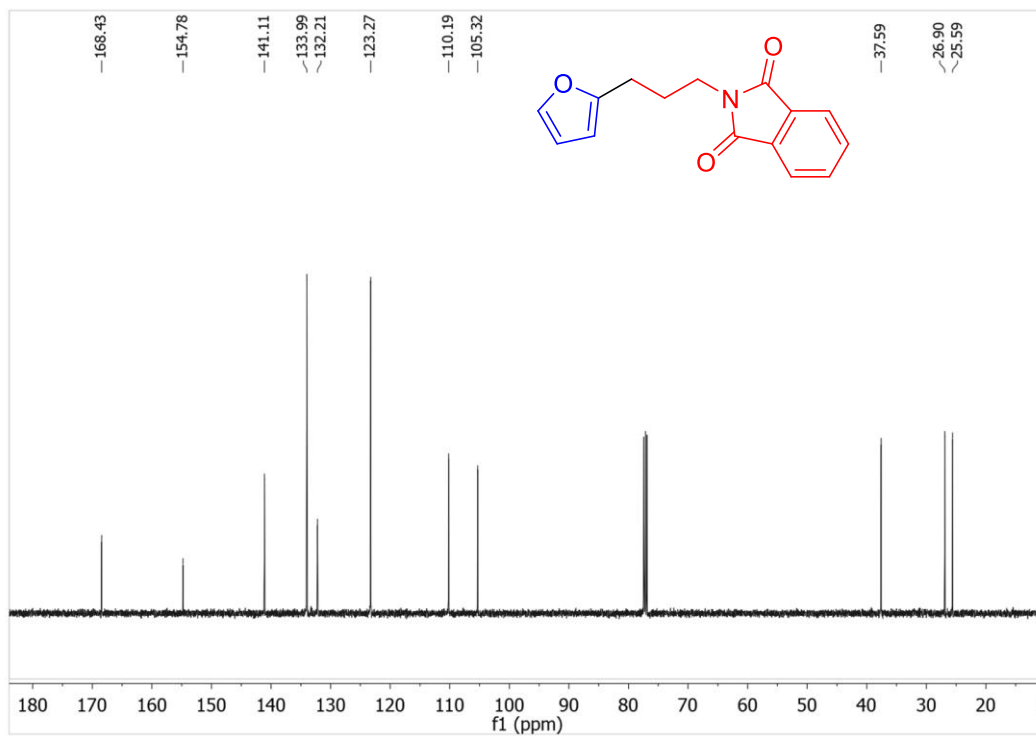


Figure S47. ¹³C{¹H} NMR spectrum (151 MHz, CDCl₃) of 2-(3-(2-furanyl)propyl)isoindoline-1,3-dione, derived from substrate **4t**.

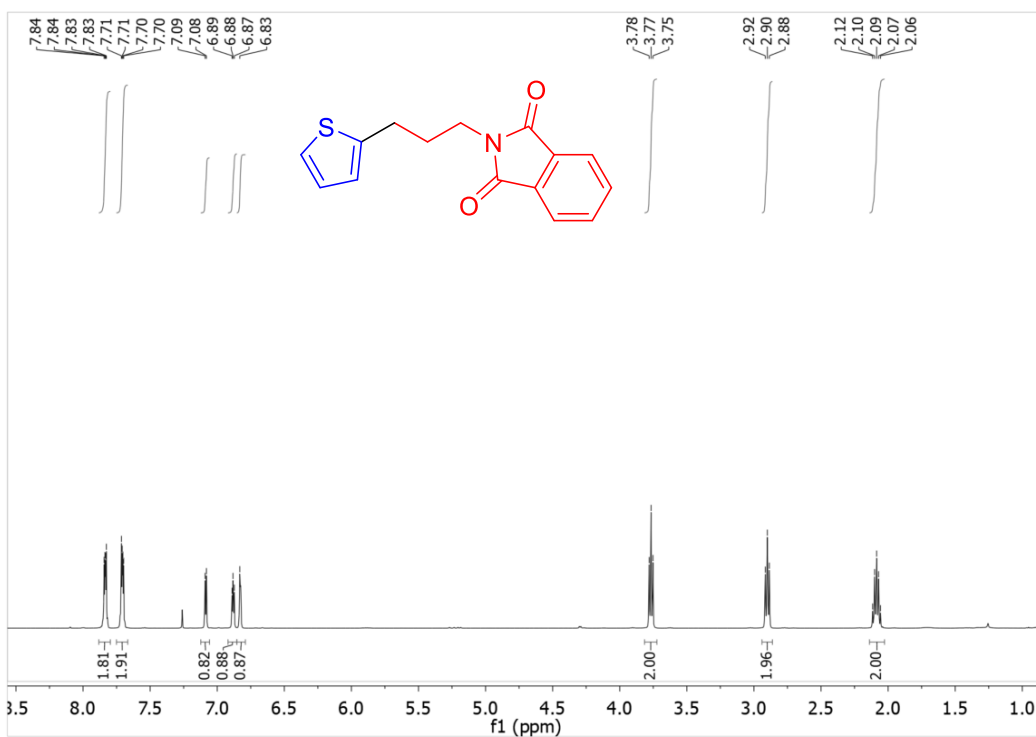


Figure S48. ¹H NMR spectrum (400 MHz, CDCl₃) of 2-(3-(2-thiophenyl)propyl)isoindoline-1,3-dione, derived from substrate **4u**.

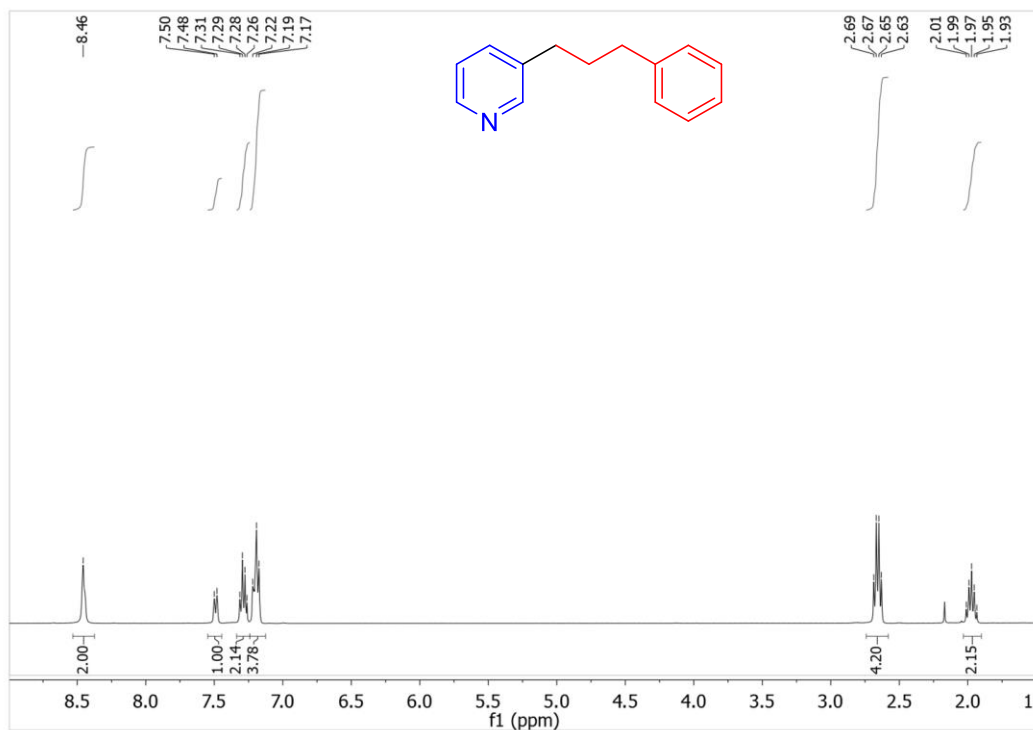


Figure S49. ¹H NMR spectrum (400 MHz, CDCl₃) of 3-(3-phenylpropyl)pyridine, derived from substrate **4v**.

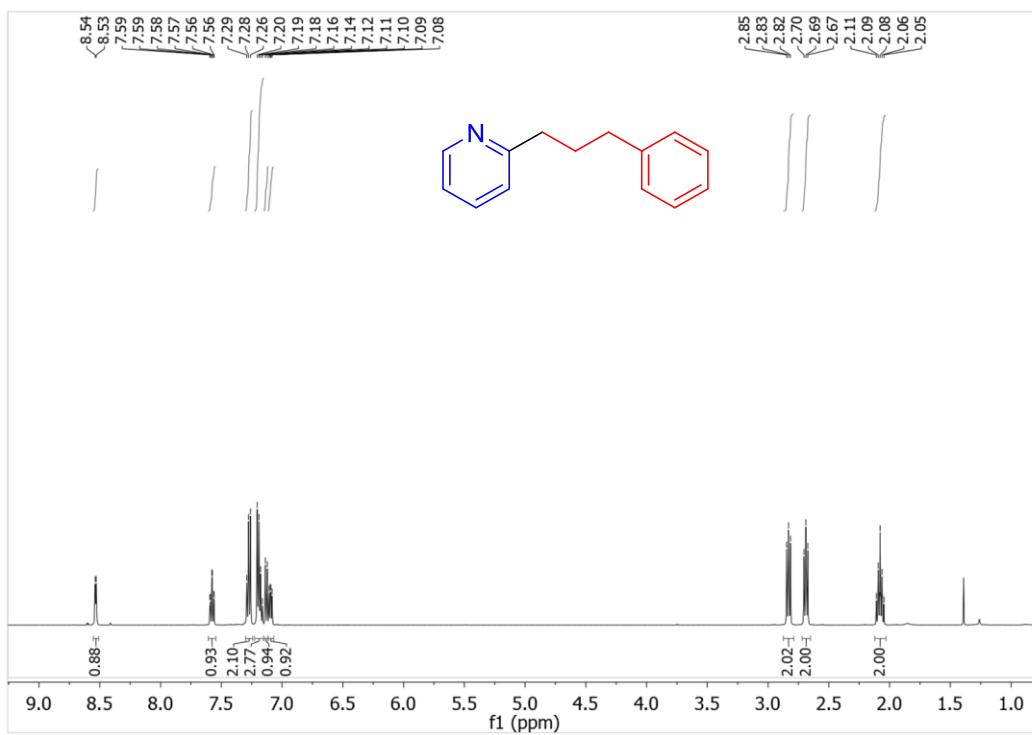


Figure S50. ¹H NMR spectrum (400 MHz, CDCl₃) of 2-(3-phenylpropyl)pyridine, derived from substrate **4w**.

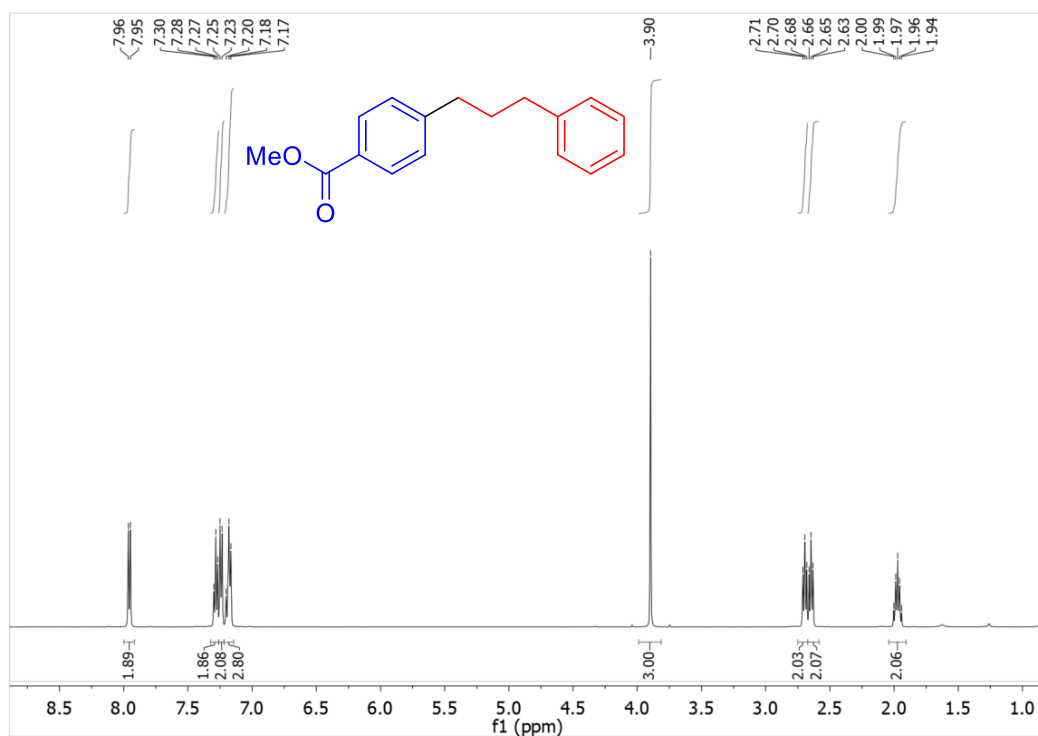


Figure S51. ^1H NMR spectrum (400 MHz, CDCl_3) of 4-(3-phenylpropyl)methylbenzoate, derived from substrate **4x**.

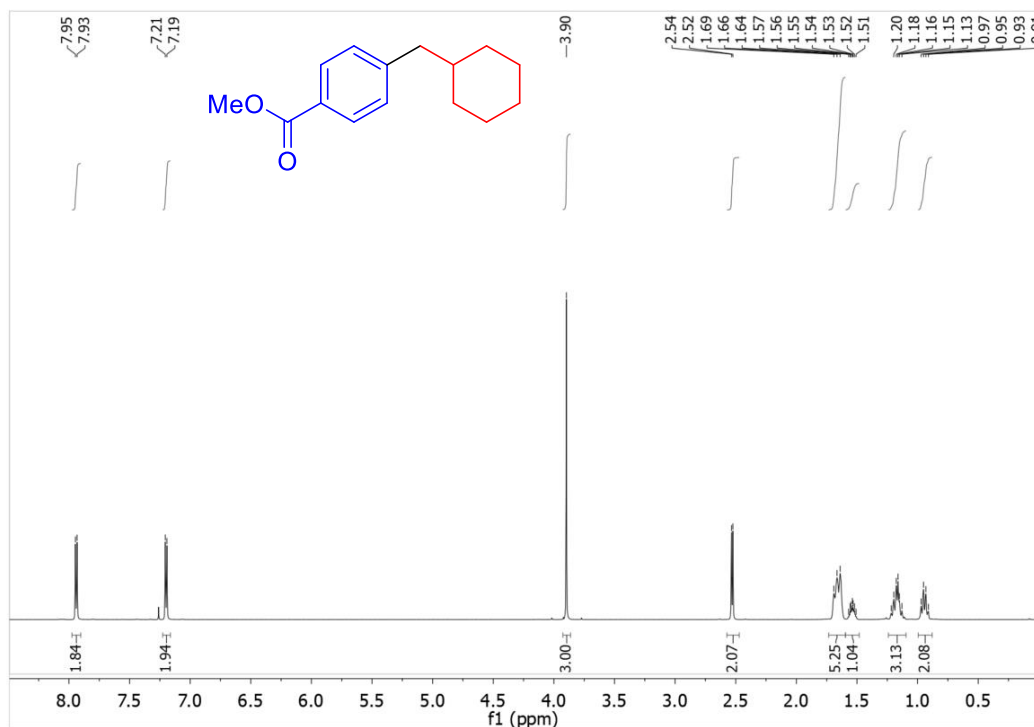


Figure S52. ^1H NMR spectrum (400 MHz, CDCl_3) of methyl 4-(cyclohexylmethyl)benzoate, derived from substrate **4y**.

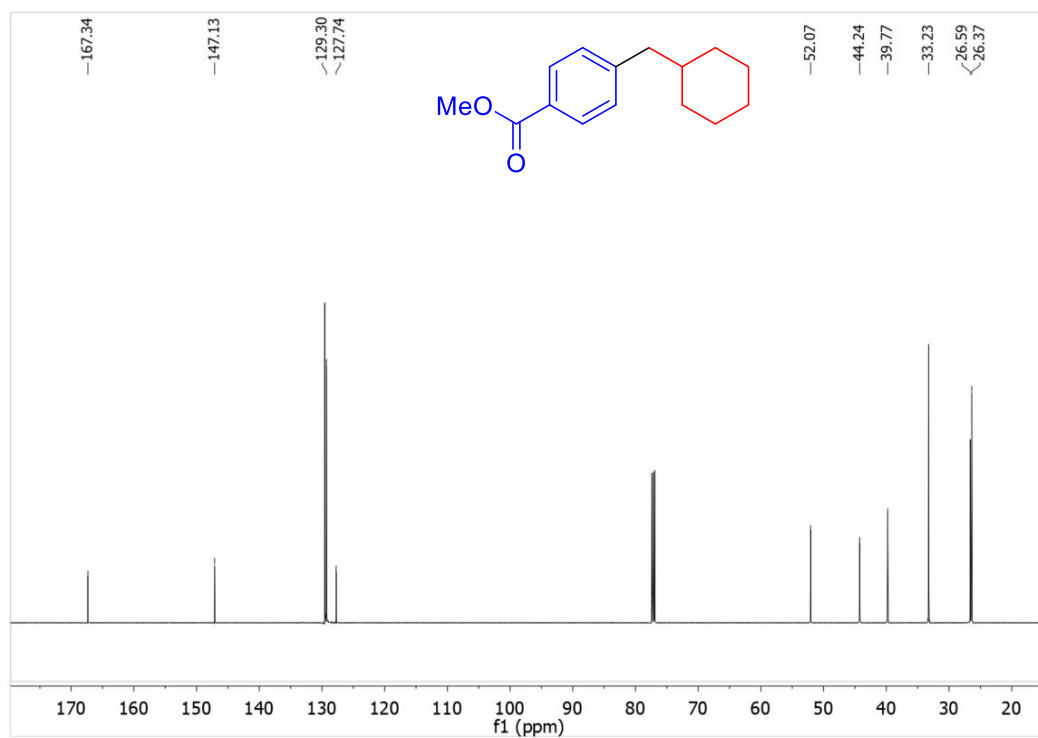


Figure S53. $^{13}\text{C}\{^1\text{H}\}$ NMR spectrum (151 MHz, CDCl_3) of methyl 4-(cyclohexylmethyl)benzoate, derived from substrate **4y**.

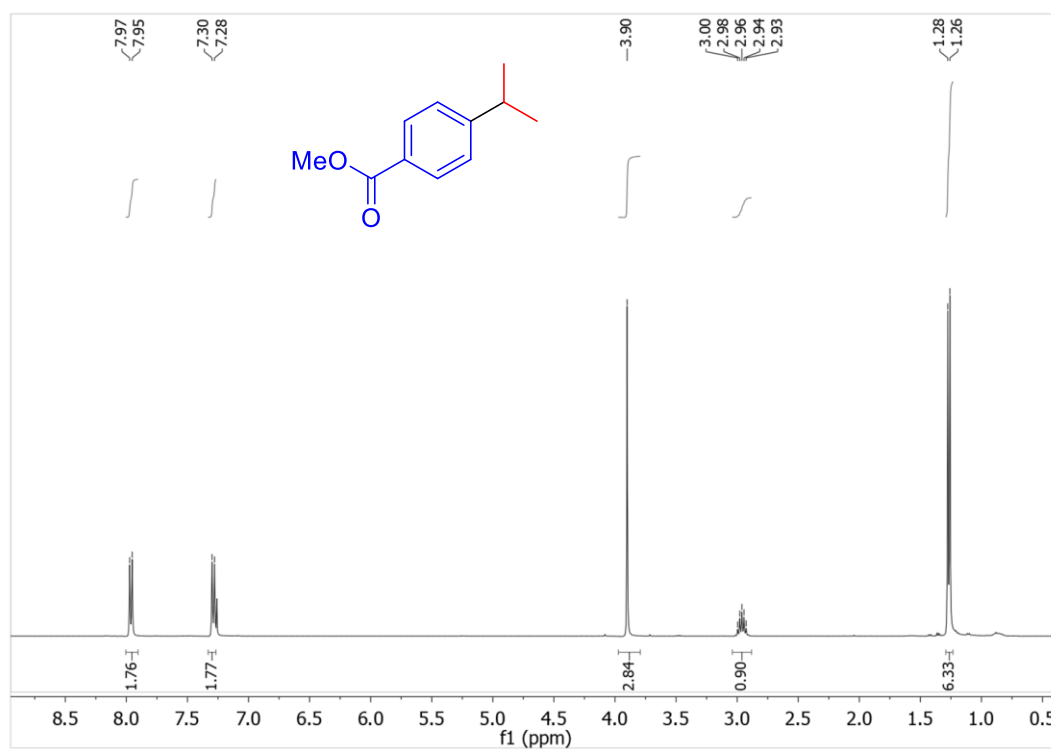


Figure S54. ^1H NMR spectrum (400 MHz, CDCl_3) of methyl 4-isopropylbenzoate, derived from substrate **4z**.

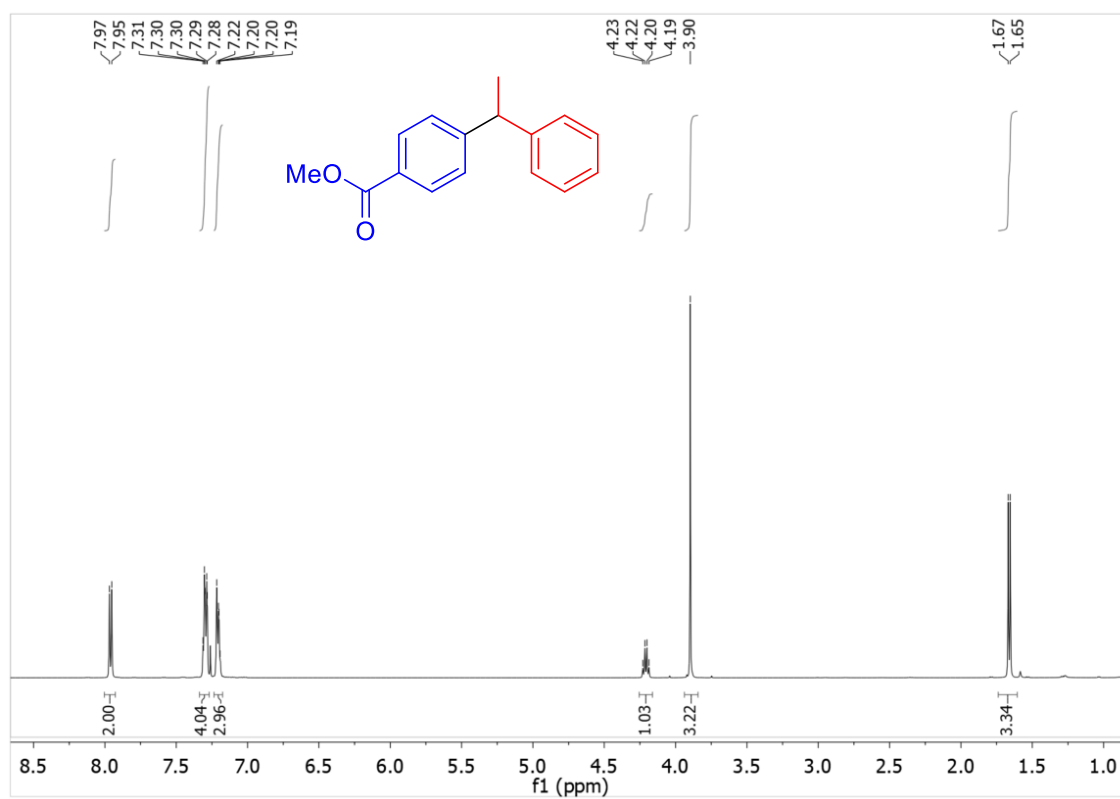


Figure S55. ¹H NMR spectrum (400 MHz, CDCl₃) of methyl 4-(1-phenylethyl)benzoate, derived from substrate **4aa**.

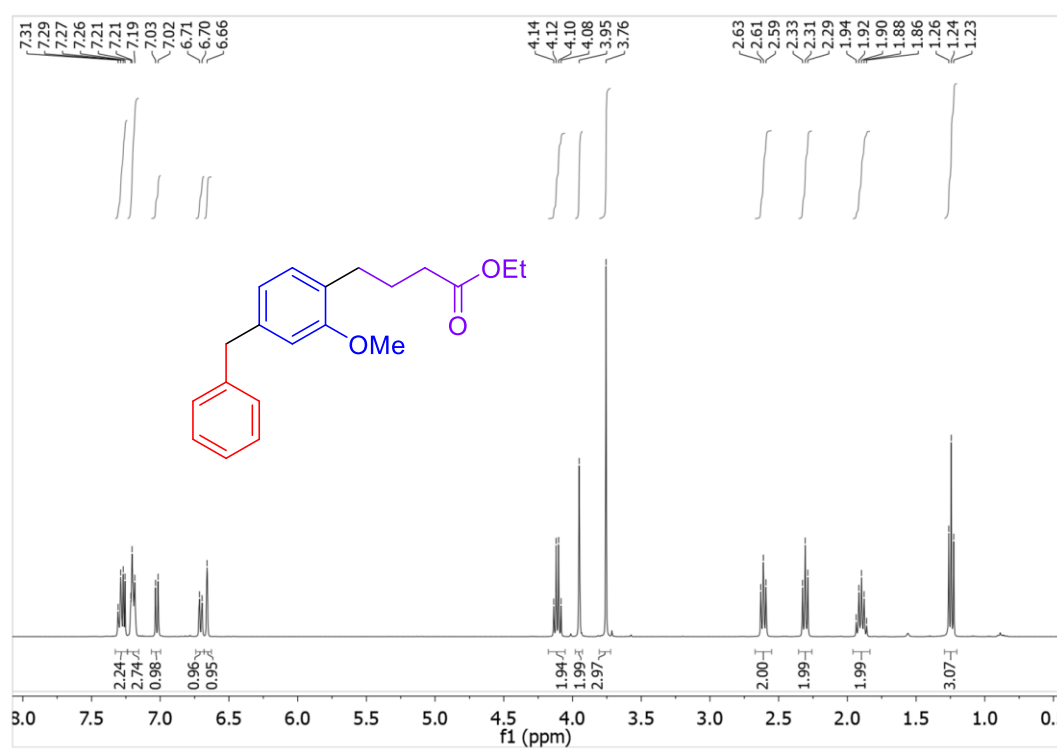


Figure S56. ¹H NMR spectrum (400 MHz, CDCl₃) of ethyl 4-(4-benzyl-2-methoxyphenyl)butanoate, Table 4, Entry 1.

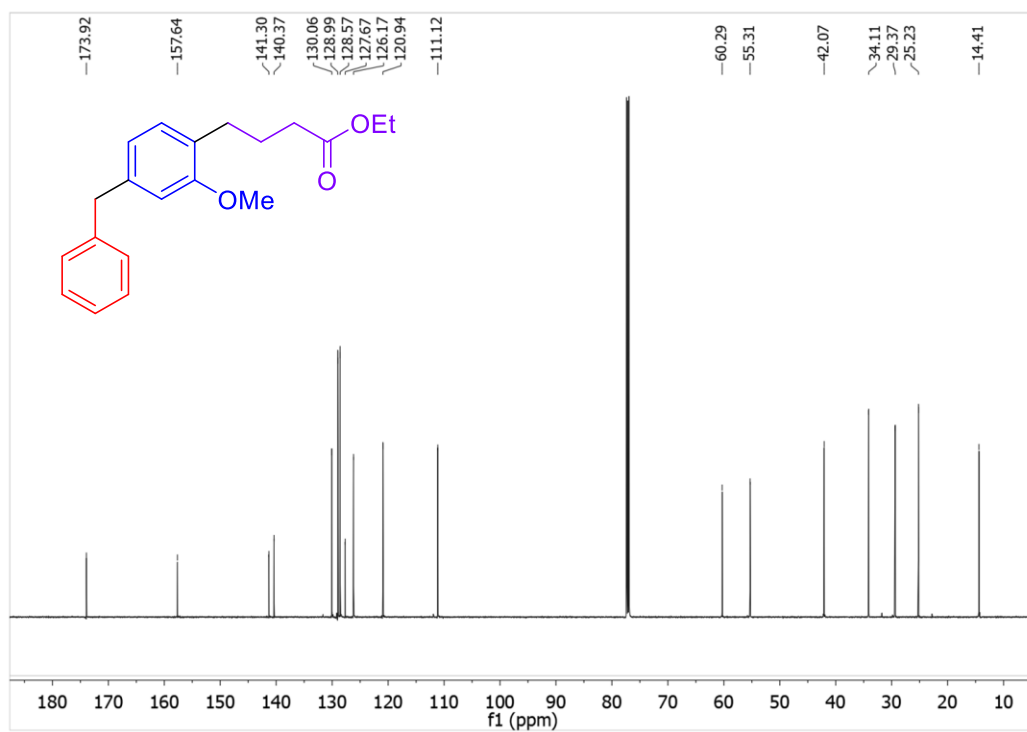


Figure S57. ¹³C{¹H} NMR spectrum (151 MHz, CDCl₃) of ethyl 4-(4-benzyl-2-methoxyphenyl)butanoate, Table 4, Entry 1.

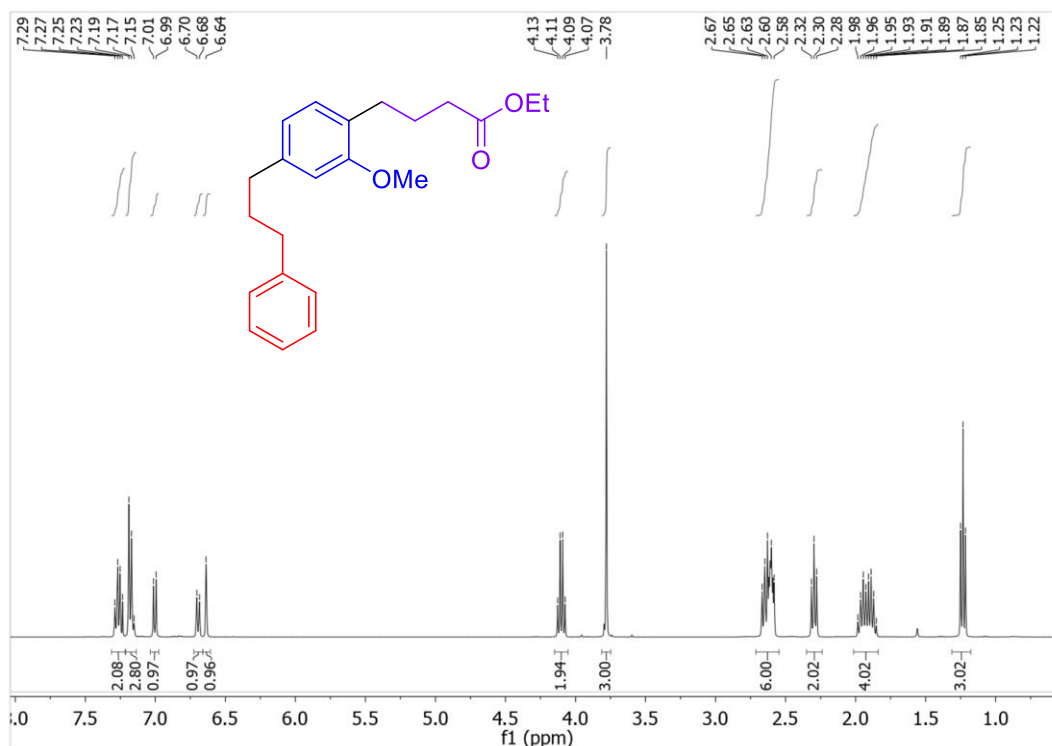


Figure S58. ¹H NMR spectrum (400 MHz, CDCl₃) of ethyl 4-(3-methoxy-4-(3-phenylpropyl)phenyl)butanoate, Table 4, Entry 2.

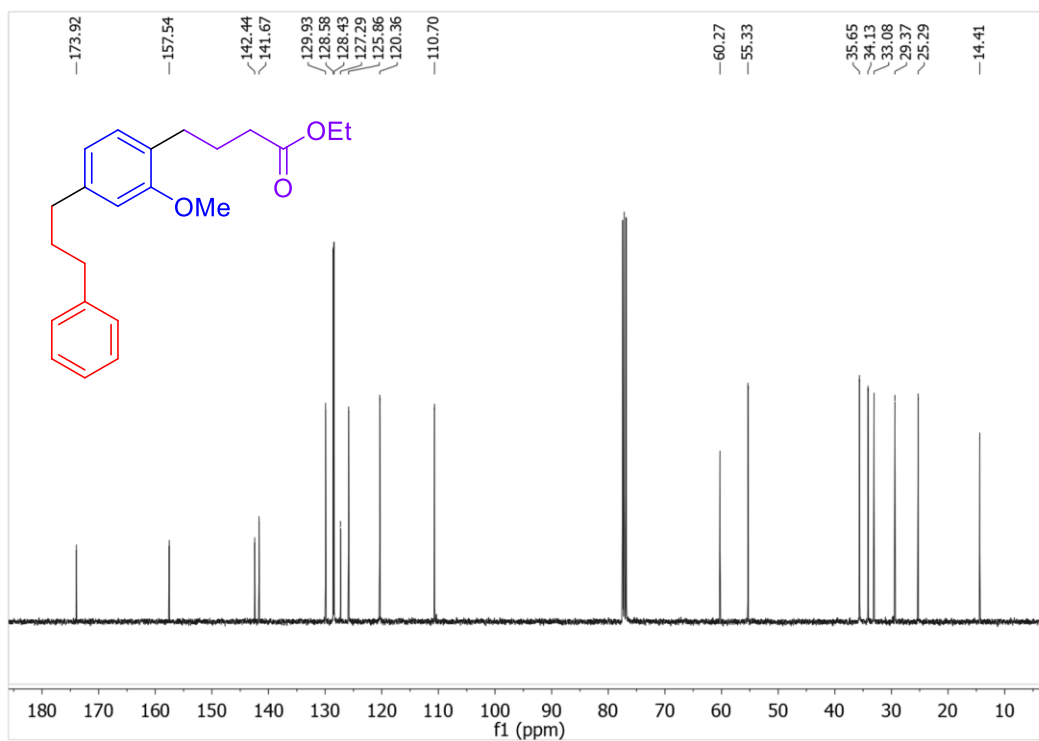


Figure S59. ¹³C{¹H} NMR spectrum (151 MHz, CDCl₃) of ethyl 4-(3-methoxy-4-(3-phenylpropyl)phenyl)butanoate, Table 4, Entry 2.

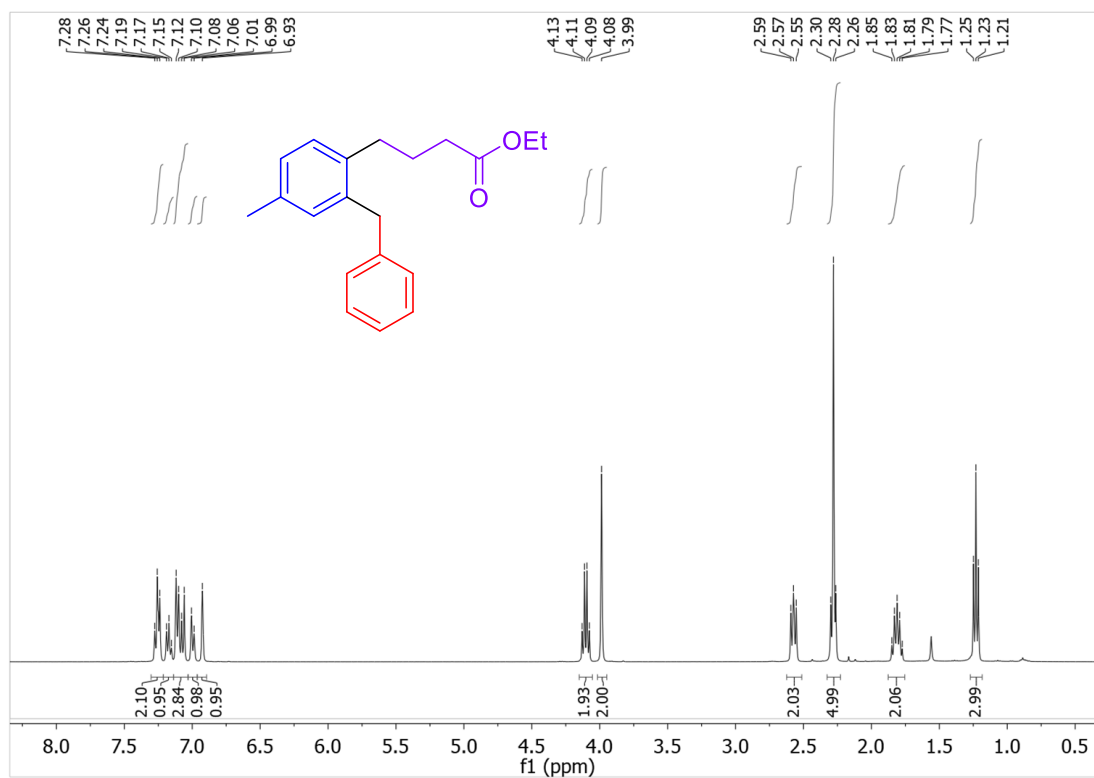


Figure S60. ¹H NMR spectrum (400 MHz, CDCl₃) of ethyl 4-(2-benzyl-4-methylphenyl)butanoate, Table 4, Entry 3.

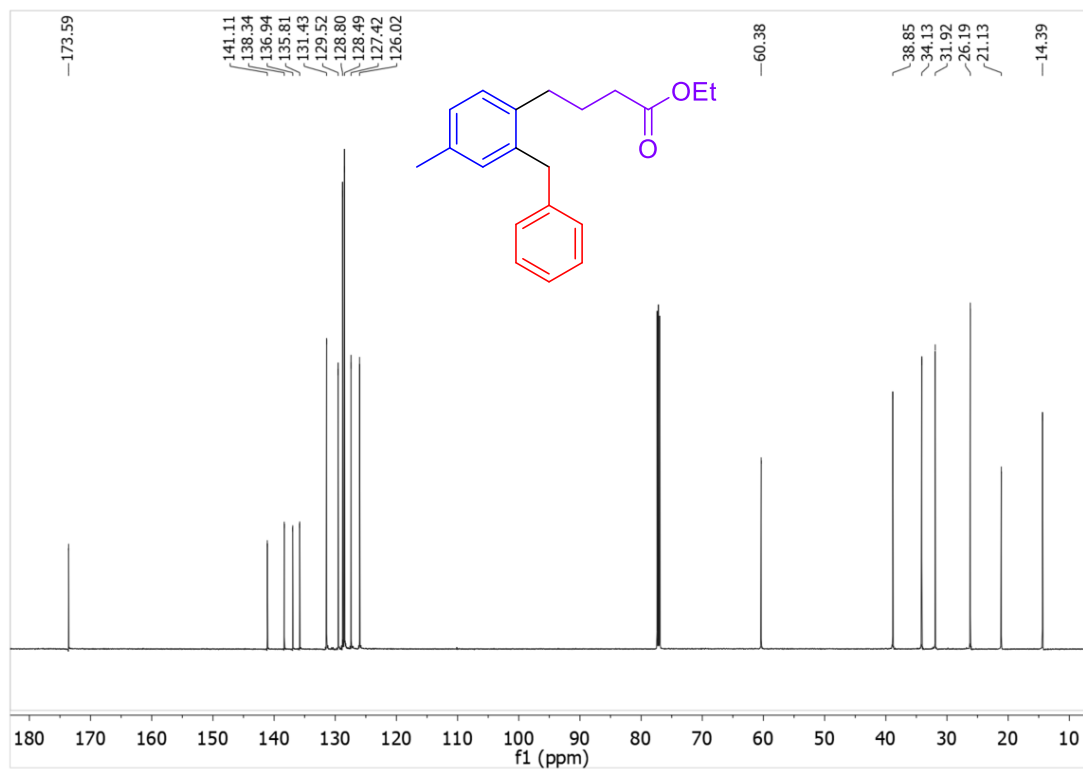


Figure S61. ¹³C{¹H} NMR spectrum (151 MHz, CDCl₃) of ethyl 4-(2-benzyl-4-methylphenyl)butanoate, Table 4, Entry 3.

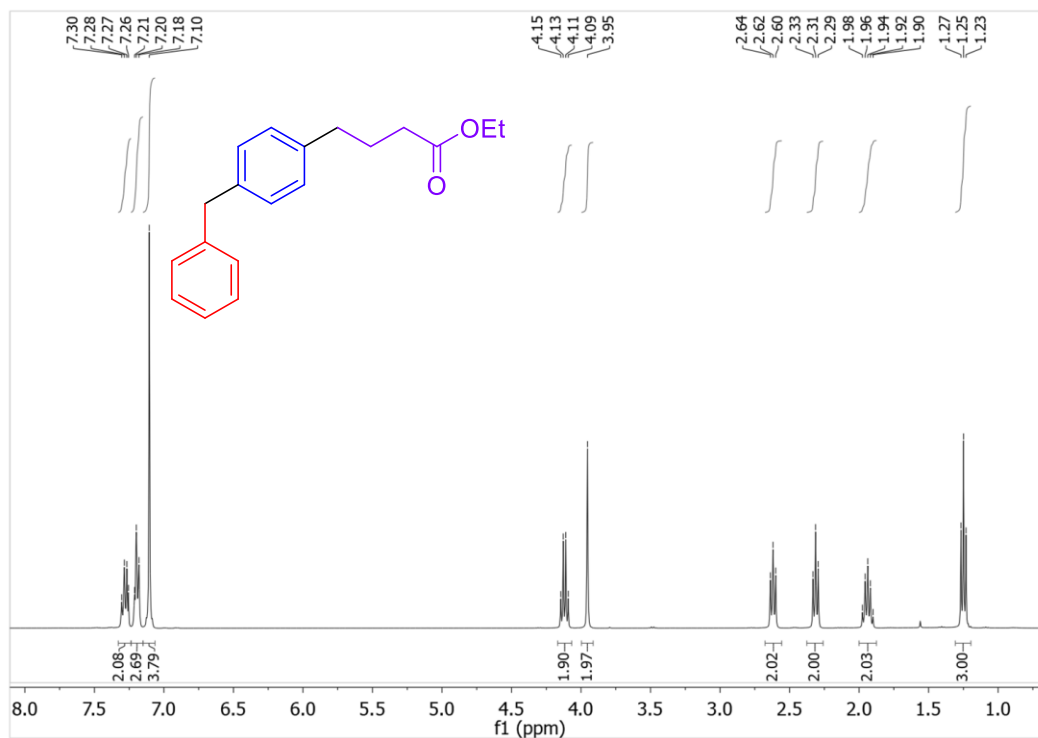


Figure S62. ^1H NMR spectrum (400 MHz, CDCl_3) of ethyl 4-(4-benzylphenyl)butanoate, Table 4, Entry 4.

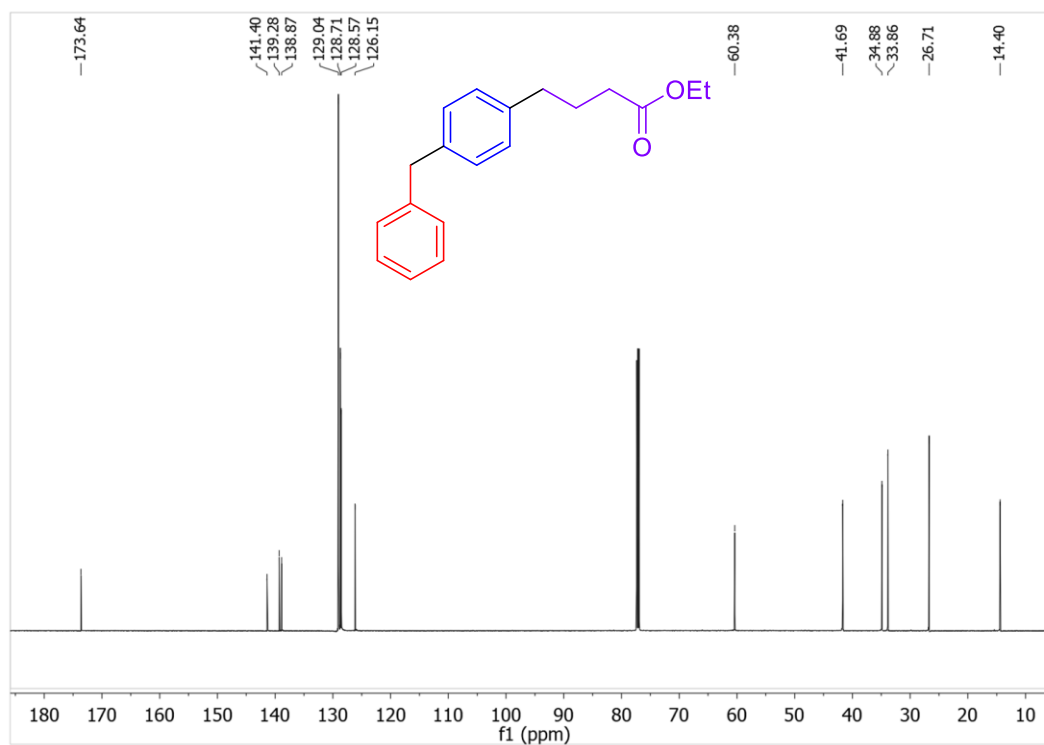


Figure S63. $^{13}\text{C}\{^1\text{H}\}$ NMR spectrum (151 MHz, CDCl_3) of ethyl 4-(4-benzylphenyl)butanoate, Table 4, Entry 4.

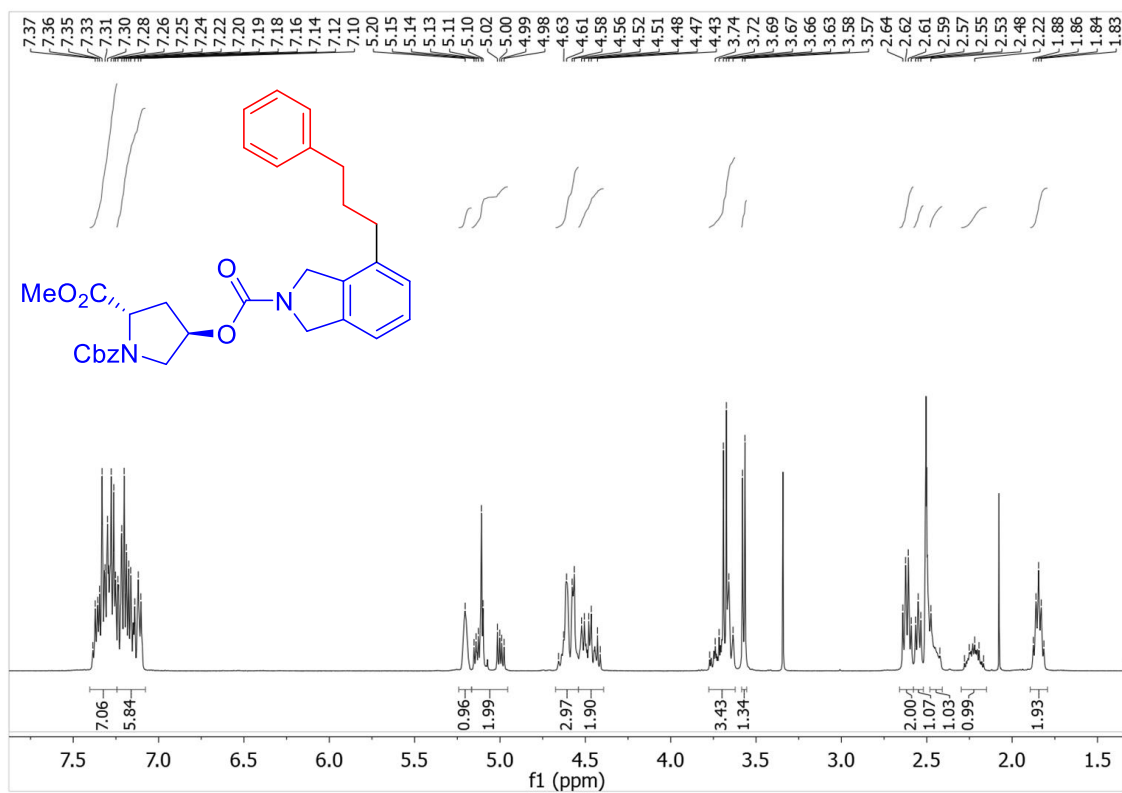


Figure S64. ¹H NMR spectrum (400 MHz, DMSO-d₆) of product derived from **5b**.

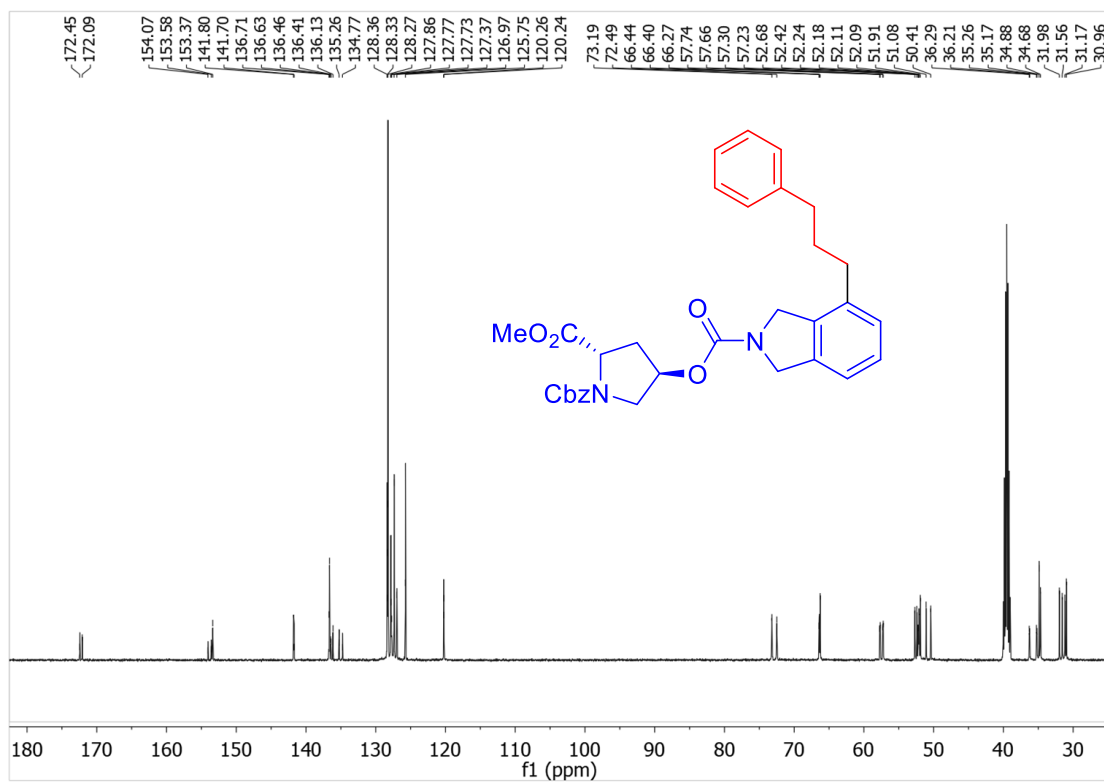


Figure S65. ¹³C{¹H} NMR spectrum (151 MHz, DMSO-d₆) of product derived from **5b**.

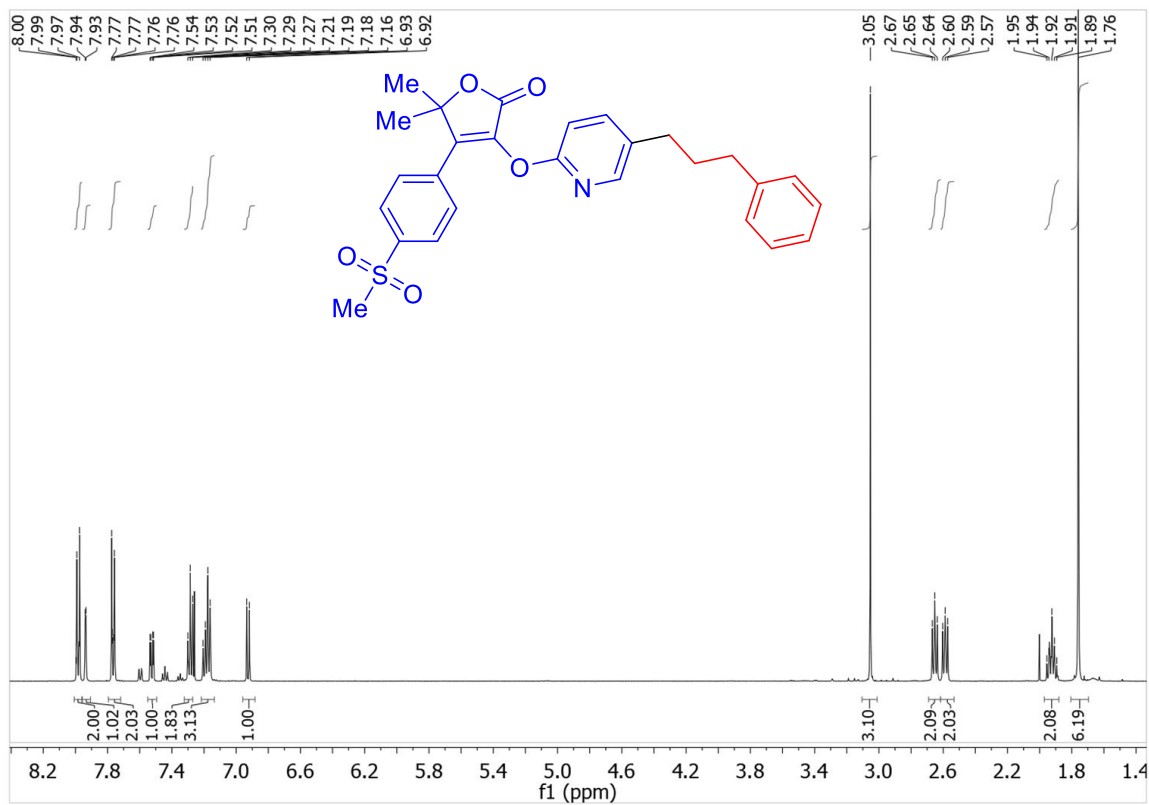


Figure S66. ^1H NMR spectrum (400 MHz, CDCl_3) of product derived from **5c**.

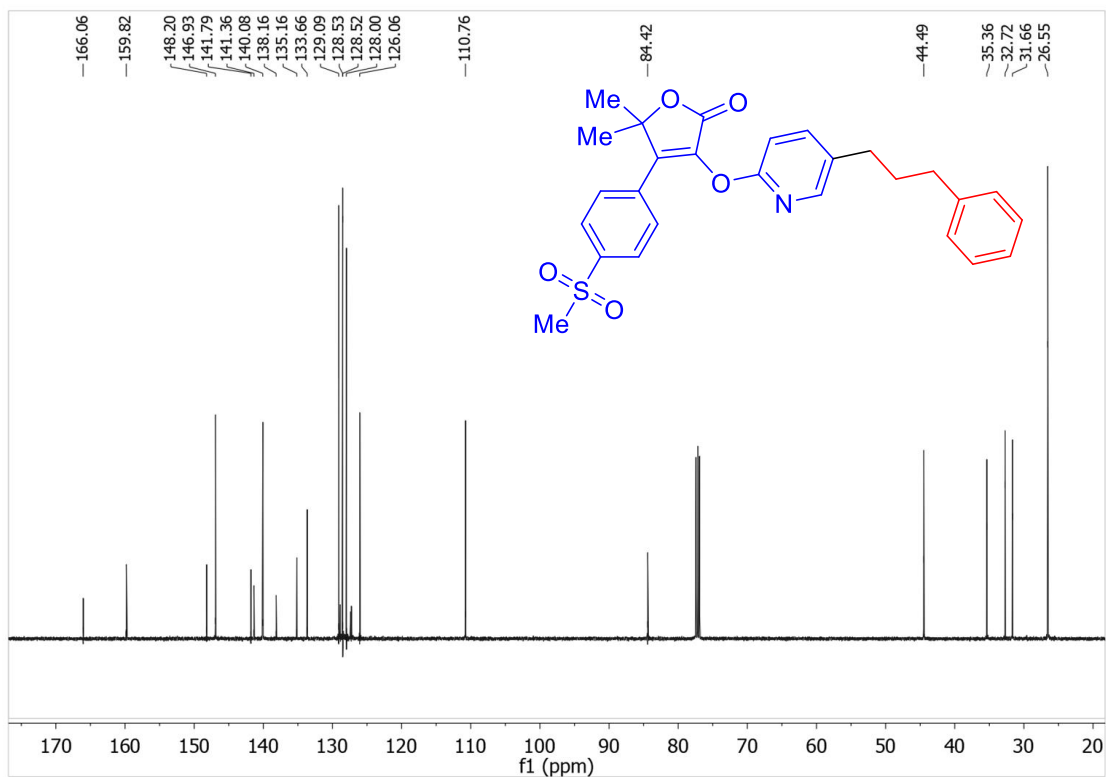


Figure S67. $^{13}\text{C}\{^1\text{H}\}$ NMR spectrum (151 MHz, CDCl_3) of product derived from **5c**.

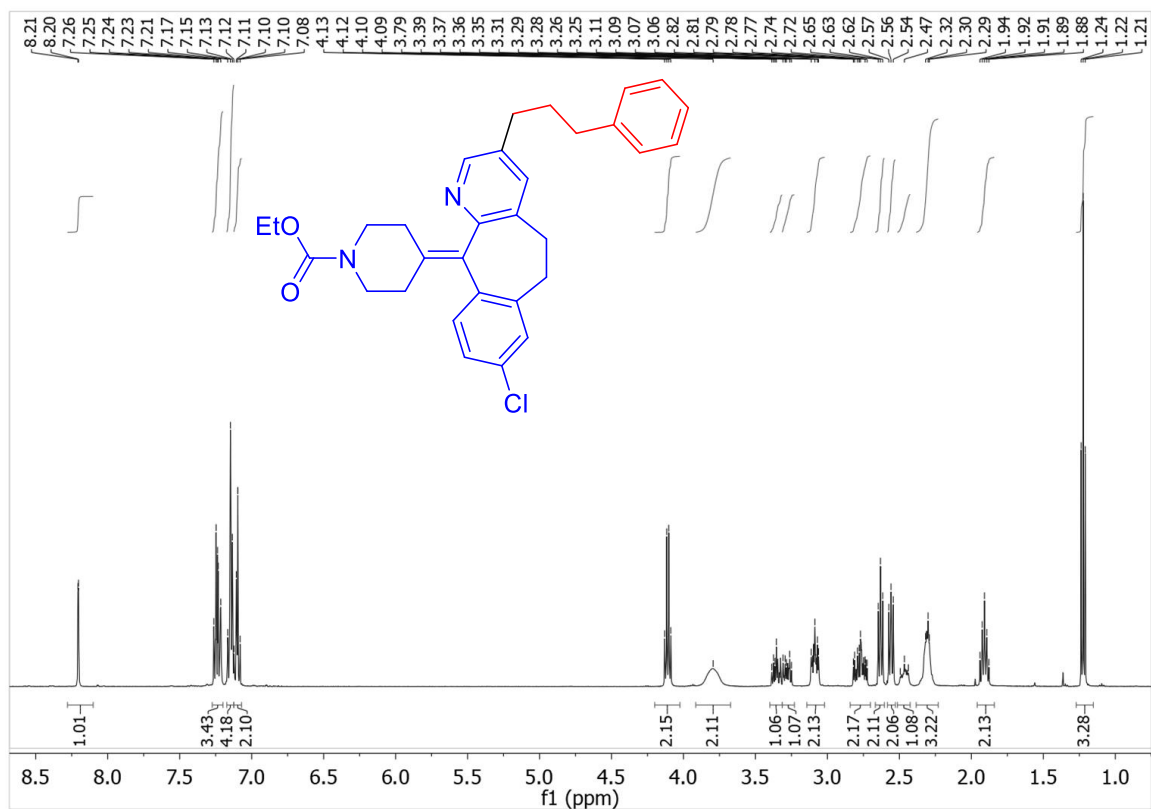


Figure S68. ¹H NMR spectrum (400 MHz, CDCl₃) of product derived from 5d.

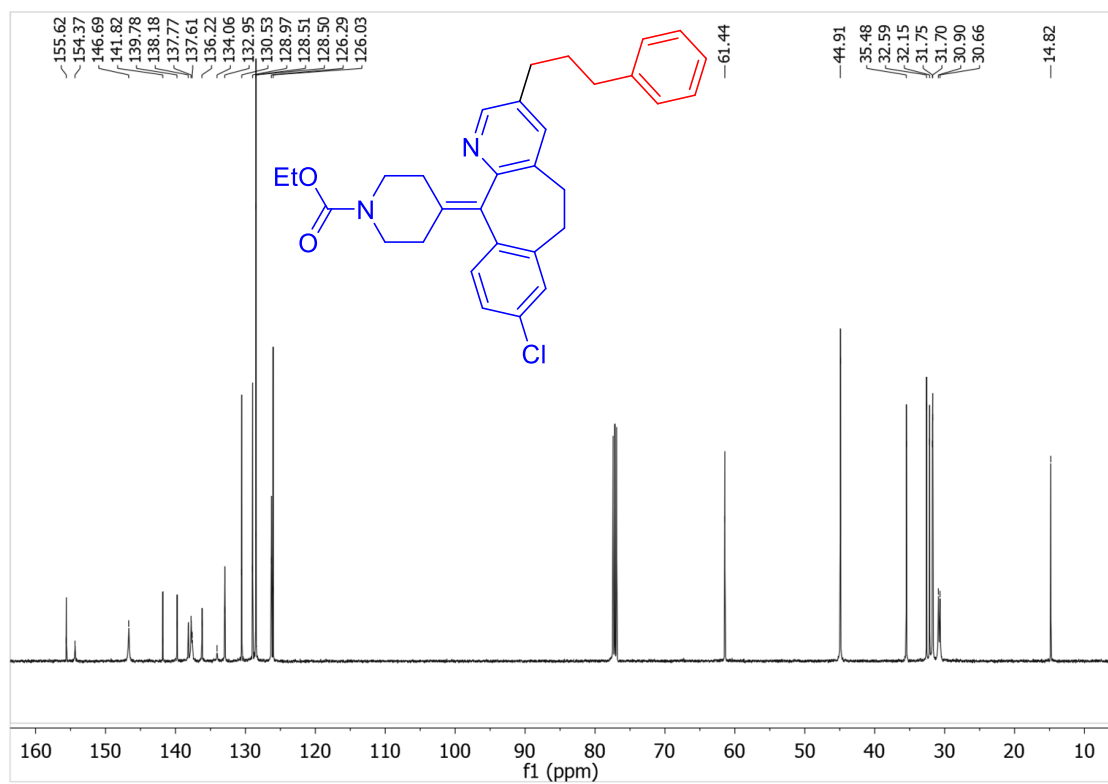


Figure S69. ¹³C{¹H} NMR spectrum (151 MHz, CDCl₃) of product derived from 5d.

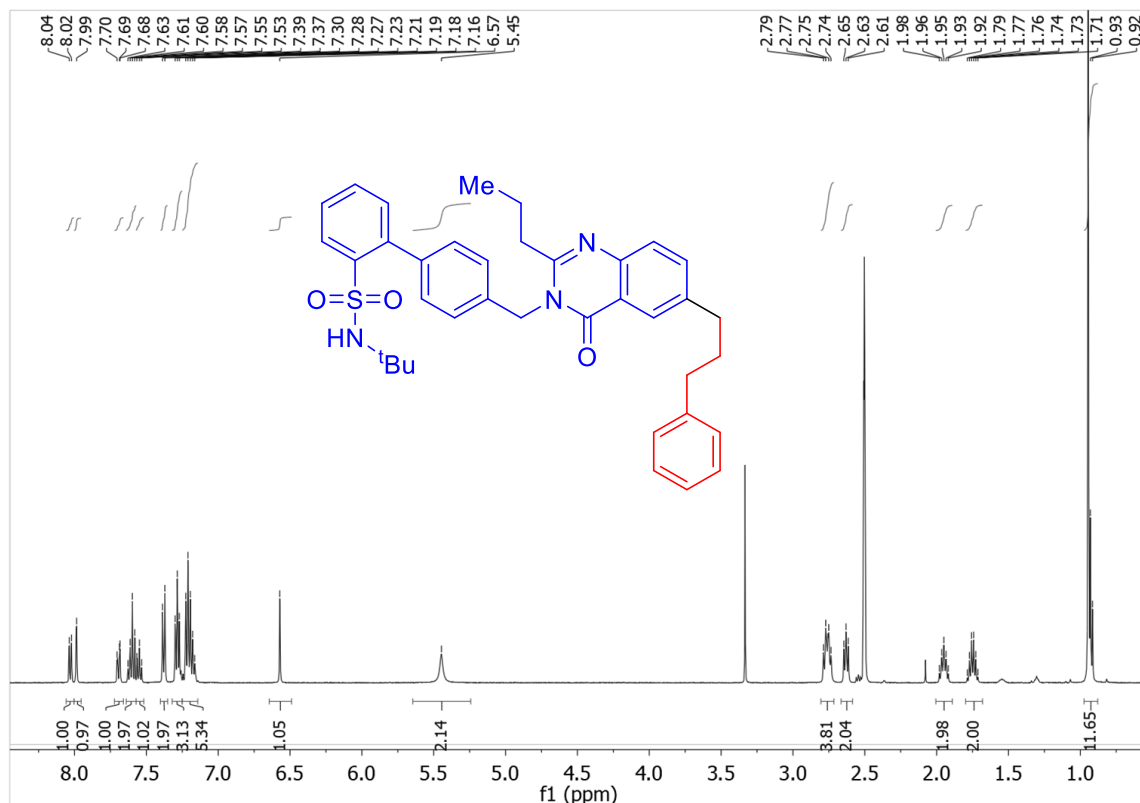


Figure S70. ¹H NMR spectrum (400 MHz, DMSO-d₆) of product derived from **5e**.

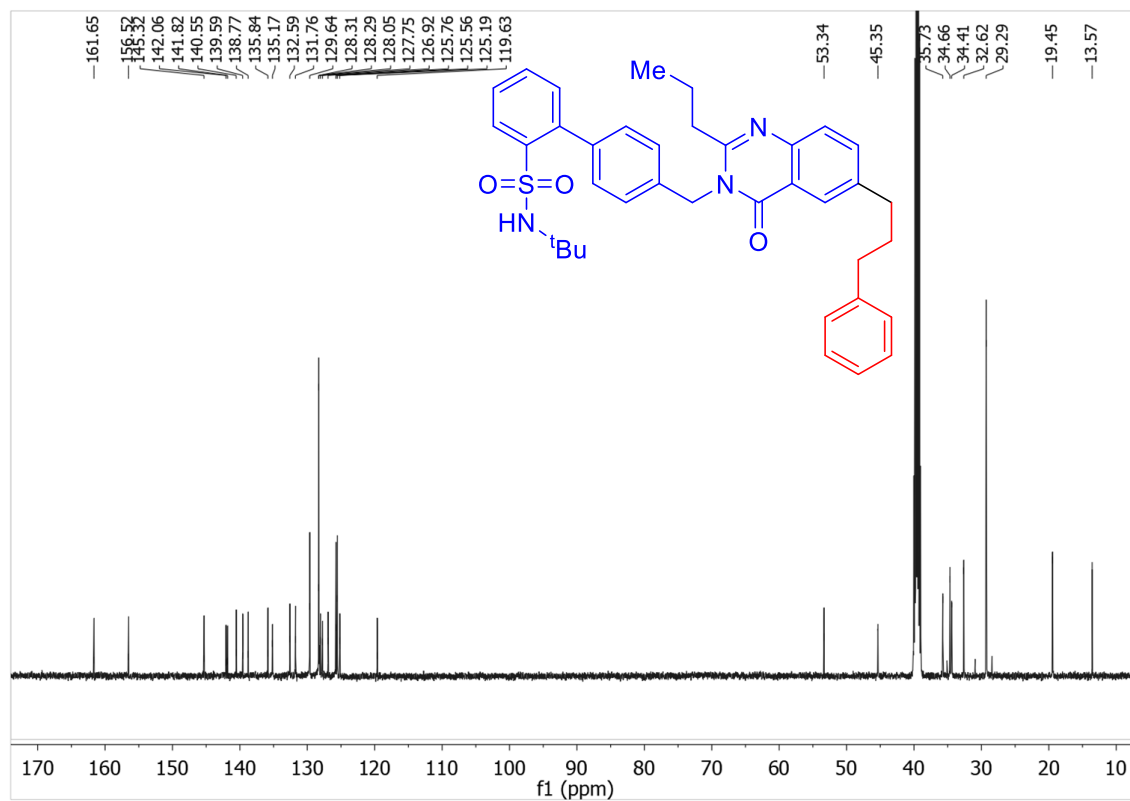


Figure S71. ¹³C{¹H} NMR spectrum (151 MHz, DMSO-d₆) of product derived from **5e**.

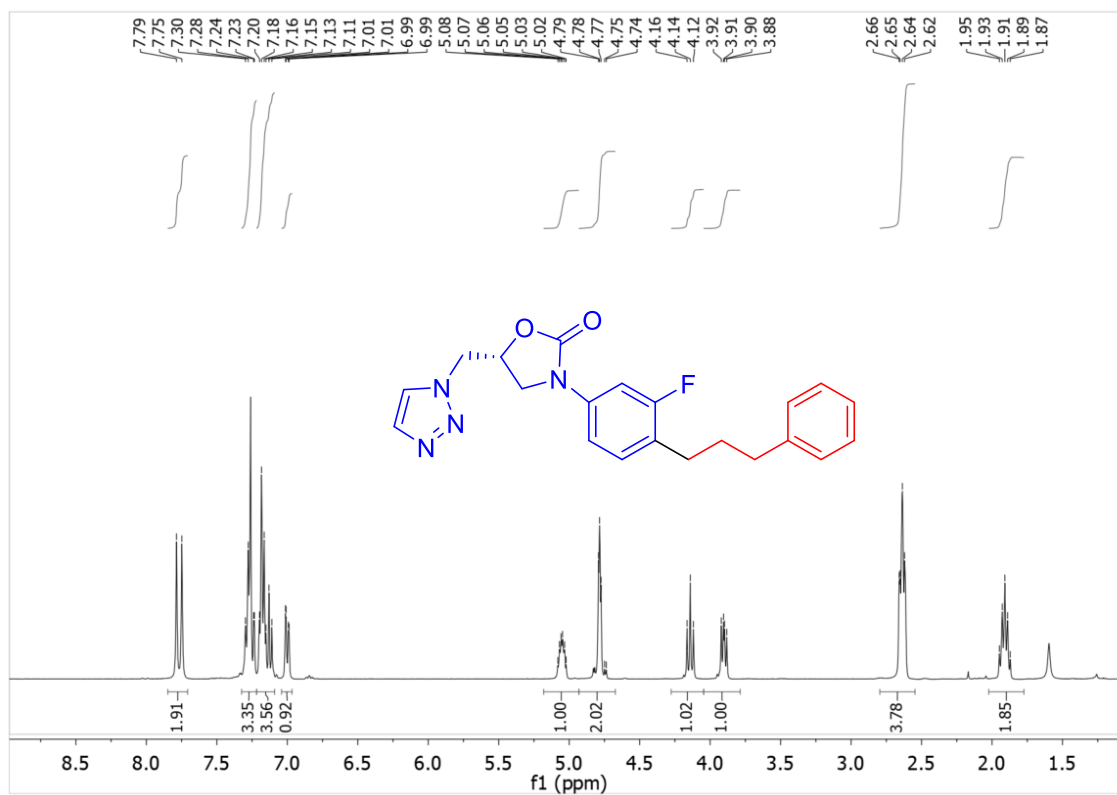


Figure S72. ¹H NMR spectrum (400 MHz, CDCl₃) of product derived from **5f**.

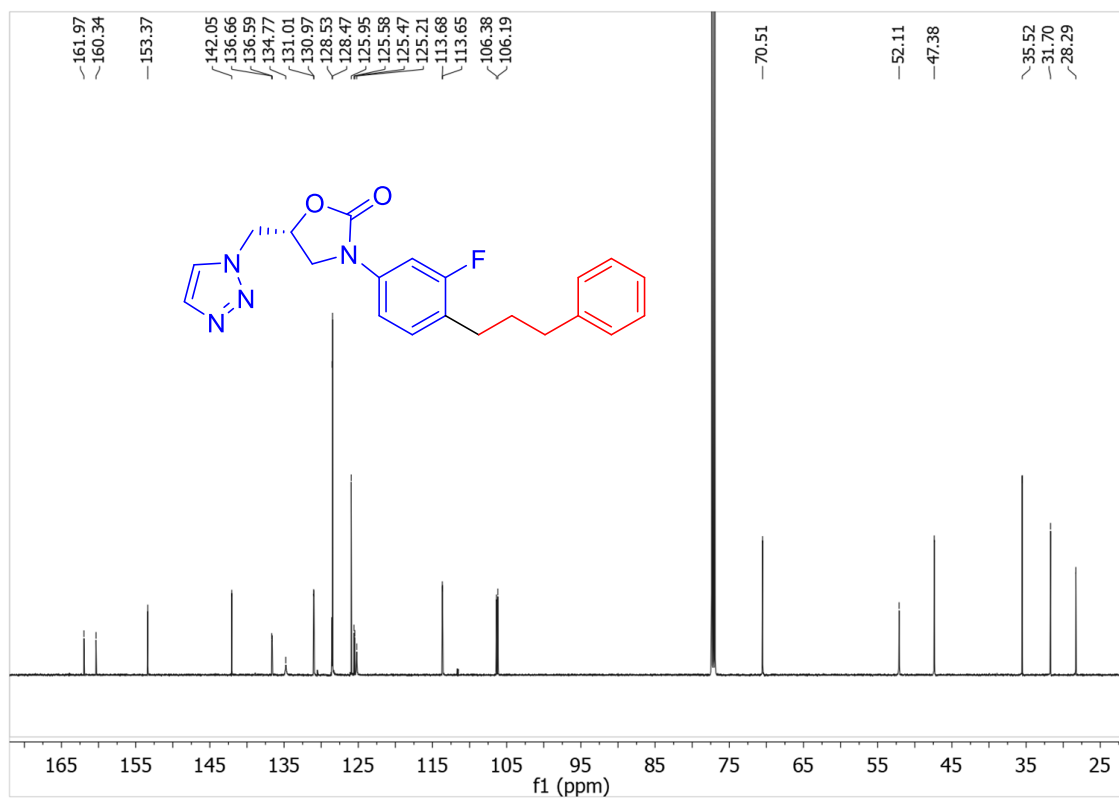


Figure S73. ¹³C{¹H} NMR spectrum (151 MHz, CDCl₃) of product derived from **5f**.

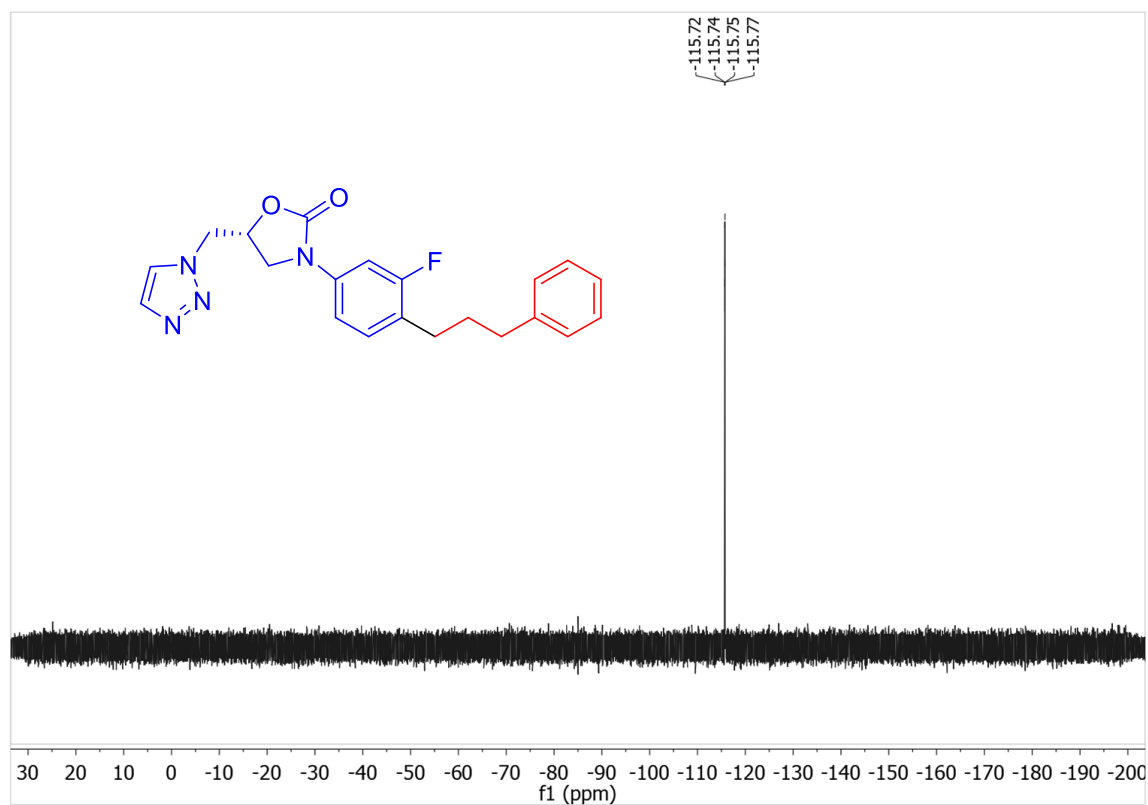


Figure S74. ^{19}F NMR spectrum (400 MHz, CDCl_3) of product derived from **5f**.

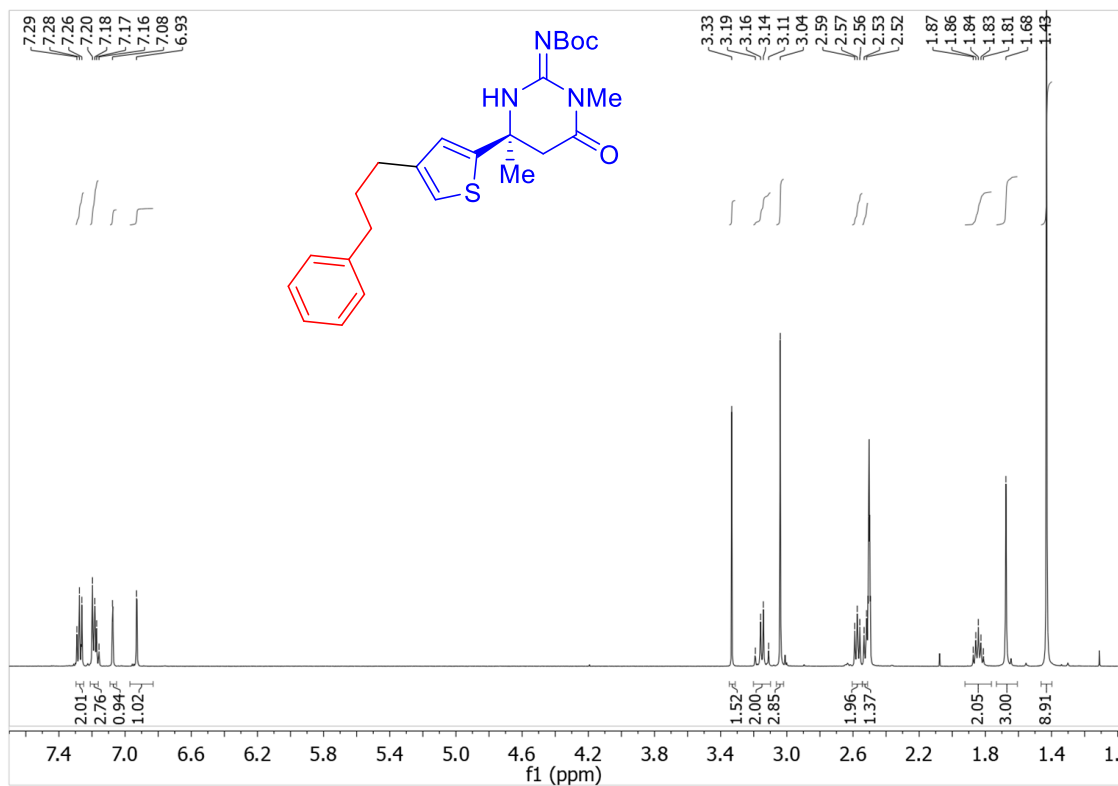


Figure S75. ¹H NMR spectrum (400 MHz, DMSO-d₆) of product derived from **5g**.

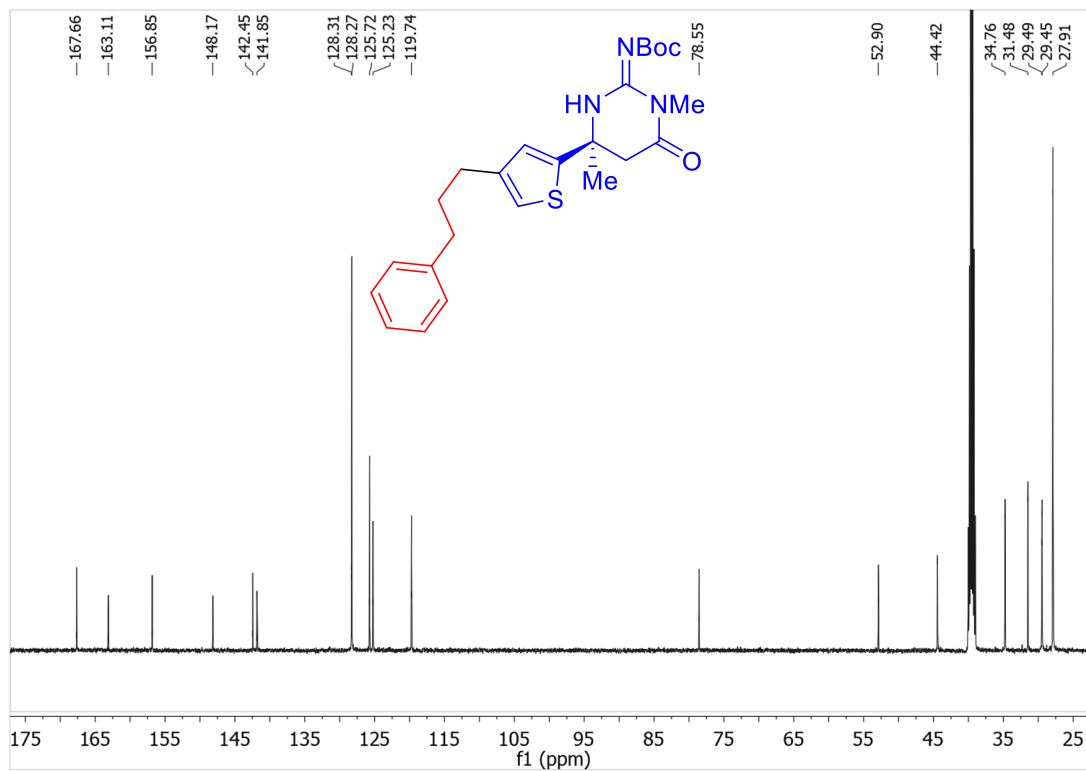


Figure S76. ¹³C{¹H} NMR spectrum (151 MHz, DMSO-d₆) of product derived from **5g**.

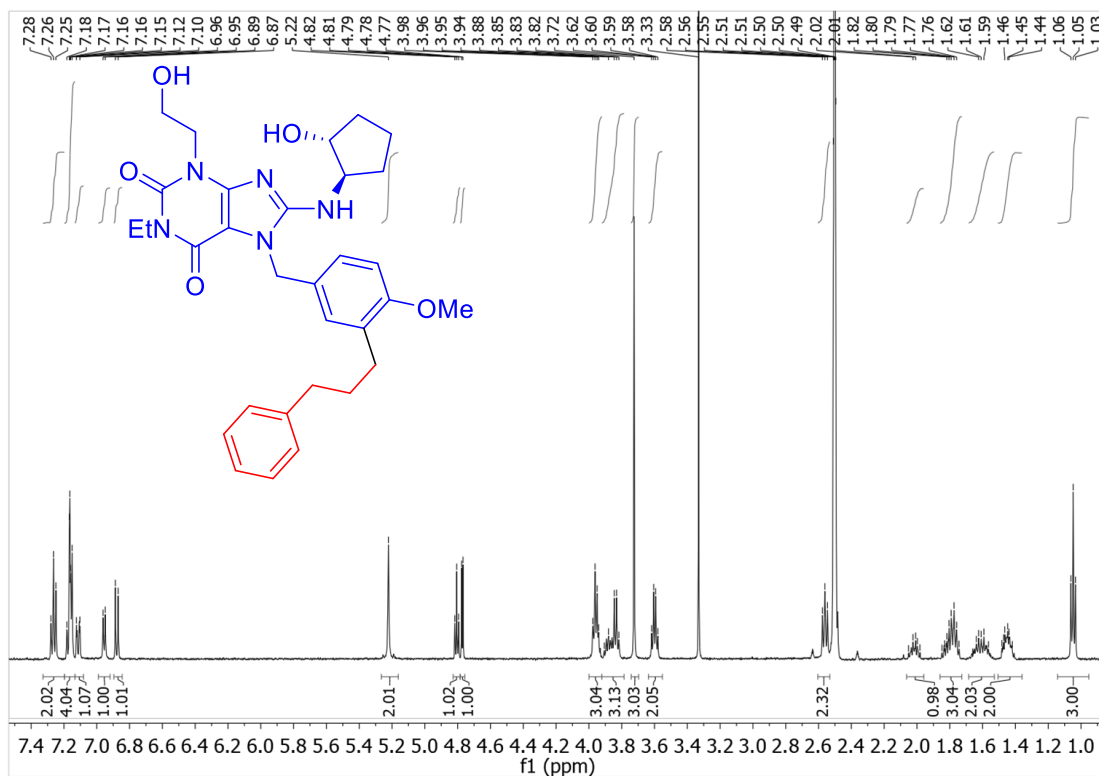


Figure S77. ^1H NMR spectrum (400 MHz, $\text{DMSO}-d_6$) of product derived from **5h**.

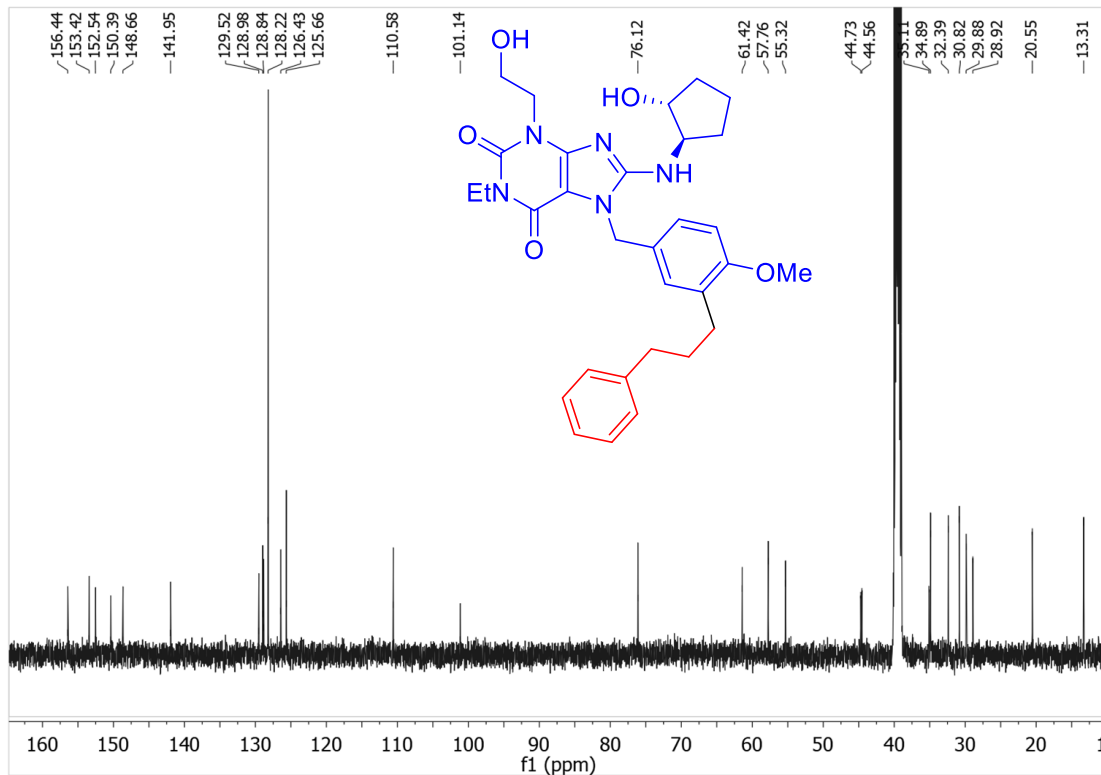


Figure S78. $^{13}\text{C}\{^1\text{H}\}$ NMR spectrum (151 MHz, $\text{DMSO}-d_6$) of product derived from **5h**.

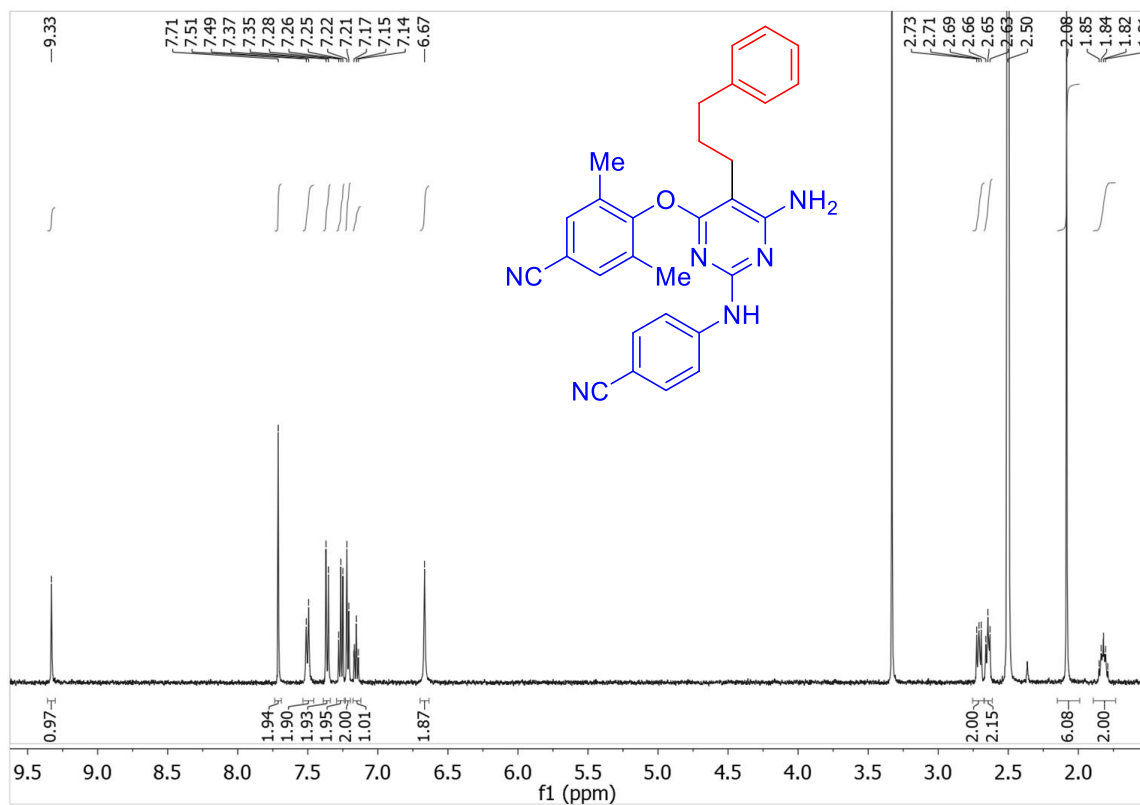


Figure S79. ¹H NMR spectrum (400 MHz, DMSO-d₆) of product derived from 5i.

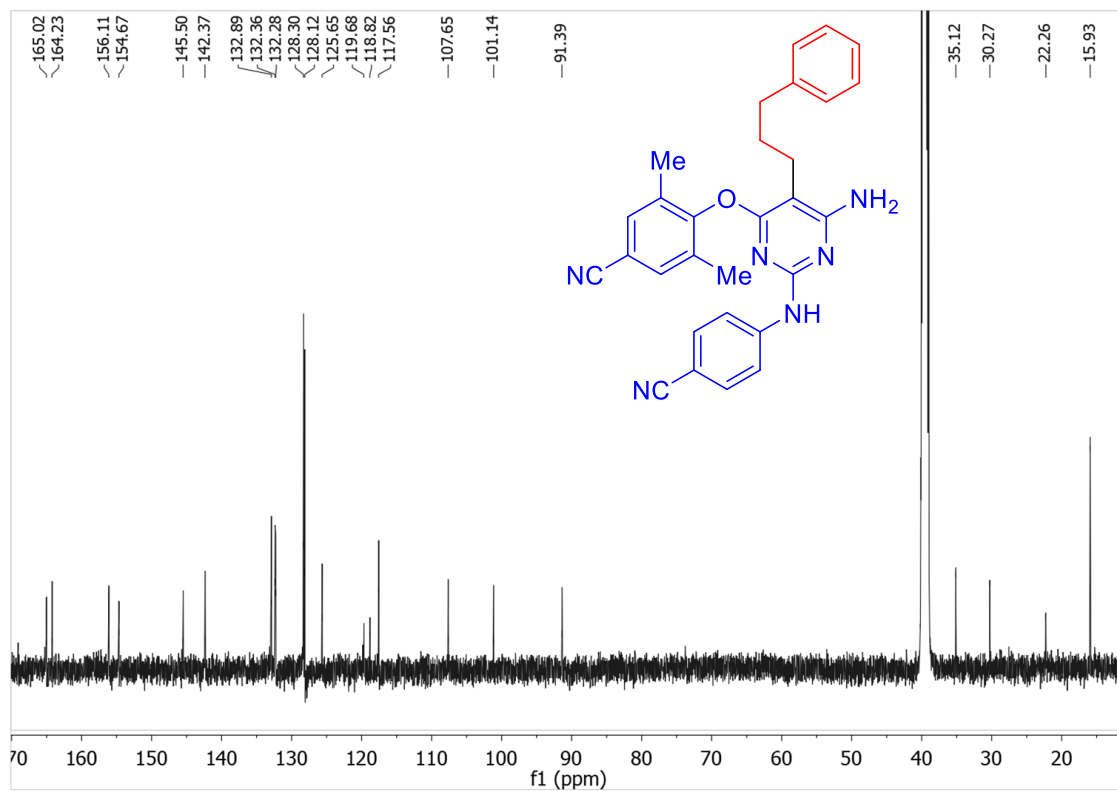


Figure S80. ¹³C{¹H} NMR spectrum (151 MHz, DMSO-d₆) of product derived from 5i.

SXXVI. UPLC Traces from HTE Experiments for Optimization of Drug-Like Aryl Halides with 1-Bromo-3-Phenylpropane

General Information:

The UPLC traces shown in this section depict the UPLC traces obtained from HTE experiments for the optimization of drug-like aryl halides with 1-bromo-3-phenylpropane (see section SXII). One UPLC trace is shown for each aryl halide, which corresponds to the conditions that were utilized to obtain ^1H NMR yields for the reaction (Figure 5 of manuscript). However, because the reaction with aryl halide **5i** was optimized further beyond HTE optimization, no UPLC trace is shown for this substrate. Some traces include an internal standard (biphenyl), but this introduced problems for data analysis (overlapping peaks) in the first set of HTE experiments and so was removed for subsequent experiments.

In the UPLC traces, product (Aryl-Alkyl) signals are colored in dark blue, aryl halide starting material signals are colored teal, biaryl (Aryl-Aryl) signals are colored orange, protodehalogenation (Aryl-H) signals are colored forest green, and internal standard (biphenyl) signals are colored violet (where applicable).

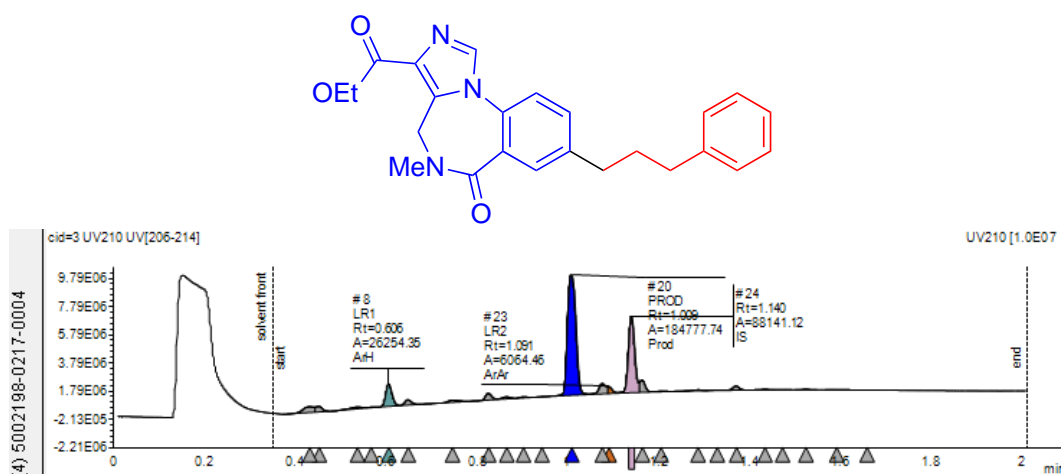


Figure S81. UPLC trace for the optimized reaction conditions of the coupling of aryl halide **5a** with 1-bromo-3-phenylpropane.

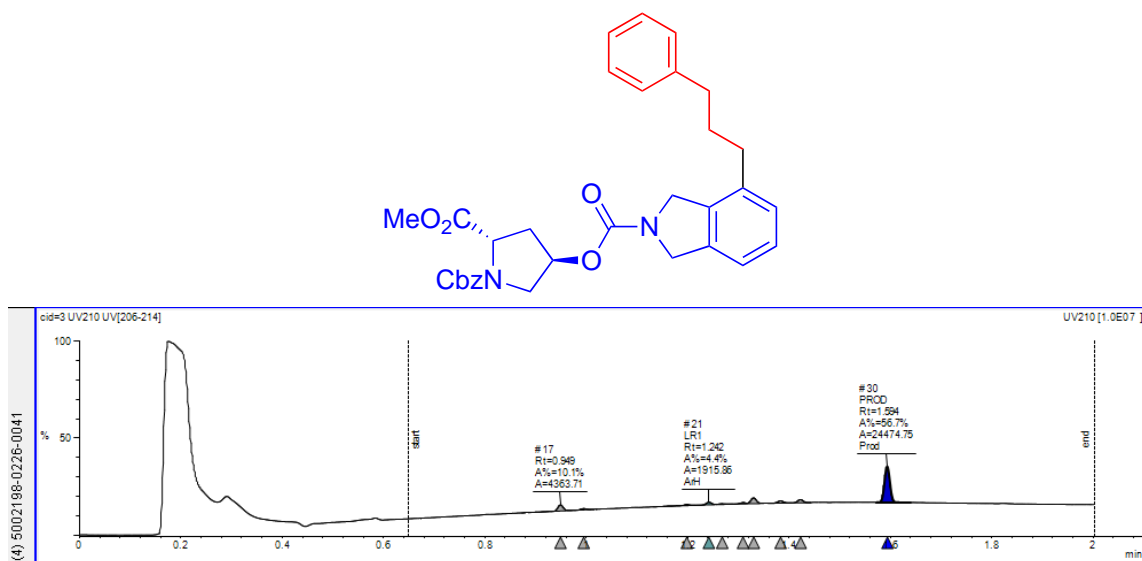


Figure S82. UPLC trace for the optimized reaction conditions of the coupling of aryl halide **5b** with 1-bromo-3-phenylpropane.

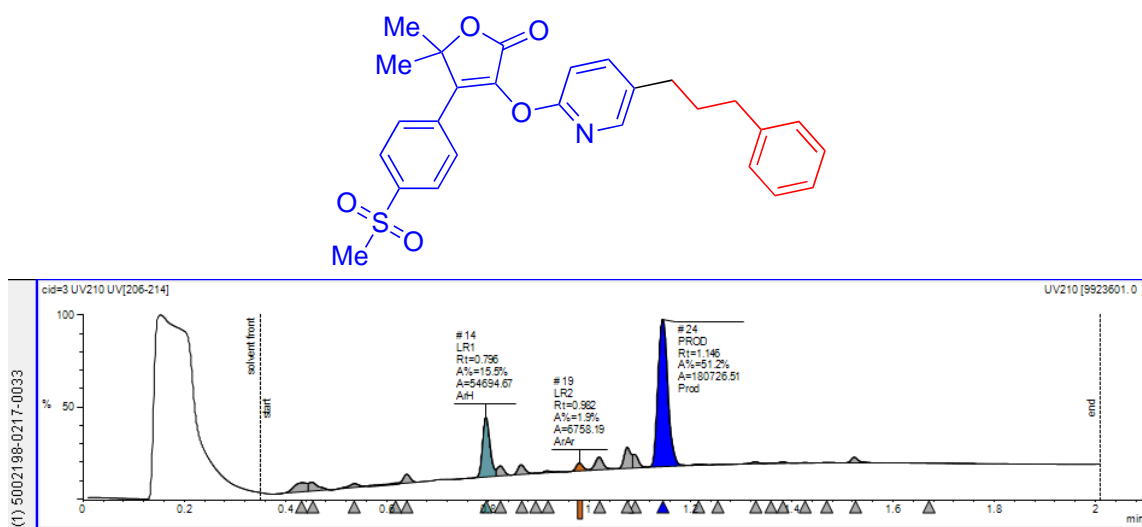


Figure S83. UPLC trace for the optimized reaction conditions of the coupling of aryl halide **5c** with 1-bromo-3-phenylpropane.

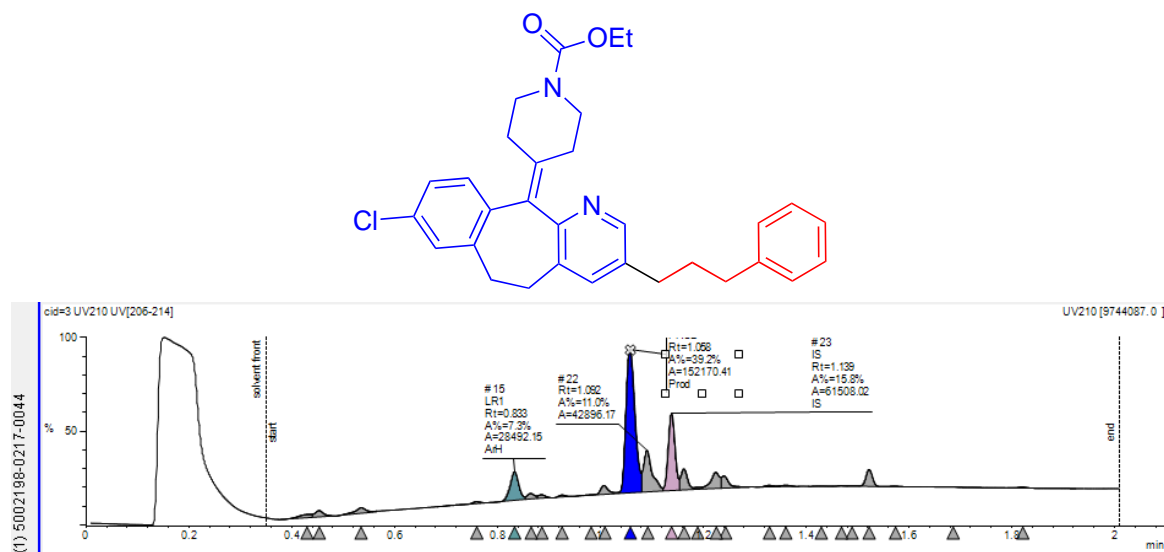


Figure S84. UPLC trace for the optimized reaction conditions of the coupling of aryl halide **5d** with 1-bromo-3-phenylpropane.

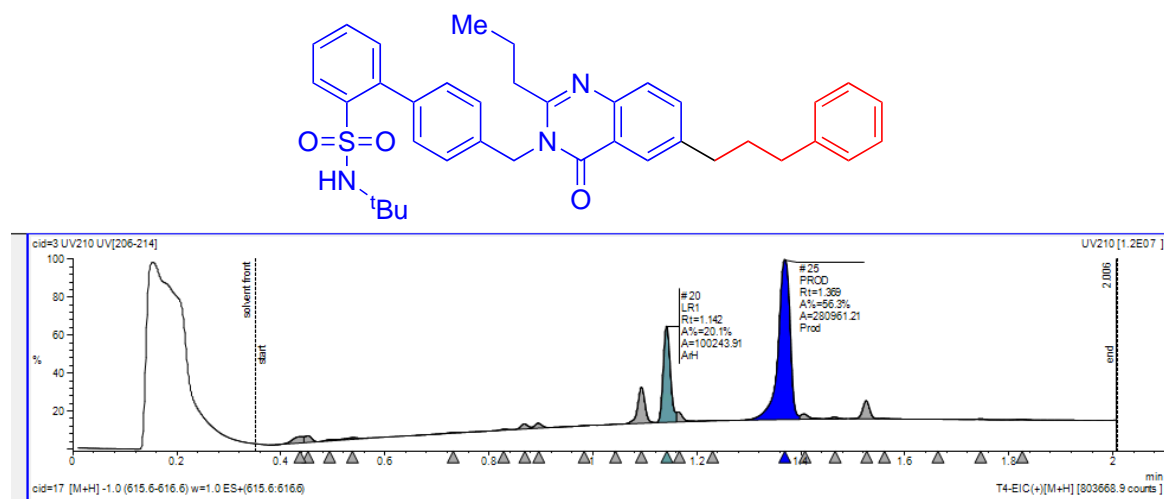


Figure S85. UPLC trace for the optimized reaction conditions of the coupling of aryl halide **5e** with 1-bromo-3-phenylpropane. Note: Aryl-Alkyl overlaps with Aryl-Iodide and Aryl-H overlaps with biphenyl internal standard in chromatograph. Low quantities of Aryl-H and Aryl-Iodide were determined by mass spectrometry ion count, consistent with the high ^1H NMR yield (91%) of the reaction.

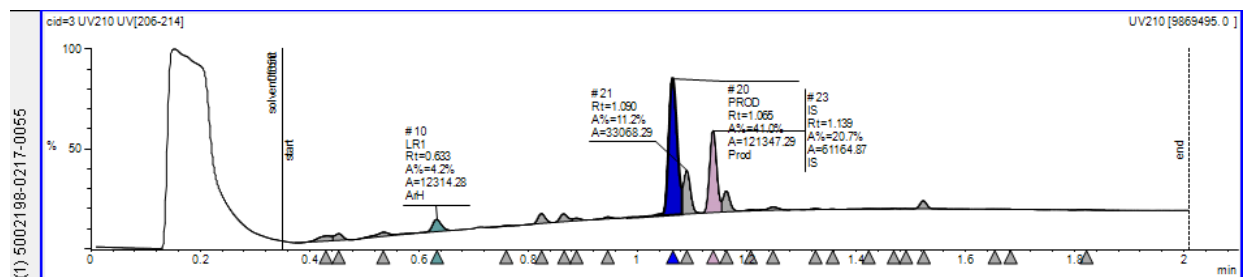
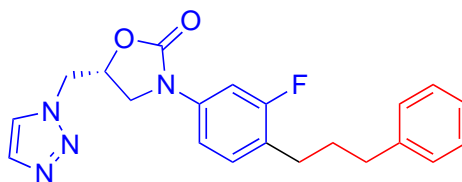


Figure S86. UPLC trace for the optimized reaction conditions of the coupling of aryl halide **5f** with 1-bromo-3-phenylpropane.

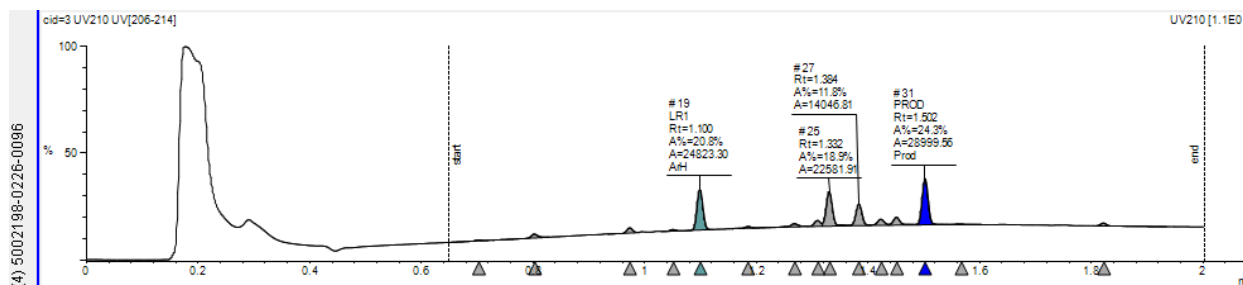
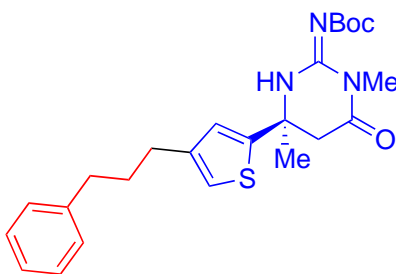


Figure S87. UPLC trace for the optimized reaction conditions of the coupling of aryl halide **5g** with 1-bromo-3-phenylpropane.

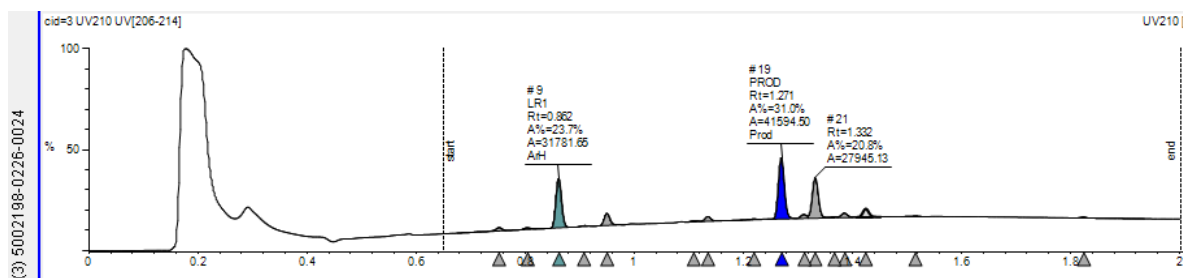
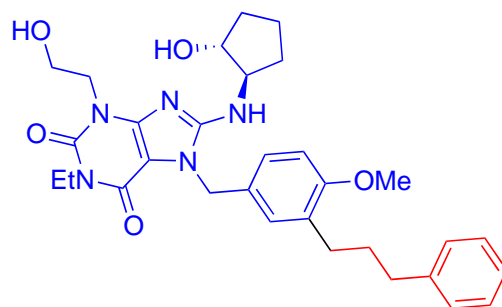


Figure S88. UPLC trace for the optimized reaction conditions of the coupling of aryl halide **5h** with 1-bromo-3-phenylpropane.

SXXVII. UPLC Traces from HTE Experiments for Parallel Library Synthesis Using Substrate **5f**

General Information:

The UPLC traces shown in this section depict the UPLC traces obtained from HTE experiments for the parallel library synthesis of substrate **5f** (see section S27).

In the UPLC traces, product (Aryl-Alkyl) signals are colored in dark blue, aryl halide starting material signals are colored teal, biaryl (Aryl-Aryl) signals are colored forest green, protodehalogenation (Aryl-H) signals are colored red.

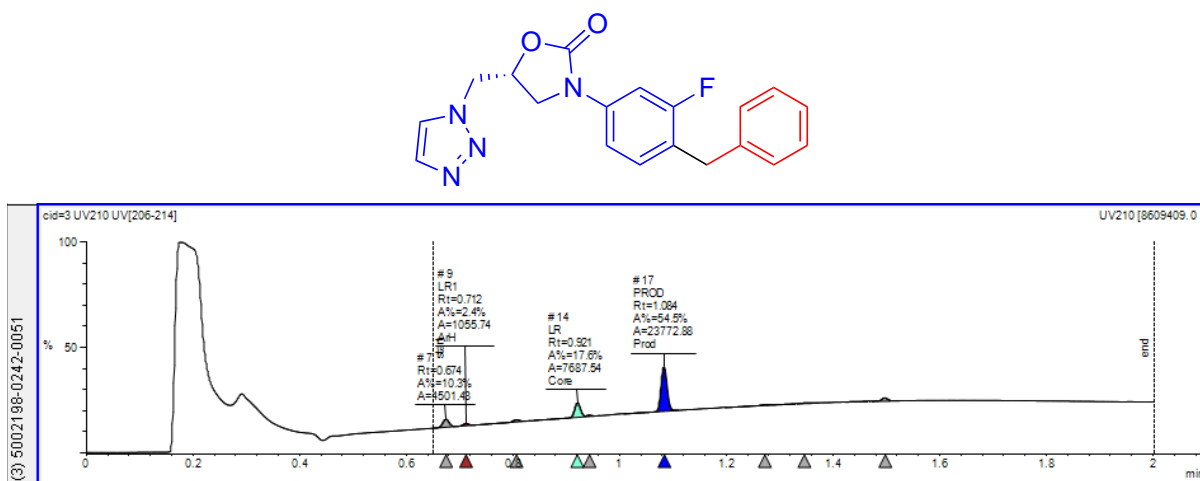


Figure S89. UPLC trace the cross-electrophile coupling of **5f** with substrate **6a**.

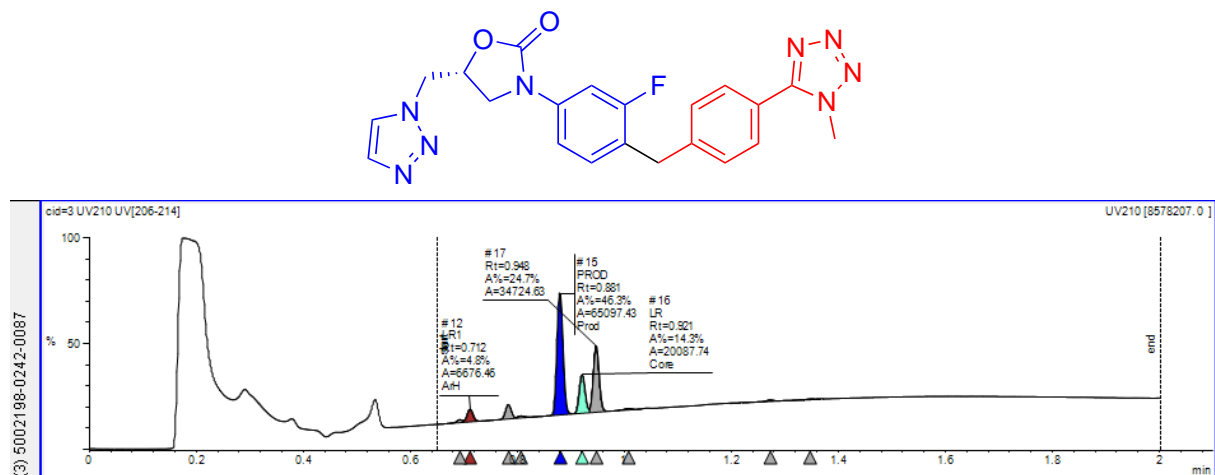


Figure S90. UPLC trace the cross-electrophile coupling of **5f** with substrate **6b**.

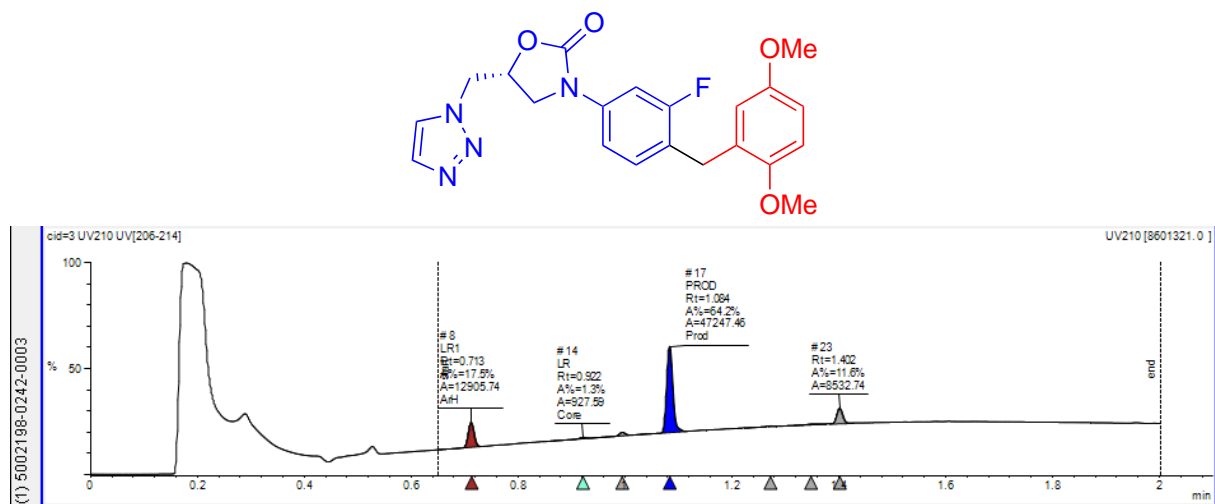


Figure S91. UPLC trace the cross-electrophile coupling of **5f** with substrate **6c**.

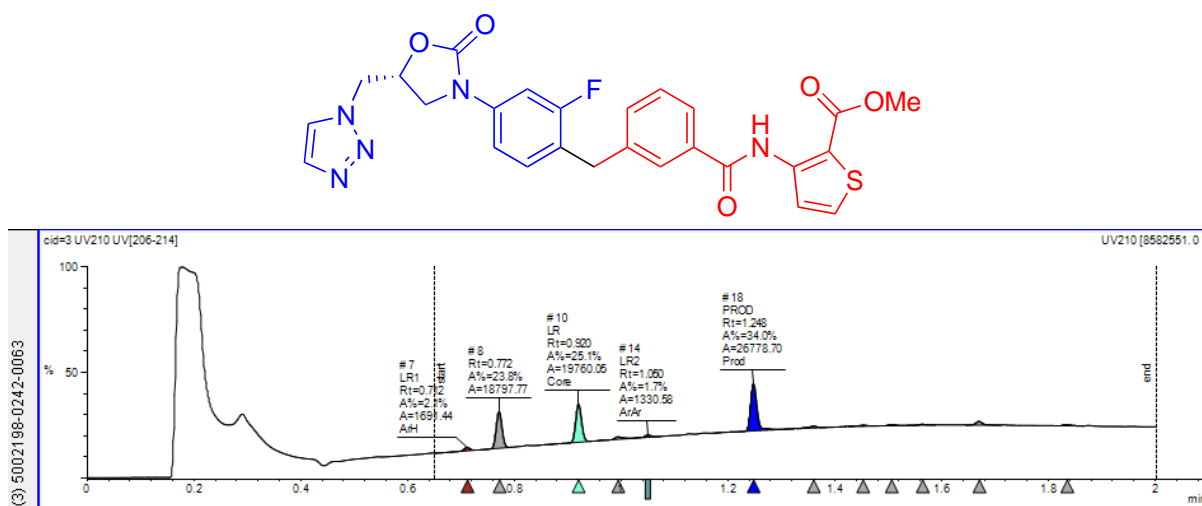


Figure S92. UPLC trace the cross-electrophile coupling of **5f** with substrate **6d**.

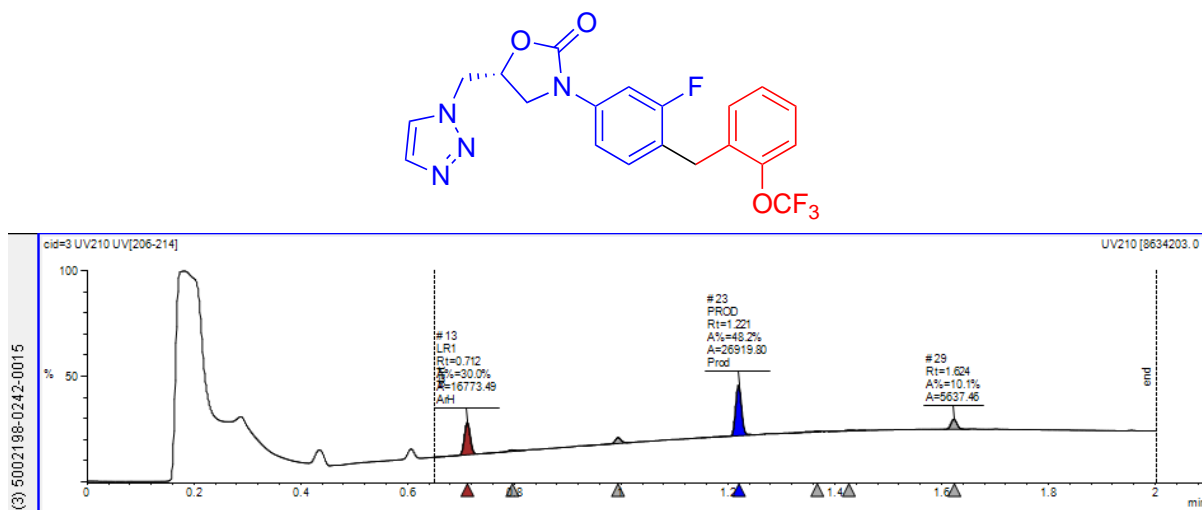


Figure S93. UPLC trace the cross-electrophile coupling of **5f** with substrate **6e**.

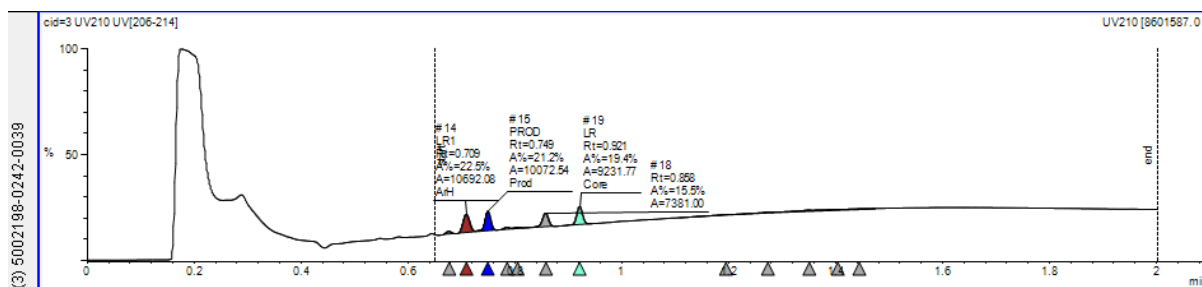
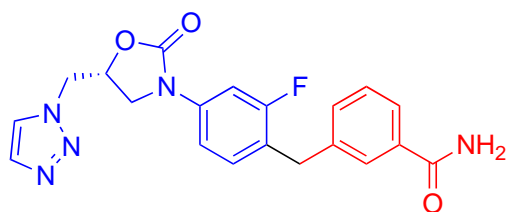


Figure S94. UPLC trace the cross-electrophile coupling of **5f** with substrate **6f**.

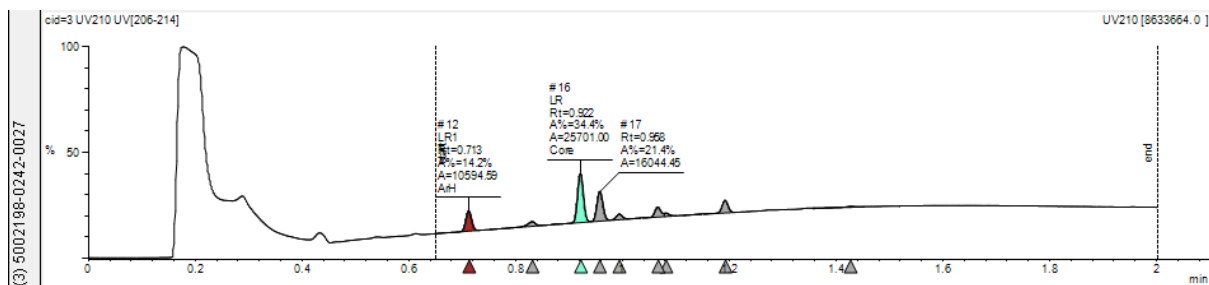
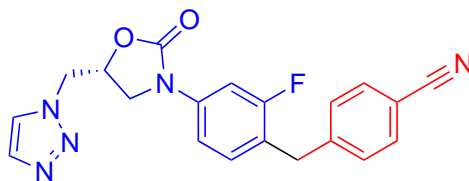


Figure S95. UPLC trace the cross-electrophile coupling of **5f** with substrate **6g**.

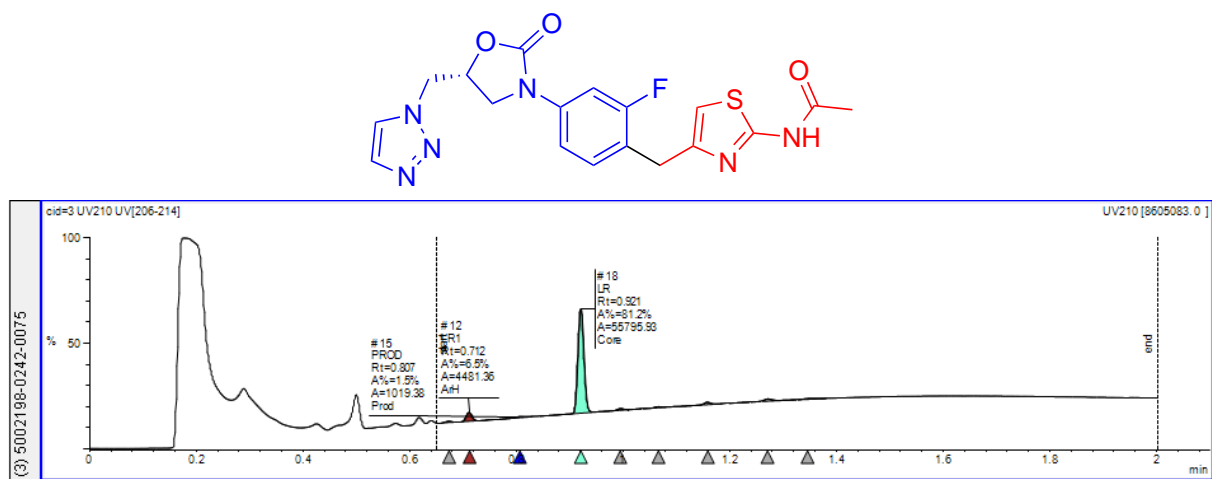


Figure S96. UPLC trace the cross-electrophile coupling of 5f with substrate 6h.

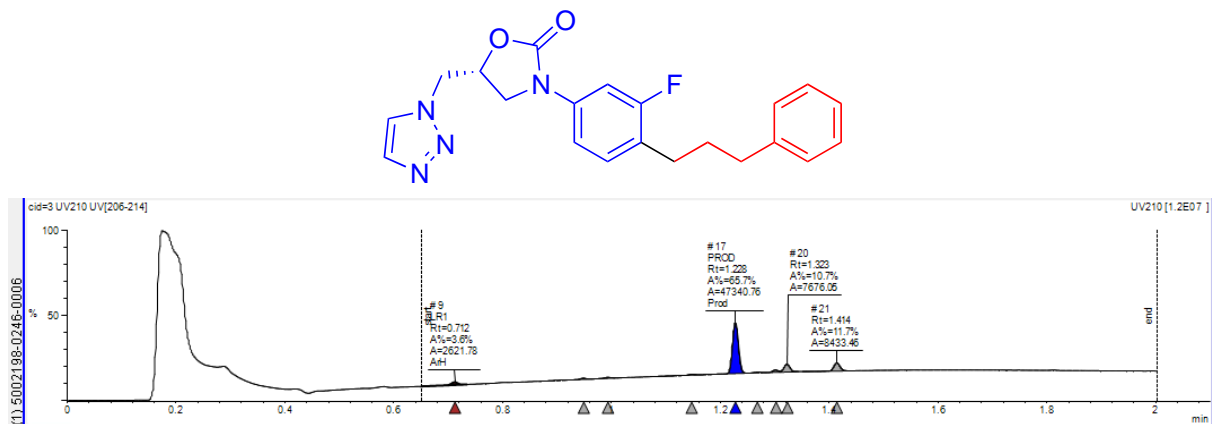


Figure S97. UPLC trace the cross-electrophile coupling of 5f with substrate 6i.

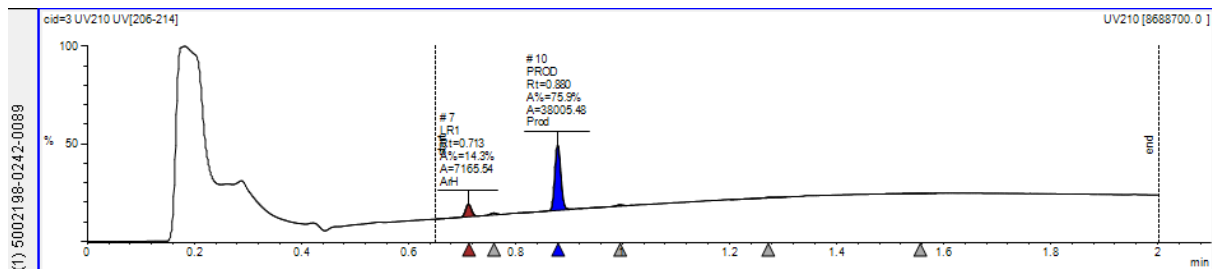
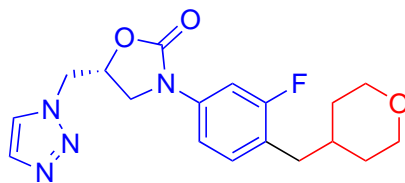


Figure S98. UPLC trace the cross-electrophile coupling of **5f** with substrate **6j**.

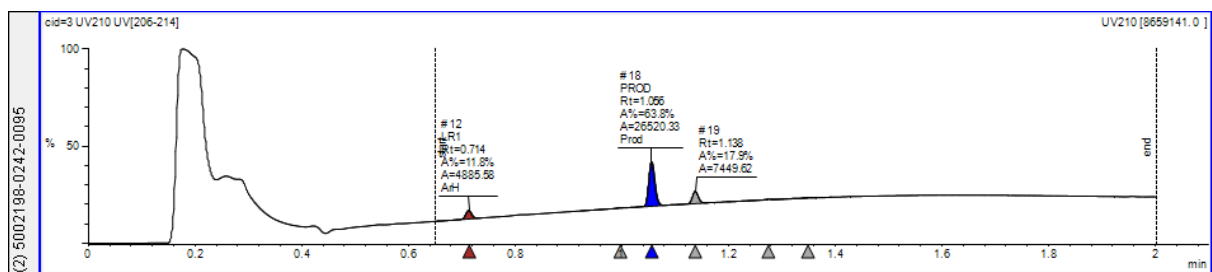
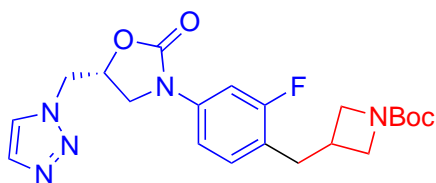


Figure S99. UPLC trace the cross-electrophile coupling of **5f** with substrate **6k**.

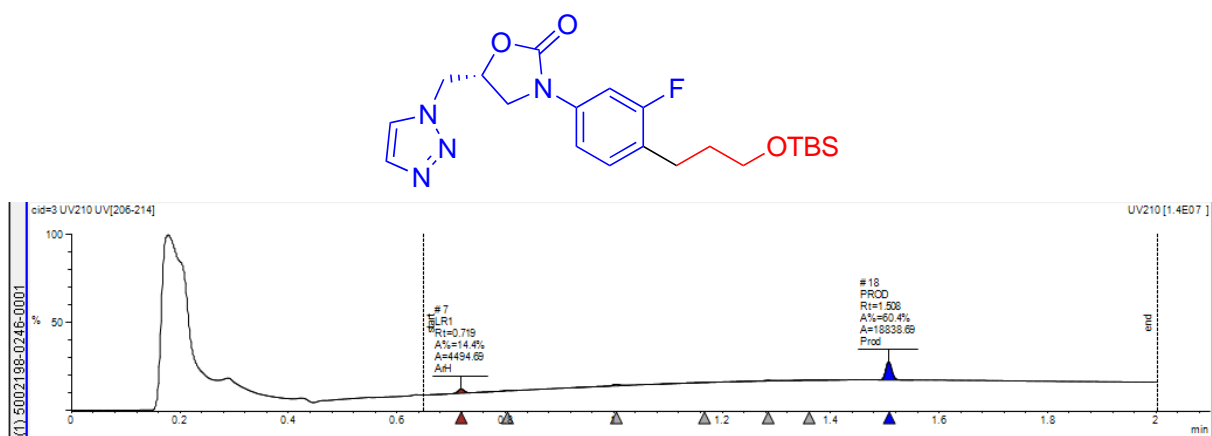


Figure S100. UPLC trace the cross-electrophile coupling of **5f** with substrate **6l**.

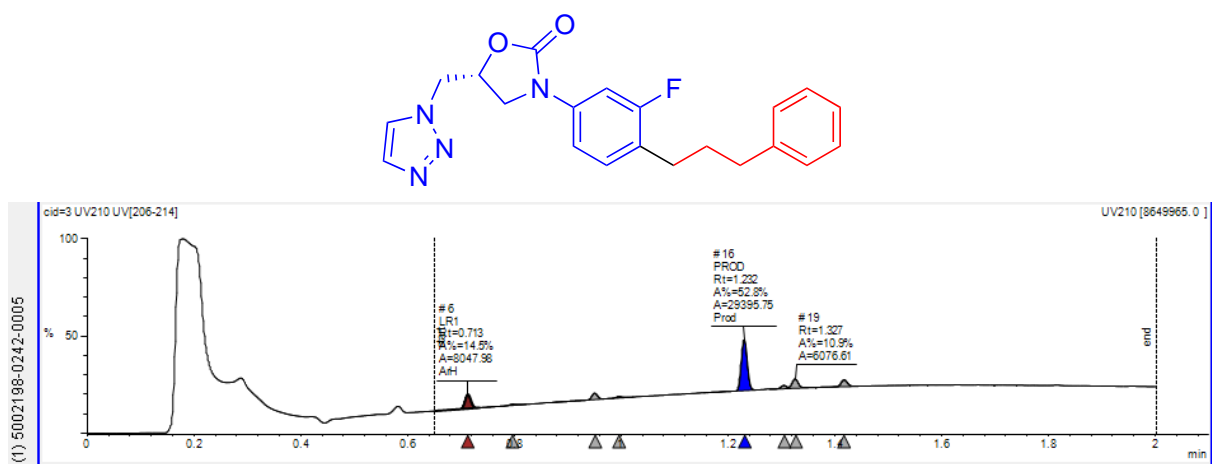


Figure S101. UPLC trace the cross-electrophile coupling of **5f** with substrate **6m**.

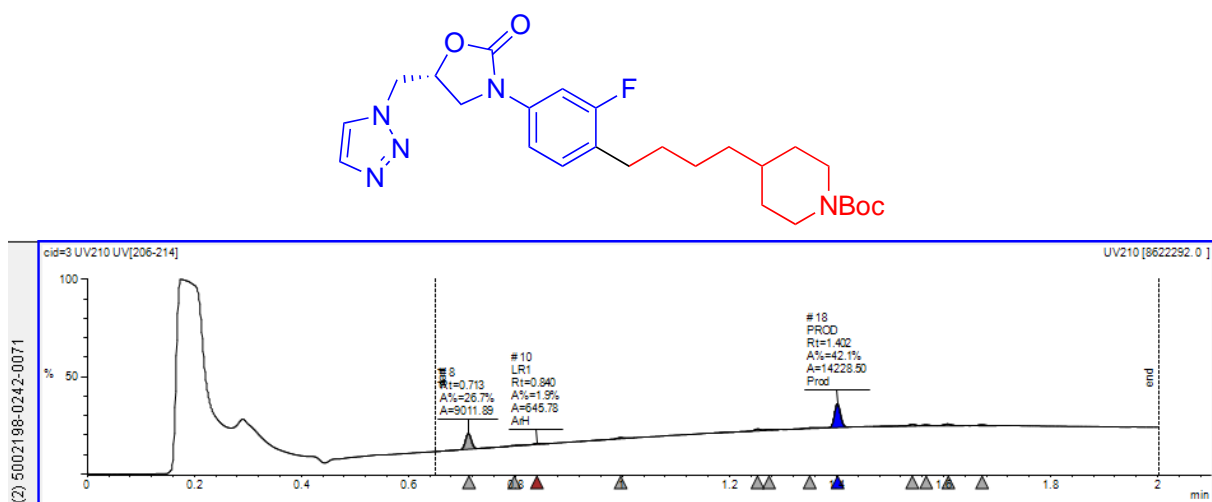


Figure S102. UPLC trace the cross-electrophile coupling of **5f** with substrate **6n**.

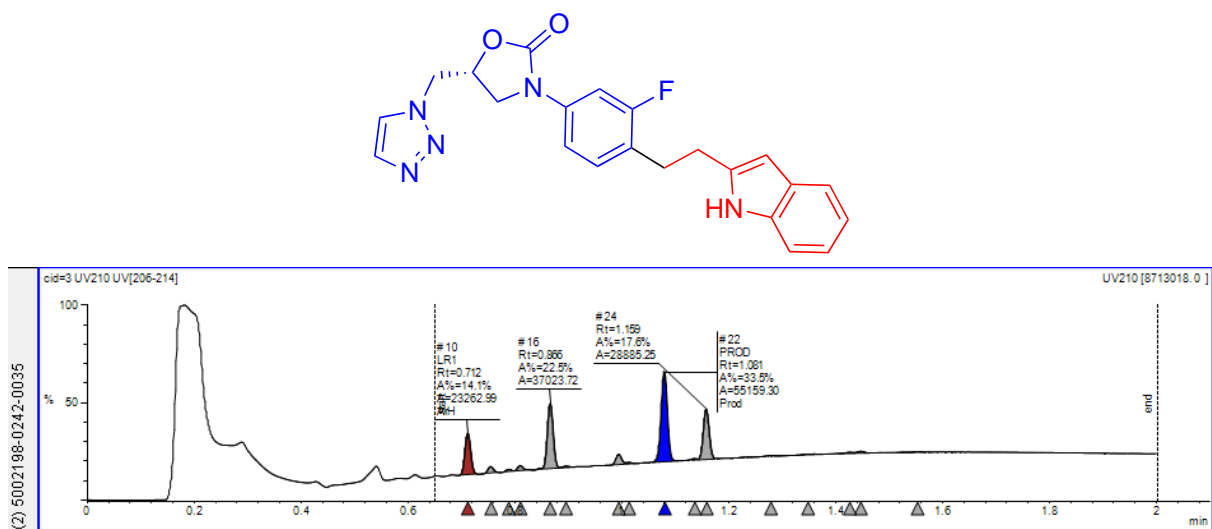


Figure S103. UPLC trace the cross-electrophile coupling of **5f** with substrate **6o**.

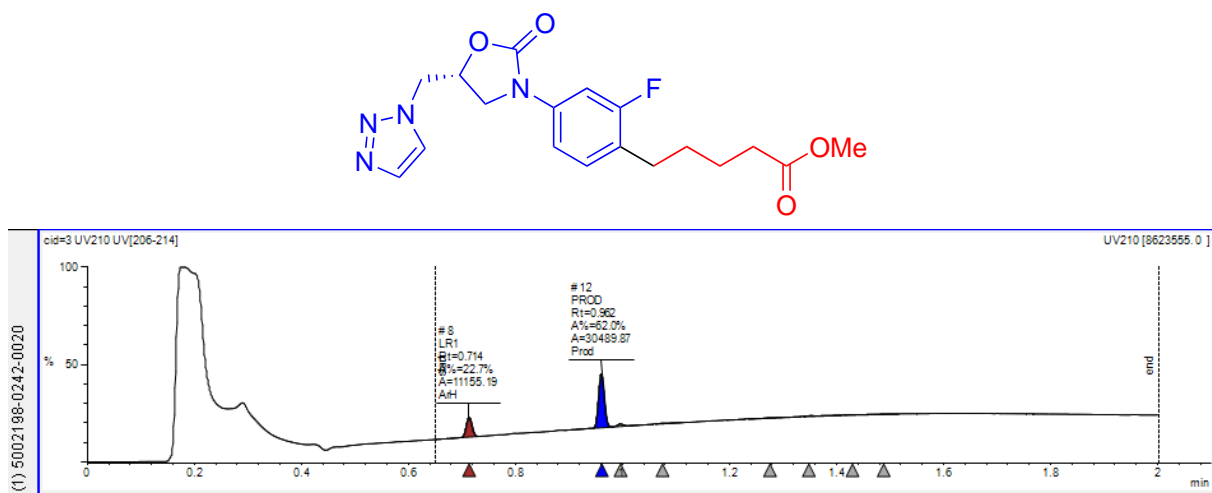


Figure S104. UPLC trace the cross-electrophile coupling of **5f** with substrate **6p**.

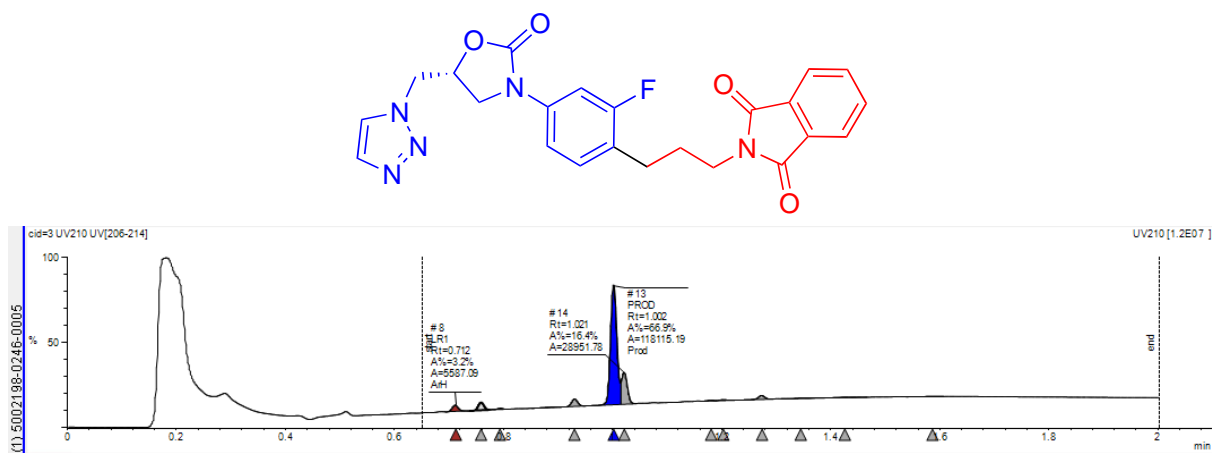


Figure S105. UPLC trace the cross-electrophile coupling of **5f** with substrate **6q**.

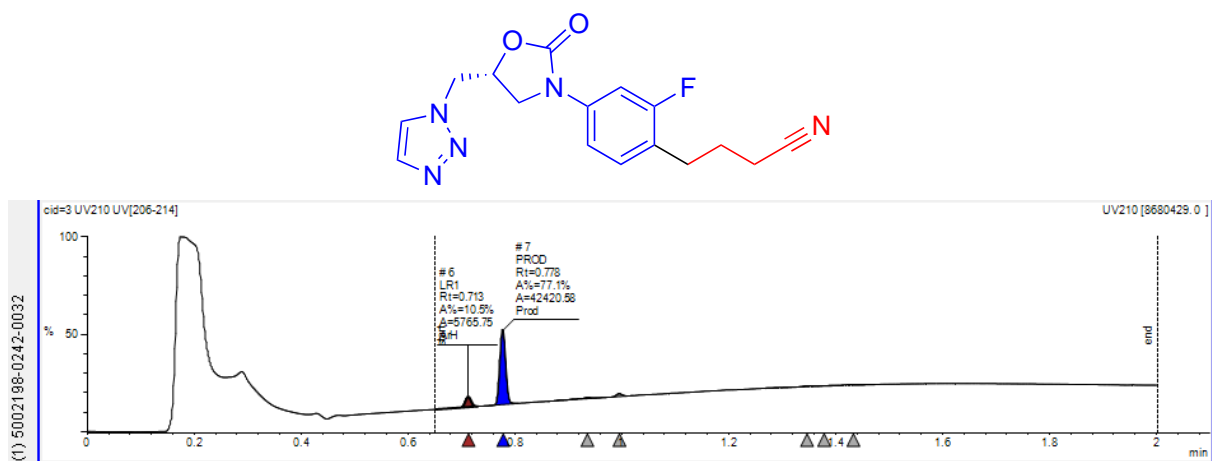


Figure S106. UPLC trace the cross-electrophile coupling of **5f** with substrate **6r**.

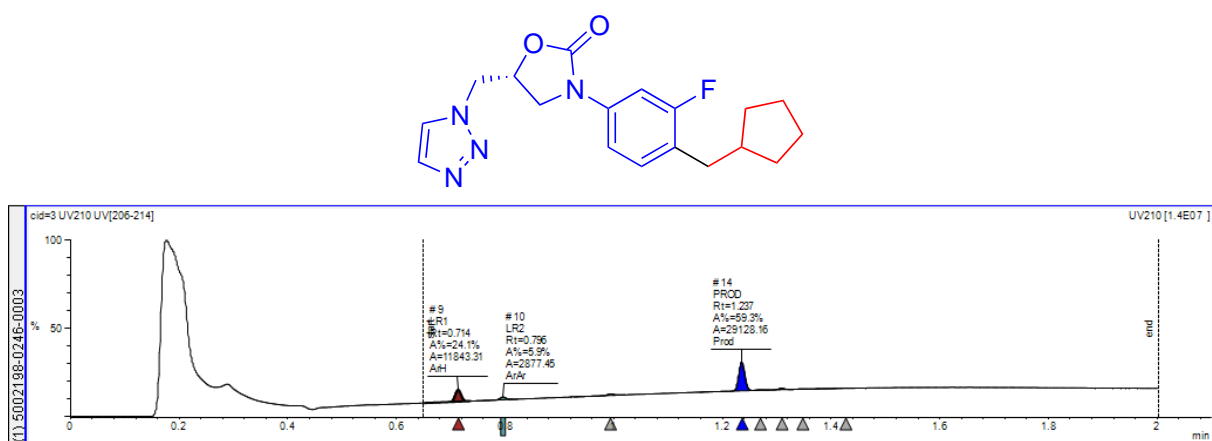


Figure S107. UPLC trace the cross-electrophile coupling of **5f** with substrate **6s**.

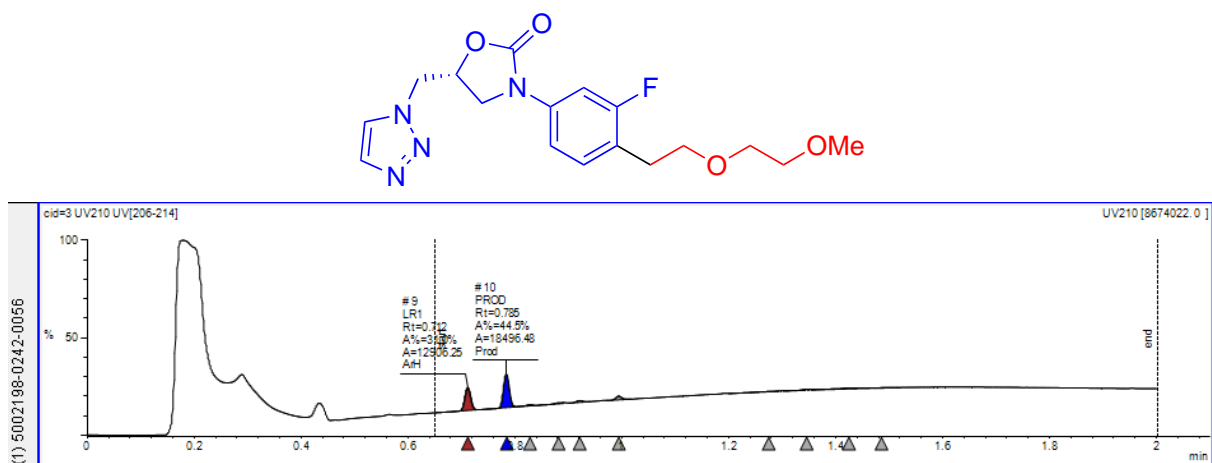


Figure S108. UPLC trace the cross-electrophile coupling of **5f** with substrate **6t**.

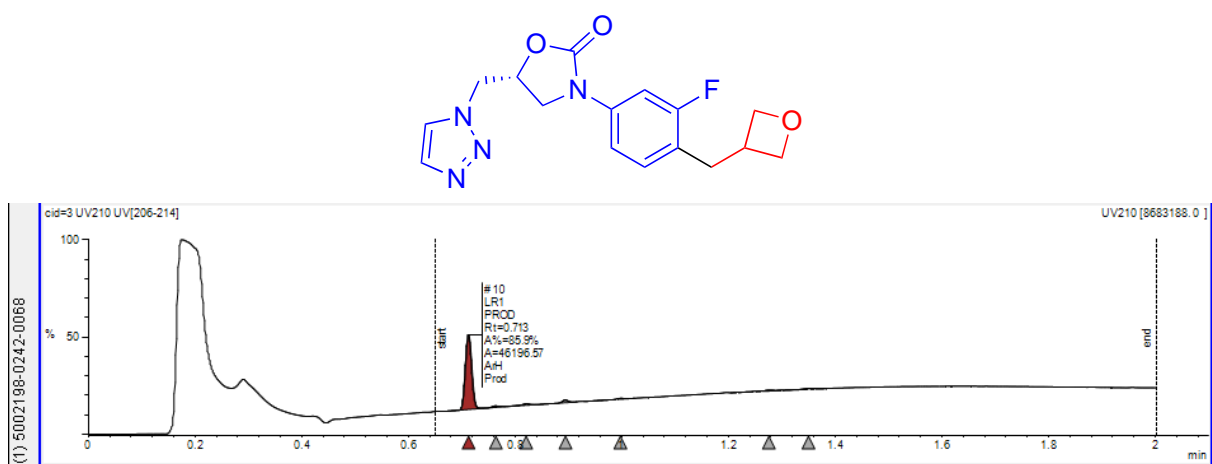


Figure S109. UPLC trace the cross-electrophile coupling of **5f** with substrate **6u**. Note: Aryl-Alkyl and Aryl-H overlap.

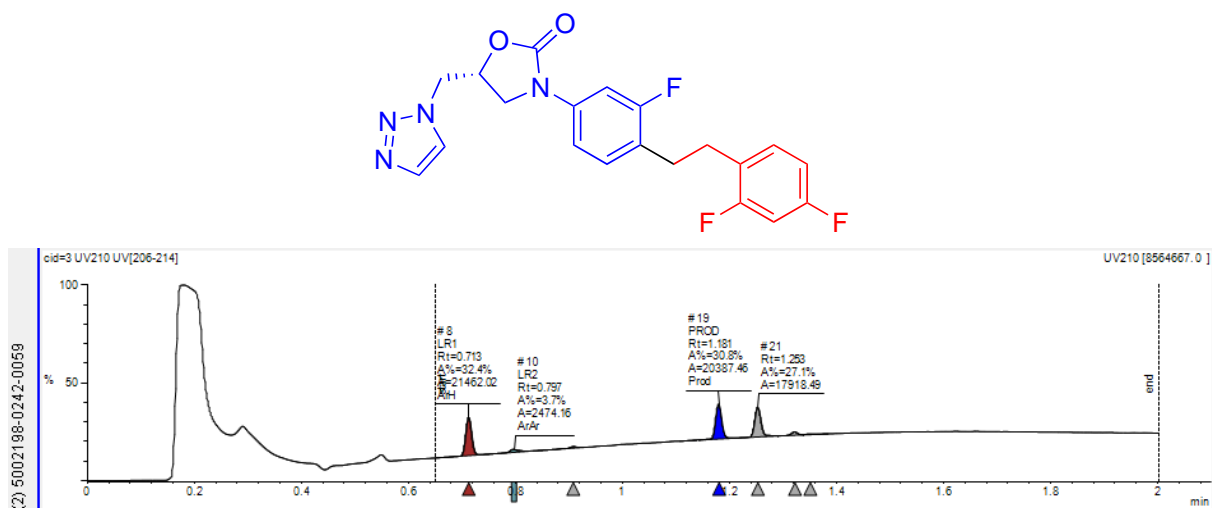


Figure S110. UPLC trace the cross-electrophile coupling of **5f** with substrate **6v**.

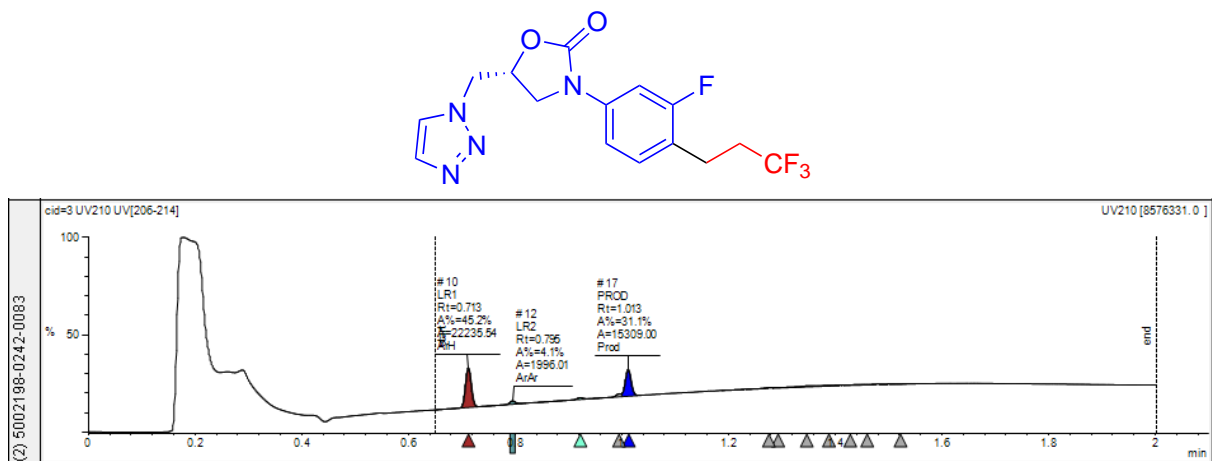


Figure S111. UPLC trace the cross-electrophile coupling of **5f** with substrate **6w**.

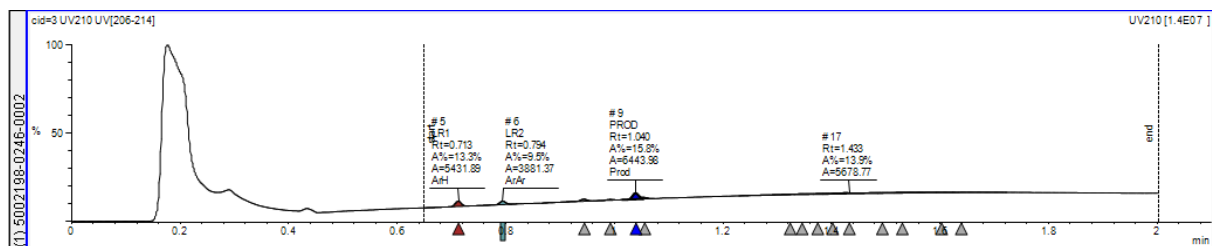
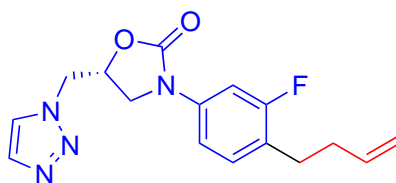


Figure S112. UPLC trace the cross-electrophile coupling of **5f** with substrate **6x**.

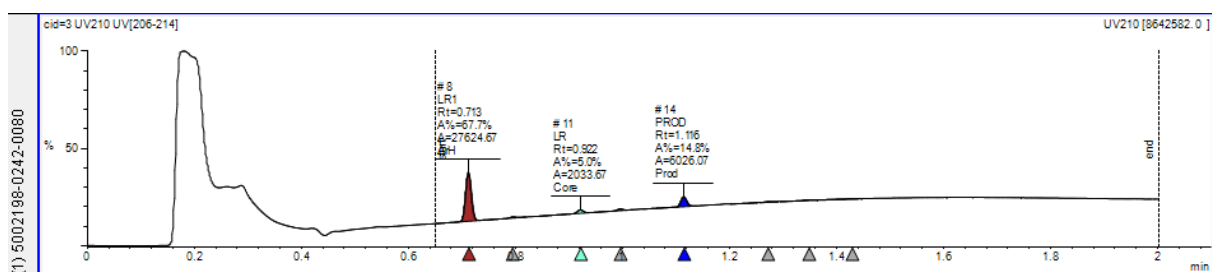
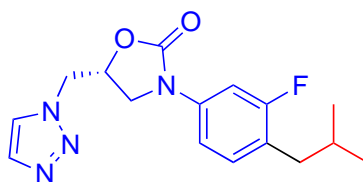


Figure S113. UPLC trace the cross-electrophile coupling of **5f** with substrate **6y**.

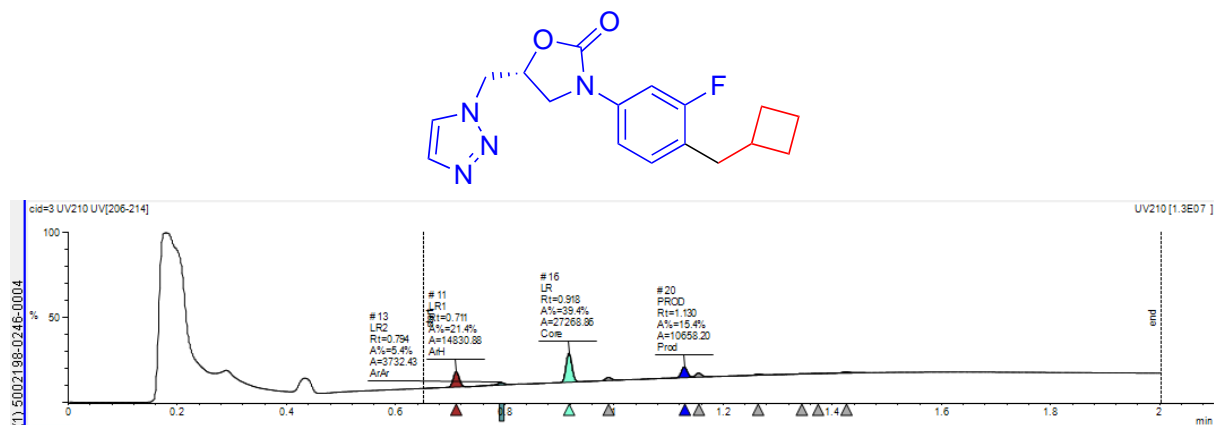


Figure S114. UPLC trace the cross-electrophile coupling of **5f** with substrate **6z**.

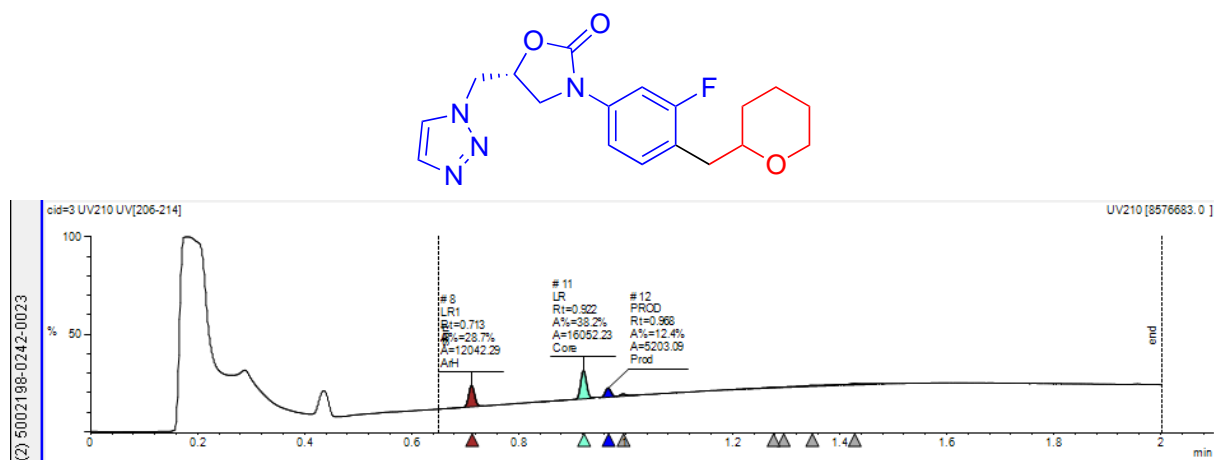


Figure S115. UPLC trace the cross-electrophile coupling of **5f** with substrate **6aa**.

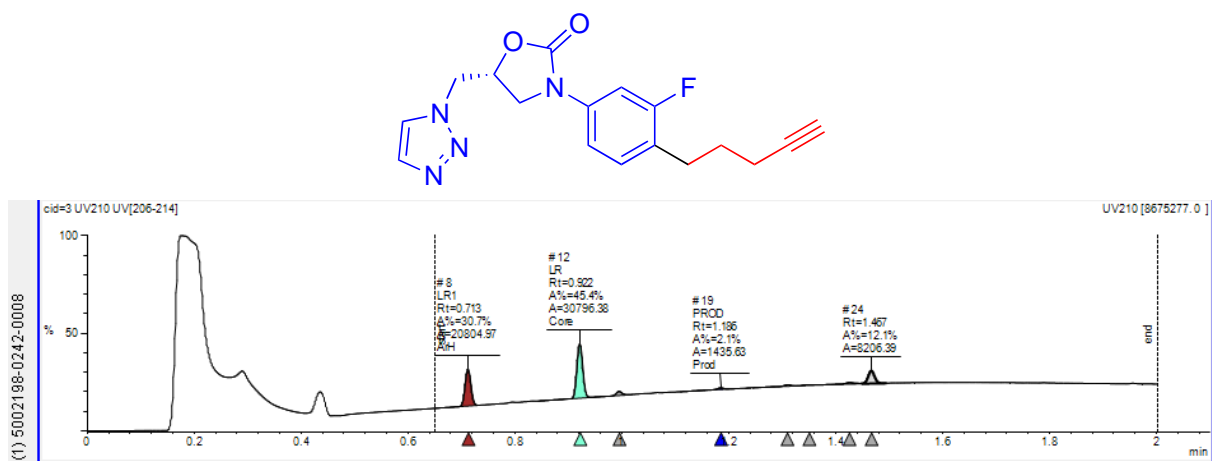


Figure S116. UPLC trace the cross-electrophile coupling of **5f** with substrate **6ab**.

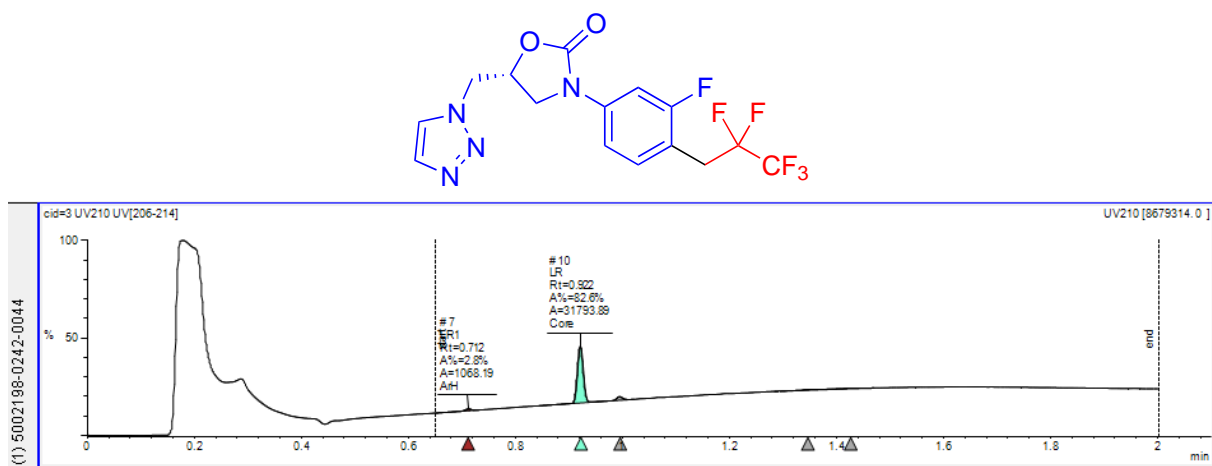


Figure S117. UPLC trace the cross-electrophile coupling of **5f** with substrate **6ac**.

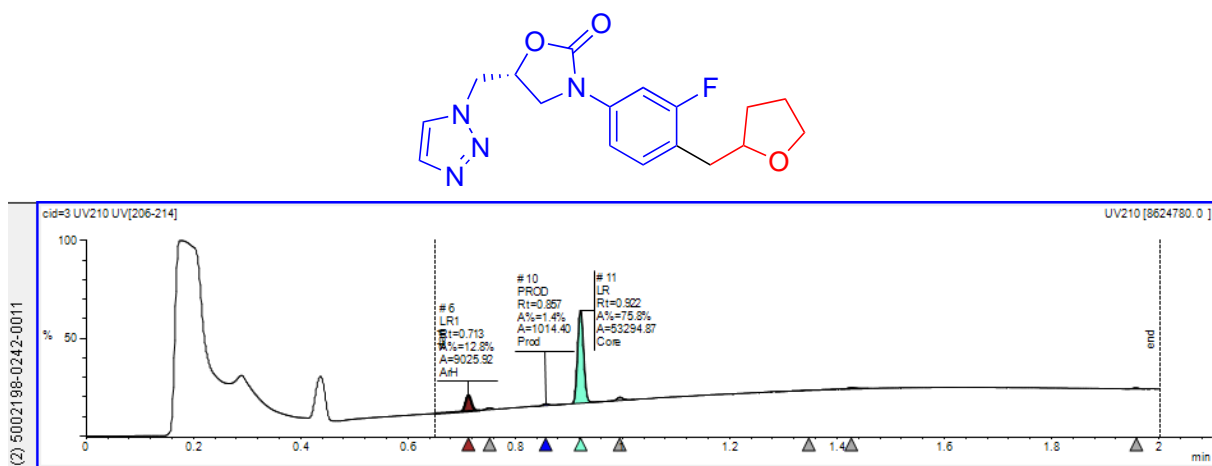


Figure S118. UPLC trace the cross-electrophile coupling of **5f** with substrate **6ad**.

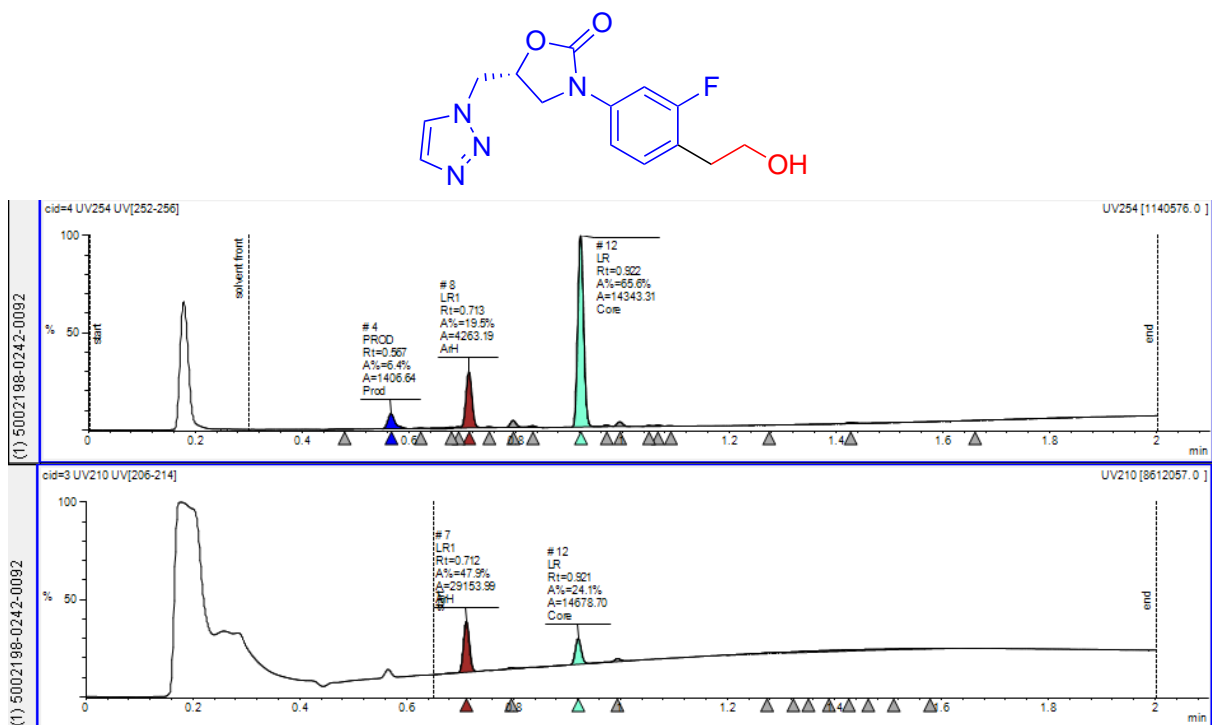


Figure S119. UPLC trace the cross-electrophile coupling of **5f** with substrate **6ae**. (Top) Trace at UV 254 nm. (Bottom) Trace at UV 210 nm.

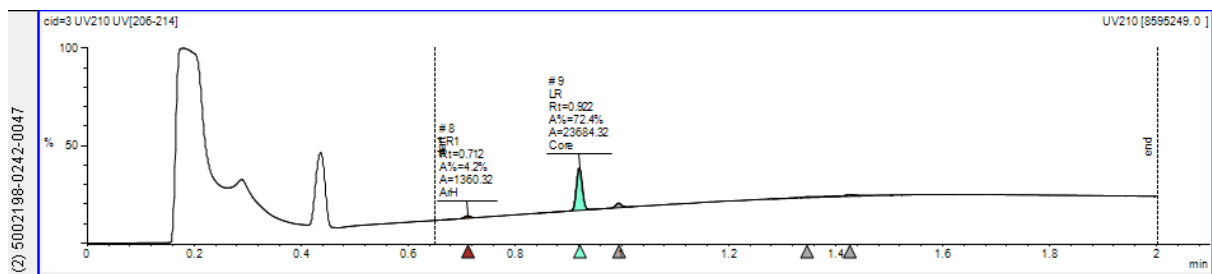
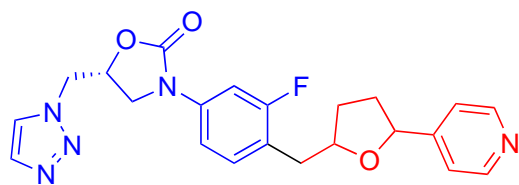


Figure S120. UPLC trace the cross-electrophile coupling of **5f** with substrate **6af**.

SXXVIII. References

- [1] K. M. M. Huihui, J. A. Caputo, Z. Melchor, A. M. Olivares, A. M. Spiewak, K. A. Johnson, T. A. DiBenedetto, S. Kim, L. K. G. Ackerman, D. J. Weix, *J. Am. Chem. Soc.* **2016**, *138*, 5016.
- [2] L. L. Anka-Lufford, K. M. M. Huihui, N. J. Gower, L. K. G. Ackerman, D. J. Weix, *Chem. Eur. J.* **2016**, *22*, 11564.
- [3] R. K. Harris, E. D. Becker, S. M. C. De Menezes, P. Granger, R. E. Hoffman, K. W. Zilm, *Magn. Reson. Chem.* **2008**, *46*, 582.
- [4] J.-W. Wu, Y.-D. Wu, J.-J. Dai, H.-J. Xu, *Adv. Synth. Catal.* **2014**, *356*, 2429.
- [5] K. A. De Castro, S. Oh, J. Yun, J. K. Lim, G. An, D. K. Kim, H. Rhee, *Synth. Commun.* **2009**, *39*, 3509.
- [6] M. Amatore, C. Gosmini, *Chem. Eur. J.* **2010**, *16*, 5848.
- [7] B.-Z. Chen, M.-L. Zhi, C.-X. Wang, X.-Q. Chu, Z.-L. Shen, T.-P. Loh, *Org. Lett.* **2018**, *20*, 1902.
- [8] Z.-L. Shen, K. K. K. Goh, Y.-S. Yang, Y.-C. Lai, C. H. A. Wong, H.-L. Cheong, T.-P. Loh, *Angew. Chem. Int. Ed.* **2011**, *50*, 511.
- [9] M. Tobisu, R. Nakamura, Y. Kita, N. Chatani, *J. Am. Chem. Soc.* **2009**, *131*, 3174.
- [10] D. A. Powell, G. C. Fu, *J. Am. Chem. Soc.* **2004**, *126*, 7788.
- [11] E. Lager, J. Nilsson, E. Østergaard Nielsen, M. Nielsen, T. Liljefors, O. Sterner, *Biorg. Med. Chem.* **2008**, *16*, 6936.
- [12] W. M. Czaplik, M. Mayer, A. Jacobi von Wangelin, *Angew. Chem. Int. Ed.* **2009**, *48*, 607.
- [13] X. Li, X. Che, G.-H. Chen, J. Zhang, J.-L. Yan, Y.-F. Zhang, L.-S. Zhang, C.-P. Hsu, Y. Q. Gao, Z.-J. Shi, *Org. Lett.* **2016**, *18*, 1234.
- [14] J. Masson-Makdissi, J. K. Vandavasi, S. G. Newman, *Org. Lett.* **2018**, *20*, 4094.
- [15] S. Laulhé, J. M. Blackburn, J. L. Roizen, *Org. Lett.* **2016**, *18*, 4440.
- [16] C. Han, S. L. Buchwald, *J. Am. Chem. Soc.* **2009**, *131*, 7532.
- [17] P. S. Campbell, C. Jamieson, I. Simpson, A. J. B. Watson, *Chem. Commun.* **2018**, *54*, 46.
- [18] P. S. Kutchukian, J. F. Dropinski, K. D. Dykstra, B. Li, D. A. DiRocco, E. C. Streckfuss, L.-C. Campeau, T. Cernak, P. Vachal, I. W. Davies, S. W. Krska, S. D. Dreher, *Chem. Sci.* **2016**, *7*, 2604.

Supporting_Information.pdf (7.19 MiB)

[view on ChemRxiv](#) • [download file](#)
